IMPACTS OF CUSTOM POWER DEVICES ON VOLTAGE STABILITY IN DG INTEGRATED RADIAL DISTRIBUTION SYSTEM

A THESIS

Submitted by

BINDUMOL E. K.

Under the guidance of

Dr. BABU C.A

for the award of the degree

of

DOCTOR OF PHILOSOPHY

DIVISION OF ELECTRICAL ENGINEERING
SCHOOL OF ENGINEERING
COCHIN UNIVERSITY OF SCIENCE AND TECHNOLOGY, KOCHI

APRIL 2017

DIVISION OF ELECTRICAL ENGINEERING
SCHOOL OF ENGINEERING
COCHIN UNIVERSITY OF SCIENCE AND TECHNOLOGY

CERTIFICATE

This is to certify that the work presented in this thesis entitled "**Impacts of Custom Power Devices on Voltage Stability in DG integrated Radial Distribution System**" is based on the authentic record of research done by **Bindumol E. K.** under my guidance towards the partial fulfilment of the requirements for the award of the degree of **Doctor of Philosophy** of the Cochin University of Science and Technology and has not been included in any other thesis submitted for the award of any degree.

Dr. C. A. Babu
(Supervising Guide)
Professor and Head
Division of Electrical Engineering
School of Engineering
Cochin University of Science and Technology

DECLARATION

I hereby declare that the work presented in this thesis entitled **"Impacts of Custom Power Devices on Voltage Stability in DG integrated Radial Distribution System"** is based on the original research work carried out by me under the supervision and guidance of **Dr. C. A. Babu**, Professor and Head, Division of Electrical Engineering, School of Engineering, Cochin University of Science and Technology, Kochi-22 and has not been included in any other thesis submitted previously for the award of any degree.

Kochi **Bindumol E. K.**
30th April 2017

ACKNOWLEDGMENT

I would like to express my profound gratitude to Dr. C. A. Babu, Professor and Head, Division of Electrical Engineering, School of Engineering, Cochin University of Science and Technology for the excellent guidance, competent advice, keen observations, persistent encouragement as well as personal attention given to me during the entire course of research work. Heartfelt thanks are due to him for the constant inspiration, motivation and freedom given to me for pursuing research. I was able to successfully complete the work and deliver this thesis only because of his able guidance and immense patience.

I am extremely thankful to Dr. Usha Nair, Associate Professor, Division of Electrical Engineering, School of Engineering, Cochin University of Science and Technology and member of Doctoral Committee for the valuable suggestions and advice during the period of this work. I take this opportunity to thank all the people in Division of Electrical Engineering, School of Engineering, Cochin University of Science and Technology specially Dr. Asha Elizabeth Daniel, Associate Professor, Dr. P. G. Latha, Associate Professor and Prof. Sheena K. M. for their constant support at all stages of this research.

I am obliged to our Principal and office staff for all other logistical support. I would like to thank all non-teaching staff of CUSAT who have helped and supported me during the entire period of work. I am thankful to all technical staff and office staff of the Electrical department, Division of Electrical Engineering, Cochin University of Science and Technology for the help given to me. I express my thanks to all library staff for the help given to me.

I express my earnest obligation to Dr. A. Amar Dutt, former Professor and Head, Department of Electrical Engineering, Govt. Engineering College, Thrissur, Kerala for her endless support, care, constant encouragement and valuable suggestions throughout this work.

I am very much grateful to Dr. B. Jayanand and Dr. M. Nandakumar, Professors, Electrical Engineering Department, Govt. Engineering College, Thrissur for spending their precious time discussing with me to clarify my doubts and to provide creative suggestions.

I have been working at Govt. Engineering College, Thrissur, during the period of my research work. I am extremely thankful to Dr. K. Vijayakumar, Director of Technical Education, Thiruvananthapuram and Dr. K. P. Indira Devi, Principal, Govt. Engineering College, Thrissur, for providing all sort of support including

administrative, to facilitate my study at CUSAT. I am grateful to all the colleagues and office staff of the college for their support.

I express my sincere thanks to Dr. Abdul Hameed K. M., Principal, Dr. C. Sreekumar, Head of the Department and all colleagues of Department of Electrical and Electronics Engineering and all office staff of Govt. Engineering College, Wayanad, Kerala for the support rendered to complete the thesis in time. Towards completion of thesis writing, I was transferred to Govt. Engineering College, Wayanad.

I remember the faculties in the training programmes I had attended during the course of my research work. The contents of the training programmes helped a lot to improve my work. I am most thankful to all the faculties for sharing their knowledge.

I express my heartfelt thanks to Prof. Mini V. and Prof. Subadhra P. R., my colleagues at Govt. Engineering College, Thrissur, for being good friends to share my anxieties and to build up confidence throughout the course of my research.

It is difficult to identify many friends who contributed so much unmentioned support. However, I am indebted to Smt. Vineetha C. P. and Smt. Bindu S. J. for helping me at many important stages during my work. I express my heartiest gratitude to all my friends for their support throughout my work.

I record my sincere and utmost gratitude to my parents Mr. E. K. Krishnan and Mrs. N. R. Soudamini for the constant encouragement and support given to me throughout my life. I am indebted to my mother-in-law, Mrs. Neeli, brother-in-law, Mr. K. Krishnan and sister-in-law, Mrs. K. A. Ammini for filling my absence at home and caring my family during the entire period of my work. I am thankful to all my family members, relatives, and well-wishers.

Words cannot express how grateful I am to my husband Dr. O.K. Mani for giving me constant guidance, motivation, and care, which I cherish throughout my life. His consistent enthusiasm and support made me sail through the hardship and provided me with the energy to overcome the various hurdles I faced. I am blessed with two lovely children, Master Mridul and Kumari Prithvy Krishna. Their love and affection had been an everlasting inspiration to complete my work at a good pace.

I thank you, the reader of this thesis for sparing your valuable time to go through my findings, in search of knowledge.

Last but not the least, I offer my heartiest salutation to the Almighty for blessing me with health, willpower, and knowledge required for completion of this work as well as getting along with life.

BINDUMOL E. K.

ABSTRACT

Growth rate in electricity supply industry (ESI) is not commensurate with growth in demand, leading to energy deficit and can even jeopardize the stable system operation. Among the various power system stability issues, voltage instability is a major challenging problem attracting focused investigation by researchers all over the world. Moreover, the customers at the far end of the distribution system suffer from severe voltage instability.

Rapid depletion, environmental impacts, increasing demand and the escalating cost of fossil fuel, etc. necessitates the search for other alternatives. Integration of renewable energy based distributed generation (DG) systems; particularly of wind and solar photo-voltaic (SPV) based systems to the grid can offer viable solutions to address these problems. Ongoing deregulation of the electricity energy market and global concerns of reducing greenhouse gas emissions result in high rate of penetration of renewable energy (RE) based DG systems. High rate of penetration of RE has resulted in increasing the awareness of power quality (PQ) issues such as voltage sag, voltage swell etc., which are concerned by both the electric utilities and end users of the electric power. A group of sophisticated power electronics based equipment called Custom Power Devices (CPDs) can be used to enhance the quality and reliability of power delivered to the customer. Increase in risks of under voltage/overvoltage caused by DG can be reduced or even be mitigating using CPD.

In this background, a Thevenin's equivalent model of the radial network has been developed incorporating a wind-based DG and a CPD, in PSCAD environment. Capability of the model in mitigating voltage sag under different fault conditions has been assessed. Developed model could successfully restore pre-fault condition with the integration of CPD.

The non-optimal allocation of DG systems adversely affects the voltage stability in terms of increase in system losses and voltage profile lower than the allowable limit. In many cases, power injection from a single point by DG may not be sufficient to improve the voltage profile, which necessitates power injection from multiple DGs at different locations. An optimization algorithm is proposed to identify the possible optimal locations and sizing of DG/DGs within the boundaries, for maintaining the voltage stability in the radial distribution network. Genetic algorithm (GA) based backward

forward sweep algorithm (BFSA) has been developed for IEEE standard radial network to secure the position of renewable energy sources (RES) within the constraints. Results showed a significant reduction in power loss and improved voltage profile. Optimal utilization of DG power results in enhanced voltage stability and considerable reduction of operating cost. Effectiveness of the algorithms is validated by implementing it on IEEE 15 bus radial distribution system (RDS) and other practical systems.

In certain circumstances, the impact of voltage instability becomes a root cause of voltage collapse or black out. Voltage stability indices help to precisely locate the origin of the crisis, through which active/reactive power support can feed for ensuring the reliability and optimum quality of power at customer end. Various stability indices are used to identify the weakest bus in the IEEE 15 bus RDS at which the voltage collapse starts first. Effectiveness has been demonstrated using different case studies.

Increased penetration of nonlinear loads results in PQ problems, which can cause economic impacts on utilities, consumers and suppliers of load equipment. Important PQ issues such as voltage sag and voltage swell can be effectively mitigated with the restructuring of existing radial network integrated with CPD. Restructuring of the system with CPDs is an effective technique to restore the voltage at the point of common coupling (PCC), for enhancing the quality of power, subject to the technical and financial constraints. Application of the BFSA gave a better voltage profile by optimally placing reactive power support in the IEEE 15 bus radial network. Combined effect of DG/DGs and CPD in the IEEE network, to reduce the power losses and improve the voltage profile has been demonstrated.

An integrated model of IEEE 15 bus system with DG and CPD are developed in MATLAB environment and observed the impacts of improving voltage profile and mitigating PQ issues. The BFSA developed in the present work for voltage stability analysis can be effectively utilized by the utilities for assessing the impact, in case of addition of any type of devices to the existing structure of the radial network.

The research work presented in the thesis demonstrates that, if the DG is properly coordinated with the CPD, proper voltage regulation can be maintained. Further, the negative impact of DG on voltage stability can be mitigated with proper integration of CPDs.

CONTENTS

LIST OF TABLES

LIST OF FIGURES

LIST OF ABBREVIATIONS

BCBV	Branch Current to Bus Voltage
BFSA	Backward Forward Sweep Algorithm
BIBC	Bus Injection to Branch Current
BVSI	Bus Voltage Stability Index
CPD	Custom Power Device
DC	Direct Current
DG	Distributed Generation
D-STATCOM	Distribution Static Compensator
DVR	Dynamic Voltage Restorer
ESI	Electricity Supply Industry
FACTs	Flexible AC Transmission System
FVSI	Fast Voltage Stability Index
GA	Genetic Algorithm
GC	Grid Code
KVL	Kirchhoff's Voltage Law
LLRI	Line Loss Reduction Index
LSF	Loss Sensitivity Factor
O&M	Operation and Maintenance
PCC	Point of Common Coupling
PE	Power electronics
PQ	Power Quality
PSCAD	Power System Computer Aided Design
PWM	Pulse Width Modulation
RDS	Radial Distribution System
RES	Renewable energy Sources
SAF	Sensitivity Analysis Factor
SPV	Solar Photo-Voltaic
SSTS	Solid State Transfer Switch
T&D	Transmission and Distribution
TOC	Total Operating Cost
VPII	Voltage Profile Improvement Index
VSC	Voltage Source Converter
VSI	Voltage stability Index
WT	Wind Turbine

ACRONYMS

V_d^{ac}	AC component of V_d
V_q^{ac}	AC component of V_q
P_j	Active load at j^{th} bus
P^{dg}	Active power generated by DG
P_{loss}^{ndg}	Active power loss without DG
θ_0	Angle of line current
θ	Angle of line current after D-STATCOM installation
α_{new}	Angle of receiving end bus after compensation
α_0	Angle of receiving end voltage
δ	Angle of sending end bus after compensation
δ_0	Angle of sending end voltage
δ_i	Angle of voltage at i^{th} bus
δ_j	Angle of voltage at j^{th} bus
k	Branch between nodes i and j
V_j^k	Bus voltage at k^{th} iteration for j^{th} node
S_j	Complex power at j^{th} node
$I(i)$	Current flow from i^{th} bus j^{th} bus
I_{dst}	Current through D-STATCOM
V_{cap}	DC bus voltage across the capacitor of DVR
V_d^{dc}	DC component of V_d
V_q^{dc}	DC component of V_q
δ_{ij}	Difference in angle of voltage at i^{th} and j^{th} bus
V_{cd}	Direct axis component of injected voltage
V_d	Direct axis component of supply voltage
I_j^k	Equivalent current injection at k^{th} iteration for j^{th} node
x_{eq}	Equivalent inductance of feeder
r_{eq}	Equivalent resistance of feeder
V_{de}	Error between reference and sensed voltage
I_j^i	Imaginary parts of equivalent current injection at k^{th} iteration for j^{th} node
$Z(k)$	Impedance of k^{th} branch
K_i	Integral gain of DC bus
I_L	Line current after D-STATCOM installation

I_{0L}	Line current before compensation
V_l	Load voltage
$P_{\max}^{dg}$	Maximum size of DG connected to the system
$Q_{\max}^{dst}$	Maximum value of reactive power injected to the system
$V_{\max}$	Maximum value of voltage at j^{th} bus
$P_{\min}^{dg}$	Minimum value of active power of DG injected at j^{th} bus
$Q_{\min}^{dst}$	Minimum value of reactive power injected to the system
$P_{\max}^{dg}$	Minimum value of reactive power of DG injected at j^{th} bus
$V_{\min}$	Minimum value of voltage at j^{th} bus
V_j^{new}	New bus voltage at j^{th} bus after compensation
V	Normal voltage
K_p	Proportional gain of DC bus
V_{cq}	Quadrature axis component of injected voltage
V_q	Quadrature axis component of supply voltage
$X(k)$	Reactance of k^{th} branch
$V_{q(r)}$	Reactive component of load voltage
Q_j	Reactive load at j^{th} bus
Q_j^{dg}	Reactive power at node j with DG
Q^{dg}	Reactive power generated by DG
Q_{loss}^{dg}	Reactive power loss with DG
Q_{loss}^{ndg}	Reactive power loss without DG
I_j^r	real parts of equivalent current injection at k^{th} iteration for j^{th} node
P_j^{dg}	Real power at node j with DG
P_{loss}^{dg}	Real power loss with DG
j	Receiving end node
V_{ref}	Reference Voltage
$R(k)$	Resistance of k^{th} branch
V_{rms}	Rms voltage
i	Sending end node
Q^{dst}	Size of D-STATCOM
P_{tl}	Total active load connected in the system

$P_{j\,loss}$	Total active power loss supplied beyond j^{th} node
P_j^{eff}	Total effective active power supplied beyond j^{th} node
Q_j^{eff}	Total effective reactive power supplied beyond j^{th} node
$Q_{j\,loss}$	Total reactive power loss supplied beyond j^{th} node
$Q_{loss(x)}^{dst}$	Total system reactive power loss with D-STATCOM of x kVAr rating
Q_{loss}^{ndst}	Total system reactive power loss without D-STATCOM
$P_{loss(x)}^{dg}$	Total system real power loss with DG of $\boldsymbol{x}$ kW rating
V_i	Voltage at i^{th} bus
V_j	Voltage at j^{th} bus
V_{pcc}	Voltage at point of common coupling
V_c	Voltage injected by DVR
$V_{0\,j}$	Voltage of bus j before compensation
V_{0i}	Voltage of bus i before compensation
VP^{dg}	Voltage profile with DG
VP^{ndg}	Voltage profile without DG

CHAPTER 1

INTRODUCTION

1.1 BACKGROUND

A planned and effective radial distribution network is the main key to cope up with an ever growing demand such as domestic, industrial and commercial load. The distribution network experience an unpredictable change in the load levels every day. The high rate of total demand for electricity affected by the economic growth and rise in per capita electricity consumption makes an imbalance in energy supply-demand. Severe environmental impacts caused by the fossil fuel based power plants and the escalating fuel costs are the major challenges faced by the ESI. Rapid depletion of fossil-based oil, coal and gas reserves and its greater demand day by day necessitates the search for other alternatives. Due to increasing air pollution, global warming concerns, diminishing fossil fuels and their increasing cost has made it necessary to look towards RES as a future energy solution. To address the global energy crisis, the RES system has attracted significant attention in the recent years. Due to increase in load demand, RES with power electronic converters, named DG, are increasingly integrated at the distribution level.

Rise or fall in voltage, deviation in system frequency due to demand-supply mismatch, injection of harmonics by power electronics based DG are the major issues in DG integrated grid system. These issues cause a high degree of PQ problem which results in poor voltage regulation at the customer end [1]. Most of the PQ issues in the power system are due to the non-linear characteristics and the fast switching of the power electronic equipment. The power electronics based electrical loads at the

various distribution ends like the adjustable speed drives, process industries, printers, domestic equipment, computers, microprocessor-based equipment, etc. have become intolerant to voltage fluctuations, harmonic content, and interruption [2]. Almost all the PQ issues are closely related to power electronic devices used in almost every aspect of the commercial, domestic and industrial application.

Voltage instability is a major issue faced in a distribution power system due to the unpredictable change in load demand. The ability of the power system to provide reactive power or the uniform consumption of reactive power by the system itself is named as voltage stability [3]. The voltage collapse first occurs at the most sensitive bus and then spreads out to other sensitive buses. Voltage stability index is an indicator to the operator about the severity of the voltage collapse, and it helps to monitor and take the initiative for the remedial action. The non-optimal location of active/reactive support can result in a wide variation in the voltage profile, with an increase in the system losses.

1.2 LITERATURE REVIEW

Distribution system is the main part of the power system network since it keeps a main link between the electricity suppliers and customers. Effective planning and restructuring of existing distribution network with some additions can make a balance between energy supply-demand. A properly designed and operated distribution network should support the energy supply at the minimum cost of operation and maintenance. To maintain the quality of service offered by ESI, the power supply should meet the specific standards such as regulated voltage, constant frequency and reliability. Distribution networks are classified as ring main distribution system and radial distribution system. Most of the distribution networks are radial in nature.

Load flow studies in RDS have not yet received appreciable attention unlike in transmission systems. Load flow analysis is very essential for the continuous evaluation of the stability of the existing power system and effective planning of other alternatives such as system expansion or DG to meet the increased load demand in future. Addition of any devices or equipment to the existing radial distribution system needs the load flow analysis, which gives real and reactive power losses and the voltage at different nodes of the system, subject to the system constraints. If the power system consists of a large number of buses, the computation is difficult and the voltage stability can be analyzed only with the help of simulation tools such as Power System Computer Aided Design (PSCAD), MATLAB, etc.

Generally, the radial distribution system is too long and its high R/X ratio causes a high voltage drop which results in low voltage stability. The efficient and reliable traditional load flow solution techniques such as Gauss-Seidel (GS), Newton-Raphson (N-R) and Fast Decoupled Load Flow (FDLF) methods cannot be used to analyze the voltage profile and computation of the losses, as discussed in the various literature [4-10]. Due to the poor convergence in the performance of these methods in RDS, a modified conventional N-R method is proposed in [11] and [12], which is quite time-consuming and complex. A ladder network based technique has been developed in [13], which appears to be complicated. In contrast to this, the algorithm in [14] is very fast, but both did not guarantee any convergence. A new compensation-based power flow method proposed in [15] and [16] used for solving radial and weakly meshed distribution networks are more efficient than the Newton-Raphson power flow technique, but needs a rigorous data preparation. Another method is presented in [17] in which only voltage magnitudes are computed, without

the bus phase angles, but both are computed in [18]. A direct method for solving radial and meshed distribution networks is demonstrated in [19] in which the node in the network is not a junction of more than three branches. This method has no convergence problem, guarantees an accurate solution for any distribution system but difficult in numbering the nodes and branches. A new and efficient method is presented in [20] for solving both radial and meshed networks with more than one feeding node. In [21], the voltage dependency of static loads and line charging capacitance are taken into account.

Fuzzy based method for weakly meshed balanced and unbalanced distribution systems are presented in [22] and based on branch-injection to the branch-current matrix (BIBC) is presented in [23]. Another method proposed in [24] for the load-flow solution of radial distribution networks with minimum data preparation in which node and branch numbering is not sequential like other available methods. A simple and efficient branch-to-node matrix-based power flow method is demonstrated in [25] in which any presence of sub-laterals complicates the matrix formation. In [26], a method has been proposed for the analysis of radial or weakly meshed distribution systems supplying voltage-dependent loads. In [27], a load-flow technique is proposed for solving radial distribution networks by calculating the total real and reactive power fed through any node, using power convergence with the help of coding at the lateral and sub lateral nodes for the large system, which increased the complexity of computation. In this method, the voltage of each receiving end node is calculated using the forward sweep, taking initial power loss as zero for solving radial distribution networks. It can solve the simple algebraic recursive expression of voltage magnitude and all the data can be easily stored in vector form, thus saving an

enormous amount of computer memory. In continuation of [27], this method is revised in [28] which is based on the technique with nodes beyond the branches using voltage convergence. Flat voltage start has been considered. The incorporation of charging admittances reduces the losses and improves the voltage profile. Even though the proposed method is computationally very efficient and provides fast convergence, it suffers from the drawback of storing nodes beyond each branch. Two new efficient load flow algorithms along with a couple of new schemes for network reconfigurations are investigated in [29]. In [30], new method of load flow analysis for radial distribution system is discussed by considering voltage independent loads and voltage dependency loads. Based on network topology, basic circuit laws and power summation technique, a ZIP model has been proposed for load flow analysis in radial and mesh distribution systems [31].

Most of the researchers have applied the widely used tools such as evolutionary computational techniques like Hereford Ranch Algorithm (HRA), Genetic Algorithm (GA), Simulated Annealing (SA), Evolutionary programming (EP), Decision Theory, Fuzzy systems, Ant Colony Optimization (ACO), Particle Swarm Optimization (PSO), Tabu Search (TS), Differential Evolution, Immune Algorithm based Optimization (IA) and Bee Colony Optimization algorithm (BCO) etc. for solving optimal DG allocation problem. An analytical approach is presented in [32] to determine the proper location of DG units on the power grid concerning the system losses. The same problem demonstrated in [33] is based on the rules of thumb methods and Bus Injection Branch Current – Branch Current Bus Voltage (BIBC-BCBV) matrices in [34]. HR algorithm is proposed in [35] to optimally locate the dispersed generation in a meshed network and [36] in the radial network. A Monte Carlo based power flow algorithm is proposed in [37] that integrates the deterministic and the stochastic natures of the new structured,

electrical distributed generation systems. GA method is proposed in [38] and [39] to determine the optimal site and size of DG in radial distribution feeders. Optimal proposed approach (OPA) is proposed in [40] to determine the optimal siting and sizing of DG with multi-system constraints to achieve a single or multi-objectives using a genetic algorithm (GA). A combination of GA and SA methods are demonstrated in [41] and quantum-inspired evolutionary programming (QIEP) in [42] to find the optimal allocation of distributed generation resources in distribution networks. The other methods such as Fuzzy-GA method is presented in [43], tabu search algorithm (TS) in [44], Immune Algorithm (IA) based optimization approach in [45] and heuristic BCO in [46] are demonstrated as a solving tool for determining the optimal position of DG for loss reduction and line capacity improvement. Further, optimal allocation and sizing of DG in a radial system using whale optimization algorithm, K-means clustering method, and Cuckoo search algorithm are discussed in [47]-[49].

Some of the researchers have developed voltage indices for finding the weakest bus which is the first origin of voltage collapse. An algorithm for voltage stability enhancement based on voltage stability index is proposed in [50] and the new sensitivity matrix L-index in [51]. In [52], the different criteria for voltage stability index is demonstrated which is helpful for voltage stability assessment. Loadability enhancement based reactive power margin can be used to identify weak buses which need reactive power [53]. Critical line and the weakest buses for the placement of D-STATCOM are identified using FVSI in [54]-[58]. A unique& novel voltage stability indicator (VSI) can identify the condition of load buses with voltage collapse point of view [59]-[62]. In [63], a framework that uses the ratio of standard deviation to mean of the magnitude of the voltage at load buses has been proposed to identify weak buses.

The economic and social developments like deregulation demand new concepts and technologies to exploit the existing power system resources to the maximum without compromising, system stability. Earlier, the shunt capacitor was considered as a good solution for correcting poor power factor due to unbalanced, harmonic current drawn by the load. Tuned filters are used to bypass harmonic currents with power electronic loads [64]. In the past, various methods like motor-generator sets (to confront interruptions) and Ferro resonance transformers (to confront voltage sags of large loads) have been proposed to confront the most widespread type of power quality disturbance such as voltage sag and interruptions [65][66]. The problem of long-term voltage changes is solved with devices such as load tap changing transformers, line voltage drop compensators and shunt capacitors. Surge arrestors are applied to protect against transient over voltages. Passive filters are used to reduce the harmonic distortion level of current flow and network voltage. The power quality mitigation device called custom power devices (CPD) [67]-[69] is used to control the power flow through the line and hence to attain stability and reliability within the limit with minimal infrastructure investment. The concept of custom power was first introduced by N.G. Hingorani [2], the term custom power pertains to the use of power electronic controllers for distribution systems. The currently used CPDs are described in [70]. The first category of such devices contains solid state breakers (SSBs) which do not need DC energy storage sources and most widely used solid-state transfer switches (SSTS) usually located to back up sensitive loads according to the type and sensitivity of load, in addition to the primary and secondary feeders which requires DC energy storage sources. The second category consists of reactive power compensation devices such as shunt connected distributed static compensator (D-STATCOM), series connected dynamic voltage restorer (DVR),

series-shunt connected unified power quality conditioner (UPQC). It plays a crucial role in the power quality improvement, power factor correction and maintaining constant voltage distribution in the distribution network.

The improper location and size of DG result in high degree of voltage instability problems in the radial network. These problems can be solved with the use of CPDs. Many of the researchers have developed algorithms to allocate the optimized CPDs in radial system. Some of the algorithms are GA, Particle Swarm Optimization (PSO), Artificial Immune System (AIS), Differential Evolution (DE), etc. Optimal placement and sizing of Static VAR Compensator (SVC) can be done using Improved Harmony Search Algorithm [71], and a hybrid Bee Colony Optimization and Harmony Search algorithms [72], and the optimal placement of UPFC can be solved using Shuffled Frog Leaping Algorithm [73]. In [74], an artificial neural network control algorithm is developed for the control of D-STATCOM for the improvement of power quality. The different formulations and methodologies based on a heuristic, artificial intelligence or hybrid techniques have been proposed to solve the optimum location of CPDs [75], [76]. The objective functions of these proposed methodologies were mostly formulated based on the cost considerations, while some limits such as bus voltage and harmonic distortion levels are considered as the constraints to control variables [77],[78]. Optimal placement of FACTS devices can be done using PSO [79] and DG [80] to improve power quality in transmission and distribution systems, but its effectiveness for optimal placement of DVR and D-STATCOM has not been investigated[81]. GA-based optimal placement approach was proposed to reduce voltage sag cost in the distribution system using power electronic controllers including SVC, STATCOM, and DVR [82].

Another GA-based optimization approach was proposed to optimally select and allocate CPDs in a distribution network to minimize the number of voltage sags [83]. The goal attainment method [84],[85] is applied to convert the multi-objective function to a single function for simplification of the optimization problem. Finally, Simulated Annealing is applied to solve the DVR optimal placement problem and mitigate voltage sag. Gravitational search algorithm (GSA) is an optimization algorithm inspired by the law of gravity [86]. Another method was proposed to enhance reliability and mitigate voltage sag propagation in power distribution systems by optimal placement of D-STATCOM using GSA [87]. A binary version of gravitational search algorithm (BGSA) is applied as a heuristic computational optimization tool to solve the optimization problem. An approach was proposed to optimally allocate DVR in distribution networks to minimize the number of voltage sags using the bottom-up approach and Dynamic Programming technique [88]. An ANN-based optimization approach was proposed to optimally locate the D-STATCOM in distribution systems to mitigate voltage sag [89]. A stochastic-based assessment using the weighted sampling method and GA was proposed to optimize the cost of placing series compensation devices including DVR and a new type of CPD named Thyristor Voltage Regulator for voltage sag mitigation in distribution systems [90]. The goal attainment method [90] is applied to convert the multi-objective function to a single function for simplification of the optimization problem.

Severe impacts of voltage sags and swells on nonlinear loads and sensitive loads are described in [91]. In an isolated power system, a series compensator (SC) is used to improve power quality [92]. In [93], a method is proposed to establish that electrical arc

furnace is a major flicker source to make power quality problems. The author [94] has formulated the derivation of an analytical model and simulation for the unified series shunt-compensator for investigating power quality in power distribution system. A new combination of a three-phase Shunt Hybrid Power Filter (SHPF) and a Thyristor Controlled Reactor (TCR) for compensating harmonic currents and reactive power are proposed in [95]. D-STATCOM for balancing source currents, power factor correction and harmonic mitigation in three phase, three wire distribution system supplying delta connected load under various source voltage conditions are demonstrated in [96]. According to [97], different methods for voltage sag source location (upstream or downstream) based on various criteria such as energy, impedance, voltage or current is simulated and compared with each other. In [98], a new current mode controller is proposed to overcome the mentioned problem. The approach uses a fixed frequency current controller to maintain voltage levels in voltage sags (dips). The mitigation of power quality disturbance in the low voltage distribution system due to voltage swells using DVR is discussed in [99]. A method is proposed in [100] to show the effect of power system deregulation on the power quality problems. In [101], proposed a technique in which FACTS devices and their switching control schemes are used for improving the power flow in the transmission network and hence improve the power quality and reliability of the low voltage distribution network.

Optimization techniques are needed to determine the optimum location, type, and size of DG/CPD. For the combination of different devices with different characteristics, the objective function has to be multi-objective, nonlinear, non-continuous, and non-differentiable [102]. In other words, it is very difficult to solve such type non-

deterministic polynomial problem due to the exponential increase of its problem size [103]. Recently, several heuristic optimization techniques have been applied to solve these kinds of multi-objective combinatorial optimization problems in power systems [104]-[106]. The searching space is limited for these algorithms because it searches for the solutions within a subspace of the total search space to find the optimum solution within a reasonable computation time [107],[108]. Since the solutions are not limited by restrictive assumptions, these algorithms give the solution near to the global optimum [109],[110]. Therefore, many researchers have concentrated on various types of heuristic optimization techniques to determine the optimal location and size of DG and CPDs in distribution systems [111].

The optimal allocation of D-STATCOM and DG in radial distribution systems using exhaustive search method to reduce the power loss and improvement of the voltage profile has been discussed [112]. The minimization of annual energy loss cost and maximization of total economic savings cost with the allocation of DSTATCOM has been carried out in [113]. In [114], the harmonic analysis has been carried out in a DG and D-STATCOM integrated radial distribution system. An effective analytical-heuristic approach has been proposed for solving optimal placement and sizing of multiple distributed generation to achieve a high loss reduction in the large-scale distribution network [115]. Determination of optimal location and sizing of DG along with D-STATCOM in the distribution network using Cuckoo Search optimization algorithm has been discussed [116]. Hardware implementation of three-phase three-level inverter based D-STATCOM has been presented to reduce the THD [117].

1.3 RESEARCH FOCUS

From the literature review, the following points observed that:

1. Load flow analysis used in [27] and [28] is superior to other methods.
2. The computational steps required for GA is much less than other optimization tools and it gives guaranteed convergence and less computation time.
3. The voltage stability indices have a role in finding the origin of voltage collapse.
4. High penetration of DG results in PQ issues so that CPDs can be used to attain better voltage stability.

Computation of power losses and voltage profile at all the nodes using BFSA for the determination of possible locations and sizing of DG has not been found attempted in literature. Even though several researchers made use of different stability indices to find the position of DG/CPD in the radial network, its position has never been confirmed with the help of case studies. Based on CPD, most of the research works are carried out by modeling and simulation of DG/CPD in two bus system (Thevenin's equivalent model) using the MATLAB/SIMULINK to mitigate the power quality issues. Effectiveness of CPDs in IEEE RDS using optimization algorithm has not yet seen in the literature. In this background, the research objectives identified are:

- Devise and implement a Thevenin's equivalent model of the test system to investigate the performance of DG and CPDs under different fault conditions.
- Develop and propose a GA based BFSA to find the possible locations of the optimal size of DG/DGs in IEEE standard radial distribution system. Restrictive assumptions are made to get the solution near to the global optimum.
- Perform case studies using different stability indices to reaffirm the size and position of DG in RDS.

- Develop and propose a GA based BFSA to find the optimized size of D-STATCOM with proper placement in the same system.

- Compare the size and location of CPD from GA based BFSA with the analytical method using stability index.

- Model and analyze the effectiveness of CPD on DG integrated IEEE standard test system and its Thevenin's equivalent model.

1.4 OUTLINE OF CHAPTERS

A brief description of the work reported in the thesis is given below:

Following Chapter 1, Chapter 2 presents the description of the radial distribution system and custom power devices.

In Chapter 3, Thevenin's equivalent model of the test system modeled in PSCAD and the effects of the wind farm as well as the effectiveness of CPDs in voltage sag mitigation under different fault conditions are investigated.

In Chapter 4, GA based BFS algorithm applied in various IEEE standard test systems and practical systems to find the best locations and optimum size of DG/DGs are presented. The technical benefits of DG in these systems are accounted with the help of two indices named Voltage Profile Improvement Index and Line Loss Reduction Index.

Chapter 5 presents various stability indices to find the most sensitive bus and position which is reaffirmed based on case studies.

Chapter 6 discusses the attempt made to find the position and corresponding optimum size of CPD alone and locations of DG and CPD together in a radial system.

In Chapter 6, IEEE radial distribution system, wind turbine system, DVR and D-STATCOM modeled in MatLab/Simulink are presented. Voltage stability analysis and PQ issues are carried out in the wind integrated radial system. As a part of this work, the equivalent circuit of the IEEE 15 bus test system is modeled in Simulink. The analysis is carried out with the integration of wind system, DVR, and D-STATCOM.

CHAPTER 2

IMPACT OF DISTRIBUTED GENERATION ON GRID

2.1 INTRODUCTION

Power system is a large interconnected network which comprises of generating stations, transmission lines and distribution systems. It is a complex system which includes different types of linear and nonlinear loads. The generators produce electrical power in sinusoidal form but due to nonlinear electrical loads, the waveform is distorted. The voltage distortion caused by these loads is a function of both the system impedance and the amount of harmonic current injected [118], [119]. Induction motor load is an important component in the voltage stability assessment of a power system. The proximity of generation capacity to the regions of demand gives many advantages such as reduced transmission losses, increased network robustness, good quality of power and greater network flexibility. It also gives the environmental benefits such as reduced usage of fuel, lower emissions of CO_2 and other pollutants and increased utilization of renewable power [120]. It is necessary to integrate the RES based systems like wind, SPV, etc. to the grid to meet the ever-increasing energy demand of the customers. The present electrical energy scenario reveals that the grid-connected wind power system can contribute to a significant part of power generation in future [121].

2.2 DISTRIBUTED GENERATION

Renewable energy is the energy, which is harvested from the natural resources like sunlight, wind, tides, geothermal heat, etc. DG refers to power generation at the point of consumption or produces electricity at a site close to customers or that are tied to an electric distribution system. These resources are naturally replenished for all practical

purposes so that it can be considered to be limitless, unlike the tapering conventional fossil fuels. The global energy crunch has provided a renewed impulsion to the growth and development of clean and renewable energy sources. Clean Development Mechanisms (CDMs) [122] are being adopted by organizations all over the world. The main advantages of using RES are the elimination of harmful emissions, significant reduction in the level of pollution and in-exhaustible resources of the primary energy.

DG refers to small-scale (typically 1 kW – 50 MW) electric power generators. Distributed generators include synchronous generators, induction generators, reciprocating engines, micro turbines, combustion gas turbines, fuel cells, SPV system and wind turbines, etc. It can increase power reliability as a back-up or stand-by power to customers and also offers the customers, a choice in meeting their energy needs. Some of the RE sources are:

2.2.1 Wind Power:

Wind power is one of the main sources of RE which is a major part of the electrical power that is available abundantly. In India, the major part of the electrical power, i.e., 60% is from wind power. In wind power system, the wind turbine captures the wind's kinetic energy in a rotor which consists of two or more blades mechanically coupled to an electrical generator that is mounted on a tall tower to enhance energy capture. The two types of configuration currently used for a wind turbine are vertical-axis configuration and horizontal-axis configuration. The horizontal axis configuration is widely used for commercial wind power generation. The wind power available at the shaft depends on both wind speed and turbine blade’s swept area [123]. The power output increases rapidly with an increase in the available wind velocity.

2.2.2 Solar power:

Solar power can be employed in such a way that the captured heat can be used as solar thermal energy with important applications in space heating. In another way, it can also be converted into electrical energy with the use of SPV cell [124].

2.2.3 Biomass:

Biomass refers to organic matter that has stored energy through the process of photosynthesis. It is one of the most plentiful and well-utilized sources of renewable energy in the world. The chemical material, organic compounds of carbon are used to generate energy. Wood from trees is the most common biomass which is widely utilized as a source of energy, probably due to its low cost and indigenous nature. It accounts for almost 15% of the world's total energy supply and 35% in the developing countries, mostly for cooking and heating. It works as a natural battery to store the sun’s energy that can yield when required.

2.2.4 Geothermal:

Geothermal energy is the thermal energy which is generated and stored within the layers of the earth. The gradient thus developed brings about an uninterrupted conduction of heat from the core to the surface of the earth which can be utilized to heat water for producing superheated steam. The steam is used to run steam turbines for the generation of electricity. The primary failure regarding geothermal energy is that it is usually limited to the regions near tectonic plate boundaries, although recent progress has led to the multiplication of this technology.

2.3 NEED FOR DISTRIBUTED GENERATION

Both electric utilities and end-users of electrical power are concerned about the quality, stability and reliability of electric power. With the increasing demand, electrical energy suppliers cannot fulfill the everyday requirements of customers. And also, due to increasing air pollution, global warming concerns, diminishing fossil fuels and their increasing cost have made it necessary to look towards RES and DG as a future energy solution.

2.4 CHALLENGES ASSOCIATED WITH DISTRIBUTED GENERATION SYSTEMS

Challenges to integrating DG into distribution network are [125]:

2.4.1 Power quality

Integration of DG may support the system or deteriorate power quality. Hence, integration of DG is a challenging task, and every possible way needs to be developed to counter PQ problems.

2.4.2 Protection scheme

Protection selectivity must be re-evaluated for each connection of DG in the distribution system. The research need is in finding the solution of nuisance tripping of breaker and issues related to fuse saving.

2.4.3 Stability

When the DG size is small, the impact on power system dynamic performance is negligible. Investigation shows that the effects of DG on the dynamics of a power system and stability strongly depend on the technology of the distributed generators. Large penetration of DG may lead to instability of the voltage profile due to the bidirectional power flows and complicated reactive power equilibrium arising when insufficient control is introduced. The voltage throughout the grid may fluctuate. The situation deteriorates if DG includes variable renewable energy sources. Therefore maintaining the stability of power system is a challenging task after integration of DG and in increased penetration.

2.4.4 Regulatory

Most of the DGs are owned by the customer. Some form of incentive schemes is in existence in many countries in the world for renewable DGs. But surveys indicate that at present situation, the majority of the countries do not have well-defined regulation and security standards. Many countries have no common guidelines for the connection of DG units to the utilities in their region. The rules for connection of DG are defined individually by the local utilities.

2.5 TECHNICAL BENEFITS OF DG

The technical benefits of DG are reliability, flexibility and upgradability, the economy of scale, diversity, and efficiency [126].

2.5.1 Reliability

Sometimes, the customers are affected by way of power failure for a long time due to the grid failure because of the storm, falling tree branches, brownouts etc. DG can localize the impact of these failures and can reduce the number of affected customers.

2.5.2 Flexibility

Big power plants such as hydel, nuclear, renewable etc. are very expensive to build. The payback period of big power plants is very high as compared to small power plants. Hence, to reduce the cost, it is better to build several small plants based on renewable sources adopting the new technologies.

2.5.3 Upgradability

The existing technology adopted in the turbine is not easy for a change. Hence, a new technology-based smaller wind farms can be used in more locations, thereby gradually increasing production without making a major investment in equipment.

2.5.4 Economy of scale

The building cost of large power plants is very high. Therefore small power plant with appropriate technology drives down the cost of mass production.

2.5.5 Diversity

DG allows a variety of power generating technologies which in turn decreases the dependence on any one resource. The strength in diversity lies in the stock portfolios, organizations, and energy.

2.5.6 Efficiency

The transmission loss depends on the distance. As the grid continues to deteriorate, energy demands keep on rising. The corporation focuses on short-term profits and therefore the need for DG increases. Electricity grids in the developed markets expect losses below 15%, but the losses by India's state utilities, over the past five years, were as high as 30% equal to about 1.5% of the country's GDP. The World Resources Institute estimates electricity transmission and distribution (T&D) losses in India to be 27 percent - the highest in the world. The T&D losses occur due to a variety of reasons such as substantial energy sold at low voltage, sparsely distributed loads over large rural areas, inadequate investment in the distribution system, improper billing and high pilferage.

2.6 POTENTIAL BENEFITS OF DG

The implementation of a DG system offers some significant economic benefits as well as imposes source limitations [127]. The various potential benefits are:

2.6.1 Economic

Transmission and distribution (T&D) costs can be dramatically reduced. It is one of the most benefits obtained with the introduction of the additional capacity closer to the consumer [128]-[131].

2.6.2 Environmental

DG promises a reduced fossil fuel consumption and lowers CO_2 emissions [131]-[134].

2.6.3 Social Benefits

Job growth is another potential benefit, and the various estimates suggest that nearly five times as many jobs will be created from investment in DG than for the equivalent level of additional conventional utility capacity. DG offers significant benefits to the developing countries. The development of rural communities serviced by household/community scale renewable sources such as SPV and wind power etc. avoids the prohibitive costs of ambitious transmission based networks [128], [135].

2.6.4 Operational Benefits

Transmission systems are currently operating closes to their stability limits due to the congestion. The network reliability is a major concern in modern power industry [131]. The enhanced operational flexibility of a DG network with the use of custom power devices offers improved power quality, which is a premium commodity for the growing electro-technology intensive commercial sector.

2.7 LIMITATIONS OF DG

Not all of the technologies that can be adopted in a distributed network offer improved performance in air emission. The move to DG sites dispersed throughout the consumer community would also mean that the emissions are released in closer proximity to the local community. The placement of electric generation units within the community could face significant community resistance from poor public perception. One could speculate that public awareness of greenhouse and energy-related issues must be fostered, particularly if the general community is to embrace the need to change

infrastructure and energy use to minimize global warming effects. Land prices for situating units within the consumer community may be prohibitive. However, this should be alleviated to a degree by the compactness of the proposed units.

2.8 APPLICATIONS OF DISTRIBUTED GENERATION SYSTEMS

i. DG can be used to meet or generate a customer's entire electricity supply or for increased reliability.

ii. In some remote locations, DG can be used as a standby or emergency generation.

iii. DG can be used to support the critical loads having very less starting time.

2.9 MEASURES OF RENEWABLE ENERGY

Over the years, RE sector in India especially wind and solar have emerged as an integral part of the grid-connected power generation capacity. It supports the growth of sustainable energy sources to meet the ever-increasing energy needs and acts as an essential player for energy access. It has been realized that RES based systems have to play a much deeper role in achieving energy security and reliability in the years ahead. Hence, it has to be incorporated as an integral part of the future energy planning process [136].

2.9.1 Energy Security:

In the present era, around 69.5 per cent of India's power generation capacity is based on coal. India's increasing dependence on imported oil is leading to the import of around 33 per cent of India's total energy needs. India's coal imports have tripled

since 2010, thus making India, the world's second-largest coal importer after China. On the demand side, the coal is of strategic importance for the country, accounting for 56 per cent of the primary commercial energy supply and 76 per cent of power generation. The coal imports in the financial year 2014-15 were at 212.103 MT, an increase of 27 per cent over the previous year, the provisional coal statistics of 2014-15. The share of electricity generated from coal worldwide declines from 40% in 2012 to 29% in 2040 [137]. Renewable energy sources offer viable option to address the energy security concerns of the country. India has one of the highest potentials for the effective use of renewable energy. India is the world's fifth largest producer of wind power after Denmark, Germany, Spain, and the USA. There is a significant potential in India for generation of power from renewable energy sources such as small hydro, biomass, and solar energy.

2.9.2 Electricity shortages:

Indian power scenario reveals that over the past 62 years even though the increase in installed capacity is more than 110 times, India is still not in a position to meet its peak electricity demand as well as energy requirement. The peak power deficit during the financial year 2001-02 was 12.2 per cent, approximately 9252 MW. However, at the end of the financial year 2014-15, the peak power deficit decreased to the order of 2.4 per cent, and in absolute terms, peak deficit was at 6103 MW. Similarly, the shortage regarding the energy availability was around 7.5 per cent at the end of the financial year 2001-02 (39,187 MU), whereas, at the end of the financial year 2015-16, it was reduced to around 1.8 per cent (89,402 MU). The planned and un-planned load-shedding measures were required to be undertaken by most of the utilities to bridge this demand-supply gap at a fallout situation.

2.9.3 Energy Access:

In any situation, India faces a challenge to ensure availability of reliable and modern forms of energy for all its citizens. Almost 85 per cent of rural households depend on solid fuel for their cooking needs and only 55 per cent of all rural households have access to electricity. However, most of the rural households face issues with quality and consistency of energy supply. Lack of energy access for rural lighting is leading to the large-scale use of kerosene. Such usages need to be reduced because it leads to increased subsidies, importing dependence and consequent pressure on other reserves.

2.9.4 Climate change:

India has taken a voluntary commitment to reducing emission intensity of its GDP by 20-25 percent from 2005 levels by 2020. In recently concluded 20th Conference of the Parties to the United Nations Framework Convention on Climate Change (UNFCCC) held at Lima, Peru, all parties to the Convention were invited to communicate Intended Nationally Determined Contributions (INDCs) towards climate change mitigation. The increased share of RE in the coming years will contribute towards achieving this goal.

2.10 BENEFITS OF WIND POWER AS A DISTRIBUTED RESOURCE

The various surveys reveal that high potential locations are available to harness the wind power than any other renewable source [138].

- No fuel cost
- Renewable and can be tapped

- Environment-friendly and pollution free
- Potential exists to harness wind energy
- Lowest gestation period and capacity addition can be in modular form
- Cost of generation reduces over a period
- Low O&M Costs
- Limited use of land
- Accommodation of other land uses
- Avoid energy losses in T&D lines
- Cleaner, quieter operation — reduced environmental impacts
- Potential to free up transmission assets for increased wheeling capacity
- Greater market independence and consumer choice — empowered customers
- Mitigation of energy price risks - costs are predictable, unlike fossil fuels
- Avoid fuel transportation costs
- Additional capability to meet peak day and night time power demands
- Enhanced power quality and reliability

2.11 LIMITATIONS OF WIND POWER

- low energy density
- Available at selected geographical locations away from cities and load centers
- Variable, irregular, unsteady and erratic
- Turbine design complex

- Large units less capital cost per kWh
- small units are more reliable
- Requires storage batteries-environment pollution

2.12 IMPACTS OF GRID INTEGRATED DG

The use of renewable power generation sources as DGs is increasing rapidly all over the world. Apart from environmental advantages, the DGs result in the reduction of power losses, improvement of bus voltages, increased system reliability, stability, power quality and ease of operation. There are various issues results from the integration of DG with the distribution system and utility grid [125].

2.12.1 Voltage Level

The improper location and coordination of DG results in a rise or drop in the voltage level from the permissible limit. Hence voltage control is an issue when DG is integrated into the distribution grid.

2.12.2 Reactive Power

Most of the DG technologies use induction generators. Even though it is meant for generating active power, it acts as a reactive load and draws more reactive power from the grid. Low power factor in induction machines results in large fault current. It is necessary to use DG with power electronic converters to inject the required amount of reactive power for the distribution line.

2.12.3 Reverse Power Flow

The improper location and increased size of DG may cause power flow from the LV distribution grid to the HV grid. Hence, the system requires well-functioning protection scheme to resist the reverse power flow.

2.12.4 System Frequency

The frequency may deviate from the rated value in the case of an imbalance between electrical energy demand and supply. The system frequency is affected by the increase in the size of DG which leads to grid failure. In this regard, the system operators and regulatory body should take the preliminary steps to avoid such serious issues.

2.12.5 Protection Scheme

When the fault occurs in a DG integrated distribution system, the location of the DG affects the magnitude, duration, and direction of the fault current occurring in a line. Hence, it is necessary to select the appropriate type of relay to protect the entire system.

2.12.6 Islanding Protection

A portion of the utility system containing DGs and some loads remain energized while isolating from the main utility system is called islanding. In such situations, the DG may energize a certain portion of the network which may cause risk to repair the faulty parts of the system. Hence, the suitable protective scheme should be placed to avoid such situations.

2.12.7 Power Quality and Reliability

The improper location and size of DG result in a rise or fall in the voltage level. The deviation in the system frequency due to demand-supply mismatch, injection of harmonics by power electronics based DG are the major issues in DG integrated into the grid system. These issues cause a high degree of PQ problem which results in poor voltage regulation at the customer end. CPDs can be adopted to mitigate the PQ problem.

2.13 GRID CODE OVERVIEW

In recent years, more and larger wind farms have been connected to the transmission networks. Each of these network levels has specific requirements when connecting to wind power generation units. The connection issues for the network are related to grid stability which is influenced by power flows and wind farm behavior in the case of network faults. Grid operators (transmission, distribution) develop rules or grid codes (GC) for connecting generators. This GC aims to ensure that wind farms do not adversely affect the power system operation concerning the security of supply, reliability, and PQ [121][139]. Essential grid code requirements are related to frequency, voltage and wind turbine behavior in case of grid faults. The most common requirement concerns:

- *Active power control*: Several grid codes (GCs) require the active control of the wind farm output power to participate in the energy dispatch as conventional power plants and prevent overloading of lines.

- *Frequency control*: Some GCs require wind turbine types (WTs) to participate in the frequency control as conventional power plants. The frequency is kept within acceptable limits to ensure the security of supply, prevent the overloading of electric equipment and fulfill the power quality standards.

- *Frequency and voltage ranges*: Range of voltage amplitude and frequency are provided for the continued operation in case the system is in trouble (i.e., voltage and frequency stability problems).

- *Voltage control*: Some GCs require WTs to perform the voltage control as in conventional power plants. This is performed by controlling the reactive power.

- *Voltage quality:* A whole set of different requirements are included in national GCs concerning rapid changes, flicker, and harmonics.

- *Tap-changing transformers*: Some grid codes require that wind farms are equipped with tap-changing grid transformer to vary the voltage ratio between the wind farm and the grid when needed.

- *Fault ride-through capability:* Some GCs require WTs to remain connected and, in some cases, to support the power system by injecting the sufficed reactive power to ensure the system stability.

- *Wind farm modeling and verification*: Some GCs require wind farm owners/developers to provide models and system data, to enable the transmission system operator to investigate the interaction between the wind farm and the power system through simulations. They also require the installation of monitoring equipment to verify the actual behavior of the farm during faults and to check the model.

- *Communications and external control:* Most GCs require that the wind farm operator provide an on-line measurement of some important variables for the system operator to enable proper operation of the power system (i.e., voltage, active and reactive power, operating status and wind speed). Only in few cases especially in Denmark, it is required to connect and disconnect the wind turbines externally.

The application of custom power devices such as DVR and the D-STATCOM is proposed as an effective way for improving the fault ride-through capability of wind turbines connected to the grid. These devices allow the compensation of voltage dips at the wind farm side of the coupling transformer (DVR) or helping the wind turbine to withstand the dip (D-STATCOM) by controlling the active and reactive power injected to the grid.

Traditionally, wind turbines are disconnected from the grid when an abnormal grid voltage occurs at the wind farm terminals. In some areas, the concentration of wind turbines is getting so high that it is not possible to disconnect an entire wind farm without affecting the system stability. Electrical utilities and system operator have specified in their recent requirements that wind turbines have to offer ride-through capability under severe voltage dips. Instead of disconnecting from the grid under fault conditions, wind turbines should be able to follow the characteristic shown in Fig 2.1. When the grid voltage goes below the curve, then only the turbine is allowed to be disconnected. In any other case, the turbine should remain connected to the grid without consuming active or reactive power during the disturbance.

If wind farms are unable to withstand voltage drops for a limited time, they will be disconnected from the system. This may cause a cascading voltage fall and the break-down of part or all in the power system. To contribute to the system stability, it is necessary that the wind turbine restores to the normal operation. A solution to this problem is to use a CPD such as D-STATCOM, DVR, etc.

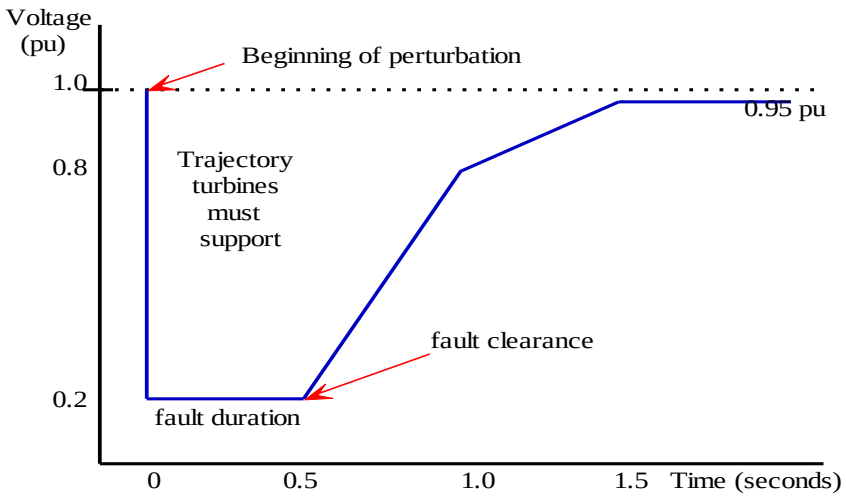

Fig 2.1: Voltage time curve during fault condition

2.14 INDIAN GRID CODES

Special technical requirements for connectivity of renewable energy generating station to the grid are [140]:

1. A generating station of renewable sources can be connected at the distribution level (below 33 kV) or transmission level (at or above 33 kV) of the state depending upon policies of the State Electricity Regulatory Commissions. A generating station of renewable sources can also be connected to the inter-state transmission system (ISTS).

2. Wind farms shall have the ability to limit the active power output at the grid connection point as per system operator's request.

3. The grid-connected wind farms shall have the ramp up/ramp down capability.

4. The reactive compensation system of wind farms shall be such that wind farms shall maintain power factor between 0.95 lagging and 0.95 leading at the connection point.

5. The wind generating machines shall be equipped with fault ride through capability.

6. Wind turbine generator protection:

    a. All the grid-connected wind farms must have protection systems to protect the wind farm equipment as well as the grid, such that no part system shall remain unprotected during faults.

    b. The protection co-ordination for the wind farms shall be done by the SEB/STU and RPC.

    c. The following are the minimum protection schemes that shall be installed for wind farm protection:

        i) Under/over voltage protection

        ii) Under/over frequency protection

iii) Over current and earth fault protection

iv) Load unbalance (negative sequence) protection

v) differential protection for the grid connecting the transformer

vi) Capacitor bank protection

vii) Tele-protection channels (for use with distance protection) between the grid connection point circuit breaker and user connection point circuit breaker

7. Wind farms shall have communication channel which is continuously available to the system operator.

8. Data Acquisition System facility shall be provided for transfer of information to the concerned SLDC and RLDC

9. Lightning protection of WTG system shall be according to IEC TR 61400-24 "Wind turbine generator systems – Part 24: Lightning protection."

10. Wind turbine grounding systems shall follow the recommendations of IEC TR 61400-24 (section 9).

11. The grid connecting transformer configuration shall be designed to provide:

i) A favorable circuit to block the transmission of harmonic currents.

ii) Isolation of transmission system side and wind farm side ground fault current contributions

2.15 SUMMARY

Integration of RES based distributed generation in the radial system can make a balance in power generation and customer demand. The different challenges to be

faced by the electrical supply industry in the case of DG integration, are discussed in this chapter. An overview of the technical benefits as well as potential benefits and its limitation are also presented. Wind power shares a major part of the electrical power generated in India. Global installed capacity of renewable energy sources in 2016 is 673GW. Out of which, wind power shares 432.419 GW, and it accounts for 64.25% of the renewable energy sources. DG based wind power becomes competitive or even cheaper than the fossil fuel based power generation. Grid codes are to be followed when renewable energy generating stations are connected to the grid.

CHAPTER 3

POWER QUALITY ISSUES AND MITIGATION MEASURES

3.1 INTRODUCTION

With the ever increasing integration of wind-based DG system and proliferation of power electronic nonlinear loads, there exists a high degree of PQ problems in the distribution systems. When the wind turbine is connected to the grid, it cannot perform voltage control on its own, and it is very sensitive to wind fluctuations [141]. And also, the faults in the power system cause voltage dips at the connection point of the wind turbine. This voltage dip will increase the stator current which leads to the destruction of converters. The only way to avoid the problem is to disconnect the system when the fault occurs and reconnect after the fault is cleared. Wind generators have to cope up with grid disturbances without disconnection, and they should supply active and reactive power after the fault has been cleared.

Due to the ongoing deregulation of the electrical supply industry almost all over the world, supplying reliable power complying appropriate PQ standards, has become a major challenge faced by the electrical utilities. They are mainly concerned about supplying reliable power with proper PQ standards [142]. PQ problems increasingly affect the supply performance to the electricity consumers and power suppliers at all levels of usage. Quality is a relative term often based on customer perception or the degree to which the supplier meets the customer expectations. IEEE standard 1159 defines PQ as "a concept of powering and grounding sensitive equipment to function within its electrical boundaries to extend their efficacy". In other words, the power quality problem is defined as "any power problem manifested in voltage, current or

frequency deviation that results in failure or misoperation of customer equipment" [143]. Hence, "Power Quality" broadly refers to maintaining a nearly sinusoidal voltage and current at rated magnitude and frequency. The issue of power quality problems is not confined to only energy efficiency and environment but more importantly on quality and continuity of supply or power quality and supply quality.

Customers and suppliers have equal responsibility in the mitigation of power quality problems. Public awareness towards the quality of power among different customers gets boosted up with the introduction of deregulation of the electric power system. During the last decade, various power filtering technology such as passive filters, active filters, hybrid filters, etc. have been applied from time to time, for giving a solution to users power quality problems. Lossless passive filters (LC tuned) are widely used to suppress harmonics. Even though it has advantages such as low initial cost and high efficiency, it has some disadvantages like instability, fixed compensation, resonance with supply as well as loads and utility impedance. To overcome these drawbacks, active filters are used in various configurations such as shunt, series, and hybrid. Current based distortion and voltage based distortion are compensated using shunt type filter and series type filter respectively. Hybrid type filter is used to eliminate the higher order harmonics. However, the customers face power disturbance problems since their ratings are very close to the load in typical applications [144].

The PQ problems can be resolved in three ways,

(i) Reducing the power supply disturbances

(ii) Improving the load equipment immunity to disturbances

(iii) Inserting corrective equipment between the electrical supply and the sensitive loads

To increase the reliability of the distribution network and to overcome the above difficulties, the concept of power electronic based corrective device called custom power device are used, and flexible AC transmission device (FACTs) are also used in the transmission system[145]. The custom power devices are preferred for PQ improvement because of the advantage like lower cost, greater flexibility, an increase of system security, etc.

3.2 NEED OF CUSTOM POWER DEVICES

The increase in the use of automated equipment like adjustable speed drives, programmable logic controllers, switching power supplies, arc furnaces, automated production lines are far more vulnerable to disturbances, so that the network comprising of such equipment are mostly affected with PQ issues such as voltage sag, voltage swell, harmonics, etc. The customers require reliability as well as the quality of power for optimal performance of their equipment. Custom power device can be used to compensate PQ issues and maintain voltage stability in the distribution network.

3.3 POWER QUALITY ISSUES

Most of the PQ issues created in power systems are due to the non-linear characteristics of loads and fast switching of PE equipment. The most sophisticated equipments have become intolerant to voltage fluctuations, harmonics, and interruption [118]. Renewable energy based systems are increasingly integrated at the distribution level to meet the increase in load demand, which utilizes PE converters for grid integration. The PQ issues can be detected from one of the following several symptoms depending on the type of problem involved.

i) Lamp flicker

ii) Frequent blackouts

iii) Sensitive-equipment frequent dropouts

iv) Ground problem

v) Locations

vi) Communication interference

vii) Overheated elements and equipment.

PQ issues encompass a wide range of disturbances such as voltage sags/swells, flicker, harmonics distortion, impulse transient and interruptions.

i) Voltage dip: A voltage dip is used to refer to a short-term reduction in voltage of less than half a second.

ii) Voltage sag: Voltage sag can occur at any instant of time with amplitudes ranging from 10 – 90% and a duration lasting for half a cycle to one minute.

iii) Voltage swell: Voltage swell is defined as an increase in rms voltage or current at power frequency for durations from 0.5 cycles to 1 min.

iv) Voltage 'spikes', 'impulses' or 'surges': These are the terms used to describe the abrupt very brief increase in voltage value.

v) Voltage transients: They are temporary undesirable voltages that appear on the power supply line. Transients are high over-voltage disturbances (up to 20KV) that last for a very short time.

vi) Harmonics: The fundamental frequency of the AC electric power distribution system is 50 Hz. A harmonic frequency is any sinusoidal frequency which is a multiple of the fundamental frequency. Harmonic frequencies can be even or odd multiples of the sinusoidal fundamental frequency.

vii) Flickers: Visual irritation and introduction of many harmonic components in the supply power and their associated ill effects.

viii) Notch: A switching disturbance of the normal power voltage waveform, lasting less than 0.5 cycles, which is initially of opposite polarity than the waveform and is thus subtracted from the normal waveform regarding the peak value of the disturbance voltage.

3.4 VOLTAGE SAG

The most common recurrent power quality disturbance in the distribution system is the voltage sag which is a momentary decrease in rms voltage magnitude in the range of 0.1 to 0.9 per unit (pu). Due to power loss occurring in the distribution network, the actual voltage available at the consumer end gets reduced. As the length of distribution line increases, the problem gets aggravates and the resulting low voltage can affect the working of equipment connected at the user end. Voltage sag occurs mostly due to system faults, drastic change of heavy loads, starting of large motors, etc. The increase in the intensity of fault at a point on distribution level may decrease the bus voltage in the entire system or a large part of it [141],[143].

The percentage of voltage sag can be calculated by using the Equation (3.1)

$$\text{Voltage sag} = \frac{V_{ref} - V_{pcc}}{V_{ref}} \times 100\% \qquad (3.1)$$

where, V_{ref} is the reference voltage normally taken as 1 pu and V_{pcc} is the voltage at Point of Common Coupling in pu.

3.5 CUSTOM POWER DEVICES

Several compensating devices are used to mitigate/improve the voltage sag and voltage swell. Such devices can be placed at three different parts in the distribution systems:

i. Utilities
ii. Customers
iii. Equipment

The custom power devices are divided into two groups [146].

- Network Reconfiguring type
  - Solid State Current limiter (SSCL)
  - Solid State Circuit Breaker (SSCB)
  - Solid State Transfer Switch (SSTS)

This category does not contain dc energy storage sources which play the role of ordinary circuit breakers. The advantage of these static key switches over conventional mechanical switches is their high switching speed. Among these devices, the most widely used type is the solid state transfer switches (SSTS) which are usually located to back up sensitive loads in addition to the primary feeder and secondary feeder.

- Compensating types
  - Distribution Static Compensator (D-STATCOM)
  - Dynamic Voltage Restorer (DVR)
  - Unified Power Quality Conditioner (UPQC)

These types of devices need dc energy storage sources that may be employed in applications such as compensating active and reactive power, eliminating harmonics and compensating for the unbalanced voltage, etc. The various issues such as sag, swell, harmonics, power flow control, etc. are to be improved to a great extent with the help of power electronic based voltage source inverter. It can be connected to the system in series (DVR), parallel (D-STATCOM) or both (UPQC)[147].

3.6 CONVERTER TOPOLOGY OF CUSTOM POWER DEVICES

The selection of compensating or custom power device is based on the application for which it is used. The compensation method is classified into three.

3.6.1 Current Based Compensation

The current based compensation is applied at which the current has to be injected. For this purpose, the power electronics based shunt device named D-STATCOM is connected at the customer side. It is widely used for power factor correction, reactive power compensation, and load balancing/load compensation when connected to the load. It can also perform voltage regulation, mitigation of voltage sag/swell, voltage dip, voltage flicker and voltage fluctuations, when connected to a distribution bus.

3.6.2 Voltage-Based Compensation

For voltage-based compensation, the voltage is injected to balance the source and load voltage. A series device named DVR is used for this purpose. It is used for the harmonic compensation, improving voltage regulation, voltage balancing, voltage flicker reduction, and removing voltage sags, swells, and dips. Apart from voltage harmonic compensation, DVR finds its application for reactive power compensation, voltage regulation, mitigation of voltage sags/swells, voltage dips and flicker.

3.6.3 Voltage and Current-Based Compensation

Many applications require a combination of both so that a combination of series with shunt device named UPQC forms an ideal choice. In dual control mode of operation,

it is considered as a versatile device, since it can inject both current (shunt) and voltage (series) simultaneously. Apart from the current and voltage based harmonic mitigation, it can perform load compensation/load balancing, reactive power compensation, power factor correction, voltage regulation, mitigation of voltage sag/swells, voltage dip and voltage flicker at the same time [148].

The mitigation techniques chosen for analysis in this project are:

i. Solid State Transfer Switch (SSTS)

ii. Distribution Static Compensator (D-STATCOM) and

iii. Dynamic Voltage Restorer (DVR)

3.7 SOLID STATE TRANSFER SWITCH (SSTS)

One of the effective ways to avoid the overloading at a critical time in the densely populated area is the rescheduling of the load from one feeder to another with the help of Solid State Transfer Switch (SSTS).

The SSTS offers continuity in the electric flow even at a critical peak time and in the case of sensitive loads. It protects the customer loads from the power quality issues by sharing the load at a critical time without service interruption.

3.7.1 Basic Configuration of SSTS

The basic configuration consists of a combination of two feeders, one the main feeder and the other one a backup feeder, connected to a common bus through two SSTS [149]. The sensitive loads are connected to this bus. The SSTS are a parallel combination of two back-to-back connected thyristors as shown in Fig.3.1.

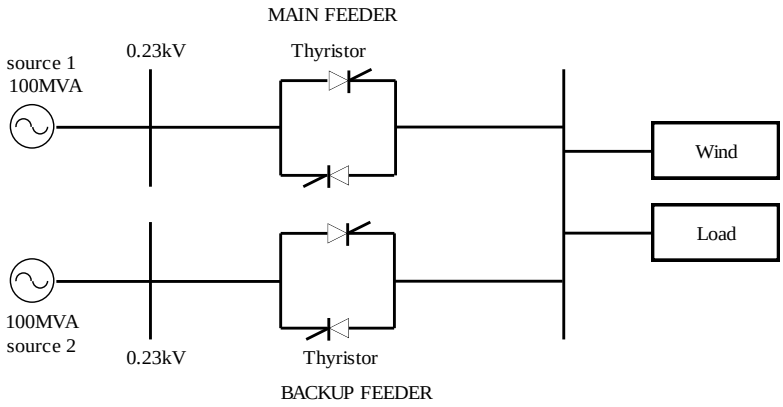

Fig. 3.1: Schematic diagram of SSTS

Under normal operating conditions, the control logic will only trigger the thyristor switch1 connected to the main feeder. At the time of any fault in the main feeder, the control logic triggers the gate signals to switch2 by removing it from switch1 and thereby transferring the load to the backup feeder. It will check whether the peak value of the voltage at every fraction of a cycle is within the prescribed limit. If an abnormal condition is detected, the control logic will give the gate signal accordingly. The control scheme will ensure that the quality of power supply in the healthy feeder by changing the load from faulted feeder to the healthy one. When the fault is cleared, and sufficient voltage is recovered, the only load is transferred back to the healthy feeder through the action of the control logic [150],[151].

3.7.2 Control logic of SSTS

The control logic will monitor the peak value of the voltage waveform every half cycle at the point of common coupling where the load is connected. At the time of fault detection, the control logic will reverse the gate signal from the faulty feeder to the healthy feeder. The maximum value of the voltage is set as 1 pu. It can be seen that the voltage at the faulty feeder is not restored by generating/absorbing reactive

power with the help of SSTS but deactivate the faulty feeder in favor of the healthy one within a fraction of a cycle. With the proper fast action of SSTS control, it provides effective protection to the sensitive loads against the power quality issues.

3.7.3 Applications of SSTS

a. It provides seamless uninterruptable power to customers and also rapid load transfer between independent feeder systems.

b. The ability to transfer seamlessly between feeders where direct interconnection is not allowed enables the device to perform load shedding easily.

3.8 DISTRIBUTION STATIC COMPENSATOR (D-STATCOM)

The main components of CPD are the voltage source converter (VSC), a dc link and a filter circuit. The various issues such as sag, swell, harmonics, power flow control, etc. are to be improved to a great extent with the help of the voltage source inverter. It is connected to the system in parallel for reactive power compensation, voltage regulation and harmonic reduction in distribution network [152],[153]. In the context of sustaining, flexible, low cost, uninterrupted standard power, suitable sensitive equipment such as D-STATCOM is proposed.

3.8.1 Basic Configuration of D- STATCOM

D-STATCOM is basically a controlled reactive source, and the operating principles are based on exact equivalence of the conventional rotating synchronous compensator. A Voltage Source Converter (VSC) is a power electronic device which generates a sinusoidal voltage of required magnitude, phase angle, and frequency to match the source and load voltage. The VSC helps to eliminate the harmonics and fluctuations by injecting the missing voltage between the source and load voltages.

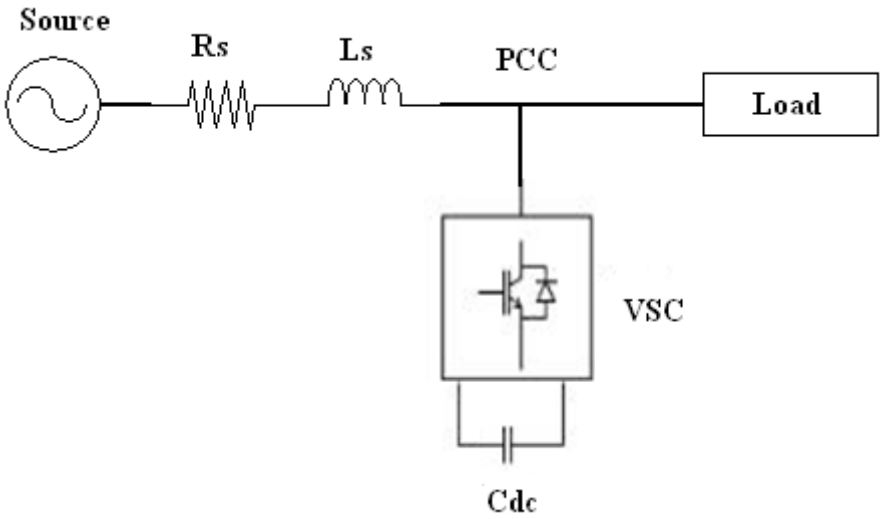

Fig. 3.2: Schematic diagram of D-STATCOM

Figure 3.2 shows the schematic representation of D-STATCOM connected in a distribution system. It shows that VSC is connected to the PCC between source and load through a filter or leakage inductance of the coupling transformer. The reactive energy storage element, a dc capacitor, carries the input ripple current of the converter, which is connected to the input of the converter. This capacitor is either charged by a battery source or recharged by the converter itself. If the output voltage of the VSC, V_c is equal to PCC voltage, V_{pcc} then no reactive power is delivered to the system. If V_c is greater than V_{pcc}, D-STATCOM is in the capacitive mode of operation and if it is less than V_{pcc}, it is in the inductive mode of operation. The amount of reactive power absorbed or injected is proportional to the difference between V_{pcc} and V_c. It is to be noted that voltage regulation at PCC and power factor correction cannot be achieved simultaneously. For a D-STATCOM used for voltage regulation at the PCC, the compensation should be such that the supply currents should lead the supply voltage; whereas, for power factor correction, the supply current should be in phase with the supply voltage.

3.8.2 Applications of D-STATCOM

The various applications of D-STATCOM are listed below [146].

a. To regulate the voltage at PCC in the distribution system.

b. To improve power factor to unity.

c. To mitigate harmonics in the distribution system.

d. For load balancing.

3.9 DYNAMIC VOLTAGE RESTORER (DVR)

DVR is one of the most effective series equipment connected before load in series with the mains using a transformer to compensate the reactive power and to improve voltage regulation [145], [154]. It is smaller in size, low cost and gives a fast dynamic response to the disturbance. Fig. 3.3 shows the schematic diagram of DVR. It consists of a two-level voltage source converter, a DC energy storage device, a coupling transformer connected in series with the ac system and the associated control circuits.

3.9.1 Basic Configuration of DVR

When the source voltage increases or decreases, the DVR injects a series voltage through the transformer so that the desired load voltage magnitude can be maintained [155], [156]. The VSC switching strategy is based on sinusoidal PWM technique. The VSC converts the DC link voltage V_{dc}, on the capacitor to a set of 3-phase ac output

voltages of adjustable magnitude and phase. These voltages are in phase and coupled with the ac system through the reactance of the coupling transformer.

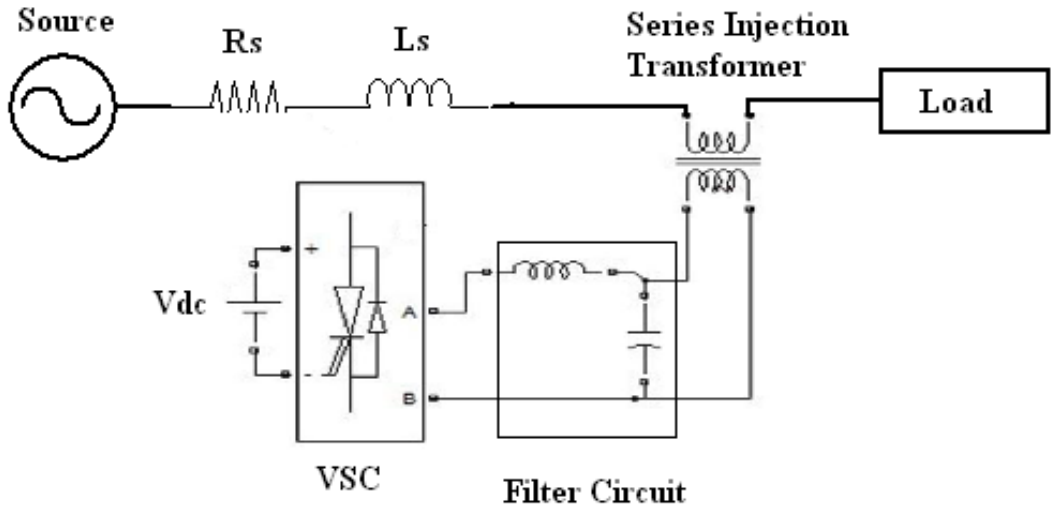

Fig. 3.3: Schematic diagram of DVR

During normal operation, the capacitor receives energy from the main source. When the voltage sag is detected, the capacitor starts to deliver energy to the inverter proportional to the missing voltage. A suitable capacitor size is required to store the energy to mitigate the voltage sag [157].

Adjusting the magnitude and phase of the DVR, the output ac voltage allows the effective control of active and reactive power exchange between DVR and the ac system. For this, a suitable modulation technique has to be used.

3.9.2 Applications of DVR

a. To protect against sags to 50% for durations of up to 0.1 seconds.

b. To mitigate the damaging effects of voltage swells, voltage unbalance and other waveform distortions.

3.10 CONTROL STRATEGY OF D-STATCOM AND DVR

Two basic control strategies of DVR are in-phase compensation and minimum energy injection strategy [158]. In in-phase compensation, during voltage sag condition, the injected voltage is in the same phase with that of the supply voltage. During swell condition, the injected voltage will be in quadrature with the supply voltage. The main advantage of this technique is that the magnitude of the injected voltage is minimum.

The custom power devices DVR and D-STATCOM consists of two-level voltage source converter (VSC), dc energy storage device, coupling transformer connected in series or shunt at the load end and the associated control circuits. The VSC switching strategy is based on sinusoidal PWM [159], [160].

The control system measures only the rms voltage at the load [121], but no reactive power measurement is required. The VSC switching strategy is based on a sinusoidal PWM technique which offers simplicity and good response. Since custom power is a relatively low-power application, PWM methods offer a more flexible option than the fundamental frequency switching (FFS) methods favored in FACTS applications. Besides, high switching frequencies can be used to improve the efficiency of the converter without incurring significant switching losses.

The VSC converts the DC link voltage V_{dc} on the capacitor to a set of 3-phase ac output voltages of adjustable magnitude and phase. These voltages are in phase in DVR and out of phase in D-STATCOM, coupled with the ac system through the

reactance of the coupling transformer. In both DVR and D-STATCOM, dc capacitor delivers/absorbs energy to the inverter proportional to the missing voltage [147][161].

Adjusting the magnitude and phase of the DVR or D-STATCOM, output ac voltage allows the effective control of active and reactive power exchange between converter and ac system. For this, suitable modulation technique such as sinusoidal pulse width modulation is used. The control scheme is used to maintain constant voltage magnitude at the load point under fault condition [160]. If V_c is the inverter voltage, V_{pcc} is the voltage at the load point and δ is the angle of V_{pcc} wrt V_c, then,

Active power

$$P = \frac{V_{pcc} \times V_c}{X} \operatorname{Sin} \delta \tag{3.2}$$

Reactive power

$$Q = \frac{V_{pcc} \left(V_{pcc} - V_c \operatorname{Cos} \delta \right)}{X} \tag{3.3}$$

If V_{pcc} less than or greater than V_c, then the error signal is obtained by comparing reference voltage V_{ref} (normally taken as 1pu) and rms value of V_{pcc}. This error signal is processed by PI controller shown in Fig.3.4 to generate the required angle δ to drive the error to zero. Then V_{pcc} is brought back to the reference voltage, V_{ref}.

If $V_{pcc} \sim V_c$ is positive, then the current flows from the ac system to the converter. The converter thereby absorbs the voltage equal to the difference between V_{pcc} and V_c or

absorbs the inductive reactive power thereby the capacitor is charged. In D-STATCOM, if $V_{pcc} \sim V_c$ is negative, then the current flows from the converter to the ac system. The reactive power flows from the converter to ac system by injecting the current. If $V_{pcc} \sim V_c$ is zero, then there is no exchange of reactive power. As long as the injected current maintains the in phase quadrature relationship with the line voltage, the converter supplies or consumes the reactive power. Any other relationship causes the flow of active power as well. But in DVR, if $V_{pcc} \sim V_c$,then the missing voltage is injected by DVR which is in phase with the ac voltage.

Figure 3.4 shows the controller scheme implemented in PSCAD/EMTDC for DVR and D-STATCOM. An error signal is obtained by comparing the reference voltage V_{ref} with the PCC voltage, V_{pcc}, then V_{in} is measured at the load point. An advantage of a proportional plus integral controller is that its integral term causes the steady-state error to be zero for a step input.

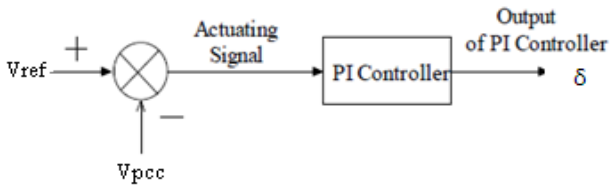

Fig. 3.4: Schematic diagram of a typical PI Controller

The PI controller processes the error signal and generates the required angle δ to drive the error to zero. Then the rms load voltage is brought back to the reference voltage. In PWM control, the converter switches are turned on and off several times during a half cycle. The modulated angle δ is applied to the PWM generators in phase A as shown in equation (3.3). The angles for phases B and C are shifted by

120^o and 240^o respectively as given in equations (3.4) and (3.5). In this PI controller, only the voltage magnitude is taken as a feedback parameter in the control scheme.

The sinusoidal signal $V_{control}$ is phase-modulated e mploying the angle and the modulated three-phase voltages are given by

$$V_a = \mathrm{Sin}\left(\omega t + \delta\right) \tag{3.4}$$

$$V_b = \mathrm{Sin}\left(\omega t + \delta - \frac{2\pi}{3}\right) \tag{3.5}$$

$$V_c = \mathrm{Sin}\left(\omega t + \delta + \frac{2\pi}{3}\right) \tag{3.6}$$

The modulated signal $V_{control}$ is compared with a triangular (carrier signal) signal, $V_{carrier}$ to generate switching signals for the VSC. The exchange of reactive power between the ac system and VSC can be controlled by varying the magnitude of VSC [160], [153].

Amplitude modulation index m_a of the signal $V_{control}$ is taken as 1pu to obtain highest fundamental voltage component at the control output.

$$m_a = \frac{V_{control}}{V_{carrier}} = 1pu \tag{3.7}$$

The frequency modulation m_f is taken as 9 by selecting switching frequency as 450Hz.

$$m_f = \frac{f_s}{f_1} = \frac{450}{50} = 9 \tag{3.8}$$

3.10.1 Advantages of PWM based switching power converter

i. Easy to implement and control
ii. Compatible with today's digital microprocessors
iii. Lower power dissipation
iv. It allows linear amplitude control of the output voltage/current

3.10.2 Disadvantages of PWM based switching power converter

i. Attenuation of fundamental component of PWM waveform
ii. Drastically increased switching frequencies
iii. Generation of high-frequency harmonic components

The major concerns of PWM technique in this analysis are

a. Low switching losses
b. Good utilization of DC power supply to give a higher output voltage
c. Good linearity in voltage/current control [153]

3.11 SUMMARY

Power quality issues are a major problem faced by the electrical power supply industry. The ultimate goal of EES is to provide good quality of reliable power to the end users. But in the radial network, the increased use of DG, as well as nonlinear loads, makes a high degree of PQ problem. Proper placement of custom power devices is a viable solution to mitigate the PQ issues. Different types of CPDs used in distribution network are discussed in this chapter.

Chapter 4

IMPACT OF CPDS IN DG INTEGRATED NORMAL DISTRIBUTION TEST SYSTEM

4.1 INTRODUCTION

Energy demand in agriculture, industrial, commercial and household sectors has increased tremendously and has placed enormous pressure in search for other alternatives [118]. Depleting resources and increasing pollution of environment due to energy use have necessitated the optimum use of its resources, which in turn requires proper energy planning to achieve energy security. There exists a wide gap between the supply and demand of crude oil in India leading to increased dependence on the imports. The Energy Policy pursued in the country encourages the promotion of RES, particularly wind and SPV based system to reduce the import of fossil fuels.

The most common type of PQ disturbance like voltage sag and voltage swell is the crucial problem faced by the ESI with the improper integration of RE sources. The PQ issues can be solved by the use of PE devices like D-STATCOM, DVR, UPQC etc. connected to the load [141]-[143], [162]. In the normal radial system, the effects of the wind farm as well as the effectiveness of CPDs in voltage sag mitigation under different fault conditions are discussed in this chapter.

4.2 DISTRIBUTION TEST SYSTEM

In this work, normal distribution test system is taken for PQ analysis. System parameters of the test system are shown in Table 4.1 and its schematic diagram is shown in Fig. 4.1. It is represented by its Thevenin's equivalent, feeding into the primary side of a 3-winding distribution transformer. Load, wind farm and CPDs are connected to the secondary side of the transformer at PCC.

Simulations are carried out on the test system shown in Fig. 4.1, to show the effectiveness of CPDs in mitigating the voltage sag.

Table 4.1: System parameters of distribution test system

System Parameters	
Power Supply	230 kV, 50 Hz
Transformer	230/11 kV
Load	R= 412.1 Ω and L= 0.1926 H
Feeder resistance	R= 0.1 Ω and L= 0.758 H

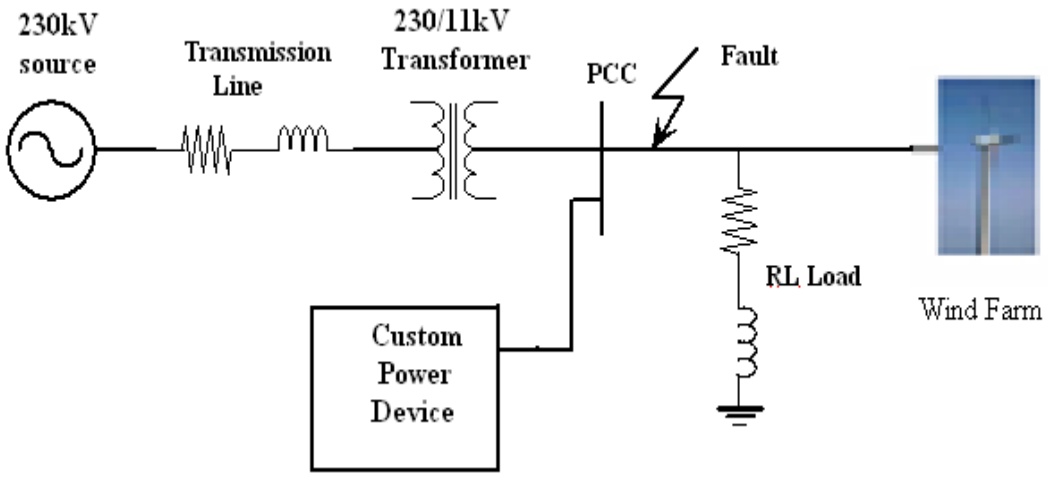

Fig. 4.1: Schematic diagram of CPD in wind integrated normal distribution test system

PQ analysis for the system has been carried out in the following cases:

i. NO fault applied to the test system

ii. Different faults applied to the test system

iii. Sag compensation with DVR

iv. Sag compensation with D-STATCOM

v. Sag compensation with SSTS

4.2.1 Test System with NO fault

Figure 4.2 shows the Thevenin's equivalent circuit of the normal distribution test system implemented in PSCAD. The system consists of voltage source of 23 kV step down to 11 kV using transformer. The linear load is connected at the secondary side of the transformer. The simulation is carried out in the test system without applying any fault. The rms voltage (V_{rms}) at PCC is measured and compared with the reference voltage (V_{ref}). The reference voltage is taken as 1 pu.

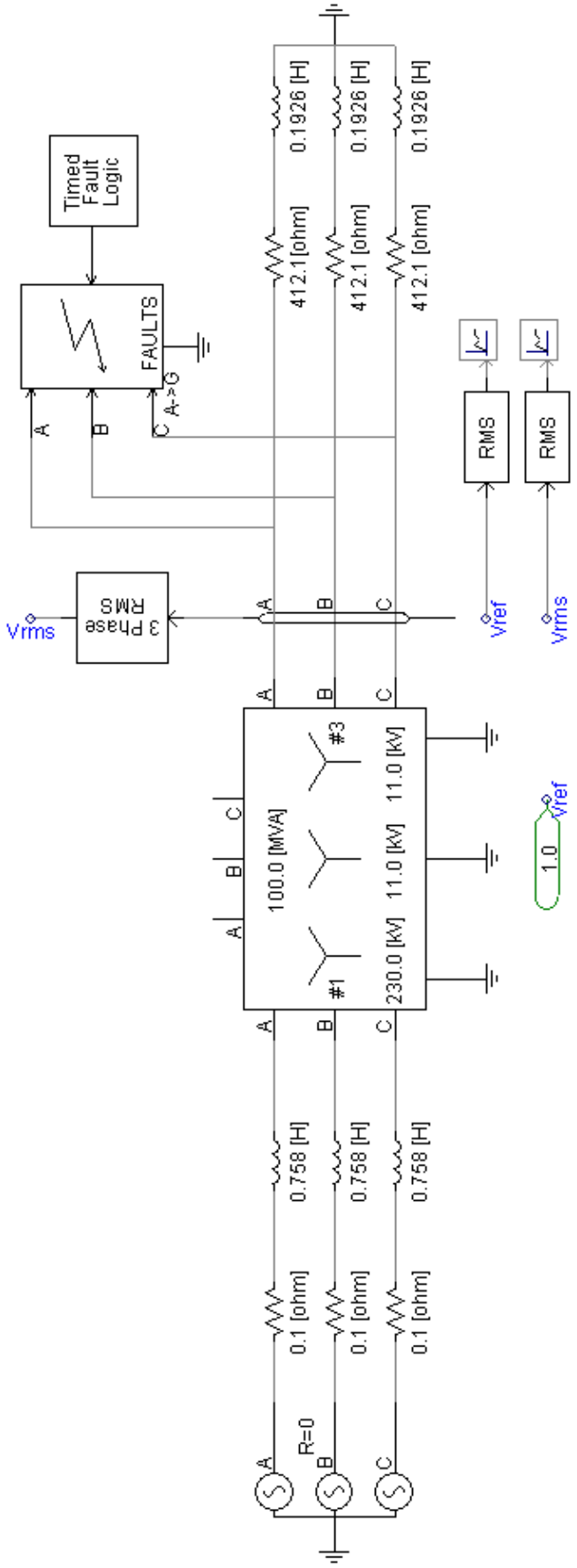

Fig. 4.2: PSCAD model of Thevenin's equivalent of normal distribution test system

Figure 4.3 shows that V_{rms} at PCC in the distribution test system is equal to the reference voltage, V_{ref} .

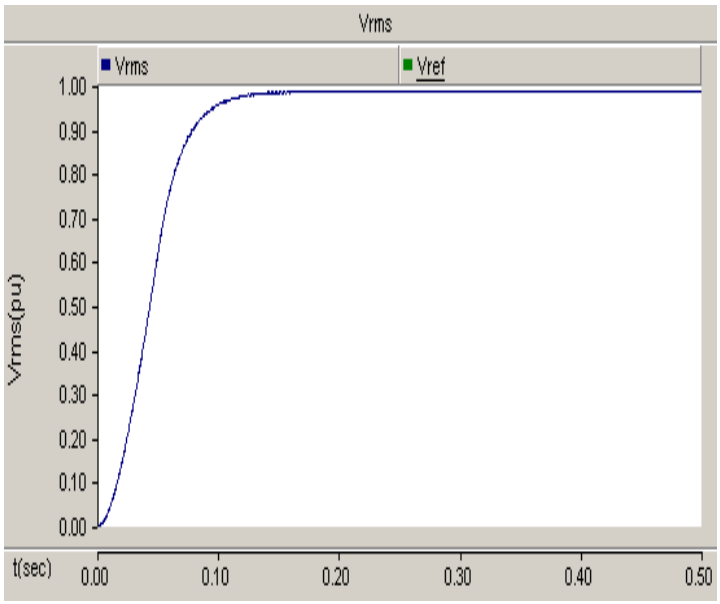

Fig. 4.3: Load voltage at PCC without fault

4.2.2 Test System with different faults

Various faults occurring in the distribution systems are the line to ground fault (LG), line-line to ground fault (LLG), line-line-line to ground fault (LLLG), line-line fault (LL), line-line-line fault (LLL). Most frequently occurring fault is the LG fault and the most severe fault is the LL fault. The simulation is carried out with the test system for which the fault is applied for 0.1 to 0.15 seconds via a fault resistance of 1Ω. Figure 4.4 shows the variation in load voltage, V_{rms} from V_{ref} at PCC. This is referred as voltage sag.

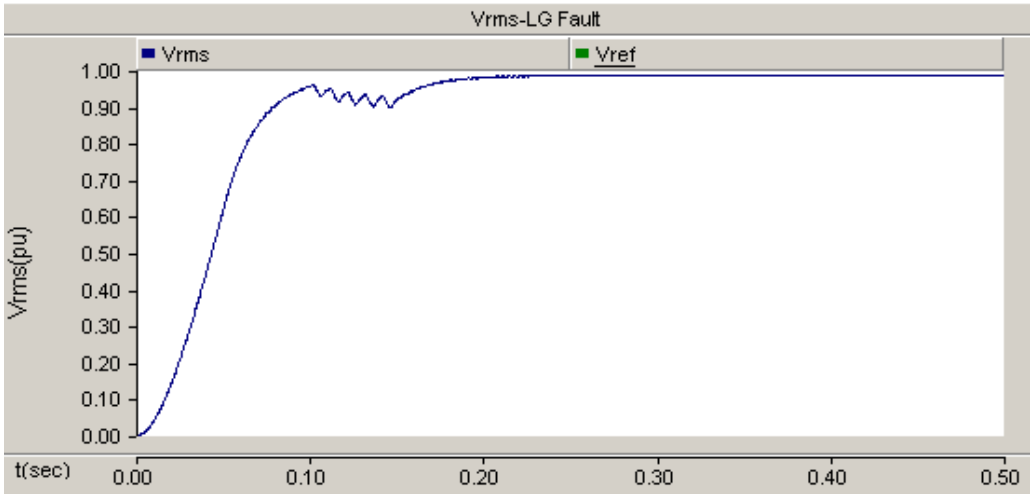

(a) LG fault

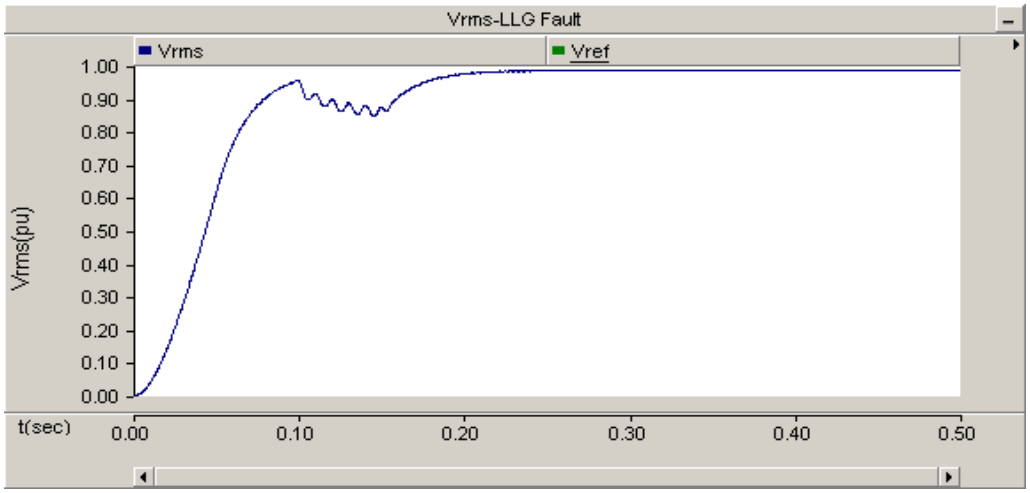

(b) LLG fault

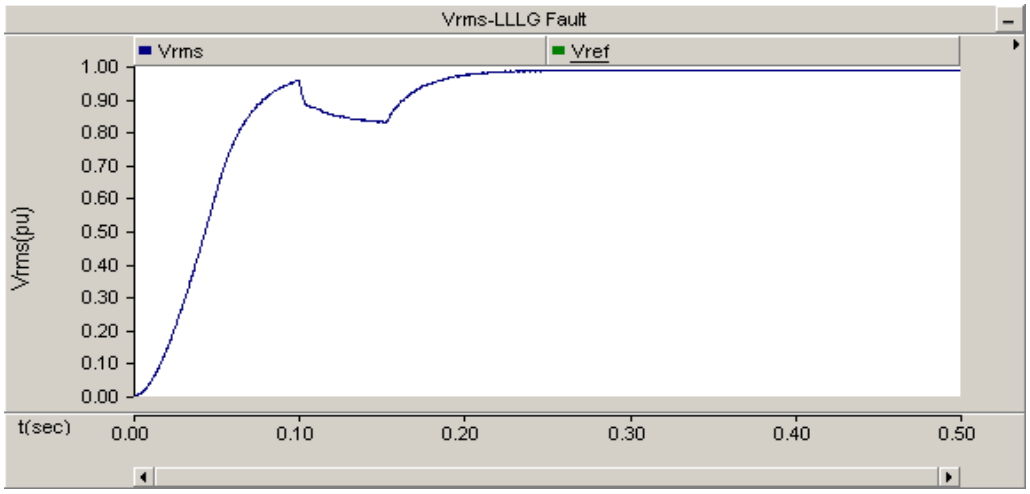

(c) LLLG fault

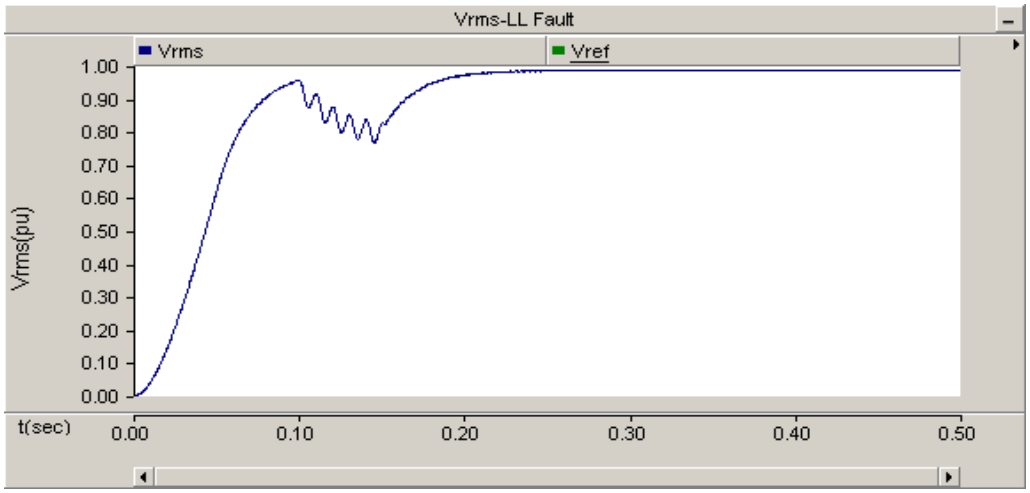

(d) LL fault

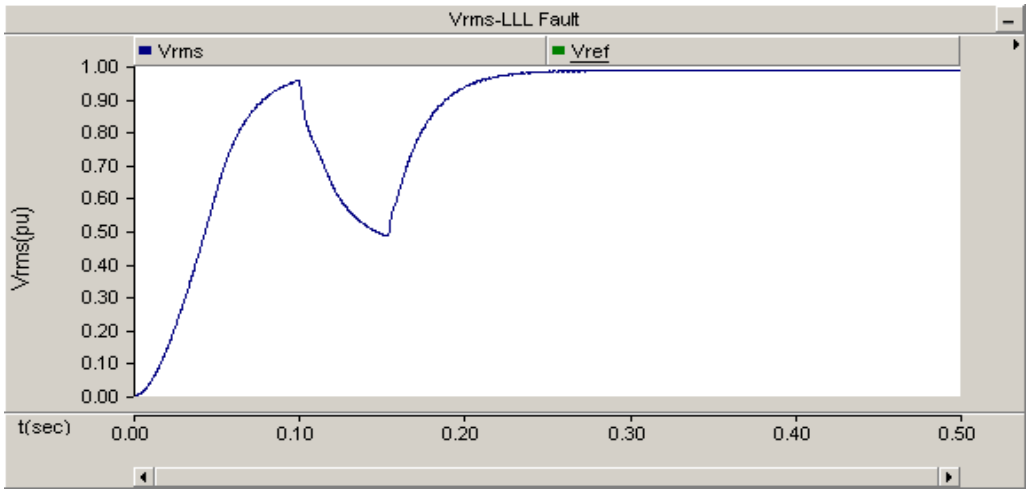

(e) LLL fault

Fig. 4.4: Load voltage at PCC under different fault condition

4.2.3 Test system with DVR

To mitigate the voltage sag, the compensating device, DVR is connected in series with the distribution line. Figures 4.5(a) and (b) show the schematic diagram and PSCAD modeling of test system integrated with DVR and its control logic. In the PSCAD simulation, the DVR will be in operation only during the fault period, analogous to a practical situation. The coupling transformer of DVR is connected in the delta in the DVR side, with a leakage reactance of 10%. The transformer turns ratio of unity was used i.e., no booster capabilities exist. The capacity of the dc storage device is 5 kV. A 750 μF capacitor on the dc side provides the DVR energy storage capability.

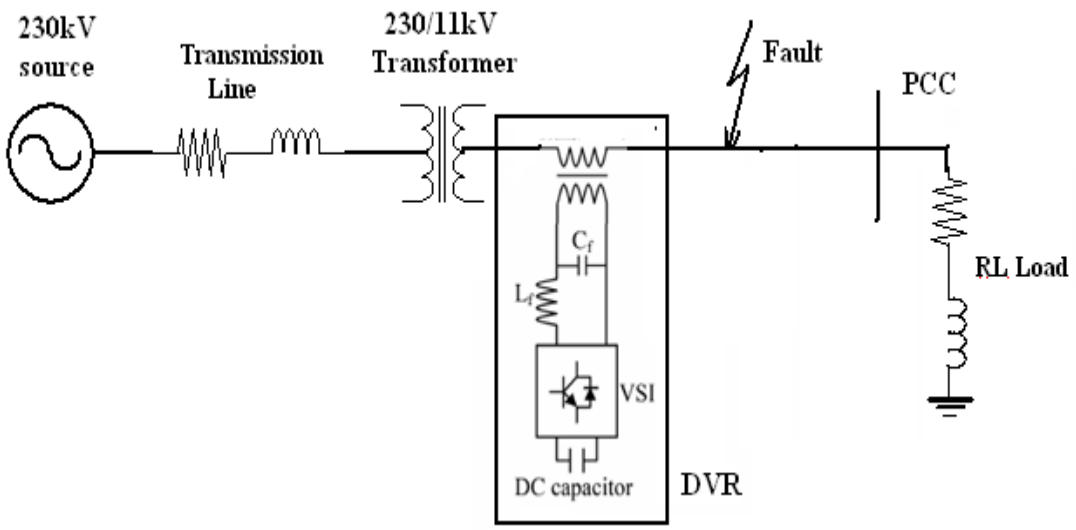

Fig. 4.5 (a): Schematic diagram of normal distribution test system integrated with DVR

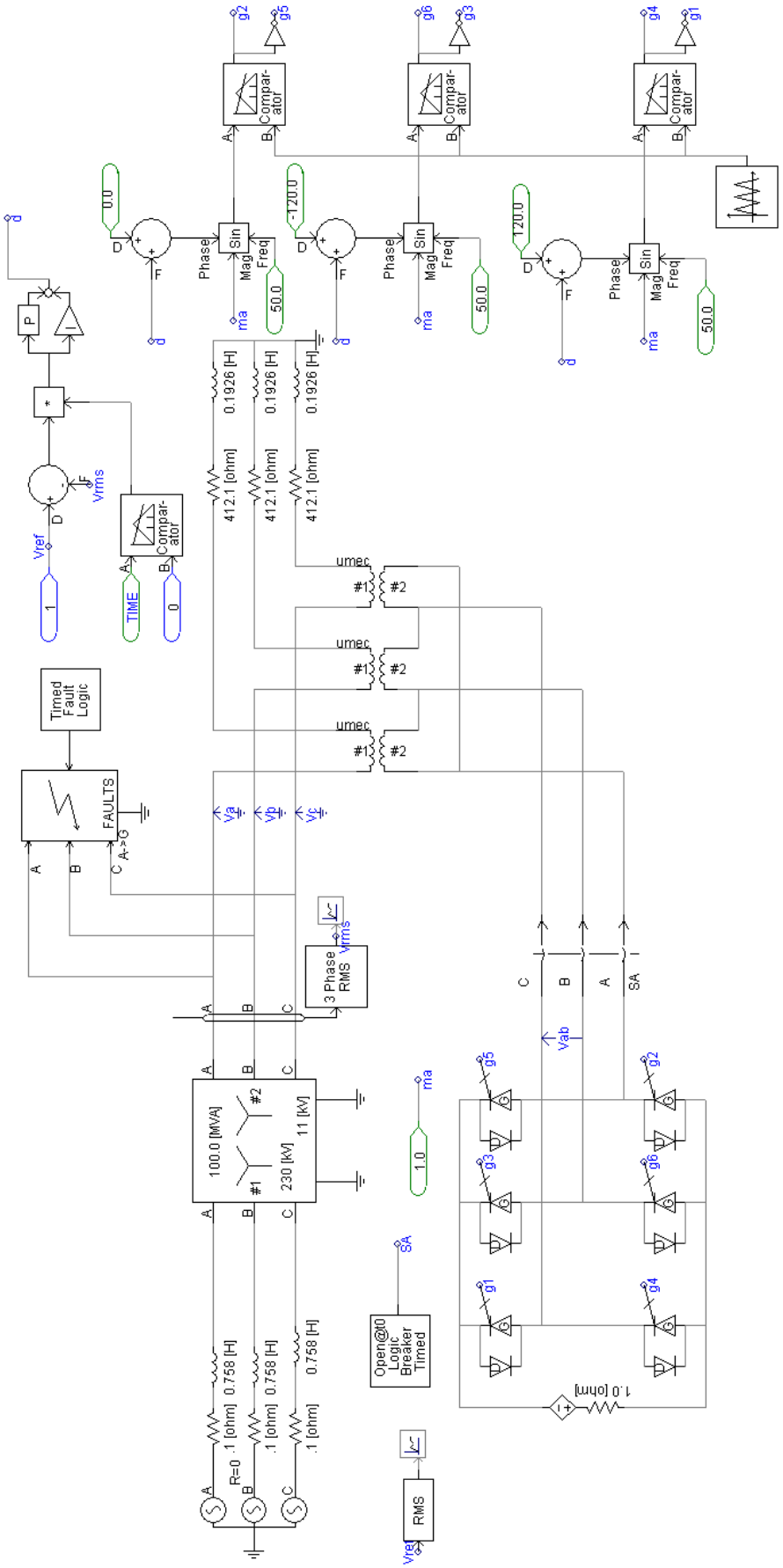

Fig. 4.5 (b): PSCAD model of normal distribution test system integrated with DVR

From Fig. 4.6, it is observed that the PCC voltage is improved from 0.901 pu to 0.995 pu with the help of DVR under LG fault condition.

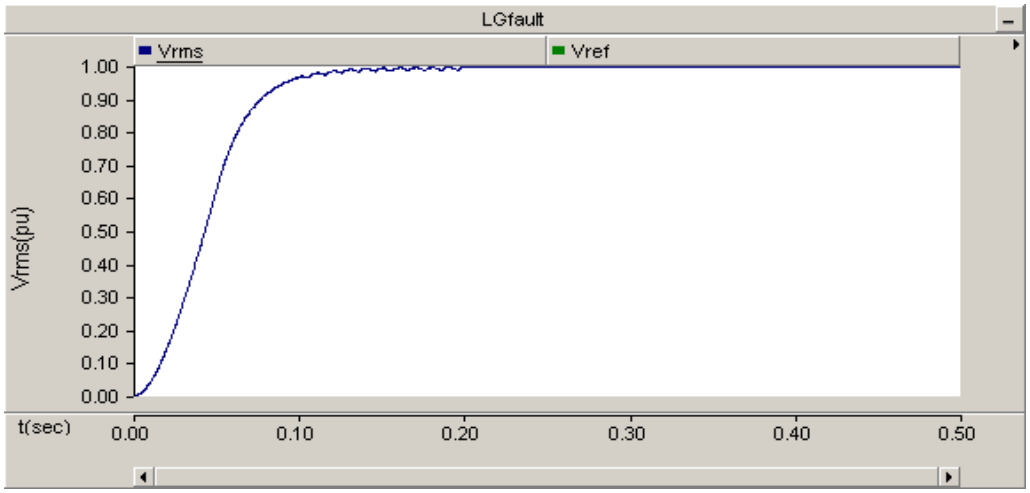

(a) LG fault

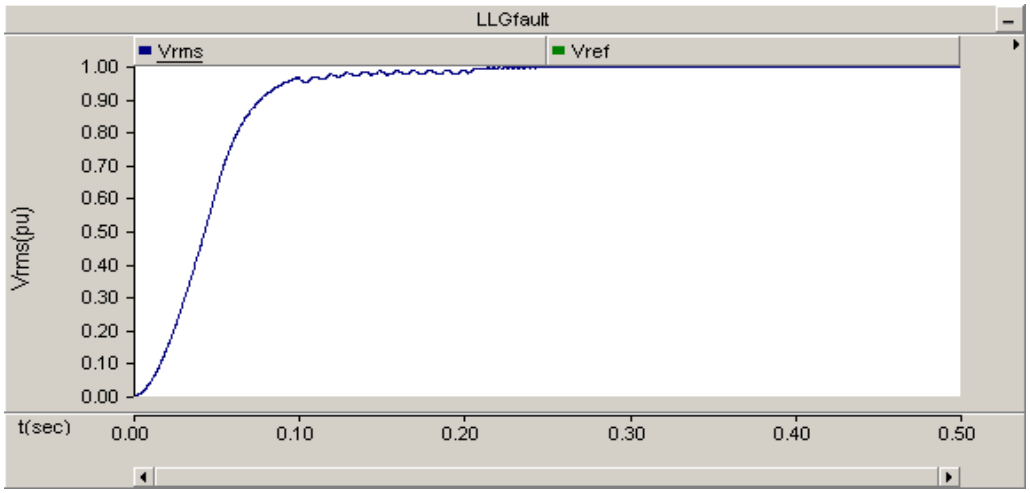

(b) LLG fault

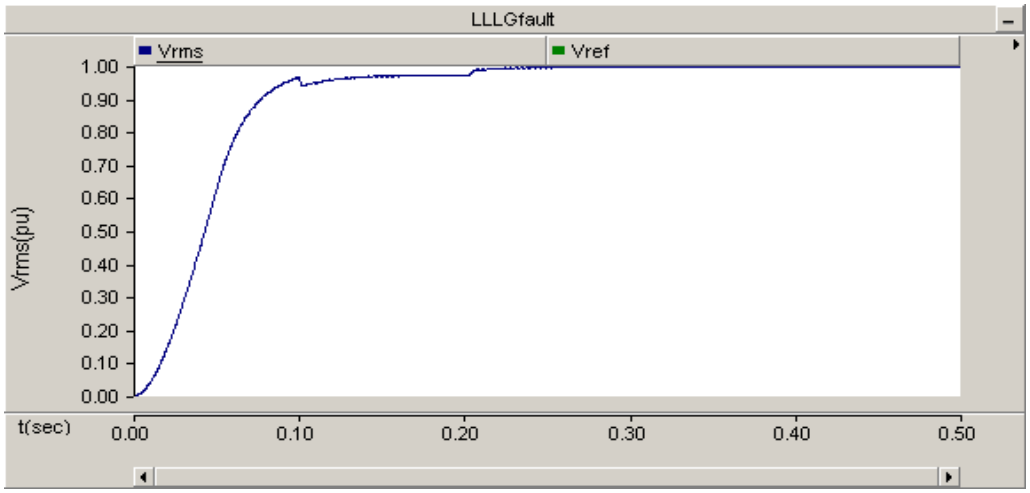

(c) LLLG fault

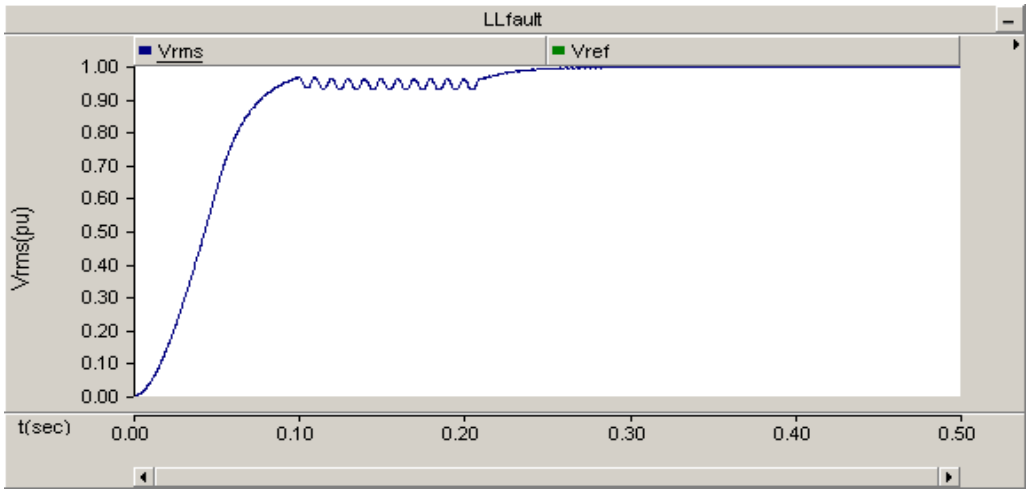

(d) LL fault

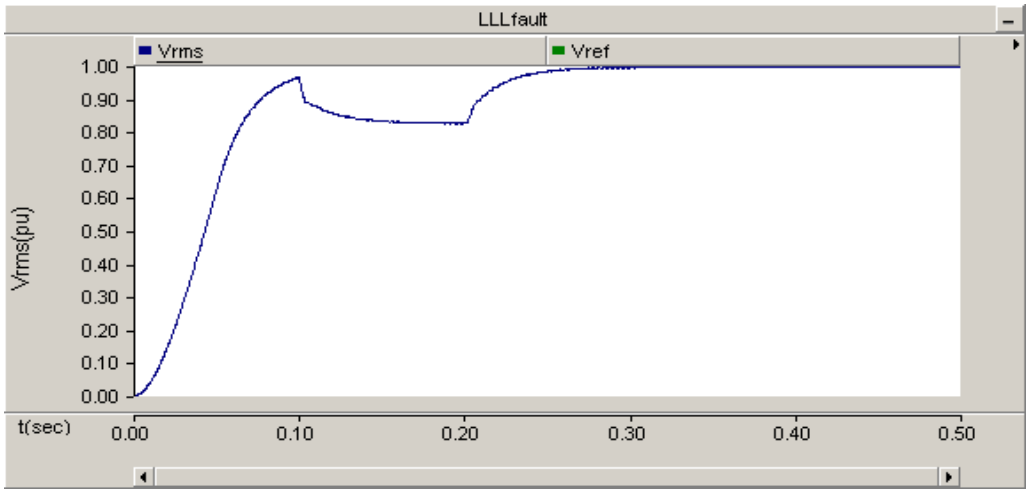

(e) LLL fault

Fig. 4.6: Recovered voltage at PCC under different fault condition with DVR

4.2.4 Test System with D-STATCOM

To study the mitigation of the voltage sag, simulation is carried out with the use of D-STATCOM connected in parallel with the distribution line. The schematic diagram and PSCAD model of normal distribution test system integrated with D-STATCOM are shown in Fig. 4.7 (a) and (b). A two-level D-STATCOM is connected to the 11 kV tertiary winding to provide instantaneous voltage support at the load point. A 750 μF capacitor on the dc side provides the D-STATCOM energy storage capabilities.

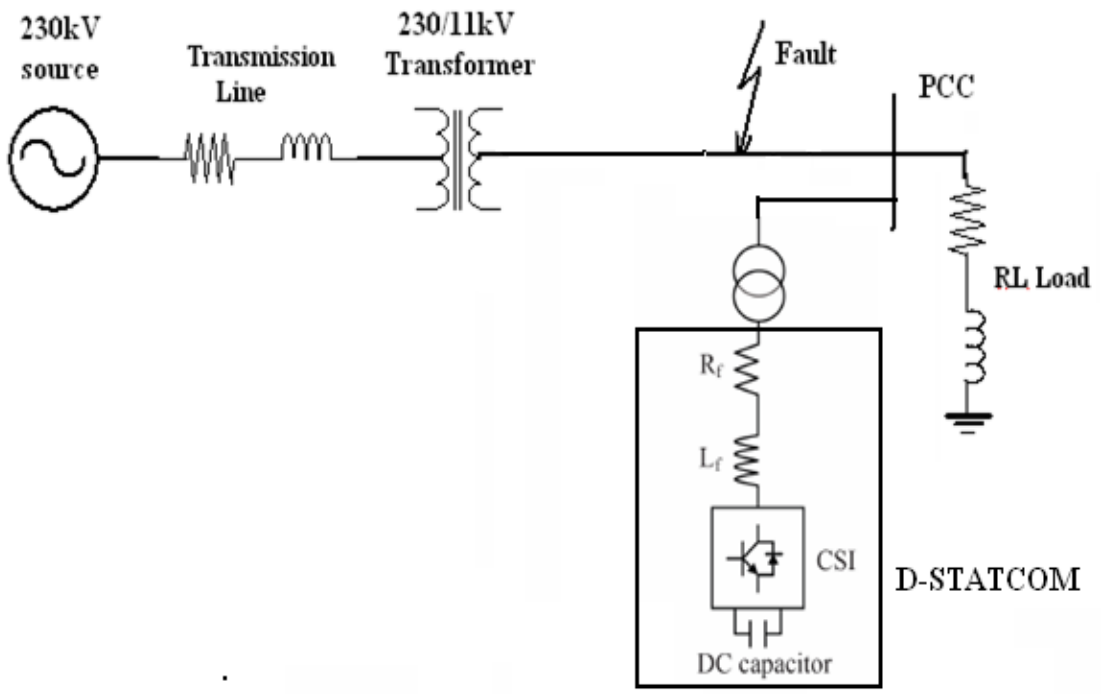

Fig. 4.7 (a): Schematic diagram of normal distribution test system integrated with D-STATCOM

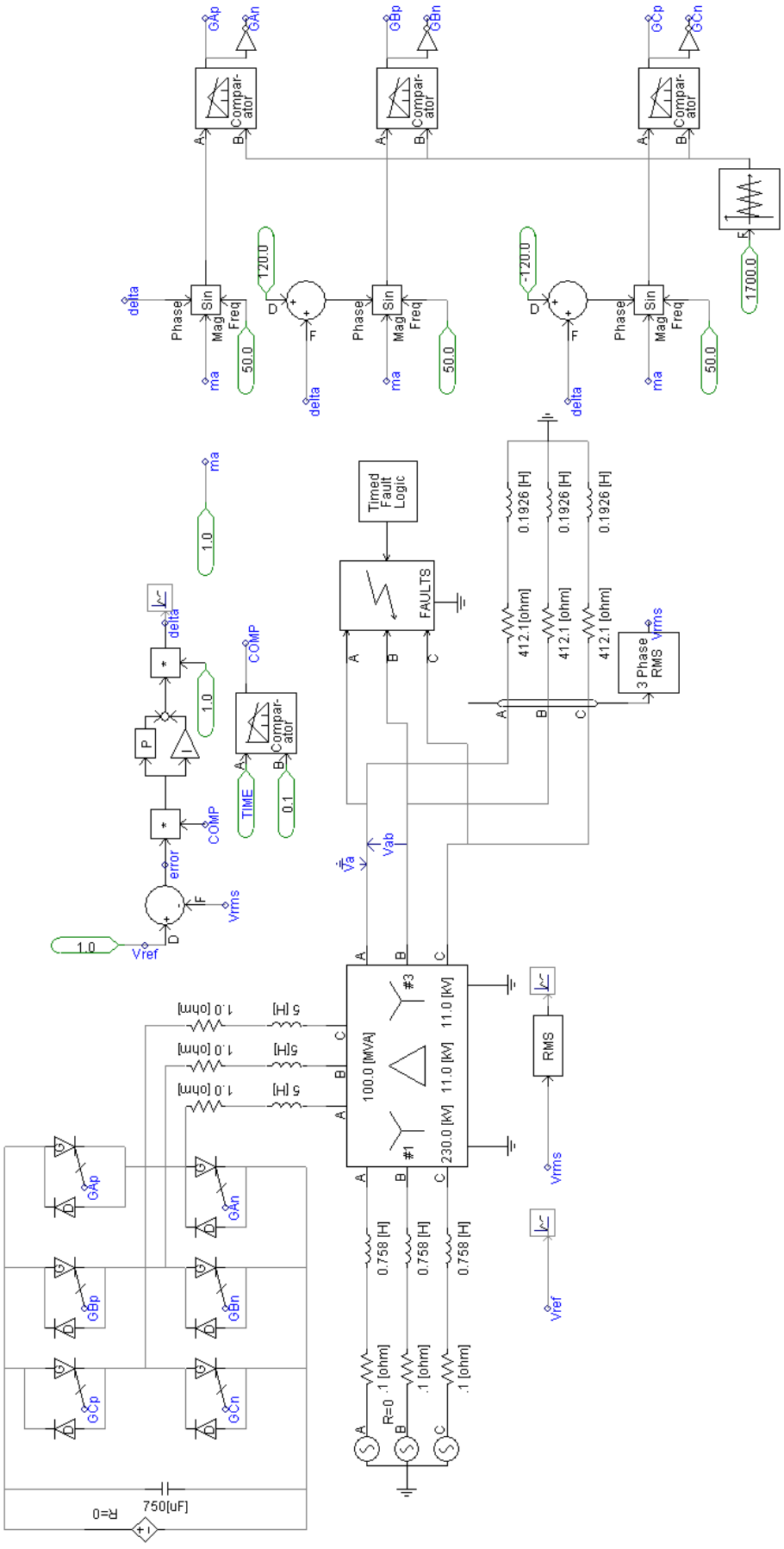

Fig. 4.7 (b): PSCAD model of normal distribution test system integrated with D-STATCOM

D-STATCOM is expected to be in operation only at the moment of occurrence of the fault. In a practical situation, during LG fault, the voltage sag is 0.901 pu which is improved to 0.996 pu with the use of D-STATCOM is shown in Fig.4.8. With the reactive power compensating property of D-STATCOM, the PCC voltage is recovered to nearly V_{ref} under this fault. The PWM technique controls the magnitude and the phase of injected or absorbed voltage provided by VSC to restore the rms voltage at the load point very effectively.

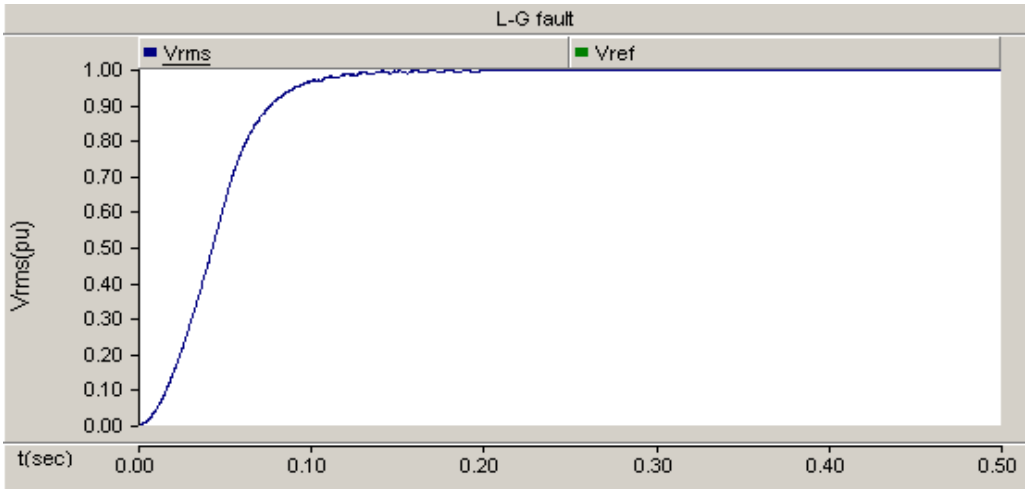

(a) LG fault

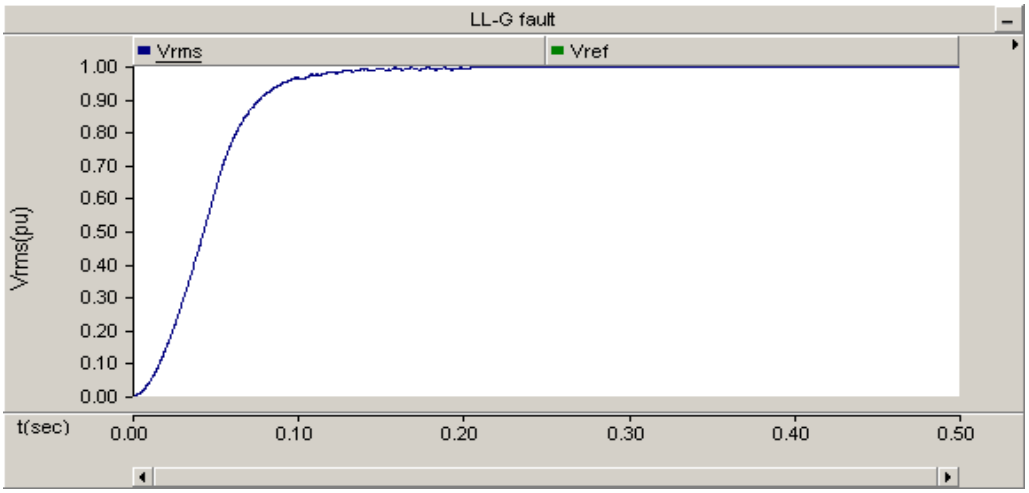

(b) LLG fault

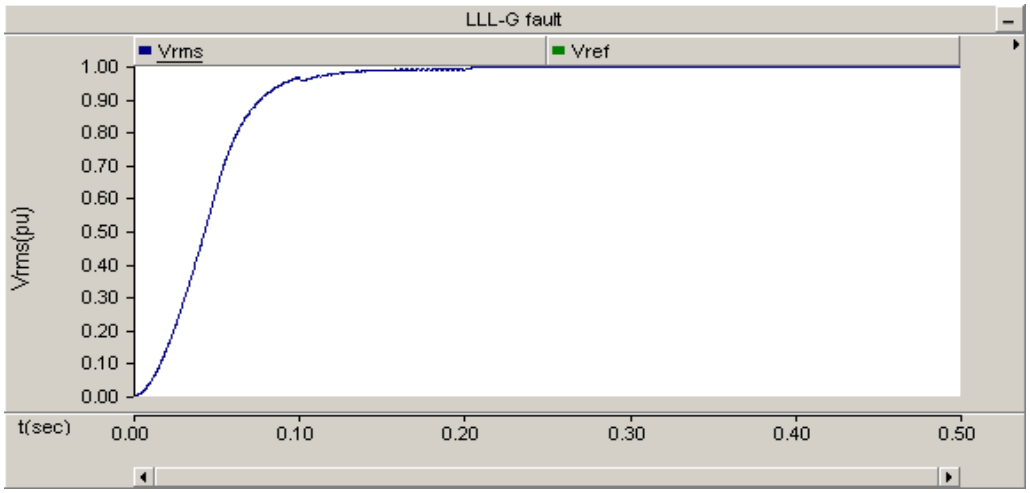

(c) LLLG fault

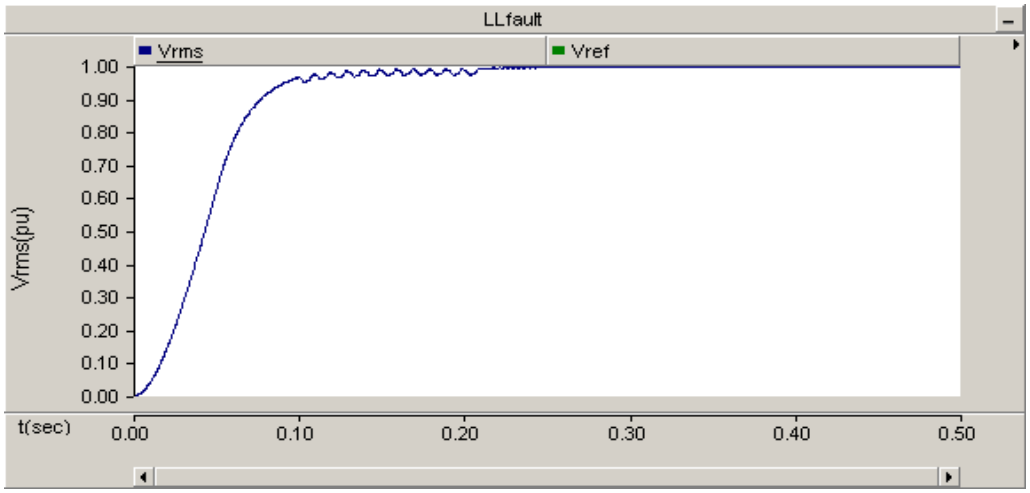

(d) LL fault

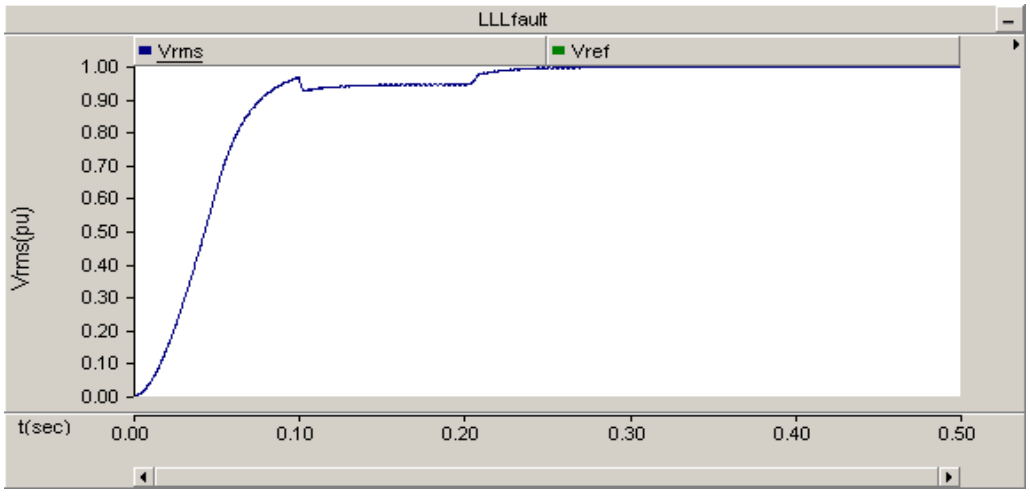

(e) LLL fault

Fig. 4.8: Recovered voltage at PCC under different fault condition with D-STATCOM

4.2.5 Test System with SSTS

The schematic diagram of test system connected with SSTS is shown in Fig.4.9. The system parameters are given in Table 4.2. The simulation is carried out on the test system comprising two identical feeders feeding to bus bar to which a sensitive load is connected through Y/Y 3-winding transformer. The effectiveness of the control scheme proposed in SSTS is analyzed under the various fault conditions [163]-[166].

Table 4.2: Parameters of test system with SSTS

System Parameters	
Power supply	230 kV, 50 Hz
Load	(412.1 + j60.5) Ω
Transformer	100 MVA, 230/11 kV

The PSCAD model of SSTS and its control scheme are shown in Fig. 4.10 (a) and (b).The control logic will monitor the peak value of the voltage waveform every half cycle at PCC where the load is connected. At the time of fault detection, the control logic will reverse the gate signal from the faulty feeder to the healthy feeder [167]. The maximum value of the voltage is set as 1 pu. It can be seen that the voltage at the faulty feeder is not restored by generating/absorbing reactive power with the help of SSTS, but the faulty feeder is deactivated in favor of the healthy one within a fraction of a cycle. With the proper fast control action of SSTS, effective protection is provided to the sensitive load against the power quality issues.

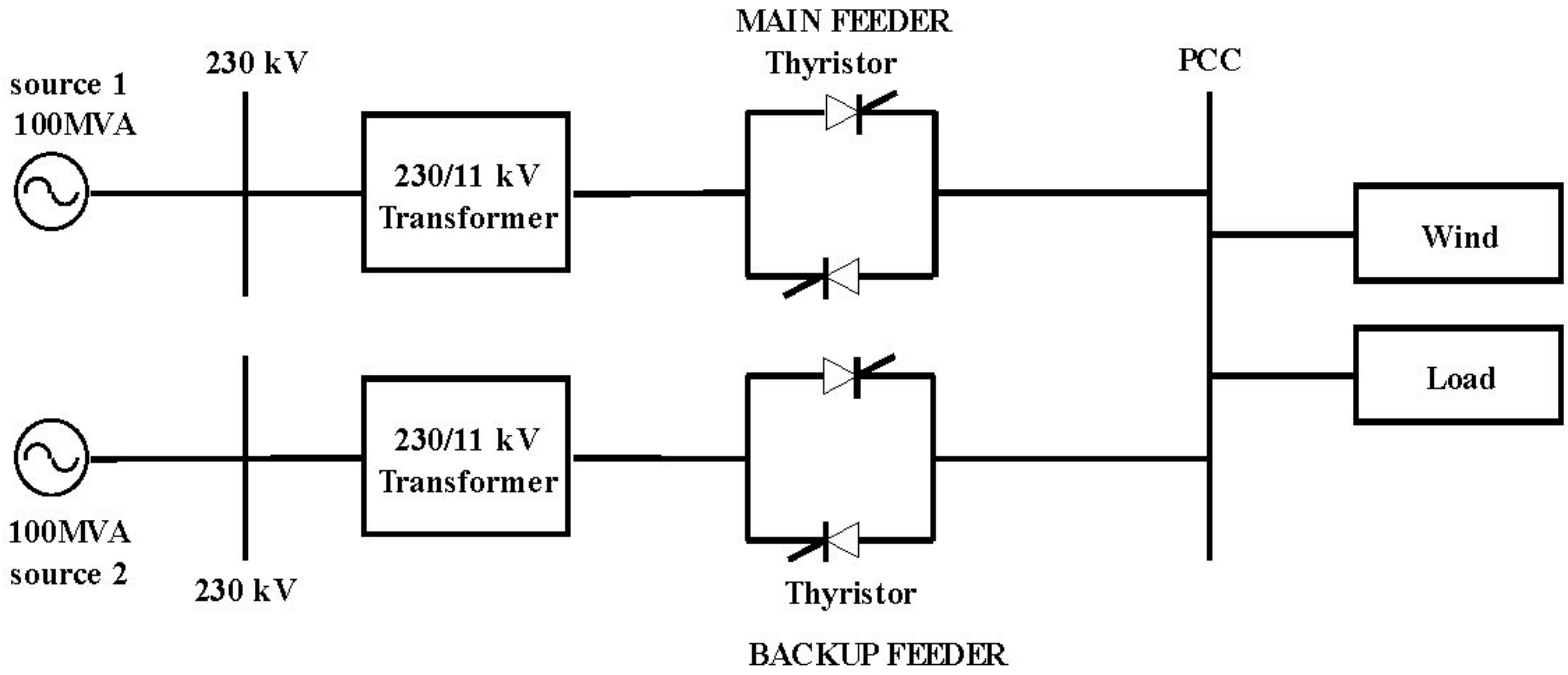

Fig. 4.9: Schematic diagram of normal distribution test system integrated with SSTS

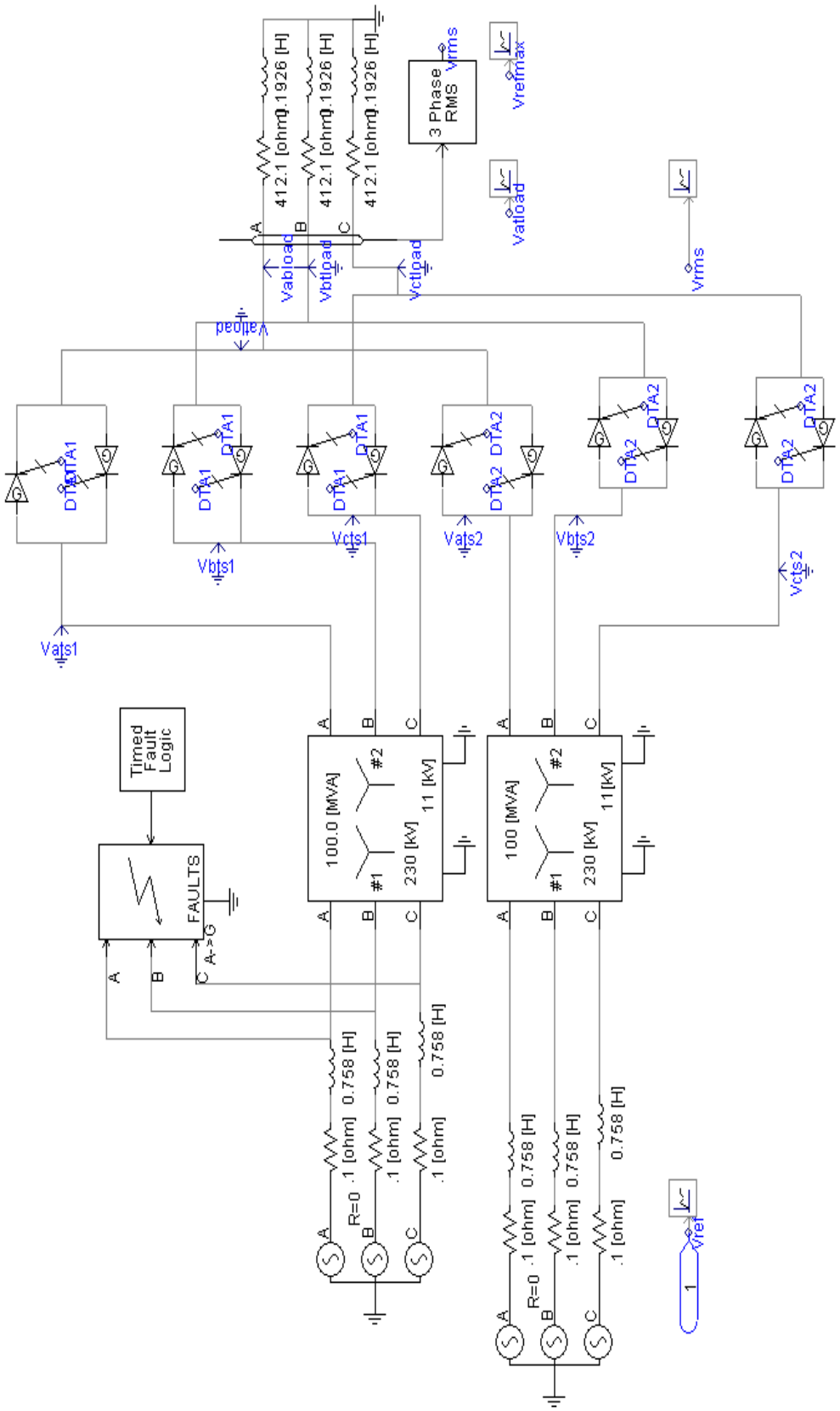

Fig. 4.10(a): PSCAD model of normal distribution test system integrated with SSTS

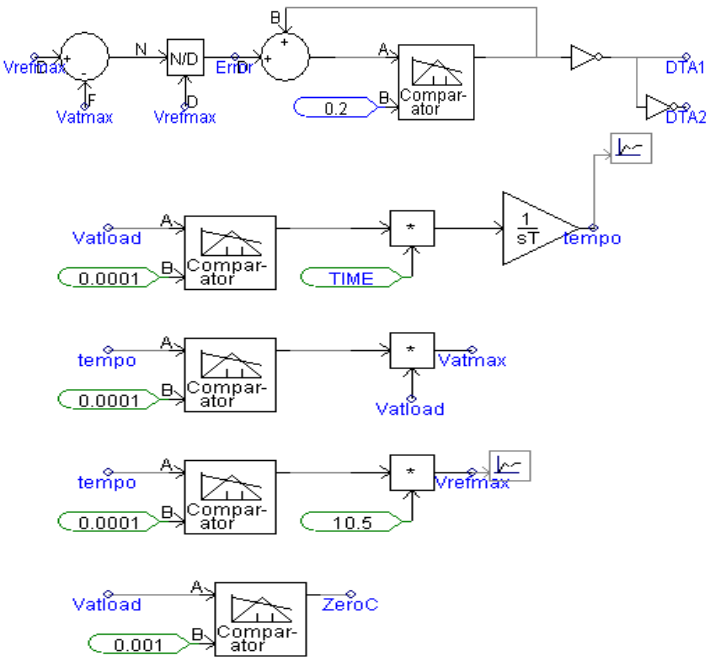

Fig. 4.10(b): Control mechanism of SSTS in PSCAD

Fig. 4.11 shows the result of simulation carried out on the test system without applying any fault. Under the normal operating condition, the PCC voltage at which the load connected is same as that of V_{ref} .

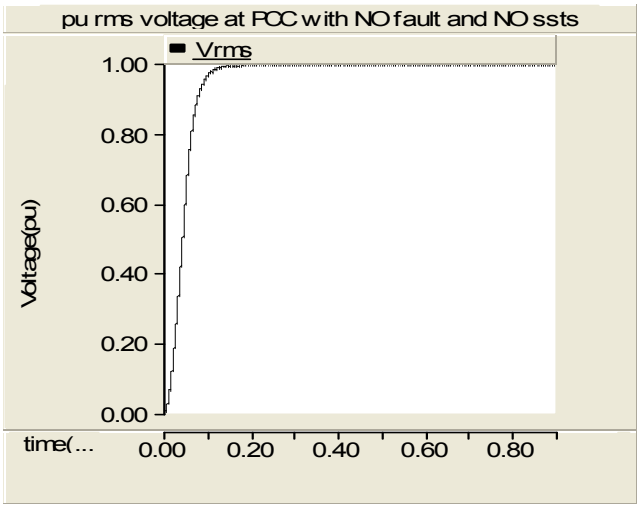

Fig. 4.11: Load voltage at PCC without fault

The simulation is carried out on the same system with NO SSTS and the different faults such as LG, LLG, LLLG, LL and LLL are applied for 0.2 to 0.5 seconds via a fault resistance of 1 Ω. From Fig. 4.12, it is observed that the voltage sag is 0.916 pu during LG fault.

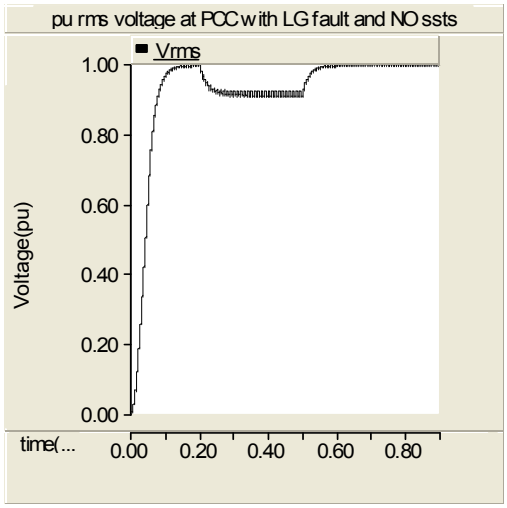

(a) LG fault

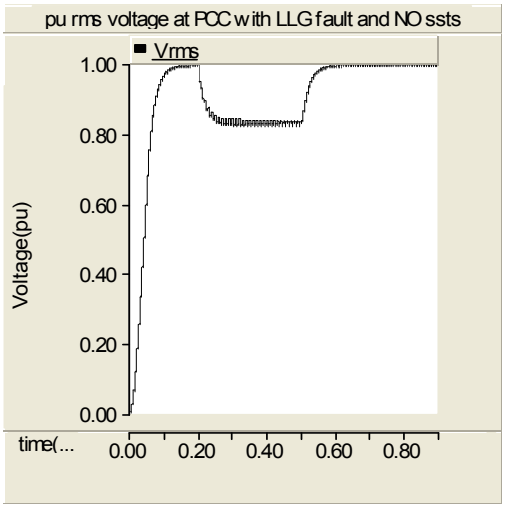

(b) LLG fault

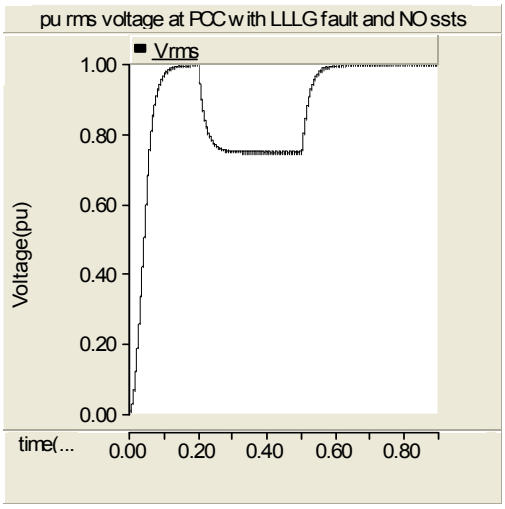

(c) LLLG fault

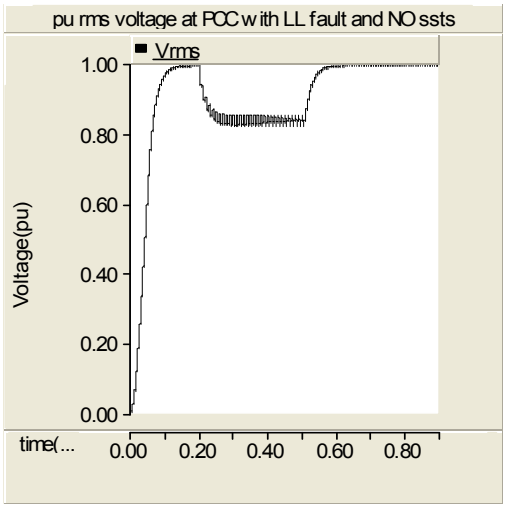

(d) LL fault

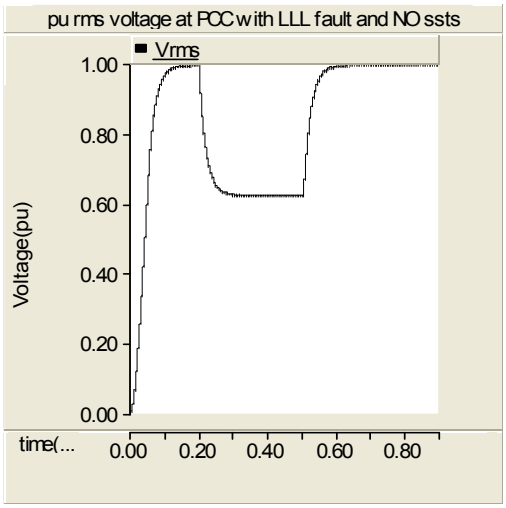

(e) LLL fault

Fig. 4.12: Load Voltage at PCC under different fault condition

The simulation is carried out on the same scenario by connecting SSTS. The pu rms load voltage at the load point or PCC under LG fault condition is recovered by SSTS as it is shown in Fig. 4.13. It is found that the load voltage is raised to 0.975 pu under LG fault condition when SSTS are under operation. In this case, the control scheme provides proper and effective control on the SSTS switches to drive back to the pre-fault voltage. Meanwhile, SSTS transfers the load from the unhealthy feeder into the healthy feeder within a fraction of half cycle.

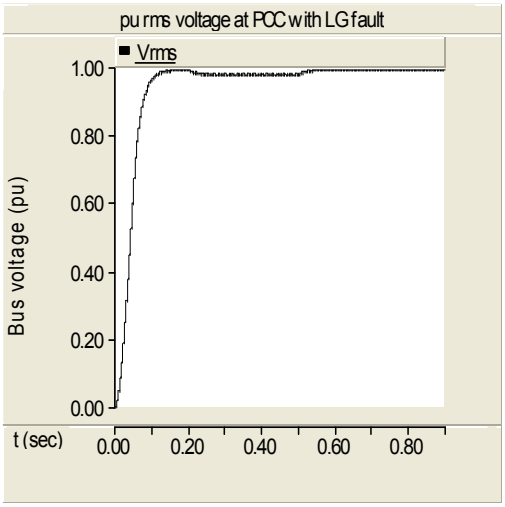

(a) LG fault

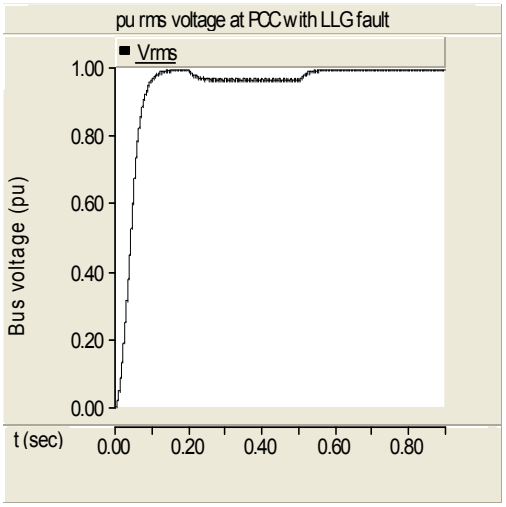

(b) LLG fault

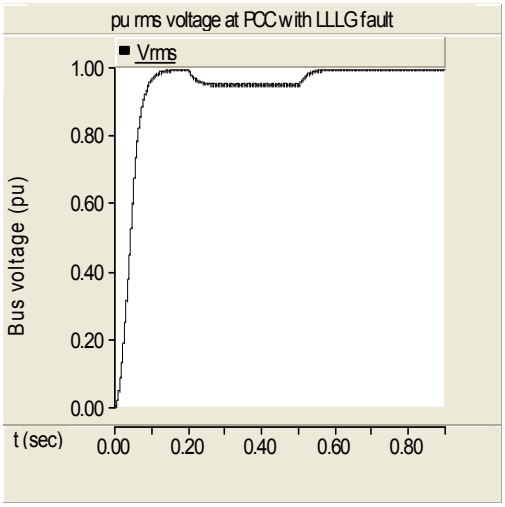

(c) LLLG fault

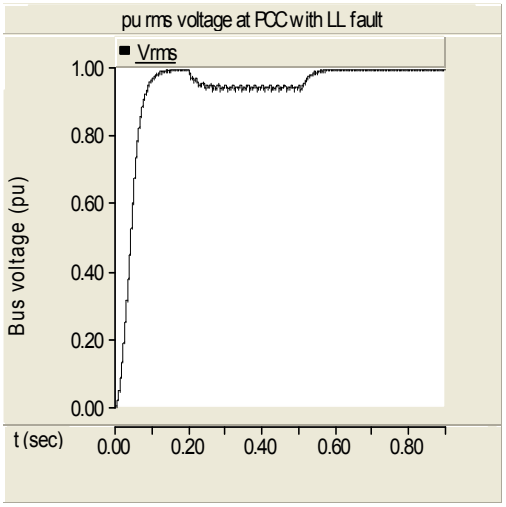

(d) LL fault

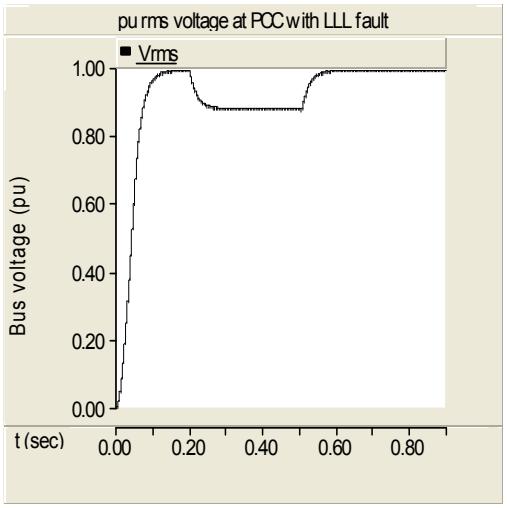

(e) LLL fault

Fig. 4.13: Recovered voltage at PCC under different fault condition with SSTS

4.3 WIND INTEGRATED DISTRIBUTION TEST SYSTEM

In normal distribution test system, a wind farm of 2 MVA at a nominal voltage of 11 kV is connected at PCC, as shown in Fig. 4.1. The simulation is carried out on the test system in which CPD is connected in series or parallel to the wind farm. The simulation is carried out first without any fault and with different faults applied during 0.2-0.25 sec. The reference voltage at PCC is set to be 1 pu.

4.3.1 Test System with NO fault

The simulation is carried out on the wind connected distribution test system without applying any fault. The circuit modeled in PSCAD is shown in Fig. 4.14. The result of simulation shown in Fig. 4.15 shows that V_{rms} at the PCC is equal to V_{ref} (= 1 pu).

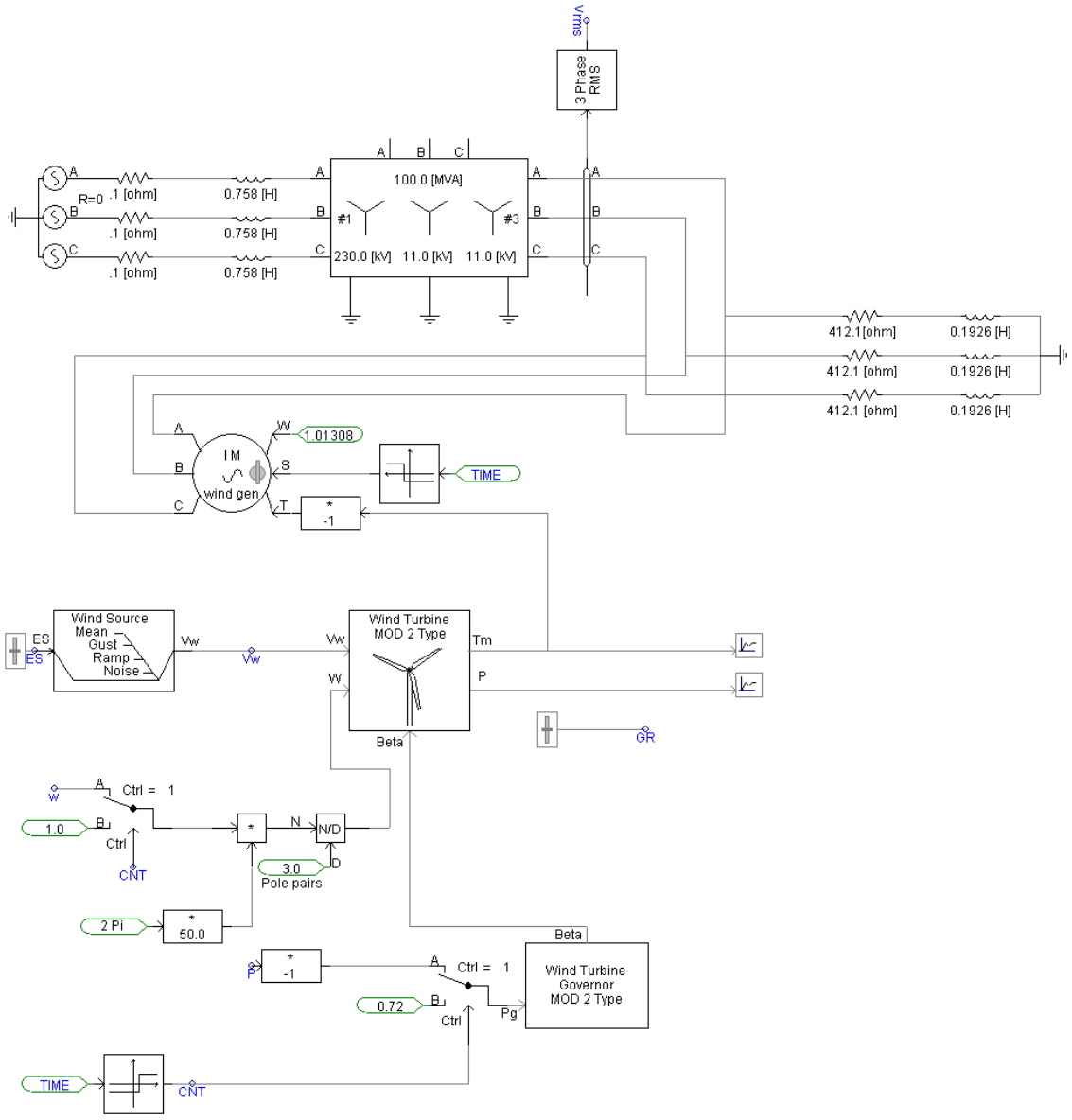

Fig. 4.14: PSCAD model of wind integrated normal distribution test system

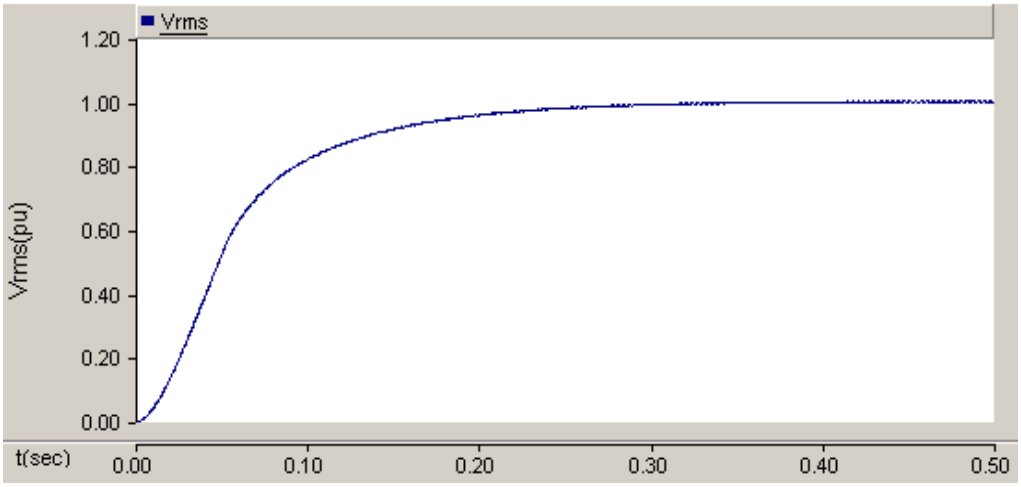

Fig. 4.15: Load Voltage at PCC without fault

4.3.2 Test System with different faults

The simulation is carried out on the same system in which different faults are applied for 0.2 to 0.25 seconds via fault resistance of 1 Ω. The voltage sag under LG fault which is given in Fig.4.16 shows that the voltage is reduced to 0.93 pu.

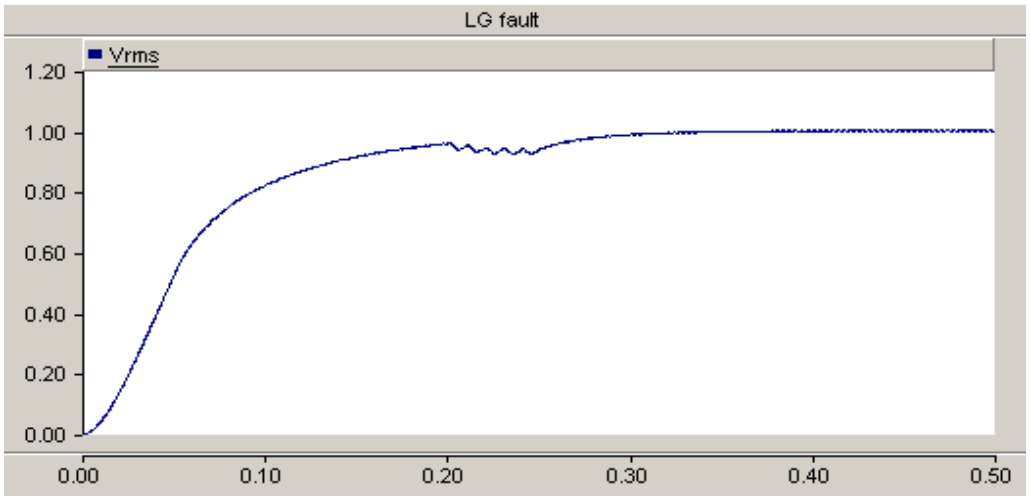

(a) LG fault

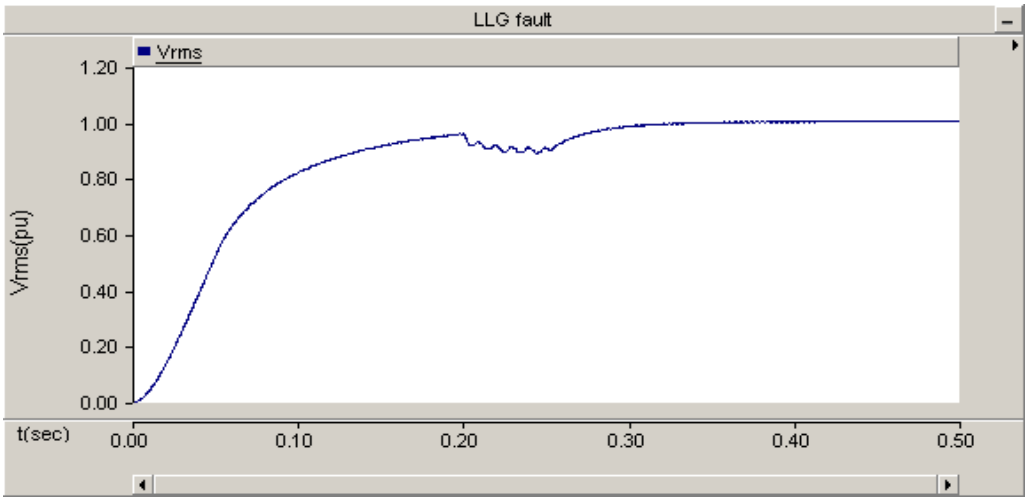

(b) LLG fault

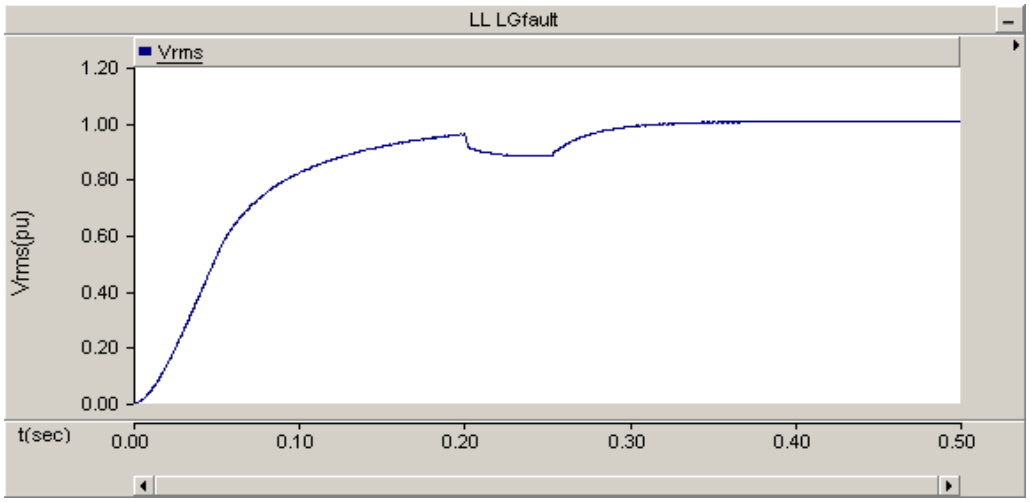

(c) LLLG fault

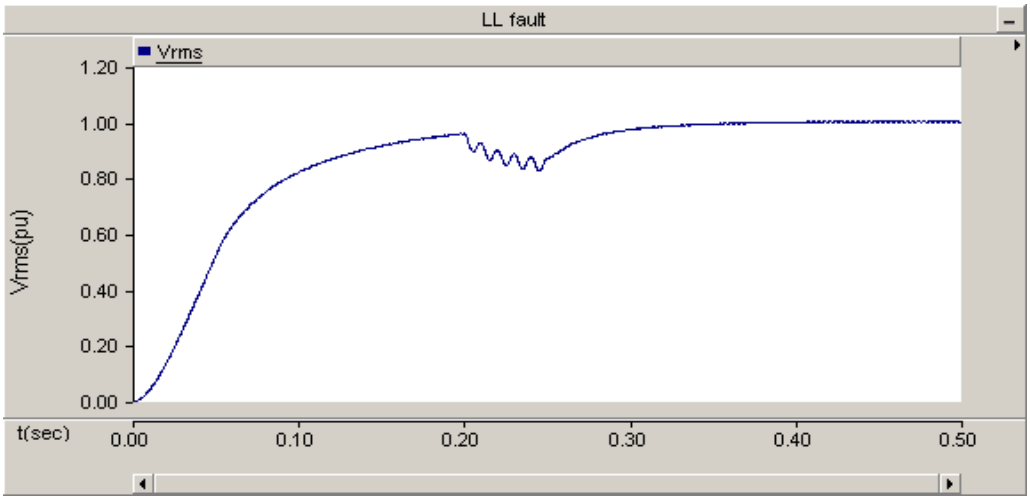

(d) LL fault

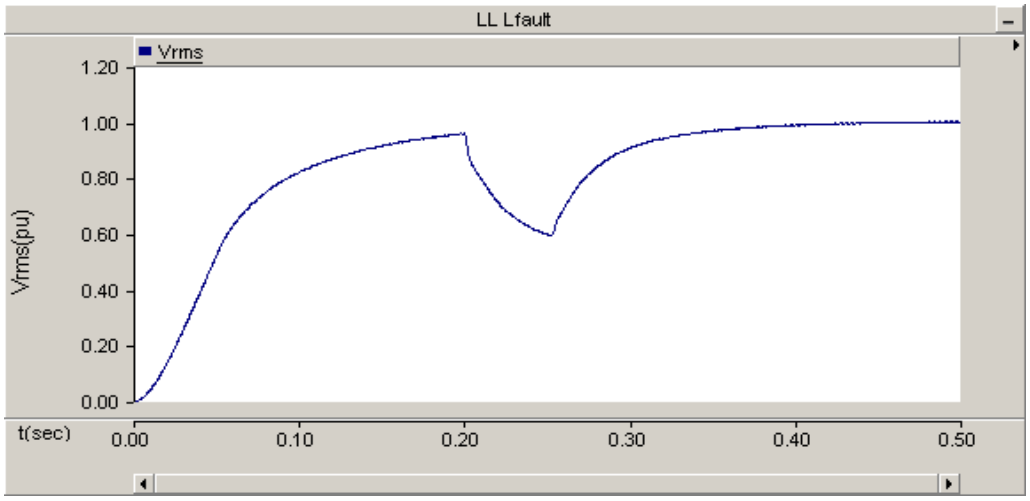

(e) LLL fault

Fig. 4.16: Load voltage at PCC under different fault condition

4.3.3 Test system with DVR

Integration of DVR in the radial network is shown in Fig. 4.5(a) to which a wind farm is connected at PCC. PSCAD model of this system is shown in Fig. 4.17, in which DVR is connected in series with the wind system at PCC. To compensate the missing voltage, a suitable capacitor connected at the input of VSC [160].

The DVR does not inject reactive power when there is no fault in the system. During fault condition, the terminal voltage at the load side decreases or increases depends on type of fault. The DVR is in active mode only when the fault is cleared. During sag condition, DVR injects the required amount of reactive power to get the normal voltage and in swell condition, it absorbs the reactive power to maintain the normal voltage.

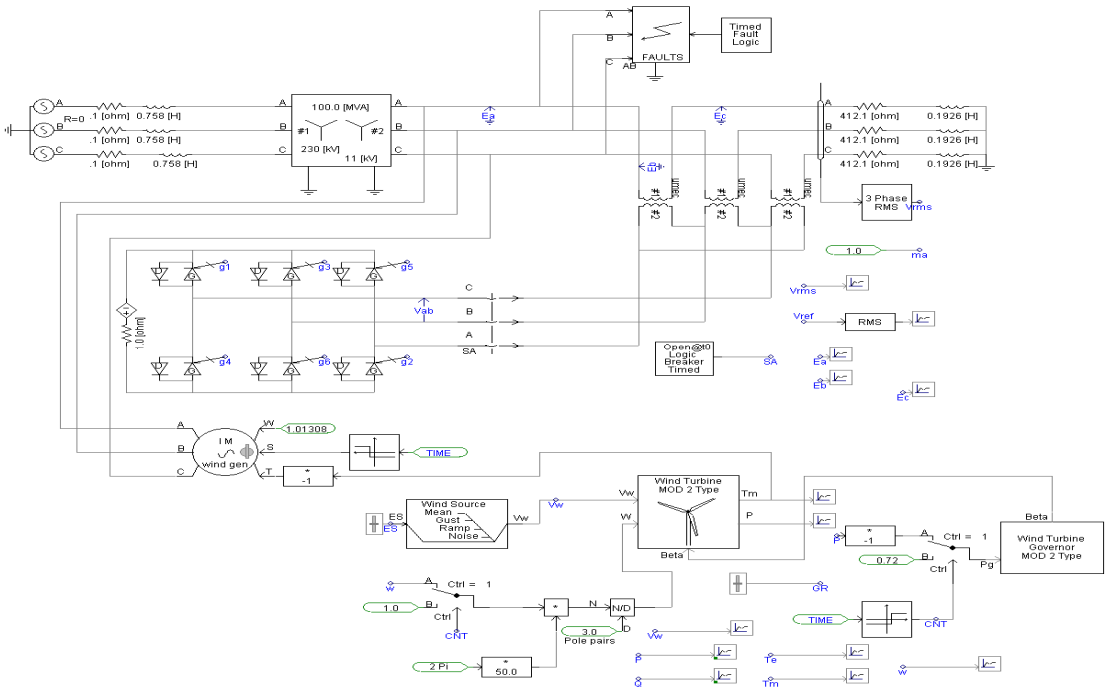

Fig. 4.17: PSCAD model of wind integrated normal distribution test system with DVR

During LG fault condition, Fig. 4.18 shows that the PCC voltage is improved to 0.95 pu when DVR is connected.

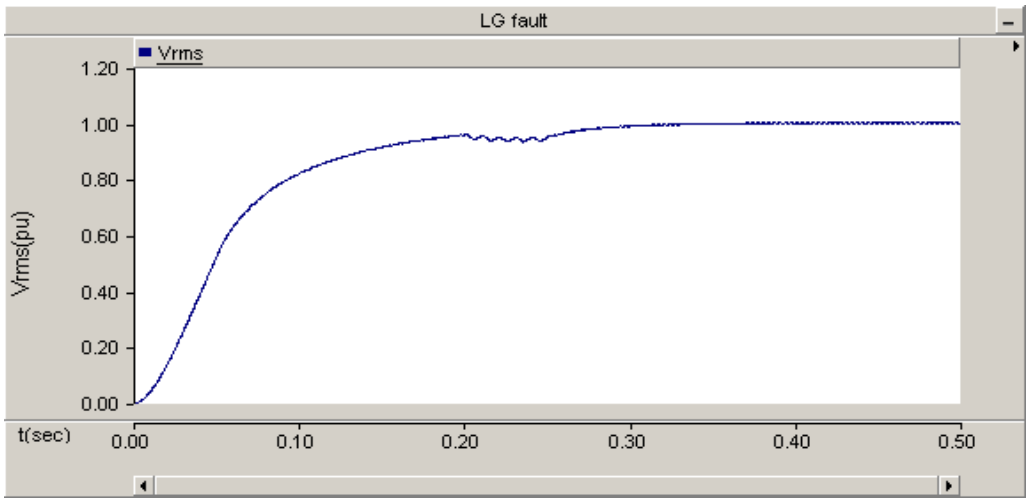

(a) LG fault

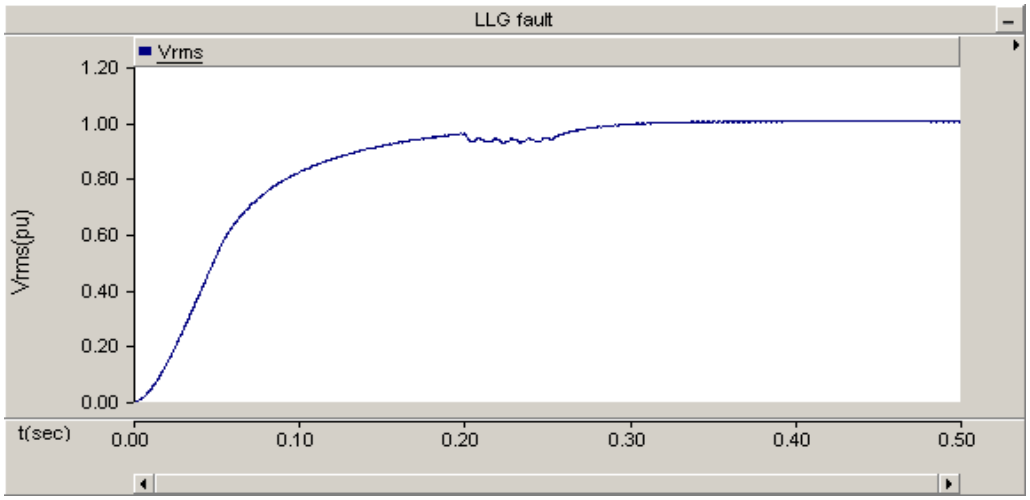

(b) LLG fault

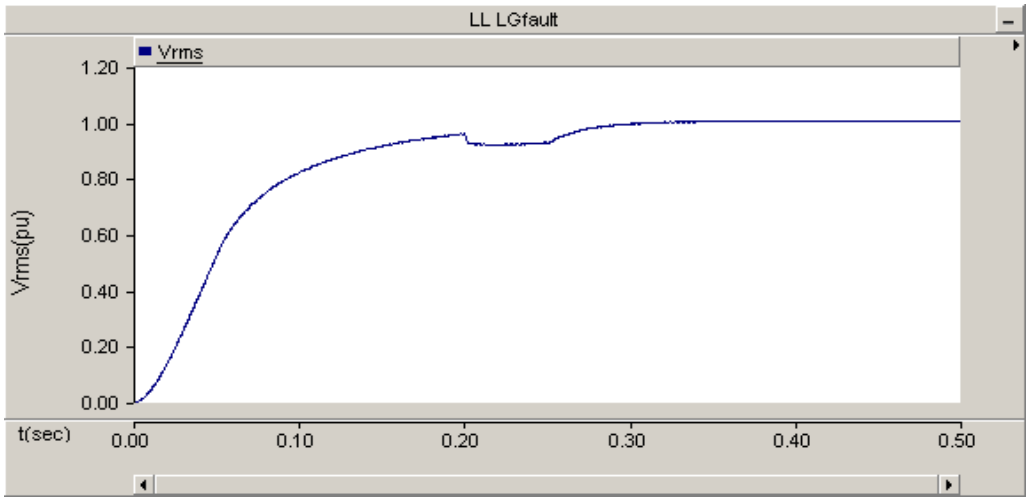

(c) LLLG fault

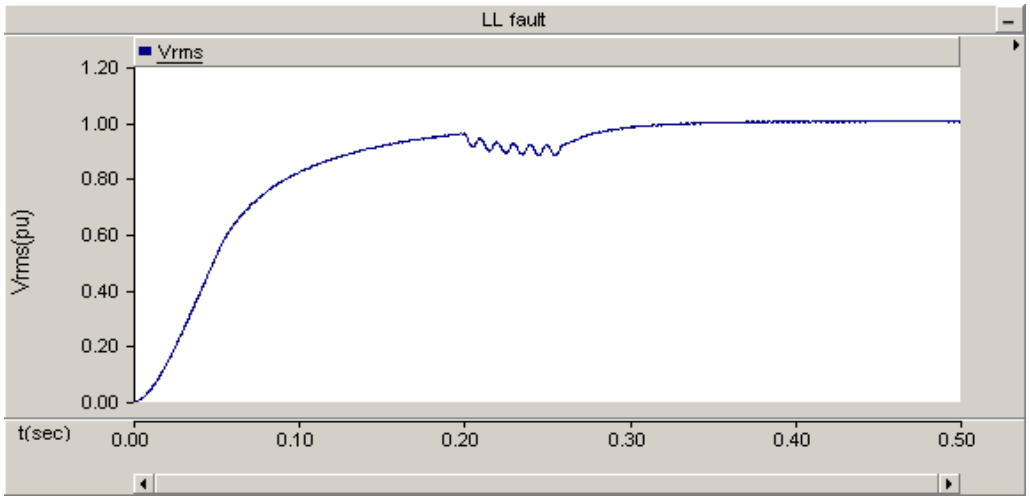

(d) LL fault

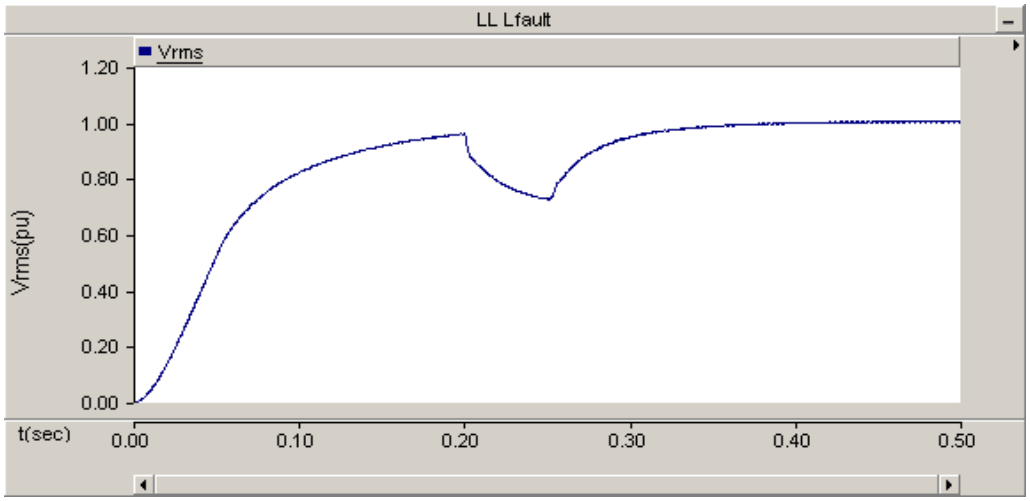

(e) LLL fault

Fig. 4.18: Recovered voltage at PCC under different fault condition with DVR

4.3.4 Test system with D-STATCOM

The schematic diagram of radial network incorporated with D-STATCOM is shown in Fig. 4.7 (a) to which wind farm is connected at PCC. PSCAD model of wind integrated distribution test system with D-STATCOM is shown in Fig. 4.19. D-STATCOM is capable of maintaining load voltage at any instant.

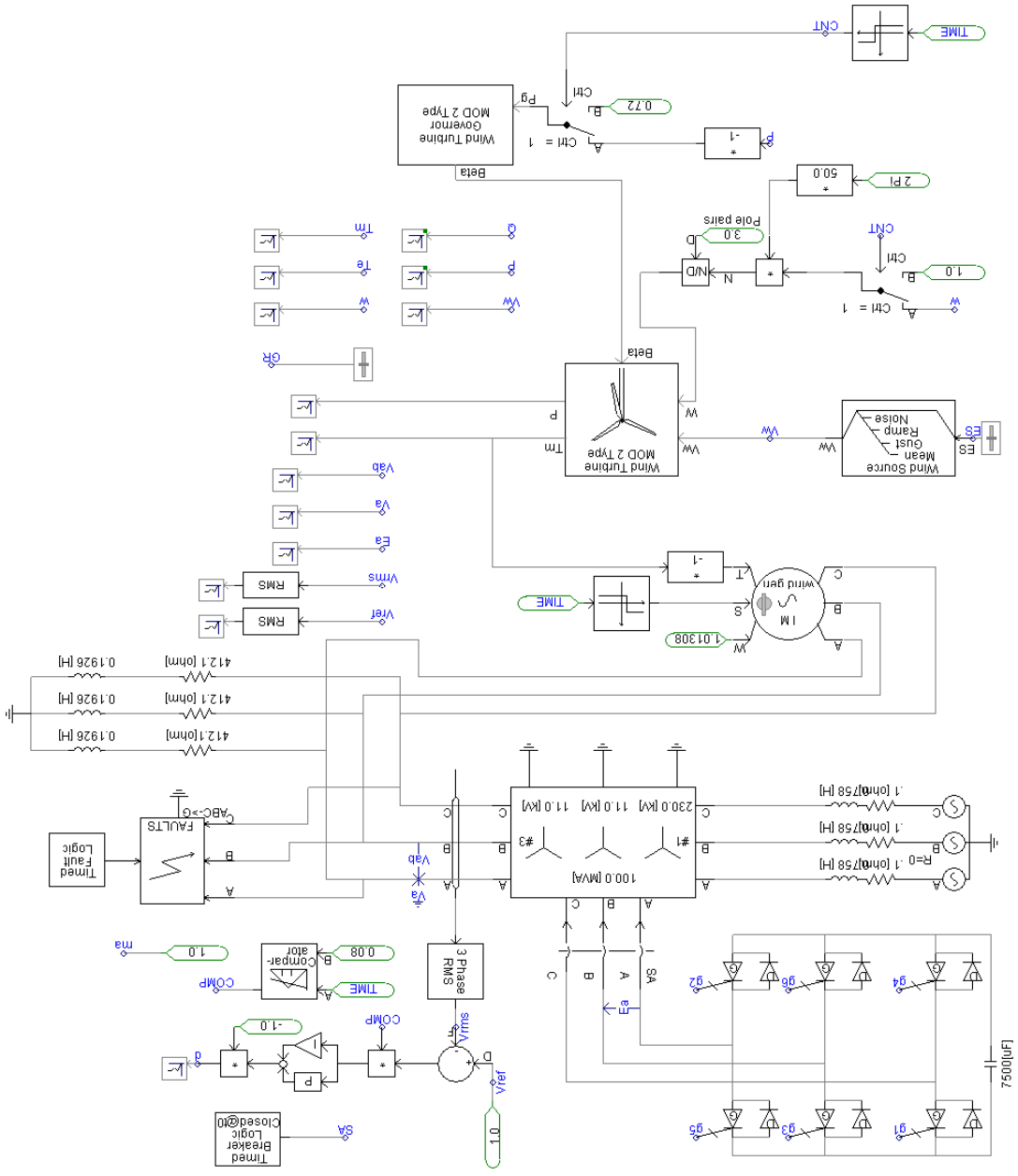

Fig. 4.19: PSCAD model of wind integrated normal distribution test system with D-STATCOM

The result of the simulation is shown in Fig. 4.20. It is seen that the load voltage at PCC is recovered from 0.93 to 0.967 pu with the help of D-STATCOM. The PWM technique controls the magnitude and the phase of injected or absorbed voltage provided by VSC to restore the rms voltage at the load point very effectively.

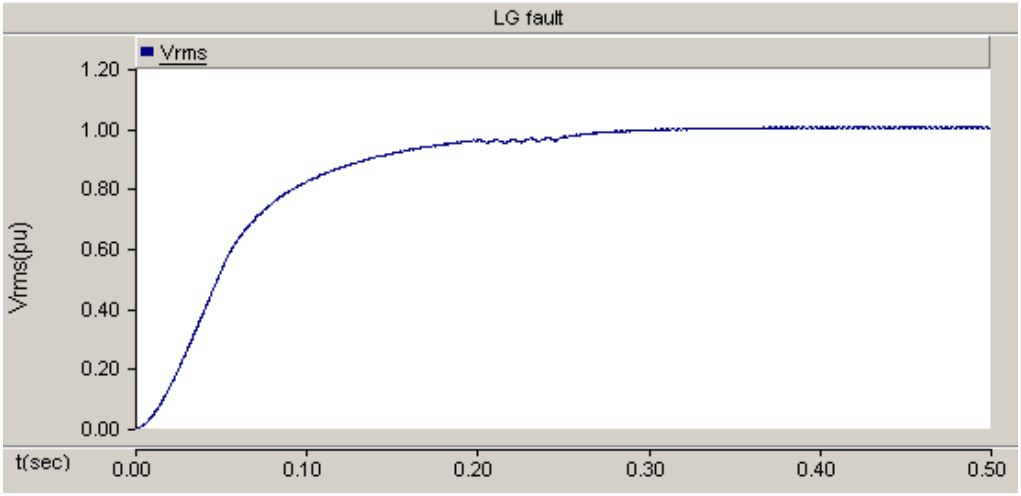

(a) LG fault

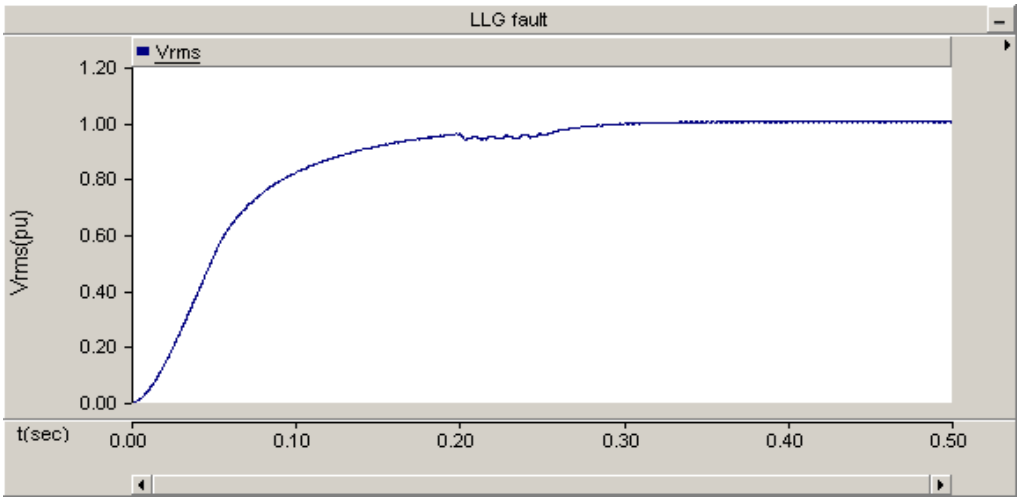

(b) LLG fault

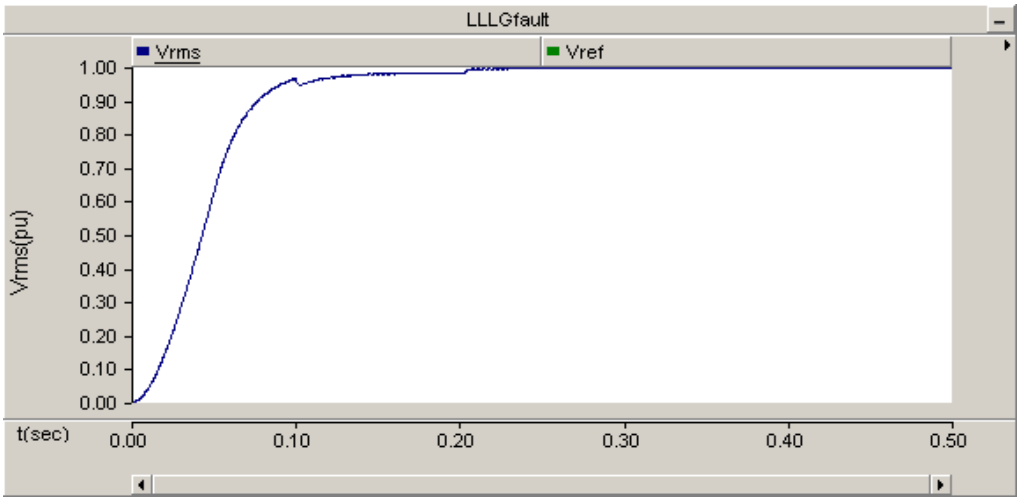

(c) LLLG fault

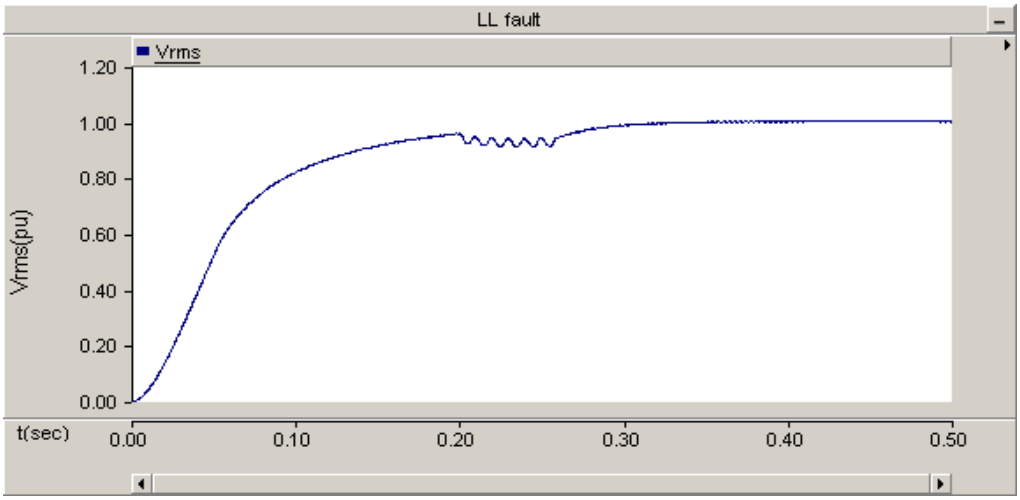

(d) LL fault

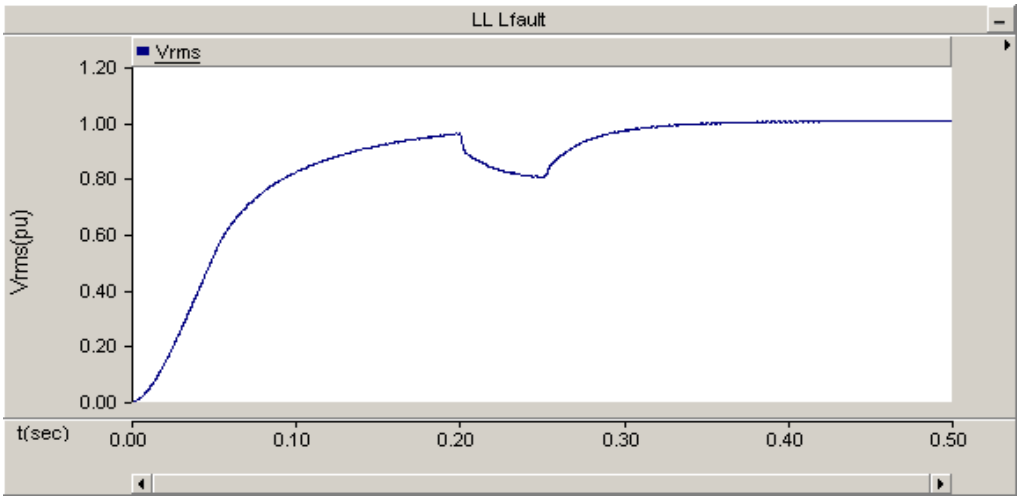

(e) LLL fault

Fig. 4.20: Recovered voltage at PCC under different fault condition with D-STATCOM

4.3.5 Test system with SSTS

A wind system of 2 MVA, 230 kV integrated with the distribution test system is shown in Fig. 4.9. The simulation is carried out to assess the effectiveness of the control scheme proposed in SSTS under various fault conditions. The circuit modeled in PSCAD is shown in Fig. 4.21.

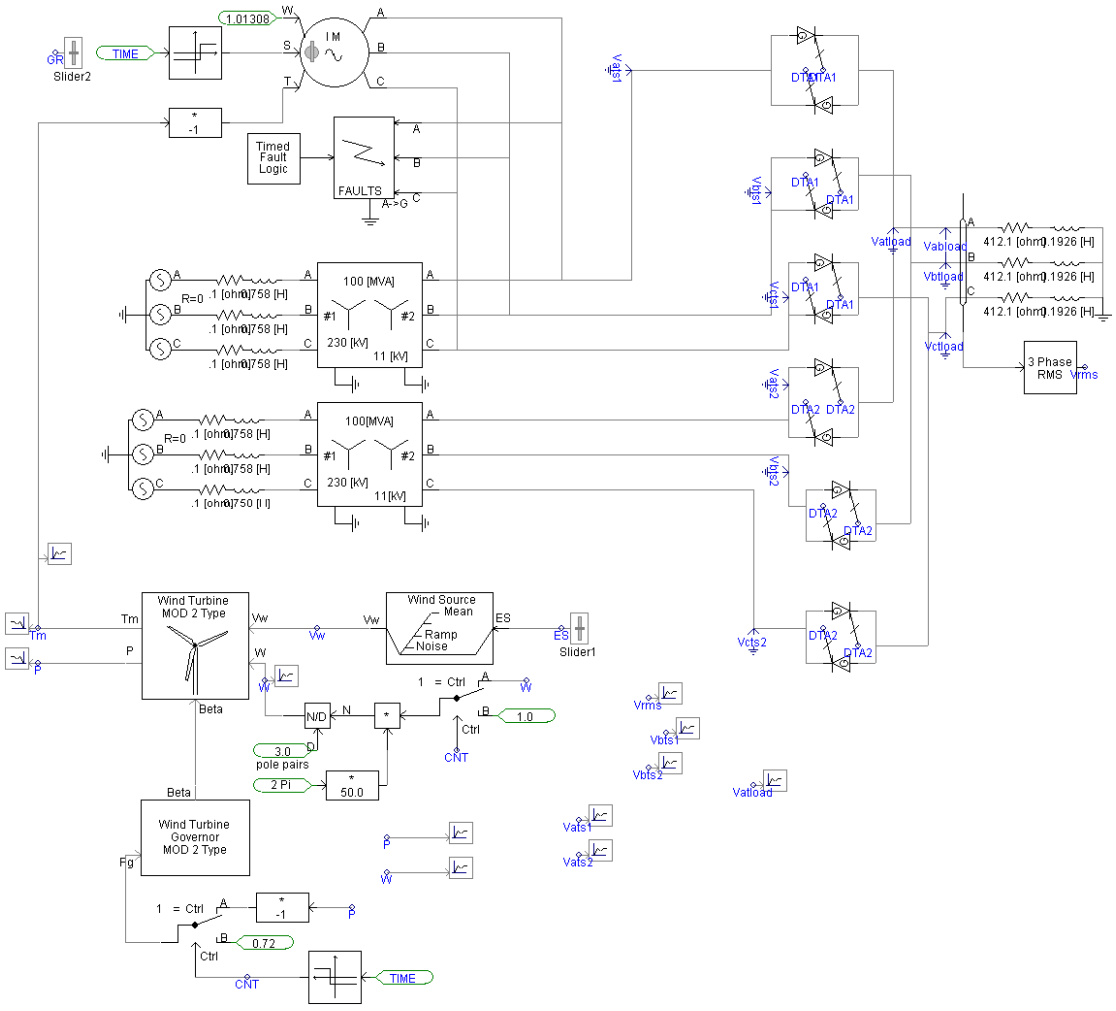

Fig. 4.21: PSCAD model of wind integrated normal distribution test system with SSTS

The simulation is carried out on the wind integrated distribution system without applying any fault. V_{rms} at PCC is measured and is nearly equal to V_{ref} i.e., 1 pu as shown in Fig 4.22.

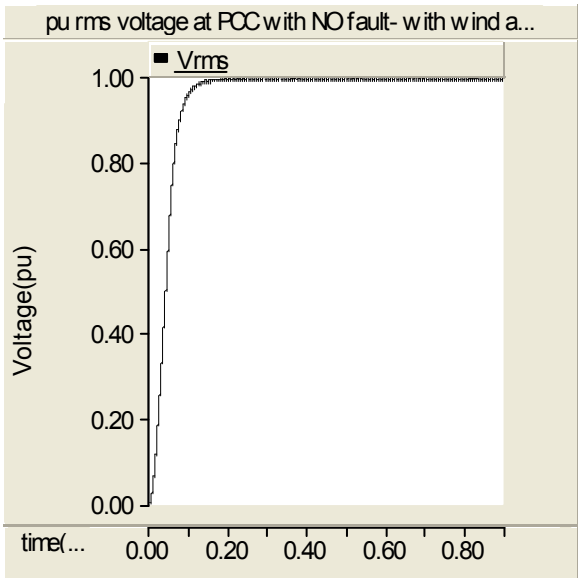

Fig. 4.22: Load voltage at PCC in wind integrated system without fault and NO SSTS

The simulation is carried out with the same system with NO SSTS and different faults such as LG, LLG, LLLG, LL and LLL are applied for a duration of 0.2 to 0.5 seconds via a fault resistance of 1 Ω. Figure 4.23 shows the variation of the load pu rms voltage at PCC under LG fault condition. It is observed that pu voltage at PCC is reduced to 0.978 pu voltage.

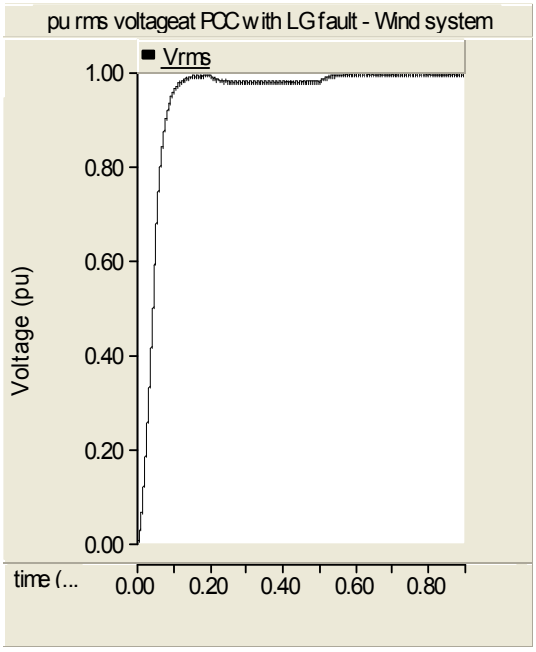

(a) LG fault

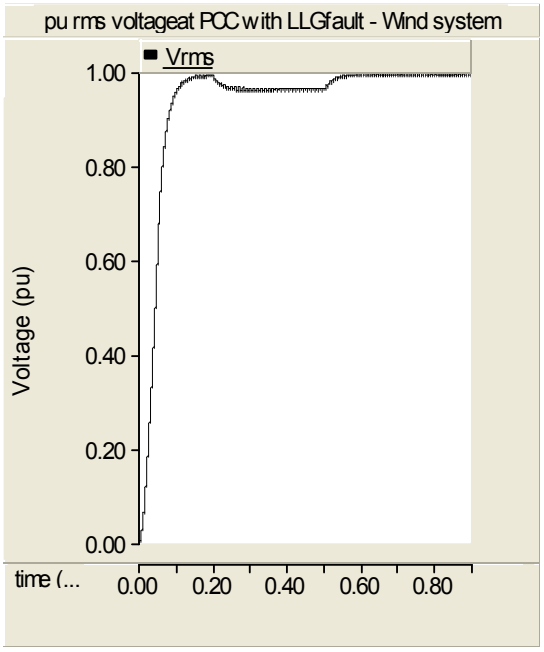

(b) LLG fault

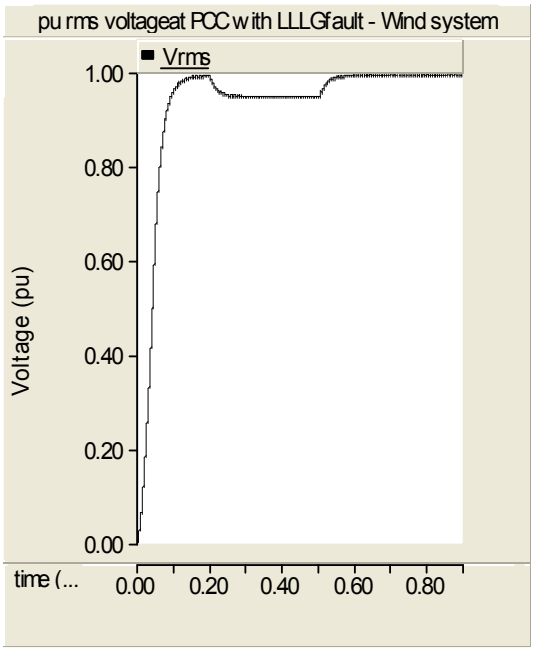

(c) LLLG fault

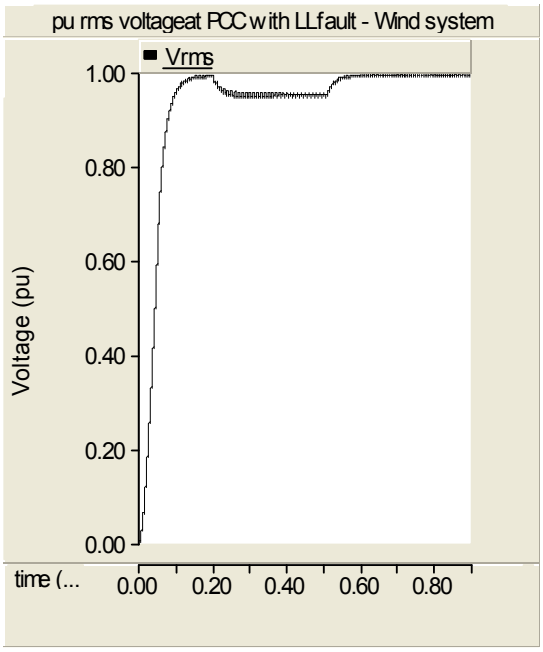

(d) LL fault

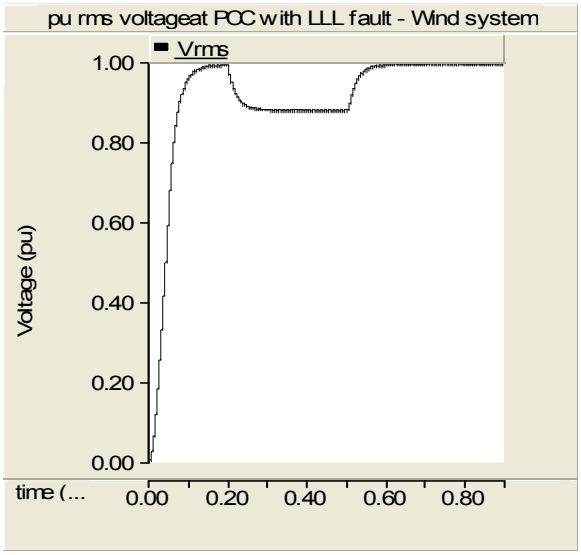

(e) LLL fault

Fig. 4.23: Load voltage at PCC under different fault condition

The simulation is carried out with the same system by connecting SSTS and the pu rms voltage at load side is shown in Fig. 4.24. The pu rms load voltage at load point or PCC under LG fault condition is recovered from 0.978 pu to nearly 1 pu by SSTS, as shown in Fig.4.25.

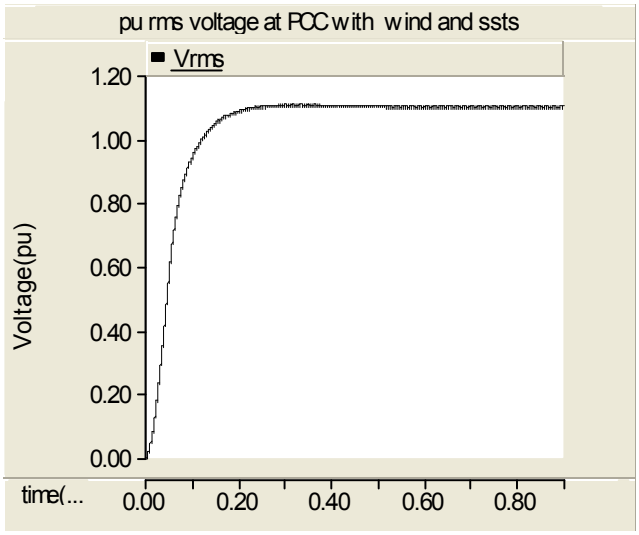

Fig. 4.24: Load voltage at PCC with SSTS and NO fault

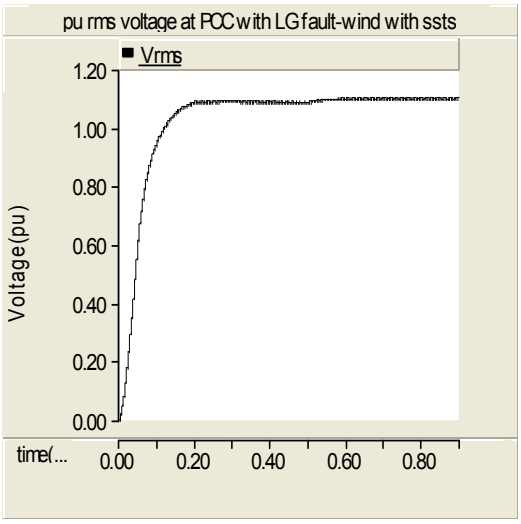

(a) LG fault

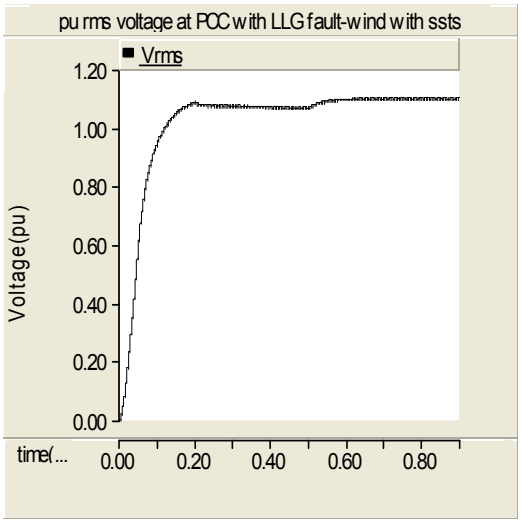

(b) LLG fault

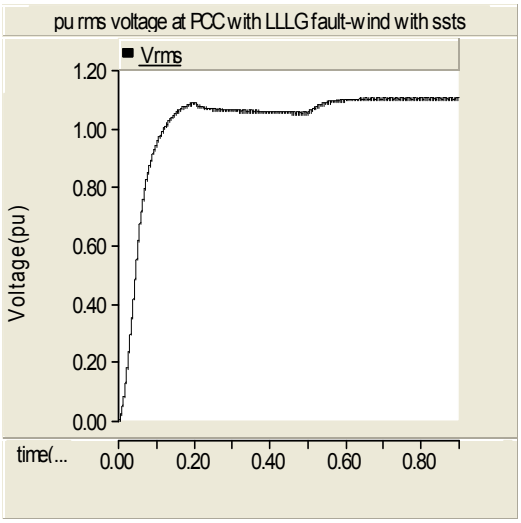

(c) LLLG fault

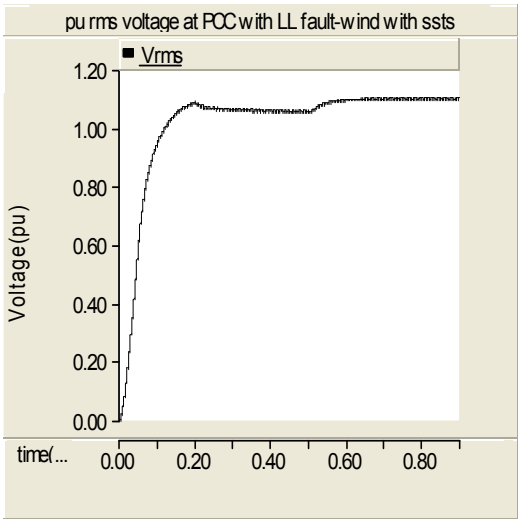

(d) LL fault

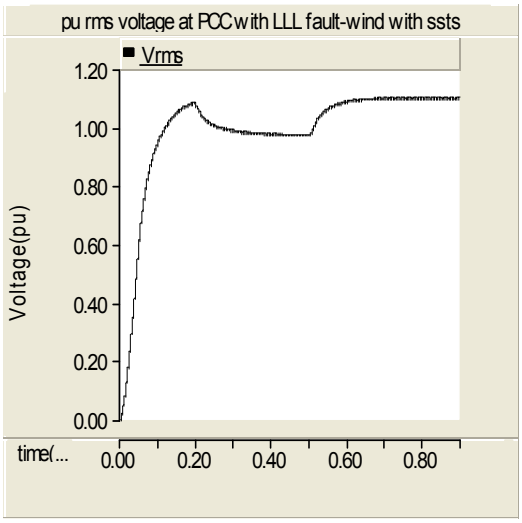

(e) LLL fault

Fig. 4.25: Recovered voltage at PCC under different fault condition with SSTS

4.4 RESULTS AND DISCUSSION

The results obtained as a result of the simulation carried out on normal and wind integrated distribution test system with and without DVR, D-STATCOM and SSTS are explained in this section.

4.4.1 Normal Distribution Test System

In normal distribution test system, various simulation studies are carried out to understand the effect of voltage sag by applying different faults in the system and its mitigation using custom power devices. Without applying any fault in the test system, it is observed that load voltage at the point of common coupling (PCC) is equal to the reference voltage, 1 pu. The voltage sag occurs, when LG, LLG, LLLG, LL and LLL faults are applied in the test system via a fault resistance. Table 4.3 shows the effects of faults in the test system. It is observed that during LG fault, the voltage is reduced from reference voltage 1 pu to 0.901 pu with voltage drop or percentage sag of 9.9%.

Table 4.3: Load voltage under different faults with and without DVR

	WITHOUT DVR			WITH DVR		
Types of faults	Voltage min (pu)	Voltage max (pu)	RMS voltage drop (%)	Voltage min (pu)	Voltage max (pu)	RMS voltage drop (%)
LG	0.901	1	9.9	0.995	1	0.5
LLG	0.857	1	14.3	0.973	1	2.7
LLLG	0.829	1	17.1	0.967	1	3.3
LL	0.789	1	21.1	0.92	1	8
LLL	0.485	1	51.5	0.801	1	19.9

Table 4.4: Load voltage under different faults with and without D-STATCOM

	WITHOUT D-STATCOM			WITH D-STATCOM		
Types of faults	Voltage min (pu)	Voltage max (pu)	RMS voltage drop (%)	Voltage min (pu)	Voltage max (pu)	RMS voltage drop (%)
LG	0.901	1	9.9	0.996	1	0.4
LLG	0.857	1	14.3	0.989	1	1.1
LLLG	0.829	1	17.1	0.983	1	1.7
LL	0.789	1	21.1	0.98	1	2
LLL	0.485	1	51.5	0.929	1	7.1

Fig. 4.26 shows the voltage sag during LG fault. The voltage at PCC is 1 pu without any fault, which is reduced to 0.901 pu under LG fault condition. Meanwhile, the voltage sag and percentage sag for other faults are shown in Table 4.3.

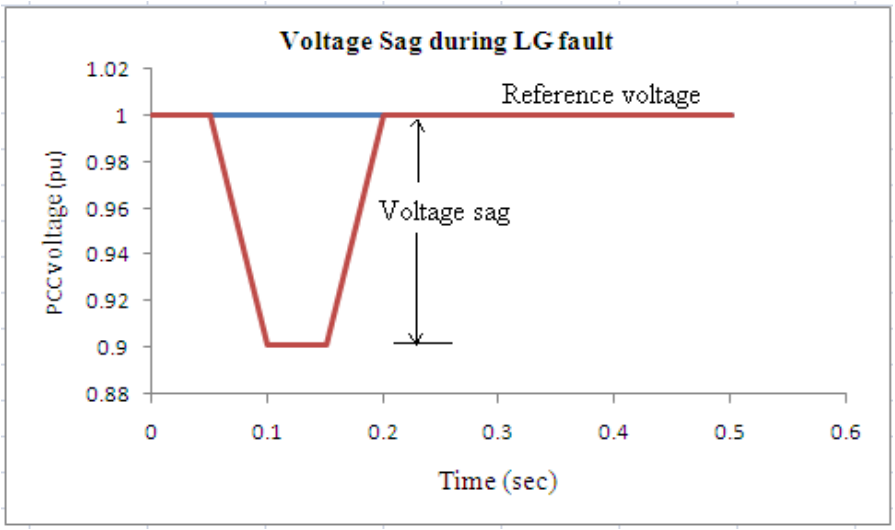

Fig. 4.26: Voltage sag during LG fault condition without D-STATCOM/DVR

Sag Compensation with DVR

When LG fault is applied during a period of 0.1-0.15 sec, a reduction of 9.9% occurs in the voltage. With DVR, the PCC voltage is raised to 0.995 pu and it is found that the percentage reduction in voltage is only 0.5%. This means that about 94.94% of sag is compensated by the use of DVR. The effectiveness of DVR for other faults are

recorded in Table 4.3. The details of voltage mitigation capability of DVR under LLL fault is demonstrated in Fig. 4.27.

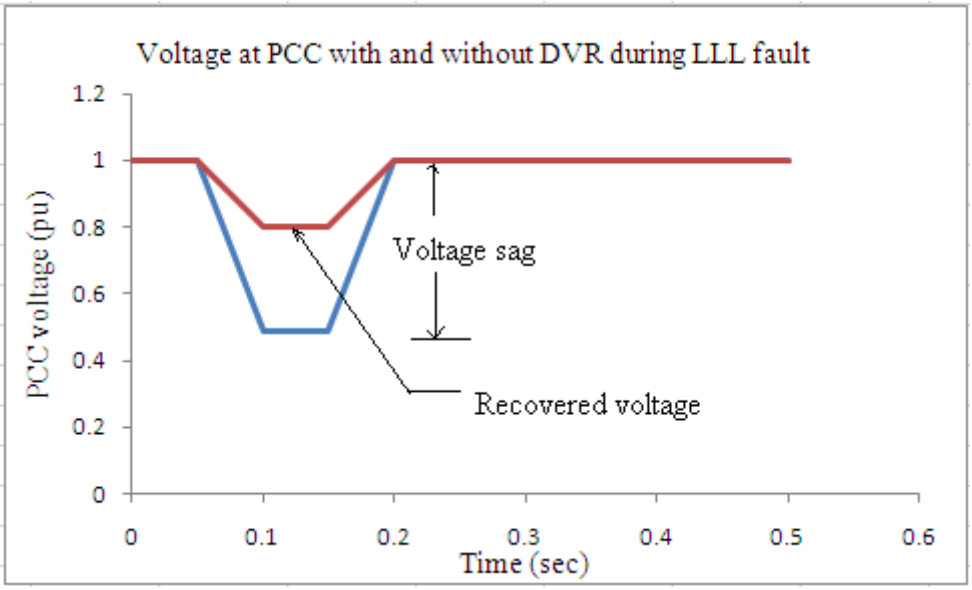

Fig. 4.27: Voltage sag during LLL fault condition without and with DVR

Sag Compensation with D-STATCOM

With the use of D-STATCOM, the PCC voltage at 0.901 pu is raised to 0.996 pu under LG fault condition. The percentage sag is reduced from 9.9% to 0.4%. Hence, a percentage sag of 95.95% is recovered The voltage sag and recovered voltage with and without the use of D-STATCOM is shown in Fig. 4.28. The effect of different faults and the effectiveness of D-STATCOM are shown in Table 4.4.

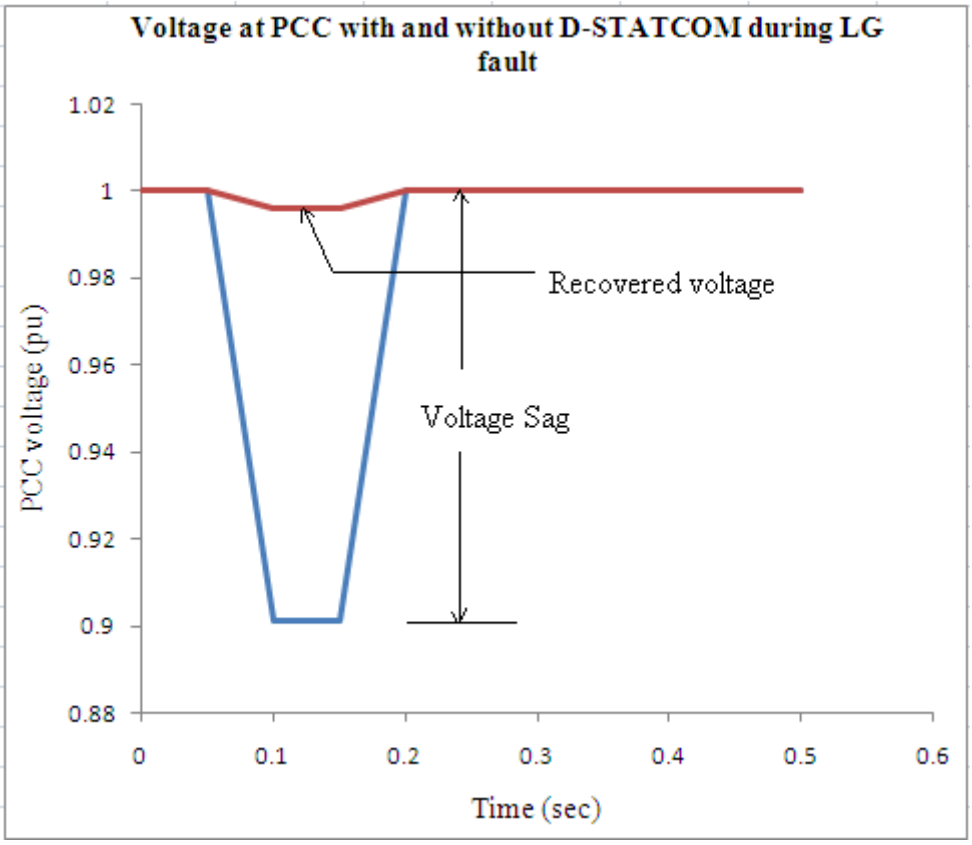

Fig. 4.28: Voltage sag during LG fault without and with D-STATCOM

Sag Compensation with SSTS

Under the normal operating condition, the rms voltage at the point of common coupling (PCC) at which the load point is normally taken as reference voltage 1 pu. When different faults are applied via a fault resistance in the system, the voltage sag occurred. During LG fault, its value which was at 0.916 pu rose to 0.975 pu with the use of SSTS with its effective control. Hence, the sag of 9.9% is reduced to 6.05%. The recovery in percentage voltage sag is found to be 38.88%. The voltage sag and its percentage sag for different fault conditions are measured and the tabulations are given in Table 4.5. The voltage sag under LG fault condition with NO SSTS is compared with SSTS in operation as can be seen in Fig.4.29. In the case of SSTS in operation, the control scheme provides proper and effective control on the SSTS

switches to drive back to the pre-fault voltage. Meanwhile, SSTS transfers the load from the unhealthy feeder to the healthy feeder within a fraction of half cycle so that the voltage at PCC is nearly equal to the reference voltage.

Table 4.5: Load voltage under different faults with and without SSTS

	WITHOUT SSTS			WITH SSTS		
Types of faults	Voltage min (pu)	Voltage max (pu)	RMS voltage drop (%)	Voltage min (pu)	Voltage max (pu)	RMS voltage drop (%)
LG	0.916	1	8.4	0.975	1	2.5
LLG	0.831	1	16.9	0.961	1	3.9
LLLG	0.745	1	25.5	0.945	1	5.5
LL	0.841	1	15.9	0.942	1	5.8
LLL	0.621	1	37.9	0.878	1	12.2

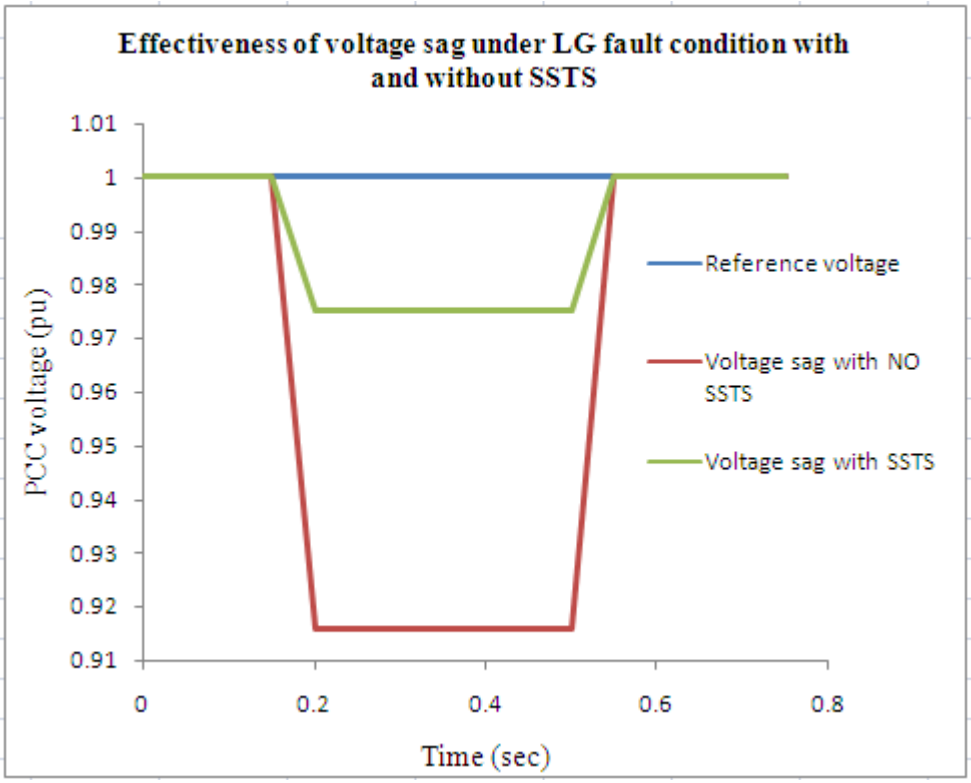

Fig. 4.29: Voltage sag during LG fault without and with SSTS

Fig.4.30 shows the PCC voltage in pu for different fault conditions and its mitigated voltage with the use of DVR and D-STATCOM.

Fig.4.31 shows the percentage voltage sag at PCC with respect to the reference voltage, for different fault conditions, with and without DVR or D-STATCOM. It is seen that the percentage voltage sag under LG fault condition is 9.9. By making use of DVR, the voltage sag is improved and the percentage voltage sag is found to be 0.5. It clearly shows that the percentage voltage recovery from fault condition to the recovered condition is 9.44.

The use of D-STATCOM gave an improvement in percentage voltage sag to 0.04. Hence, the percentage recovery in voltage sag from fault condition to the recovered condition for LG fault condition is 9.5. This means that the voltage sag occurring under LG fault condition is found to be compensated effectively. The capability of DVR and D-STATCOM for other faults is shown in Fig. 4.30 and 4.31.

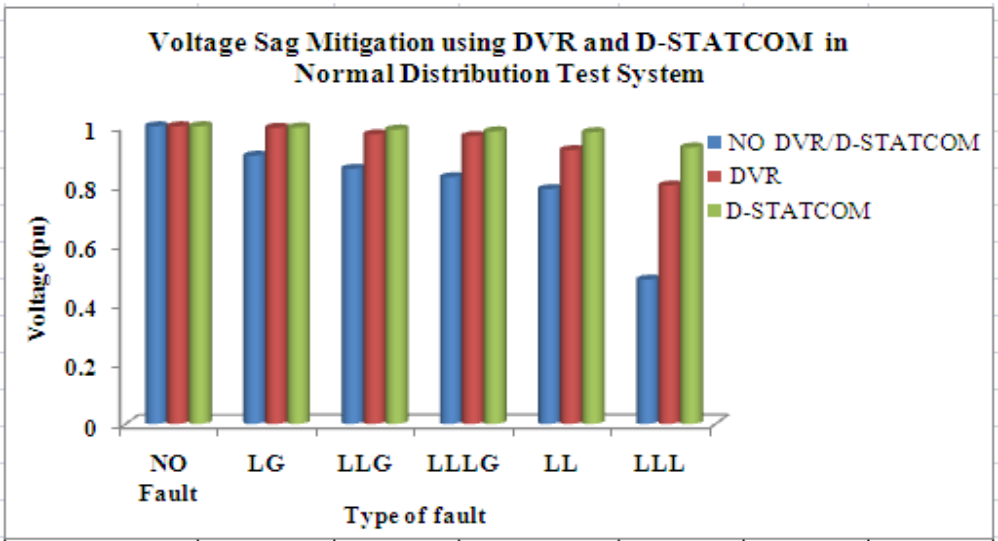

Type of fault	NO Fault	LG	LLG	LLLG	LL	LLL
NO DVR	1	0.901	0.857	0.829	0.789	0.485
DVR	1	0.995	0.973	0.967	0.92	0.801
D-STATCOM	1	0.996	0.989	0.983	0.98	0.929

Fig. 4.30: Voltage at PCC in normal distribution test system without and with DVR/D-STATCOM

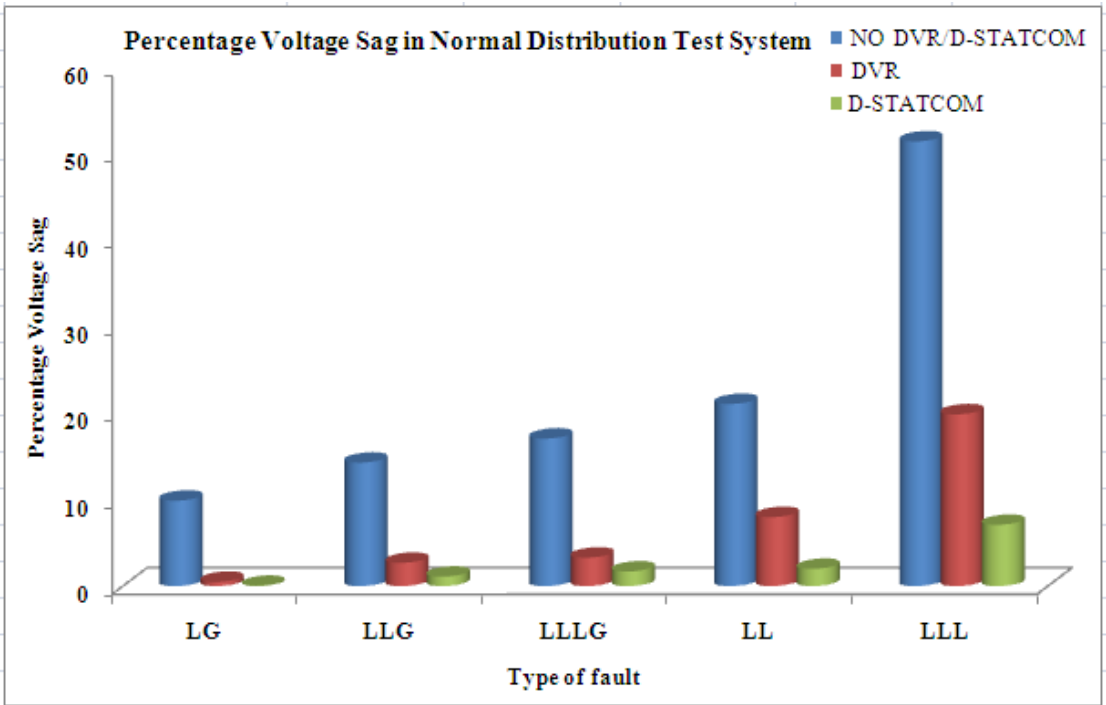

Type of Fault	LG	LLG	LLLG	LL	LLL
NO DVR/D-STATCOM	9.9	14.3	17.1	21.1	51.5
DVR	0.5	2.7	3.3	8	19.9
D-STATCOM	0.04	1.1	1.7	2	7.1

Fig. 4.31: Percentage voltage sag in normal distribution test system without and with DVR/ D-STATCOM

The load voltage at PCC with and without the use of SSTS is shown in Fig.4.32. From Fig. 4.33, it is found that, under LG fault condition, the percentage sag concerning pre-fault voltage is 8.4 which is reduced to 2.5 with the effective use of SSTS. It is found that the percentage sag improvement from fault condition to the recovered condition is 6.05.

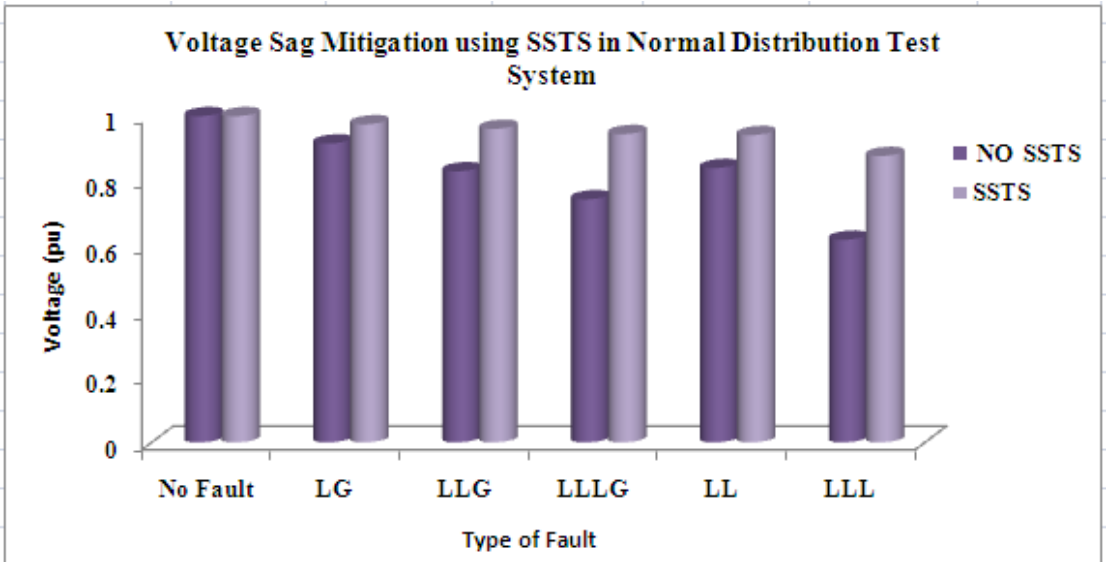

Type of fault	NO Fault	LG	LLG	LLLG	LL	LLL
NO SSTS	1	0.916	0.831	0.745	0.841	0.621
SSTS	1	0.975	0.961	0.945	0.942	0.878

Fig. 4.32: Load voltage at PCC in normal distribution test system without and with SSTS

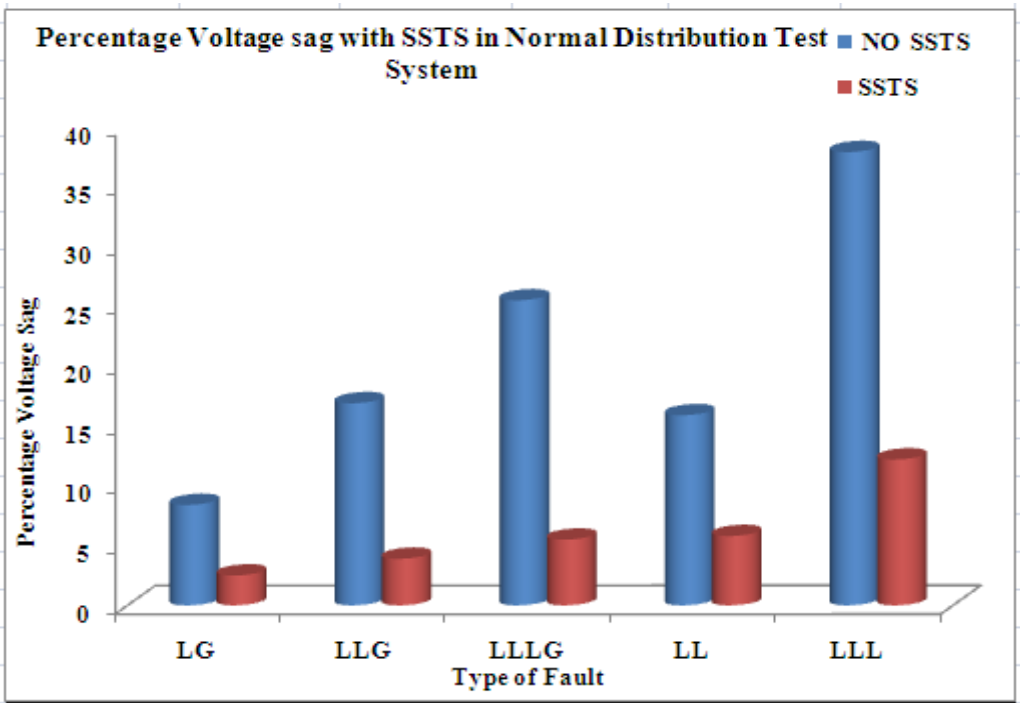

Type of fault	LG	LLG	LLLG	LL	LLL
NO SSTS	8.4	16.9	25.5	15.9	37.9
SSTS	2.5	3.9	5.5	5.8	12.2

Fig. 4.33: Percentage voltage sag in normal distribution test system without and with SSTS

4.4.2 Wind integrated Distribution Test System

In the wind integrated normal distribution test system, the voltage sag occurring at different fault conditions and its mitigation using DVR and D-STATCOM are presented in Fig.4.34. It is observed that the PCC voltage is much improved with the use of DVR and D-STATCOM.

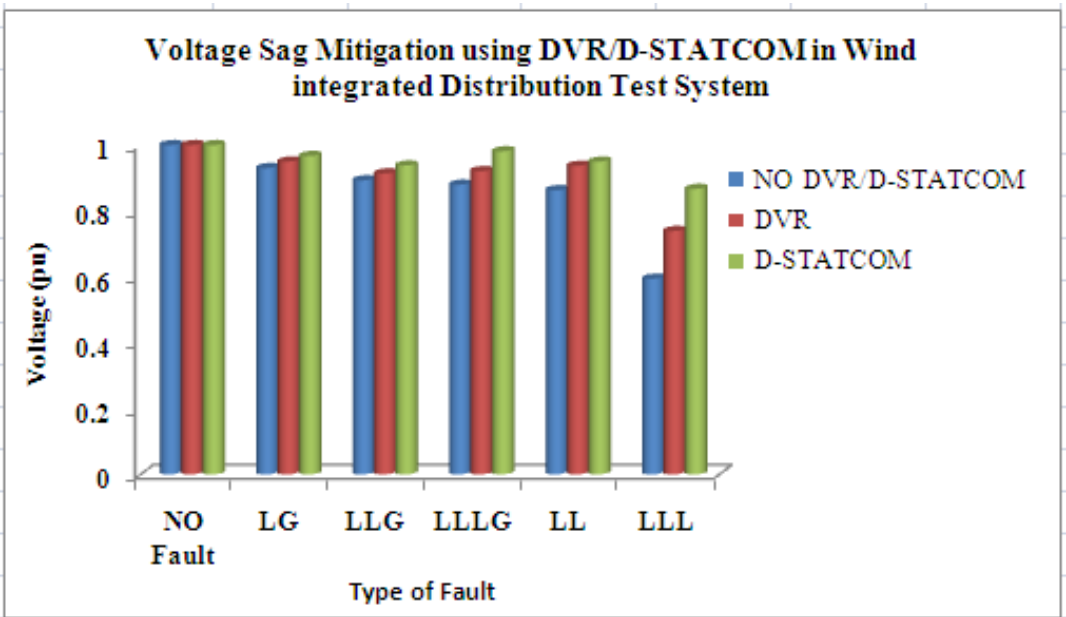

Type of fault	NO Fault	LG	LLG	LLLG	LL	LLL
NO DVR	1	0.93	0.893	0.88	0.863	0.594
DVR	1	0.95	0.914	0.921	0.937	0.739
D-STATCOM	1	0.967	0.938	0.981	0.95	0.867

Fig. 4.34: Load voltage at PCC in wind integrated normal distribution test system without and with DVR/D-STATCOM

Fig.4.35 shows a comparison of percentage sag obtained by DVR, D-STATCOM with NO DVR/D-STATCOM. Under LG fault condition, the percentage sag which was found to be 7.0, is reduced to 5.0 with the integration of DVR and to 3.3 with the use of D-STATCOM. Details of other faults are shown in Fig. 4.35.

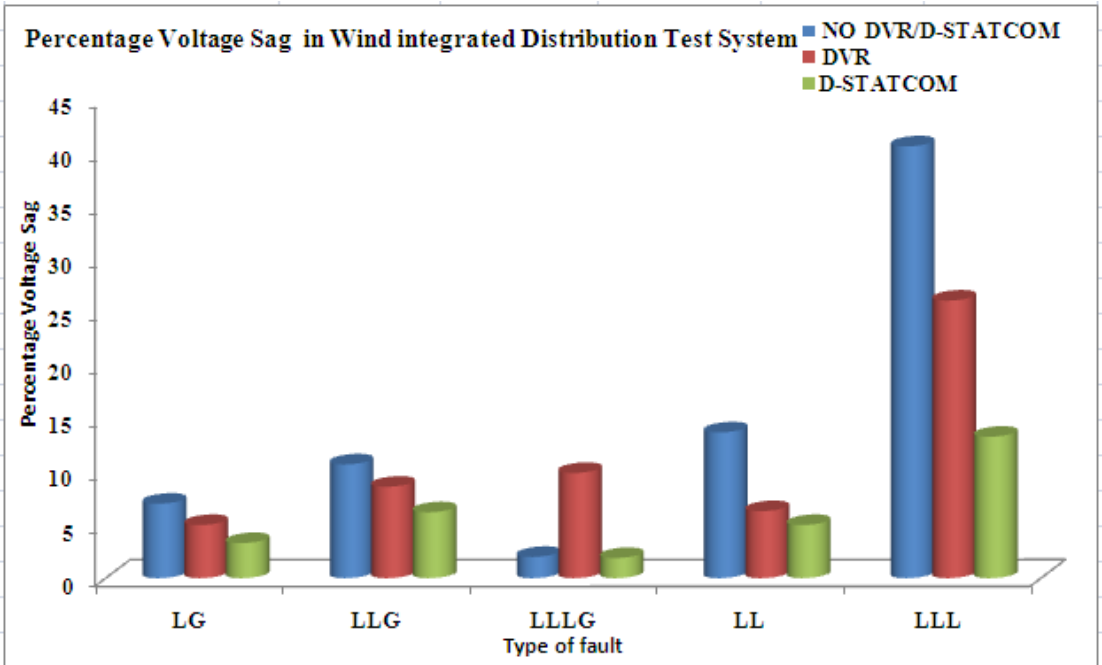

Type of Fault	LG	LLG	LLLG	LL	LLL
NO DVR/D-STATCOM	7	10.7	12	13.7	40.6
DVR	5	8.6	9.9	6.3	26.1
D-STATCOM	3.3	6.2	1.9	5	13.3

Fig. 4.35: Percentage voltage sag in wind integrated normal distribution test system without and with DVR/DSTATCOM

The voltage sag under different fault conditions with and without SSTS is shown in Fig. 4.36. It is seen from Fig.4.37 that the percentage sag under LG fault condition is 2.2 which is completely compensated with the use of SSTS. It is observed that the control scheme of SSTS effectively mitigated the sag for faults except for LLL fault.

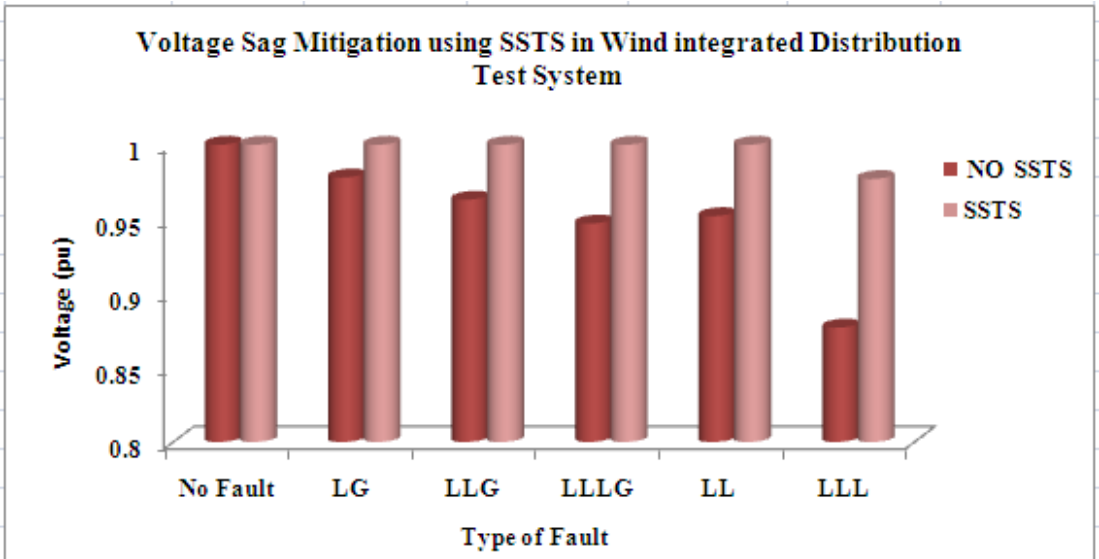

Type of fault	NO Fault	LG	LLG	LLLG	LL	LLL
NO SSTS	1	0.978	0.963	0.947	0.952	0.877
SSTS	1	1	1	1	1	0.977

Fig. 4.36: Load voltage at PCC in wind integrated normal distribution system without and with SSTS

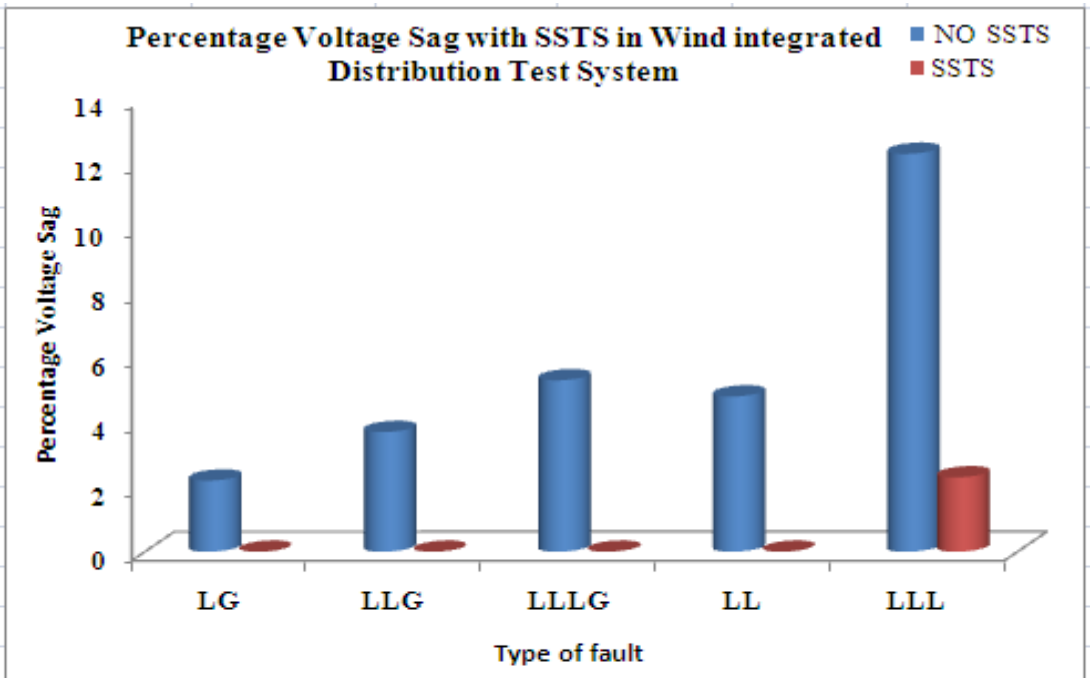

Type of fault	LG	LLG	LLLG	LL	LLL
NO SSTS	2.2	3.7	5.3	4.8	12.3
SSTS	0	0	0	0	2.3

Fig. 4.37: Percentage voltage sag in wind integrated normal distribution test system without and with SSTS

With the integration of wind as well as SSTS, the rms voltage is maintained at PCC in fault conditions. SSTS only deactivate the faulty feeder in favor of a healthy feeder but the wind system regulates the voltage by absorbing or generating reactive power.

4.4 SUMMARY

Power quality issues such as voltage sag in a normal distribution test system as well as in the wind integrated distribution test system analyzed using PSCAD is presented. In the wind connected system, the voltage at the load side is not much reduced than the normal system under different fault conditions. Essentially, it is due to the reactive support given by the wind generator. In this work, it is found that D-STATCOM gave a better improvement in PCC voltage than DVR with an effective PWM control. D-STATCOM is mainly meant for voltage regulation at the customer side and DVR helps to reduce the interference on the source side. From the analysis, it is found that the voltage sag that occurs at different fault conditions in both systems is mitigated by DVR and D-STATCOM, since it injects reactive power to maintain voltage level within limits. Simulation results show that the voltage regulation in wind connected system is less compared to the normal distribution system, under different fault conditions. Even though SSTS does not mitigate the voltage drop, it helps to transfer the power from faulty feeder to the healthy feeder at a very high speed.

CHAPTER 5

OPTIMAL ACCESS POINT AND SIZE OF DG IN RADIAL DISTRIBUTION SYSTEM

5.1 INTRODUCTION

Electrical supply industries are facing some crucial problems to satisfy their consumers against the violation of voltage limits, unscheduled power interruptions, poor power quality and reliability. The uninterrupted power with sinusoidal voltage and frequency within the tolerable limit allows the end user equipment to function in its intended manner. The distribution feeder with uninterrupted power makes use of industry to meet their targeted production which results in profit generation. The present scenario reveals that the consumption of electrical energy is sharply increasing in an unpredictable manner [168]. In the recent years, ESI cannot cope up with the customer's requirements at peak hours because the energy consumption is not in step with the possible capacity of generation. The ultimate goal of energy suppliers is to plan and maintain reliable power with proper power quality standards demanded by the end user. One of the effective ways to meet the customer's demand is the integration of distributed generation such as wind, SPV based systems etc., to the grid. A viable option to avoid overloading at the critical time in the densely populated area is, to reschedule the load from one feeder to another with the help of solid-state transfer switch (SSTS) [169], [170].

Addition of DG, CPD etc. to the existing system requires the detailed load flow analysis. In contrast to the transmission system, LF studies in radial distribution system have not yet received the appreciable attention of the researchers. Load flow analysis is very essential for the continuous evaluation of the stability and reliability of the existing power system and effective planning of other alternatives such as DG or system expansion to meet the increased load demand in the future. Because of some peculiarities, the radial system is categorized in a state of ill-condition.

The special features of the distribution network are as follows:

i. Radial or weakly meshed networks
ii. Too long
iii. High R/X ratio
iv. Multi phase, unbalanced operation
v. Unbalanced distributed load

Advantages of the radial distribution system are [171]:

- Minimum initial cost
- Planning, design, and operation are simple.

Its disadvantages are:

- Low reliability factor
- Poor voltage regulation.

Traditional load flow methods such as Gauss-Siedel and Newton-Raphson technique cannot be used to analyze the voltage profile and to compute the losses [172], [173]. And these algorithms do not guarantee any convergence and a chance to give an inaccurate result. Hence a fast and efficient load flow algorithm is required to fulfill the objectives of the load flow analysis. Backward and Forward Sweep Algorithm (BFSA) [171], [174] is proposed for conducting load flow analysis in the radial distribution network and hence to find the voltage at each bus. This method is computationally more efficient since it involves only algebraic equations of the magnitude of the voltage. Also, it saves a lot of computer memory by storing all the necessary data in the vector form.

Since almost 90% of distribution systems are radial, the customer at far end suffers from high voltage regulation. Integration of Distributed Generation (DG) having optimum size at proper location helps in improving voltage profile as well as a reduction in system losses [62]. Deployment of DG has led to the emergence of new concepts like hybrid and smart grid technology. In this regard, it helps in achieving highest reliability and efficiency [175], [176].

Voltage stability is the ability of the power system to maintain steady, acceptable voltages at all buses in the system under normal operating conditions and after being subjected to a disturbance. An unacceptable voltage level leads to instability which may be a cause for the voltage collapse or even blackout [177]. In DG integrated radial distribution system, one of the major challenges faced by electrical supply industry towards system stability is the islanding operation of DG [178]. The improper location and size of DG make a high degree of PQ problem in DG integrated grid system.

Several optimization techniques such as Particle Swarm Optimization (PSO), Genetic Algorithm (GA), Immune Algorithm [179] etc. are used to solve the multi-objective problems like the position and size of multi DG in the radial system [180], [181]. The determination of the possible locations and sizing of DG, to reduce the power losses and to improve voltage profile using BFSA, has not been found attempted in the literature. In this background, a Genetic Algorithm based BFSA is proposed, to find the optimal size of single DG with proper placement in a radial distribution system which alleviates the adverse effect such as the deployment of losses and degradation of voltage profile.

5.2 DISTRIBUTION SYSTEM

The distribution system is the final stage of electrical power system network which carries electrical power from the secondary transmission system to the individual customers. The feeders carry medium voltage up to 11 kV from secondary transmission transformer to distribution transformer located near the customer's premises.

Distribution networks are classified into two:

i. Ring main distribution system
ii. Radial distribution system

5.2.1Ring Main Distribution System

Ring main distribution network made in a way that one ring network of distributors is fed by more than one feeder. It starts at the substation and is connected to the customer area serving one or more distribution transformers or load centers. The conductor of the system returns to the same substation. In this system, the fault or

maintenance of the feeder will not affect the other feeders since the ring distributor is still energized by other feeders connected to it. Generally, the ring main system is not preferred in low voltage generation side or distribution side because its construction requires more switches and conductors. The construction cost is very high and hence it is more expensive than radial distribution system.

5.2.2 Radial Distribution System

Single substation feeding power to one end of the distribution network is called radial system. Power is delivered from the main branch to the sub-branches, and then it is split out from the sub-branches. Radial distribution systems are classified into main feeder type and main and lateral feeder type. Systems without sub-branches are called main feeder type and with sub-branches are named as main and lateral feeder type. The radial network is cheapest and reliable because this configuration has no loops. Each bus is connected to the source via exactly one path and hence it is widely used in thickly populated areas. The main advantage of the radial distribution system is its simple construction, low initial cost and useful when generation is at low voltage. But the major drawback is that in case of any feeder failure, the power supply of end users is interrupted. The radial network is preferred when the substation is located in the centre of the load.

5.3 METHODOLOGY

The electrical equivalent circuit of 15 bus, 11 kV balanced radial distribution system is shown in Fig.5.1. Line shunt capacitance is negligible at the distribution voltage level. Consider a two bus network having sending end voltage $V_i \angle \delta_i$ and receiving

end voltage $V_j\angle\delta_j$. Load at bus *'j'* is $P_j + jQ_j$ and $I(i)$ is the current flowing from the bus *'i'* to bus *'j'* [171]. The impedance of the feeder line is $R(k) + jX(k)$.

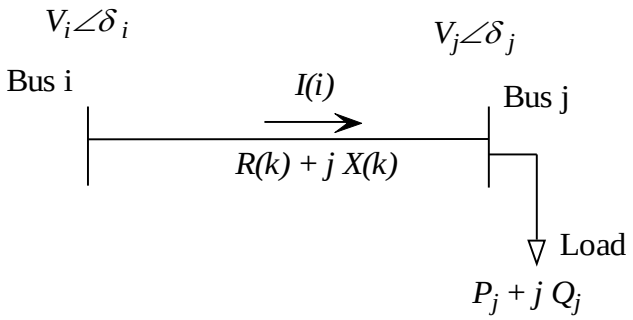

Fig. 5.1: Schematic diagram of radial distribution system with two buses

$$I(i) = \frac{|V_i|\angle\delta_i - |V_j|\angle\delta j}{R(k) + jX(k)} \tag{5.1}$$

Also,

$$I(i) = \frac{P_j - j\,Q_j}{V_j^*} \tag{5.2}$$

from the above equations (1) and (2)

$$|V_j| = \left\{ \left[\left(P_j R(k) + Q_j X(k) - 0.5|V_i|^2 \right)^2 - \left(R(k)^2 + X(k)^2 \right)\left(P_j{}^2 + Q_j{}^2 \right) \right]^{1/2} \left(P_j R(k) + Q_i X(k) - 0.5|V_i|^2 \right) \right\}^{1/2} \tag{5.3}$$

where P_j and Q_j are total real and reactive power loads through node j

P_j = sum of real power loads of all the nodes beyond node *'j'* plus real power load of node j itself plus the sum of real power losses (P_{loss}^{ndg})of all the branches beyond node j

Q_j = sum of reactive power loads of all the nodes beyond node j plus reactive power load of node *'j'* itself plus the sum of reactive power losses (Q_{loss}^{ndg}) of all the branches beyond node j.

Real and reactive power losses in branch *'k'* is

$$P_{loss}^{ndg} = R(k) \times \frac{\left| P_j^{\,2} + Q_j^{\,2} \right|}{|V_j|^2} \tag{5.4}$$

$$Q_{loss}^{ndg} = X(k) \times \frac{\left[P_j^{\,2} + Q_j^{\,2} \right]}{|V_j|^2} \tag{5.5}$$

For MATLAB simulation, the nodes and branches beyond a particular node have to be identified which helps in finding the exact load feeding through that particular node. If all the nodes and branches are identified, it is very easy to calculate voltage magnitudes at nodes with the help of equation 5.3. In successive iterations, the solution gets converged, if the difference between real and reactive power delivered from the substation is less than 0.1 kW and 0.1 kVAr [182]-[185]. The above algorithm is used to find the voltage at different nodes and active and reactive power losses at different branches. Active and reactive supports are given to the branch having high active and reactive power loss employing DG and Custom Power Devices to maintain the voltage stability [186], [187].

5.4 FORWARD BACKWARD SWEEP ALGORITHM (BFSA)

Backward and Forward Sweep Algorithm (BFSA) is a simple, efficient and accurate algorithm that can be implemented to find the voltage profile and hence total real and reactive power losses of a radial distribution system. It converges very fast since node voltages are evaluated directly from Kirchhoff's Voltage Law [171]. Backward/forward sweep method for the load-flow computation is an iterative method in which, two

computational stages are performed in every step of the iteration. Load flow of a single source network can be solved iteratively from two sets of recursive equations. First set of recursive equations for the calculation of power flow through branches starting from the last branch and proceeding in the backward direction towards root node. It starts from the branches in the last node and moves towards the branches connected to the root node. The updated effective power flows in each branch are obtained by considering the bus voltages of the previous iteration. Hence, the bus voltages obtained in the forward path are held constant during the backward propagation and updated power flows in each branch are transmitted backward along the feeder using backward path.

The other set of recursive equations are used to calculate the voltage magnitude and angle of each node starting from the root node and proceeding in the forward direction towards the last node. In this case, Forward Sweep is used for updating bus voltages starting from branches in the first node to the last node. The feeder substation is to be taken as the first node and the voltage of this node is set to $1\angle 0$ pu. The effective power in each branch is held constant to the value obtained in the backward path. Since radial system consists of main feeders as well as lateral feeders, it is necessary to identify the nodes and branches beyond a particular node. BFS algorithm helps in finding the net load feed through each node. IEEE 15 bus radial distribution test system has been taken for the application of BFS Algorithm.

5.5 ALGORITHM FOR LOAD FLOW ANALYSIS

The steps for computing power loss and bus voltages are:

Step 1 : Read the system Data.

Step 2 : Identify the nodes and branches beyond each node.

Step 3 : Calculate the exact load feeding through each node.

Step 4 : Assign bus with larger capacity as Slack.

Step 5 : Assign flat start profile 1pu (per unit).

Step 6 : Perform BFSA to find node voltage.

Step 7 : Check for convergence of node voltage.

Step 8 : If not converged, replace node voltage with updated value, otherwise go to step 8.

Step 9 : Set node voltage.

Step 10 : Calculate net Real and Reactive power losses.

Step 11 : Store net Real and Reactive power losses.

Step 12 : Print the result.

5.6 FLOW CHART OF LOAD FLOW ANALYSIS

Flow chart of load flow algorithm is shown in Fig. 5.2.

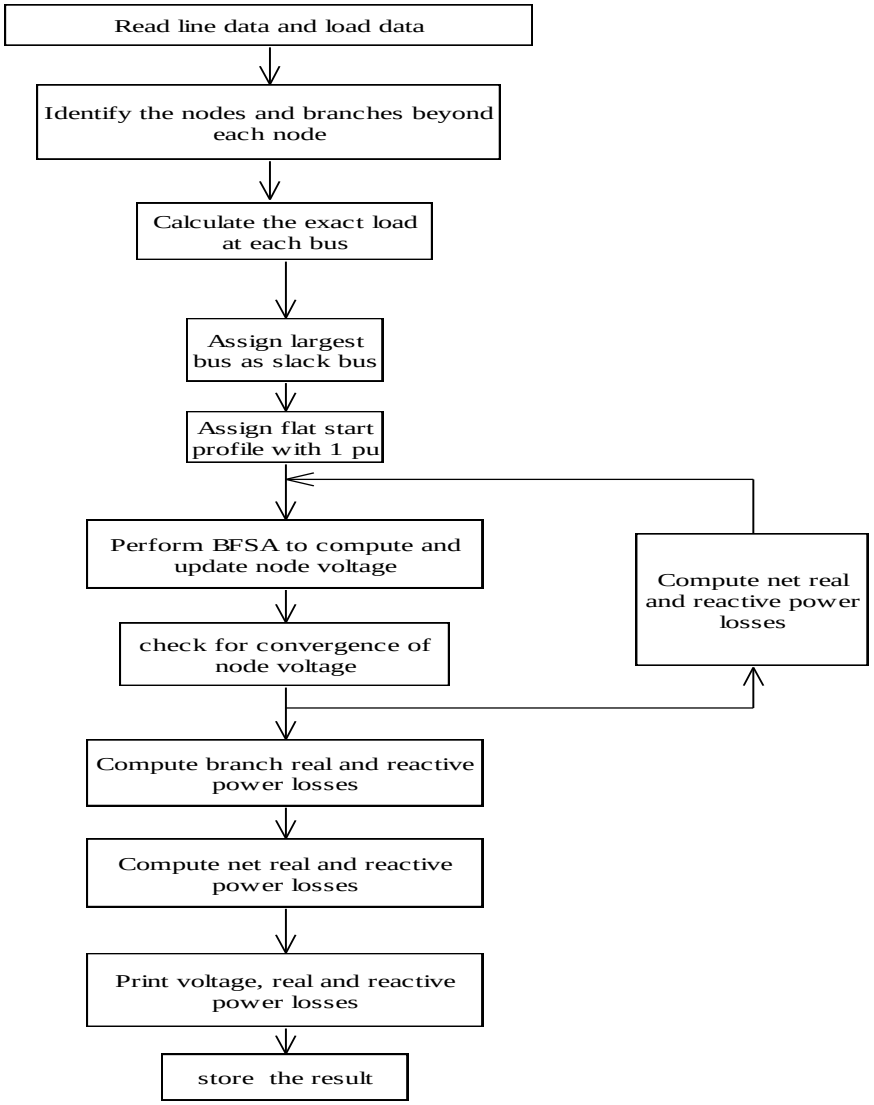

Fig. 5.2: Flow Chart for finding bus voltage and power loss

5.7 GENETIC ALGORITHM

Genetic Algorithm (GA) is one of the computerized search and optimization algorithm in problem-solving, that has inspired from the natural reproduction in fresh life based on Darwinian's principle of evolution "survival of the fittest"[188]-[190]. So GA maintains a population of chromosomes associated with fitness values. It

provides a global optimal solution rather than local optimum for nonlinear problems. GA depends entirely on the responses from its environment and operations such as selection, cross over and mutation, which starts with no knowledge of the real solution. It considers the population is having a number of chromosomes that represent candidate solution [191]. Chromosomes are composed of genes, representing binary strings of fixed length to optimize the various characteristics. Each chromosome is as n- dimensional real values vector where m, the number of optimized parameter and therefore each optimized parameter represents the dimension of searching space.

Parents are selected to mate by their fitness, producing offspring via a reproductive plan. Consequently, highly fit solutions are given more opportunities to reproduce, so that offspring inherit characteristics from each parent. GA processes a number of solutions simultaneously.

In the first step, make population having n individuals or chromosomes that are generated by pseudo-random generators whose individuals represent a feasible solution. This is a representation of solution vector in a solution space and is called initial solution. Then individual members of the population are evaluated to find an objective function value. Finally, the objective function is mapped into a fitness function that computes a fitness value for each member of the population.

5.8 ALLOCATION OF DG ON RADIAL NETWORK

The rating of Distributed generation (DG) ranges from 100 kW to 1500 kW. It can be connected at the substation or any point on the feeder or the load point of the customer. Integration of DG improves the system stability and reliability by reducing feeder loading and thereby lowering energy costs in high demand periods.

The feeder point at which the DG is to be connected can be assigned with the help of power loss minimization or using various indices. In this work, both methods are used for identifying the location of DG. BFS algorithm is adopted to compute bus voltage and power losses. DG is modeled as a negative load so it is independent of the terminal voltage. It is connected in parallel to the load point of the feeder.

Real power at node j with DG, $P_j^{dg} = P_j - P^{dg}$

Reactive power at node j with DG, $Q_j^{dg} = Q_j - Q^{dg}$

where, P_j and Q_j is the real and reactive power of the load connected to j^{th} node and P^{dg} and Q^{dg} are the real and reactive power of the DG connected to j^{th} node. In this work, Q^{dg} is taken as 0 kVAr.

5.8.1 Objective Function

The power loss is computed for different ratings of DG placed at each feeder point. To find the optimal size of DG, power loss minimization is taken as the objective of the problem. GA is used to optimize the size of DG.

$$P_{loss}^{ndg} = \sum_{k=1}^{N-1} R(k) \times \frac{\left| P_j^{\,2} + Q_j^{\,2} \right|}{\left| V_j \right|^2} \tag{5.6}$$

where, P_{loss}^{ndg} is the power loss without DG. Then, the objective function is:

Minimize:

$$g_{(x)} = \frac{P_{loss(x)}^{dg}}{P_{loss}^{ndg}} \tag{5.7}$$

where, x represents the chromosome value, that is, size of DG in kW. $P^{dg}_{loss(x)}$ is the total system real power loss with DG of x kW rating.

5.8.2 Constraints

The active power generated by each DG (P^{dg}) is restricted by lower and upper limits ($P^{dg}_{\min}$ and $P^{dg}_{\max}$). It is based on the total connected load of the system network.

So the constraints used for the optimization of the DG capacity is

$$P^{dg}_{\min} \le P^{dg} \le P^{dg}_{\max} \tag{5.8}$$

$$V_{\min} \le V \le V_{\max} \tag{5.9}$$

5.8.3 GA Parameters

Binary type coding is used to represent the capacity of DG. It is taken as 0000 to 1111 where 0000 represents NO DG unit and 1111 represents 15 DG units of 100 kW (1.5MW). The decoding of GA solution is based on the same idea by translating a number in the chromosome into the respective DG unit.

GA parameters used are

1. Selection : Roulette wheel selection
2. Cross over : one point cross over with a cross over rate of 0.95
3. Mutation : Bitwise mutation with a mutation rate of 0.05
4. Population Size : 30 individuals

5.8.4 Flow Chart

Flow chart for finding size and location of DG is shown in Fig. 5.3.

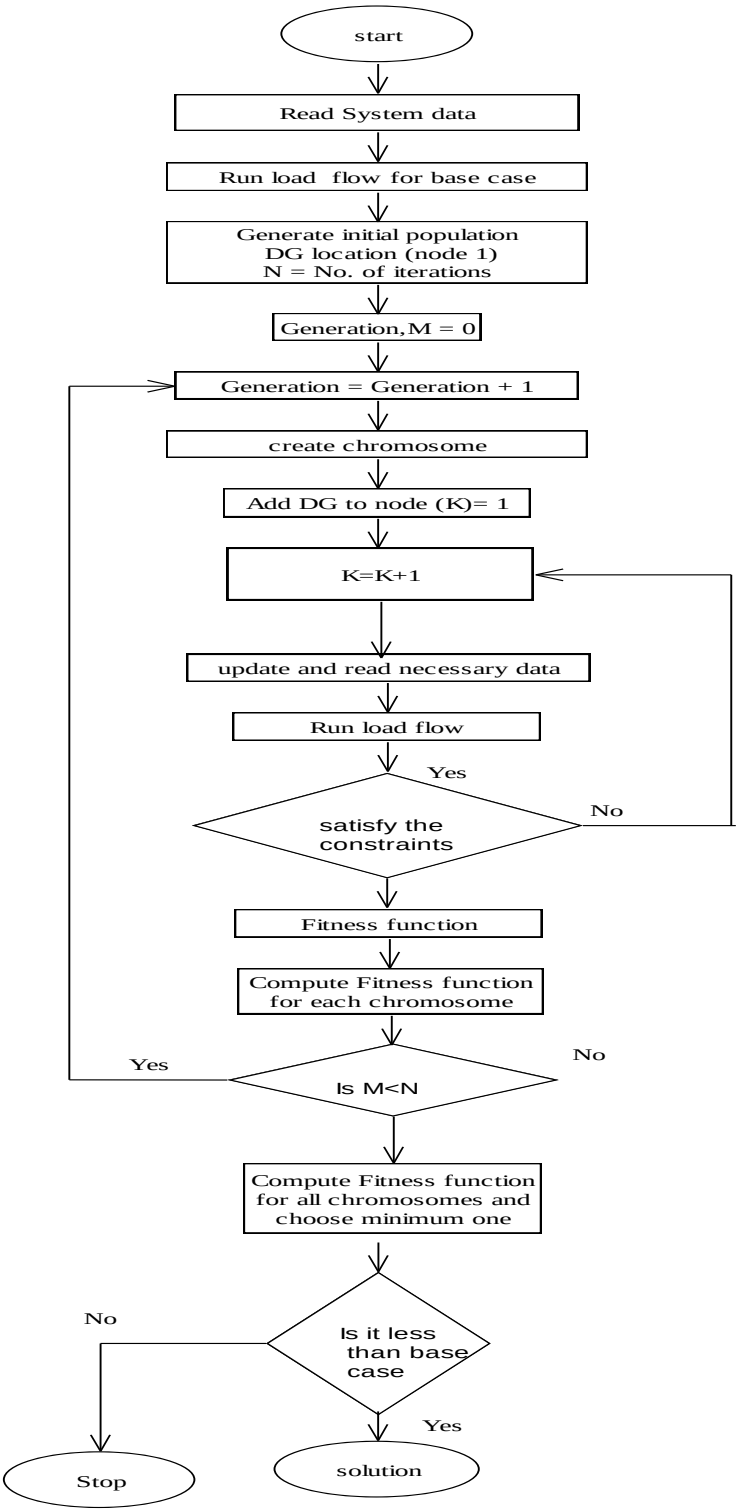

Fig. 5.3: Flow Chart for finding size and position of DG

5.9 MAIN FEEDER TEST SYSTEMS

In main feeder type RDS, the first feeder is originated from the substation and each subsequent feeder is connected to its previous feeder. It is mainly used for bulk consumers. The voltage profile of the customers at the far end is not seriously affected. The primary feeder takes power from the distribution substation and feeds it to the loads connected to it through other feeders. For a group of customers, only one substation is acting as a power source.

In this work, IEEE 10 bus and IEEE 12 bus are taken as main feeder type test systems [190], [192]-[197]. There are no lateral branches in these systems. The base voltage and base MVA of IEEE 10 bus and 12 bus are 23 kV, 100 MVA and 11 kV, 100 MVA respectively. In 10 bus system, there are 9 main feeders and 10 buses, and 11 main feeders and 12 buses in 12 bus system. In both systems, bus 1 is taken as a slack bus or substation bus and its voltage is $1\angle 0^{\circ}$.

5.9.1 IEEE 10 bus and 12 bus Test Systems

The single line diagram of IEEE 10 bus and 12 bus test systems are shown in Figures 5.4 and 5.5. In 10 bus test system, the total connected active and reactive loads are found to be 12.368 MW and 4.186 MVAr respectively and in 12 bus system, it is found to be 0.435 MW and 0.405 MVAr respectively.

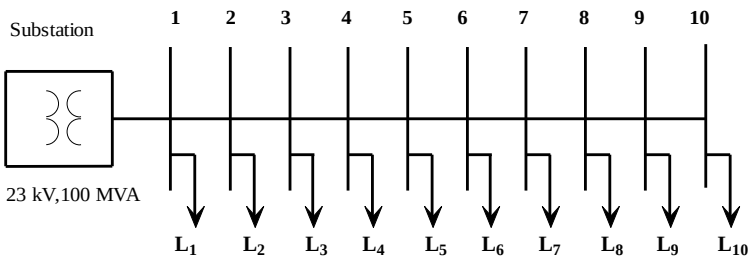

Fig. 5.4: Single line diagram of 10 bus main feeder test system

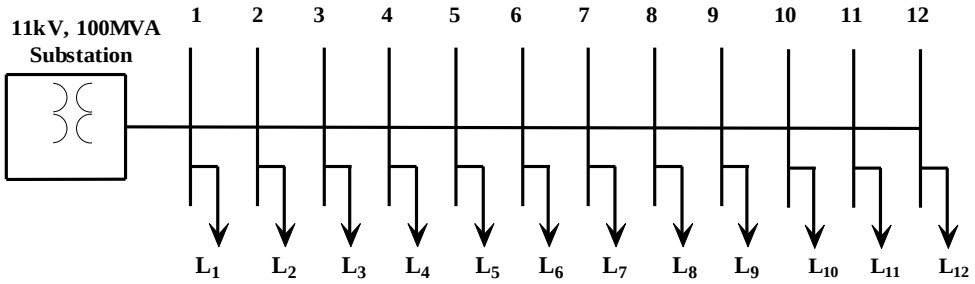

Fig. 5.5: Single line diagram of IEEE 12 bus main feeder test system

Simulation is carried out on both systems to find the voltage profile and power loss with and without DG. The first step is to compute the power loss and voltage profile with no integration of DG. Then, the different size of DG is placed at each bus and the power loss and voltage profile are computed. Both results are compared to observe whether the integration of DG is beneficial or not.

5.9.2 Power Loss and Voltage Profile

From the analysis of 10 bus system without DG, it could be observed that:

i. Bus voltage is 1 pu (23 kV) at node 1(substation), and 0.8424 pu (19.38 kV) is the lowest voltage occurring at node 10 is shown in Fig. 5.6. The voltage at load terminal is limited to $23 \pm 6\%$ (22.94 kV). But, it is seen that the customers at the far end suffer from severe voltage shortage.

ii. Active power loss and reactive power loss are found to be 0.80729 MW and 0.9689 MVAr respectively. It means that 6.527% of connected active load and 23.146% of connected reactive load are found to be as total active and reactive power loss in the system.

iii. The network requires active or reactive power support to maintain the voltage stability in the system.

From Figures 5.6 to 5.8, it is seen that the integration of suitable size of single DG at proper location gave a positive impact on voltage profile and power loss. It is observed that the power loss decreases first and then increases as the size of DG increases.

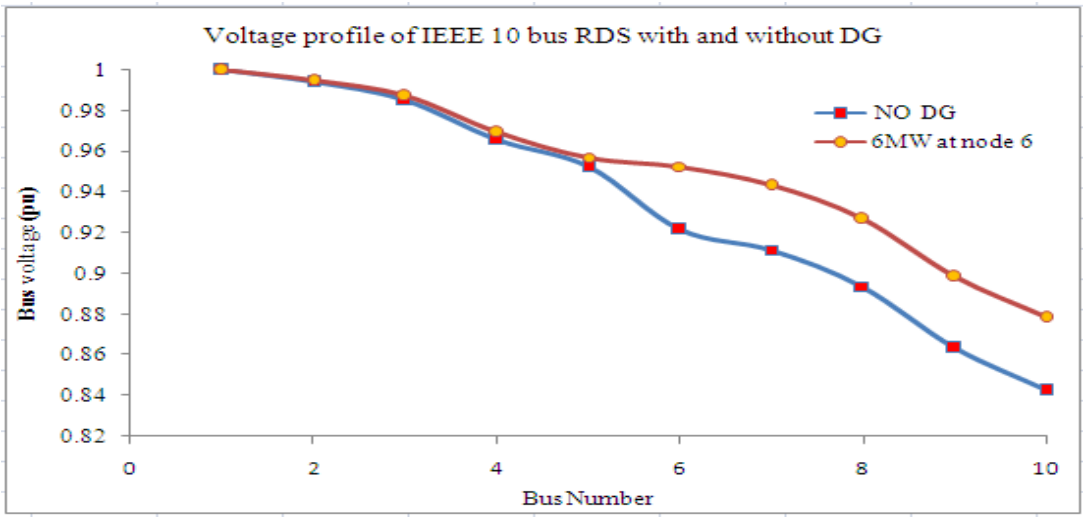

Fig. 5.6: Voltage profile of IEEE 10 bus RDS without and with DG

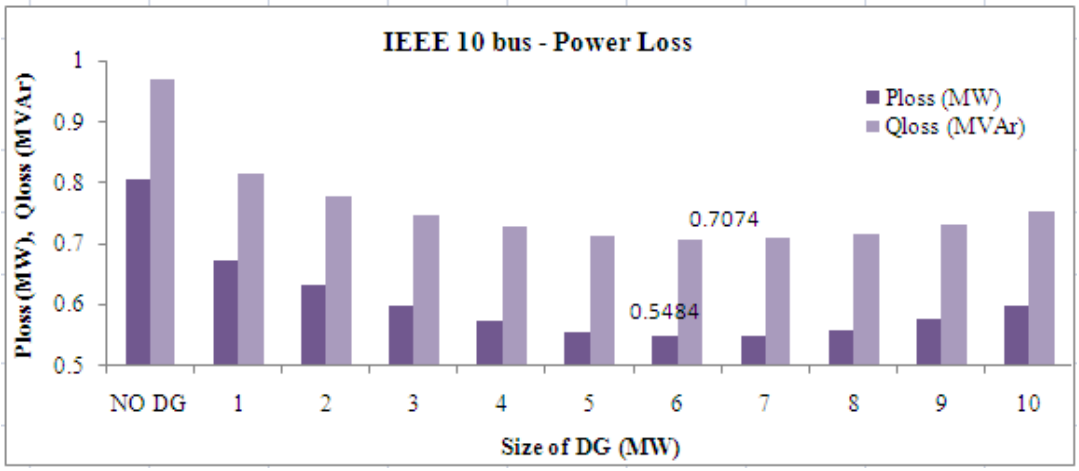

Fig. 5.7: Power loss of IEEE 10 bus RDS when different size of DG placed at bus 6

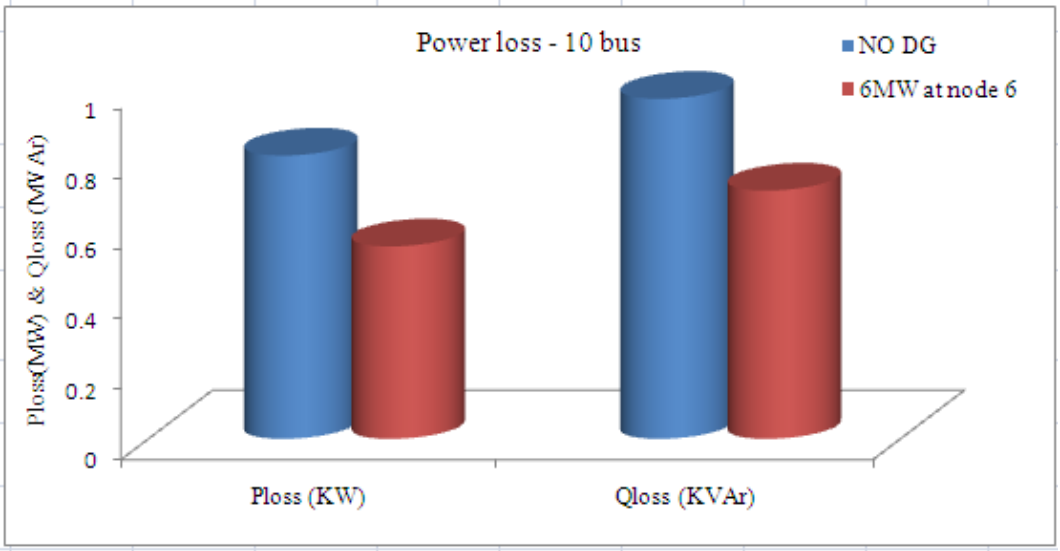

Fig. 5.8: Comparison of power loss without and with DG in IEEE 10 bus RDS

In 10 bus system, by adding DG of size 6 MW at node 6, it is seen that:

a. Voltage profile is improved because the voltage at node 10 is increased from 0.8424 pu to 0.8783 pu (20.2 kV). But this voltage does not lie in the permissible limit (± 6%). Installation of multiple DGs can improve the voltage to these limits.

b. Active and reactive power losses are reduced to 0.54846 MW and 0.70745 MVAr respectively with a loss reduction of 32.06% and 26.98% respectively.

c. Loss reduction with single DG is computed as 0.25883 MW.

Simulation results of 12 bus system are shown in Figures 5.9 to 5.11. The following observations are noted.

i. Improved voltage profile is obtained with the integration of 0.3 MW size of DG at bus 5. The lowest voltage observed is at bus 12 and it is improved from 0.9434 pu to 0.9527 pu. This voltage is within the permissible limit.

ii. Active and reactive power loss is reduced from 0.02069 MW to 0.01761 MW and 0.00806 MVAr to 0.006786 MVAr respectively. Hence, it can be seen that a single DG can reduce 14.88% of active power loss and 15.8% of reactive power loss.

iii. Loss reduction with single DG is computed as 0.00308 MW.

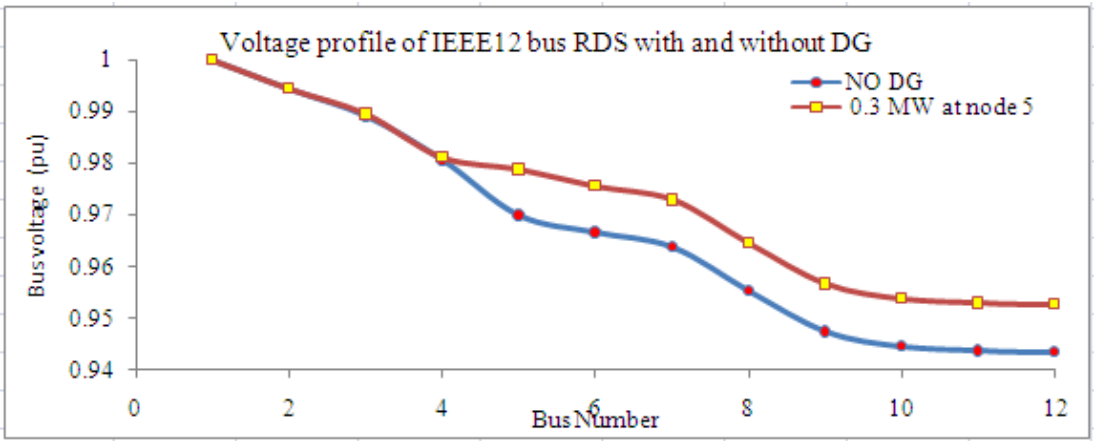

Fig. 5.9: Voltage profile of IEEE 12 bus RDS without and with DG

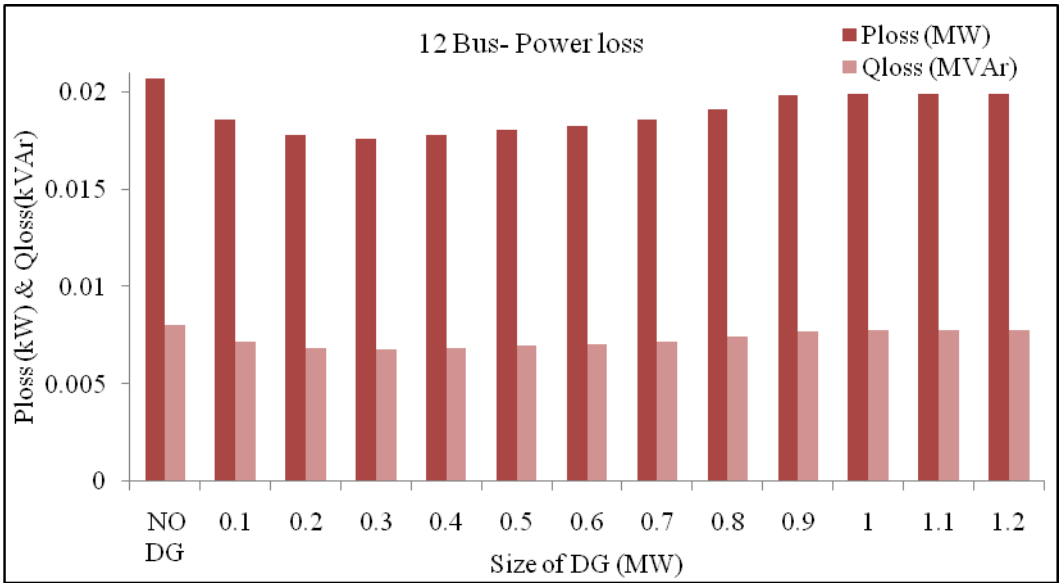

Fig. 5.10: Power loss of IEEE 12 bus RDS when different size of DG placed at bus 5

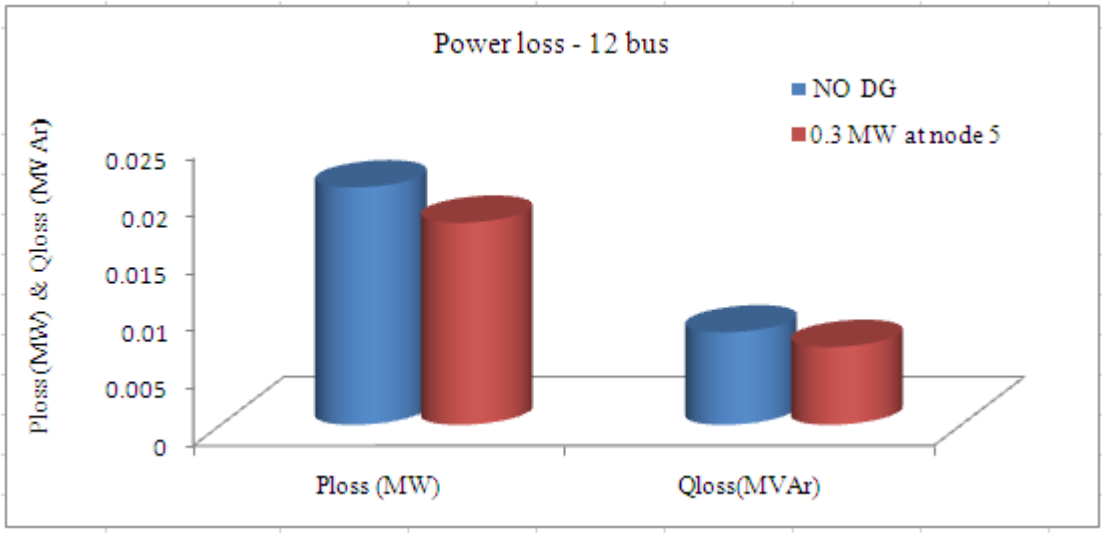

Fig. 5.11: Comparison of power loss without and with DG in IEEE 12 bus RDS

5.10 MAIN AND LATERAL FEEDER TEST SYSTEMS

Main and lateral feeder type radial network consists of lateral feeders which are connected to the main feeder so that the far end customers suffer from poor voltage regulation. The main feeder type radial systems have no lateral feeders.

5.10.1 IEEE 15 bus Test System

In this work, 15 bus, 11 kV radial distribution system connected to the substation is taken as main and lateral feeder type test system is shown in Fig. 5.12. This system consists of 4 main feeders and 10 lateral feeders and the total load connected to this system are 1.2264 MW and 1.251 MVAr respectively. The power factor of the load is treated as 0.7. Loads are represented as constant power and the shunt capacitances are neglected. It is assumed that the three-phase radial distribution networks are balanced and loads are assumed to be constant. The substation consists of a step down transformer with voltages 230/11 kV [171], [198]-[200]. The substation is taken as the slack bus, and its voltage is taken as 1 pu. It is assumed that the slack bus generates the real and reactive power required for meeting distribution losses.

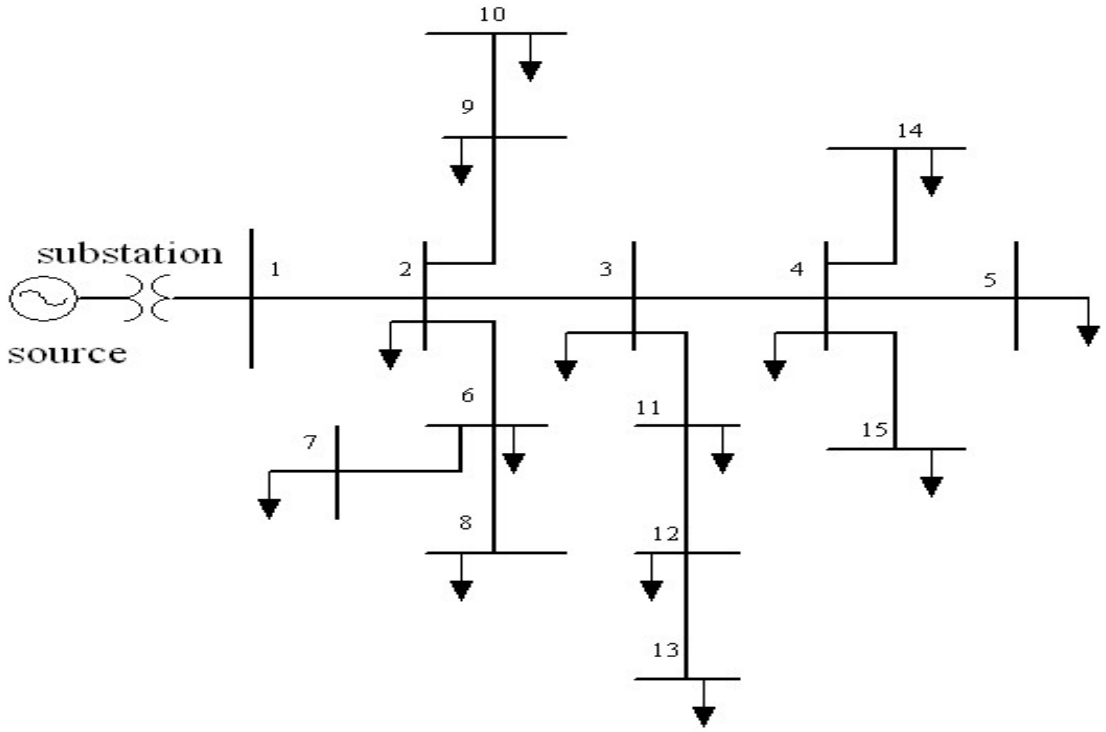

Fig. 5.12: Single line diagram of IEEE 15 bus distribution feeder

5.10.2 Power Loss and Voltage profile

The effectiveness of GA based BFS algorithm has been demonstrated for an 11 kV, 15 bus radial distribution system with constant load condition. In this analysis, DG is to act as a source of active power.

From the analysis of radial network without DG, it was observed that:

a. Bus voltage is 1 pu (11 kV) at node 1(substation voltage) and 0.9445 pu (10.38 kV) is the lowest voltage occurring at node 13 with a drop of 5.55% is shown in Fig. 5.13. The bus having a maximum voltage of 0.9713 pu (10.68 kV) is bus number 2 with a drop of 2.87%. It is observed that the voltage at lateral feeder buses is not within a permissible limit.

ii. Active power loss and reactive power loss are found to be 0.06179 MW and 0.05729 MVAr respectively. It means that 5.038% of connected active load and 4.58% of connected reactive load are found to be total active and reactive power losses in the system. The power loss exceeds the permissible limit (± 4 - 5% of connected load).

In normal operation, the power flow is from generating station to distribution line and it acts as a passive network. Integration of DG changes this scenario with the conversion of the passive distribution network to active network. DG provides power locally to the loads which reduce the current flow in this part of the network. Consequently, there is a considerable reduction in line losses which are dependent on line current through the respective branches. Similarly, the location and size of DG affect the voltage drop in the lines due to the change in line current. DG with power electronic converters provides sufficient amount of reactive power required by the line. The positive impact of DG on voltage profile and power loss is acquired by avoiding the flow of reactive power over large distances. The far end buses experience low voltage due to voltage drop in the lines. The locations of DG near to

the load counter the poor voltage regulation. Hence, the integration of proper size of DG at suitable location increases the overall energy efficiency and system reliability.

To assess the impact of DG on bus voltage, power loss in each branch and total power loss, DG of size 100 kW to 1500 kW with a step size of 100 kW have been placed on individual nodes in a sequential manner. The size of DG is selected in such a way that the maximum size of DG that can be placed in the system is its total active power load plus total power loss in the system. The variations in the above mentioned three parameters have been observed during the placement of one DG at each node individually from node 2 to node 15. Further, for each individual node, the capacity of DG has been varied in the above manner to reach an optimal rating.

It can be seen from Figures 5.13 and 5.14 that the power loss in some branches, particularly 1-2, 2-3 and 2-6 decreased with the integration of DG. This means that the DG reduces the current flow through these branches and hence decreases the power loss.

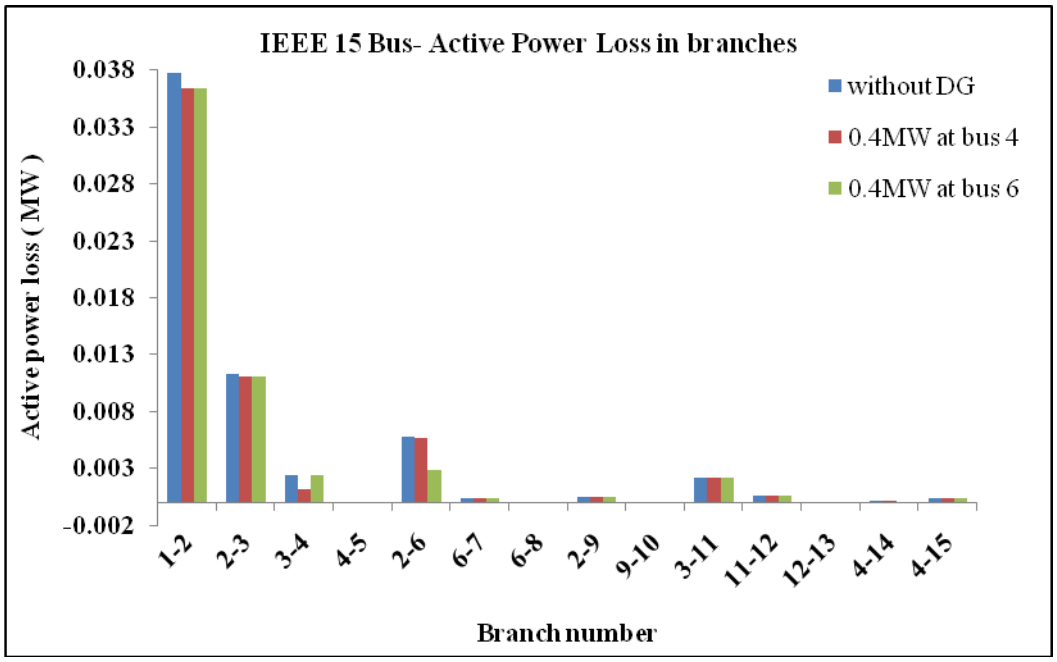

Fig. 5.13: Active power Loss in branches without and with DG

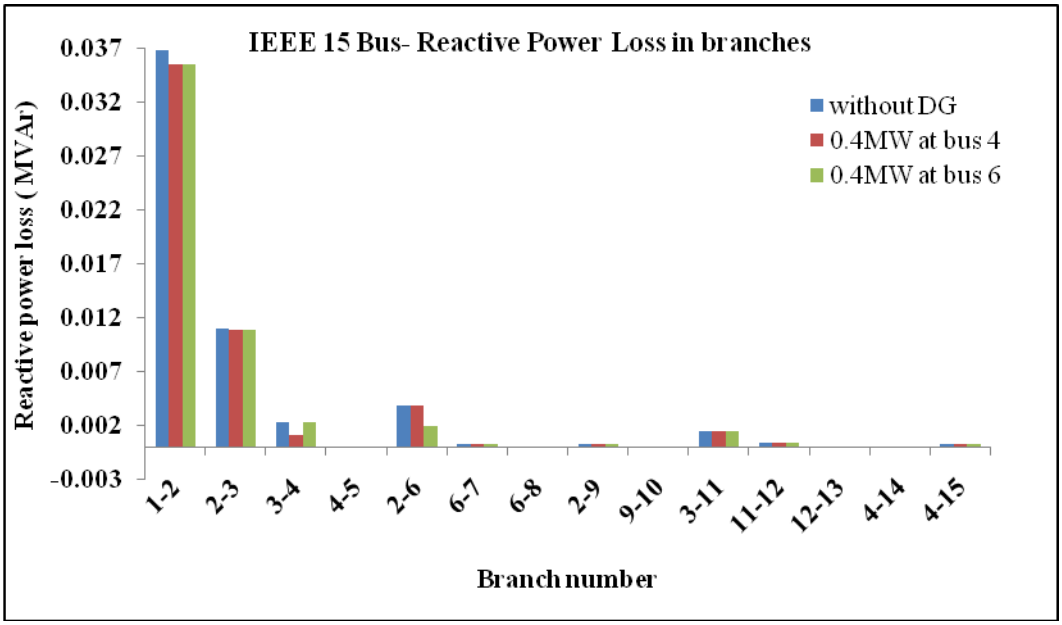

Fig. 5.14: Reactive power loss in branches without and with DG

The impact of the different size of DG at bus 6 on power loss can be seen from Fig. 5.15 and it is observed that as the size of the DG increases, the power loss decreases initially and then increases. Results show that, when DG of size 0.4MW is integrated at bus 6, then the power loss is minimum. The impact of 0.4 MW size DG at each individual node on power loss is shown in Fig. 5.16. Power loss at bus 2 and bus 3 are considerably low compared to bus 4 and bus 6, but these buses are near to the substation; hence it doesn't require any active power support. Moreover, the size of DG obtained is comparatively large and not economical. The analysis showed that 0.4 MW size DG placed at bus 6 and bus 4 provide a power loss of 0.05738 MW and 0.059 MW respectively. On comparing the results shown in Figures 5.17 and 5.18, it is concluded that more reduction in power loss can be attained with the integration of 0.4 MW size DG at bus 6 than at bus 4.

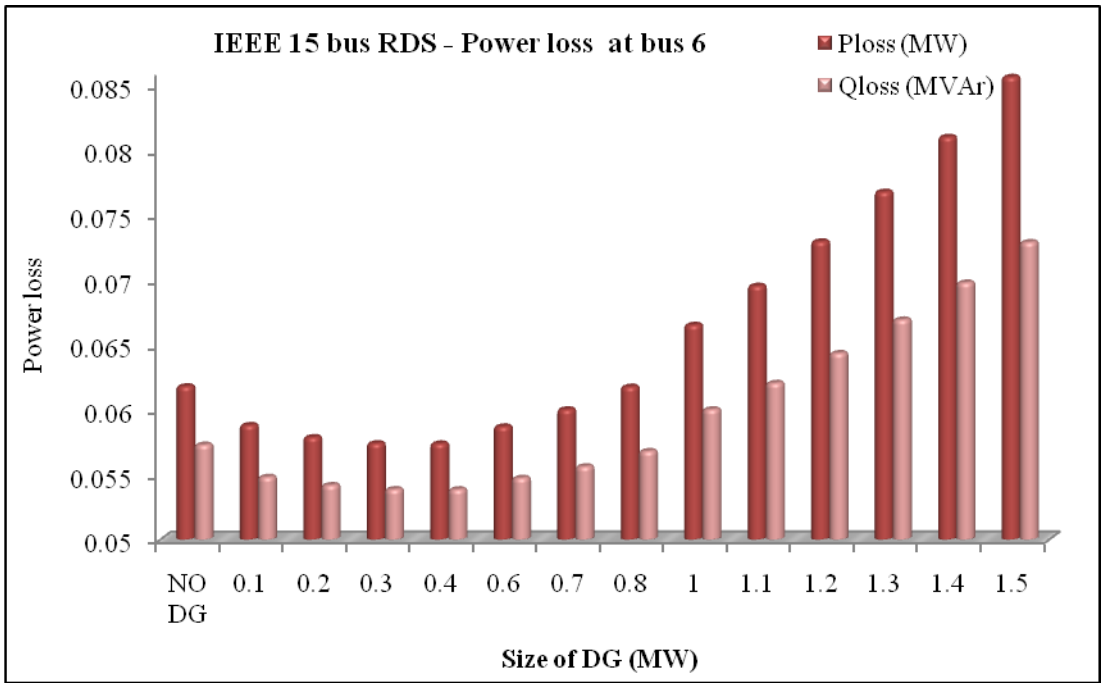

Fig. 5.15: Power loss of IEEE15 bus RDS when different size of DG placed at bus 6

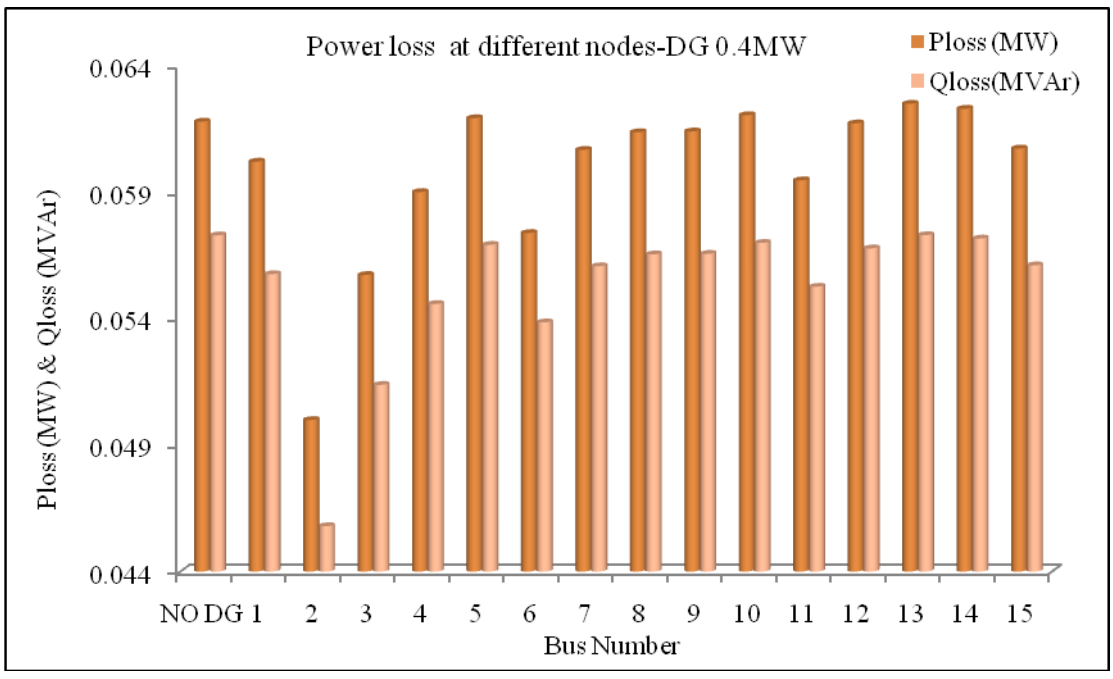

Fig. 5.16: Power loss of IEEE 15 bus RDS when 0.4 MW size of DG placed at different buses

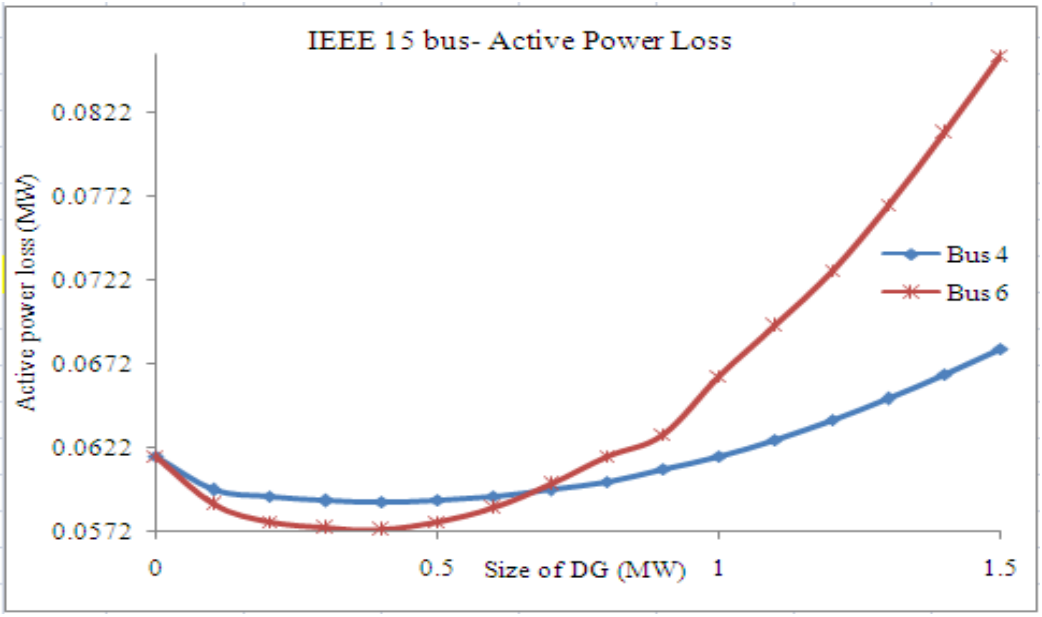

Fig. 5.17: Active power Loss when different size of DG placed at bus 4 and bus 6

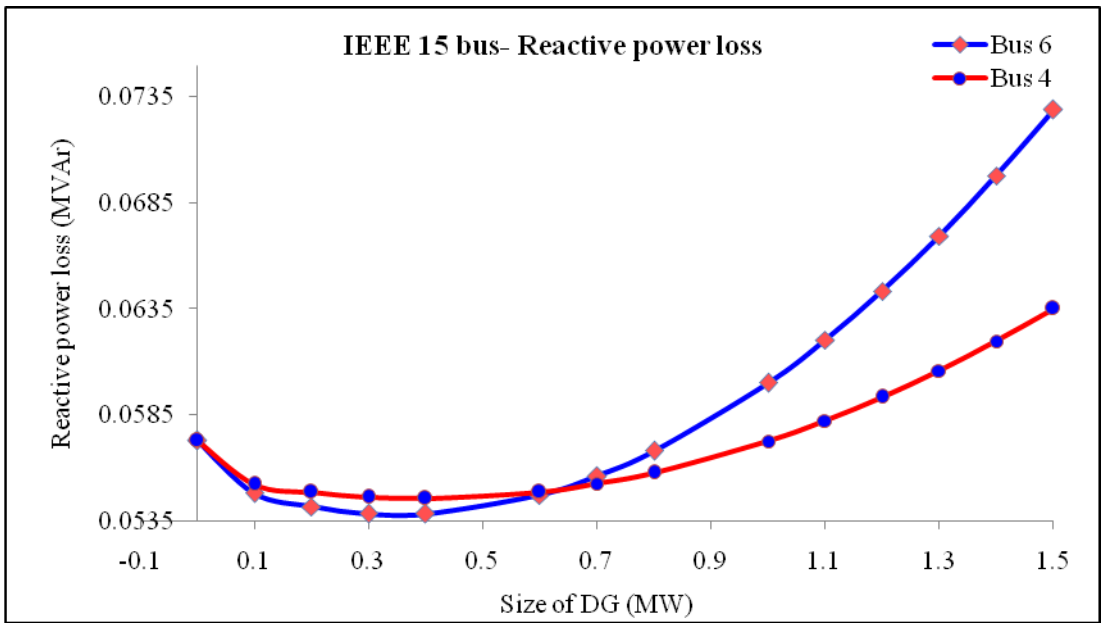

Fig. 5.18: Reactive power loss when different size of DG placed at bus 4 and bus 6

The voltage profile of IEEE 15 bus test system without DG integration and placing of 0.4MW DG at bus 4 and bus 6 are shown in Fig. 5.19. It can be seen that the integration of 0.4MW DG placed at bus 4 and bus 6 gave a positive impact on the bus

voltage. Variation in power loss with the integration of different size of DG at individual nodes is tabulated (shown in Appendix). Further, it is observed that the integration of DG at some nodes may result in considerable reduction in the voltage profile and also an increase in the power loss. Hence, it is inferred that improper location and size of DG can give negative impact on the grid in terms of increased power loss and voltage instability of the whole network.

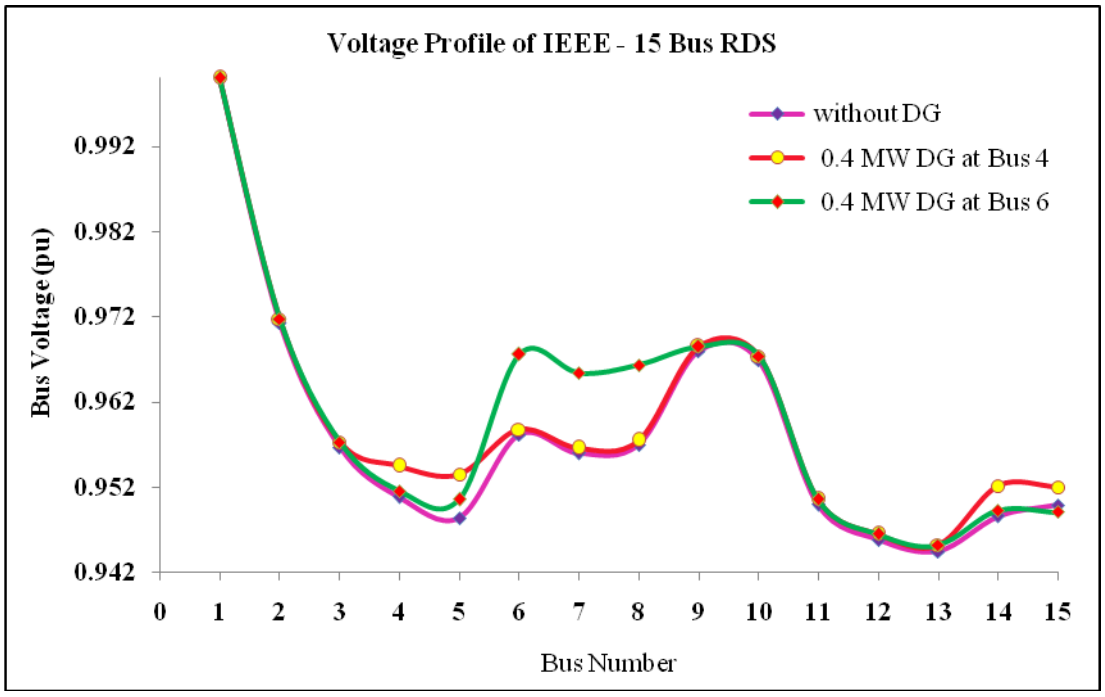

Fig. 5.19: Voltage profile of IEEE 15 bus RDS without and with DG

It is seen from Fig. 5.19 that when 0.4MW DG is integrated at bus 4, the voltage gets improved at some buses. When integrated at bus 6, voltage improvement takes place at some other buses.

Adding DG of size 0.4 MW at node 6, it was seen that:

a. Active power loss is reduced from 0.06179 MW to 0.059 MW and reactive power loss from 0.05729 MVAr to 0.05458 MVAr with the integration of 0.4 MW DG placed at bus 4. Active power loss is reduced to 0.05738 MW and reactive power loss to 0.05385 MVAr with the integration of same capacity of DG placed at bus 6. The reduction of active power losses is about 4.52% and 7.13% for buses 4 and 6 respectively. The corresponding reductions in reactive power losses are found to be 4.73% and 6.0%.

b. Voltage profile is improved and the voltage at node 13 is increased from 0.9445 pu to 0.9452 pu (10.4 kV). This voltage lies in the permissible limit (± 6%). The percentage reduction in voltage is 5.48% and 2.82% respectively. Hence, it is clear that the minimum and maximum voltages at bus 2 and 13 are recovered with 0.074% and 0.05%.

c. It is seen that the integration of 0.4 MW size of DG placed at 6 gives an improved voltage profile than the same capacity of DG placed at node 4.

d. Loss reduction with single DG is computed as 4.41 kW.

5.10.3 Line Loss Reduction Index and Voltage Profile Improvement Index

The objective of the integration of DG is to improve the voltage profile in the way of reducing power losses. Technical benefits of DG are evaluated and quantified with the help of two indices named Line Loss Reduction Index (LLRI) and Voltage Profile Improvement Index (VPII) [191]. The value of these indices should be below unity. Both indices can also be considered for the identification of optimal location and sizing of DG in radial system.

Line Loss Reduction Index

With the integration of DG, the line current is reduced, which helps in reduction of system losses. So the proposed index LLRI can be defined in terms of total losses with and without DG. Line loss reduction index is:

$$LLRI = \frac{P_{loss}^{dg}}{P_{loss}^{ndg}} \tag{5.10}$$

The benefits can be evaluated by this index shown in Equation 5.8 as:

LLRI < 1, Line losses are reduced with the integration of DG

LLRI = 1, No change in line losses with the integration of DG

LLRI > 1, Line losses are increased with the integration of DG

Voltage Profile Improvement Index

This index quantifies the improvement in the voltage profile with the integration of DG. It can be defined as:

$$VPII = \frac{VP^{dg}}{VP^{ndg}} \tag{5.11}$$

Equation 5.9 is used to show the impact of DG on voltage profile of radial network.

VPII < 1, Voltage profile is improved with the integration of DG

VPII = 1, DG has no impact on voltage profile

VPII > 1, Not beneficial

Voltage Profile, $VP = \sum_{j=1}^{N} \left| V_j - V_{ref} \right|$, where V_j and V_{ref} are the magnitudes of j^{th} bus voltage and slack bus voltage (= 1 pu) and N is the total number of buses.

Both indices for 10 bus, 12bus and 15 bus test systems are computed and found that its value is less than unity, as shown in Table 5.1. The improvement in voltage profile and reduction in power loss are attained with the integration of DG to the utility grid. This implies that the net power loss reduction is maximized by minimizing LLRI.

Table 5.1: VPII and LLRI of DG integrated 10 bus, 12 bus, and 15 bus RDS

Index	10 bus	12 bus	15 bus
Voltage Profile w/o DG	0.6694	0.4019	0.6278
Voltage Profile with DG	0.4908	0.3275	0.5928
VPII	**0.7332**	**0.8149**	**0.9442**
Line Loss without DG	807.29	0.02069	0.061794
Line Loss with DG	548.4	0.01761	0.057259
LLRI	**0.6793**	**0.8511**	**0.9266**

5.10.4 Power Loss Reduction

The most important objective of DG integration is to reduce the power loss and improve the voltage stability, by giving active or reactive support at the proper location. The active power loss reduction in 10 bus, 12 bus, and 15 bus are found to be 32.06%, 14.88%, and 7.33% respectively and that of reactive power loss reduction are 26.98%, 15.8% and 6% respectively. Hence, it can be seen that computation of reduction in power loss also yielded encouraging results.

5.10.5 Penetration level of DG

The penetration level of DG [201] in a distribution network can be calculated using equation 5.12.

$$\text{Penetration level of DG} = = \frac{P^{dg}}{P_{tl}} \times 100\% \tag{5.12}$$

where, P^{dg} and P_{tl} are the size of DG and total active power load connected to the system. The penetration level of DG in 10 bus, 12 bus, and 15 bus radial systems are shown in Table 5.2.

Table 5.2: Penetration level of DG in 10 bus, 12 bus and 15 bus RDS

Test System	Penetration level (%)
10 bus	48.51
12 bus	68.96
15 bus	32.61

5.10.6 Total Operating Cost

Integration of DG can minimize the operational cost. To compute total operating cost, the two components, cost of real power supplied from the substation and cost of real power supplied by the installed DG have to be considered. It can be obtained in terms of total power loss of the system and the amount of real power drawn from DG [195]. Hence the total operating cost is

$$TOC = C_1 P_{loss}^{dg} + C_2 P^{dg} \tag{5.13}$$

where C_1 and C_2 are the cost coefficient of real power supplied by the substation and DG in \$/kW. The cost components are taken as C_1 = 4 \$/kW and C_2 = 5 \$/kW respectively. The net operating cost of DG can be reduced as

$$\Delta OC = \frac{TOC}{C_2 P_{\max}^{dg}} \tag{5.14}$$

$$P_{\max}^{dg} = 0.6 \times \sum_{j=1}^{N} P_j \tag{5.15}$$

where j is the bus number. Total operating cost and net operating cost of 10 bus, 12 bus, and 15 bus are given in Table 5.3.

Table 5.3: Operating cost of 10 bus, 12 bus, and 15 bus RDS

Test System	$TOC\,(\$)$	$\Delta OC\,(\$)$	$P_{\max}^{dg}$ (kW)
10 bus	5193.84	0.14	7420
12 bus	1570.44	1.203	261
15 bus	2236	0.6077	735.84

5.11 OTHER IEEE TEST SYSTEMS USED IN CASE STUDIES

The effectiveness of proposed algorithm has been tested on 13 bus, 28 bus, 33 bus, 69 bus and 85 bus IEEE test systems. These buses are main and lateral feeder type test systems which are feeding on single substation only.

5.11.1 Power Loss and voltage Profile

Voltage profile for these buses is shown in Figures 5.20 to 5.24 and power loss in Figures 5.25 and 5.26. Analysis of power loss of the radial network with DG gave confirmed reduction in power loss as compared to that in the radial network without DG. Further, this helps to improve the voltage profile with the injection of active power by DG.

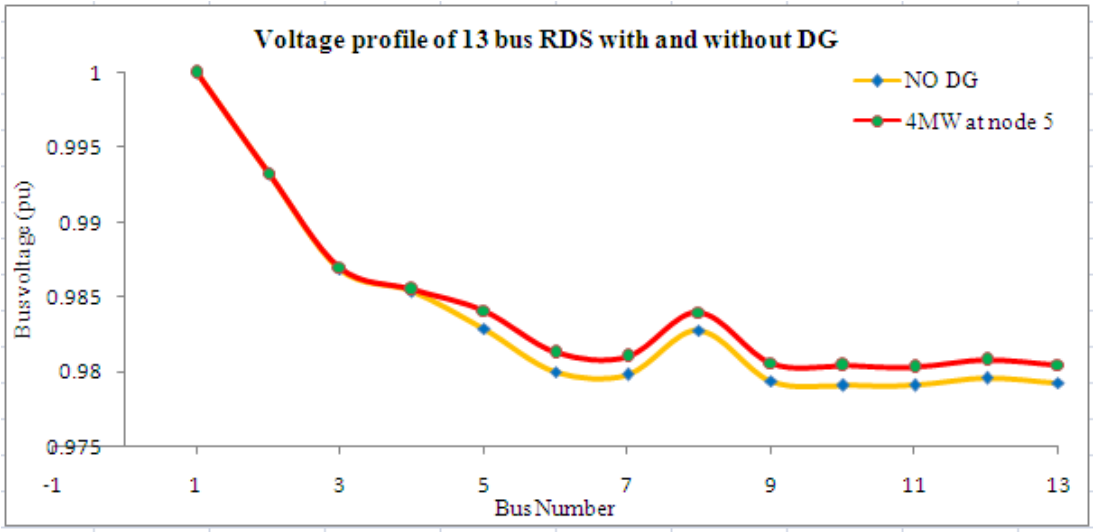

Fig. 5.20: Voltage profile of IEEE 13 bus RDS without and with DG

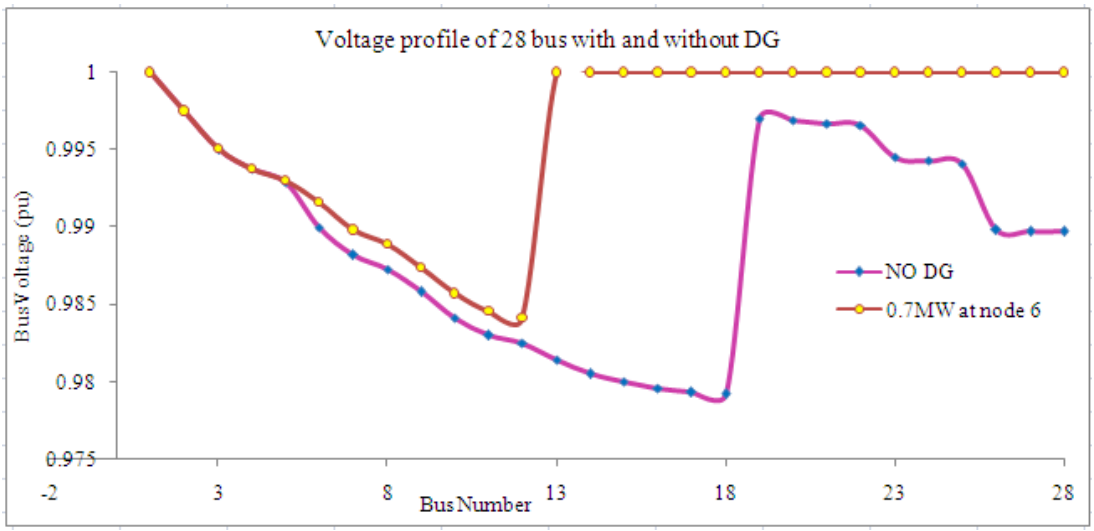

Fig. 5.21: Voltage profile of IEEE 28 bus RDS without and with DG

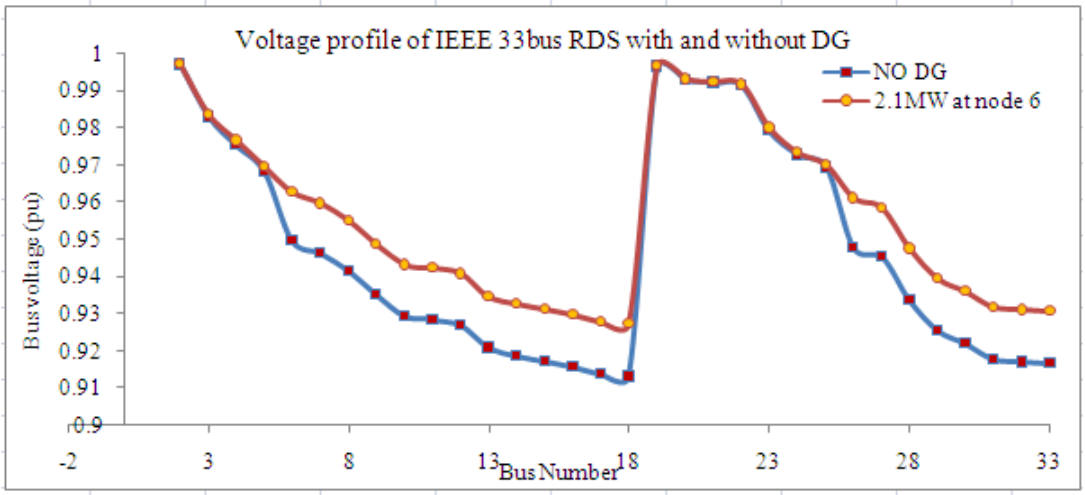

Fig. 5.22: Voltage profile of IEEE 33 bus RDS without and with DG

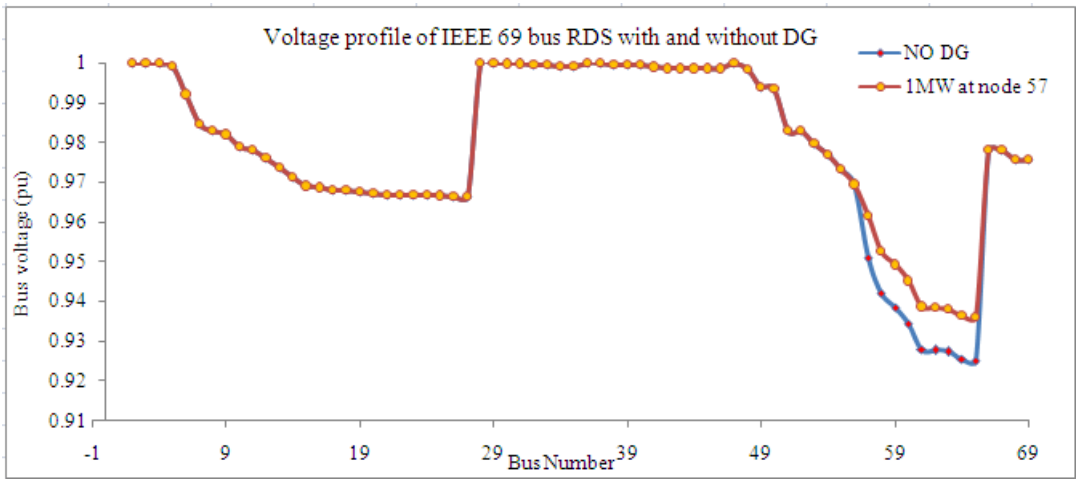

Fig. 5.23: Voltage profile of IEEE 69 bus RDS without and with DG

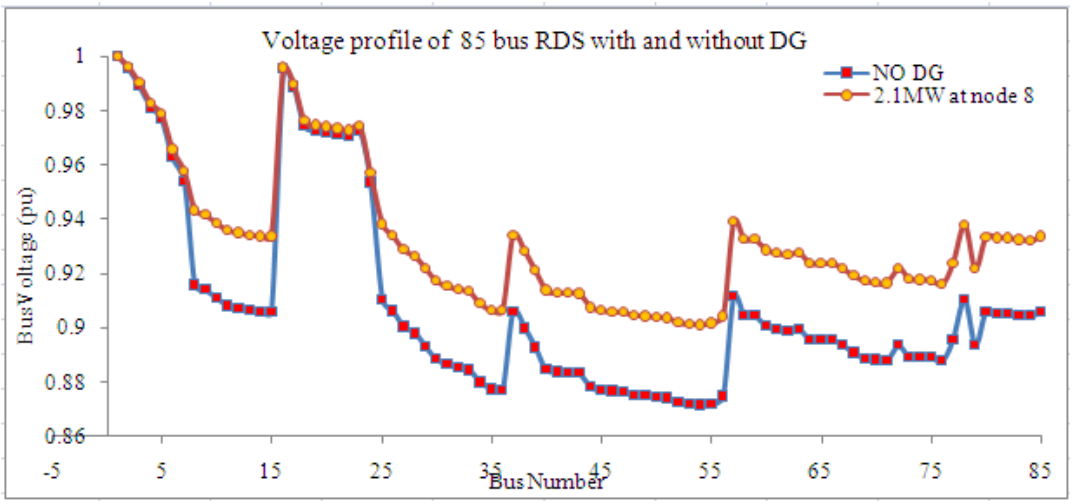

Fig. 5.24: Voltage profile of IEEE 85 bus RDS without and with DG

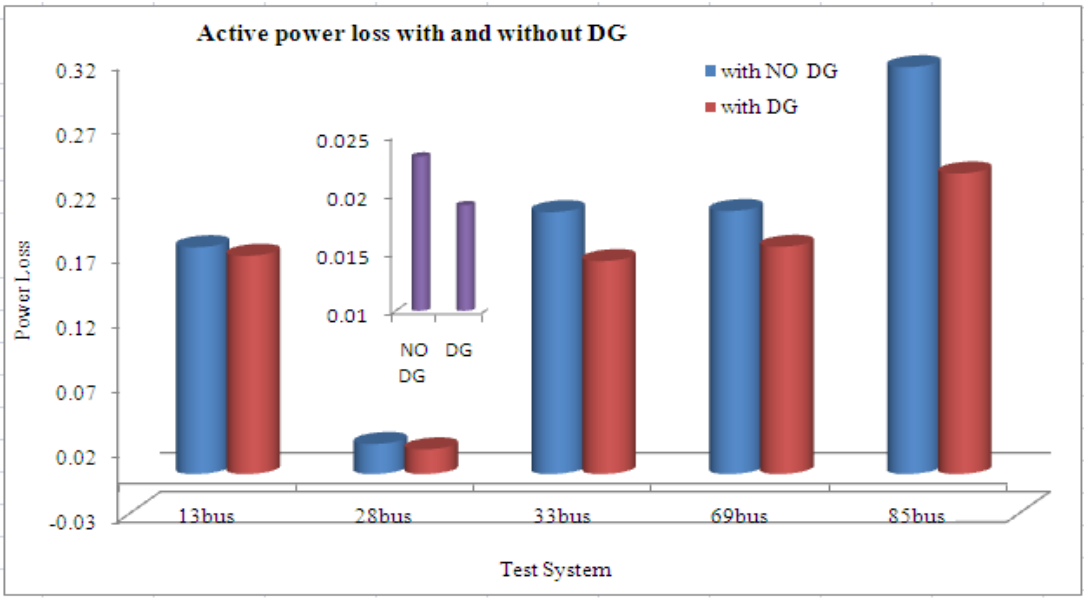

Fig. 5.25: Active power loss of different IEEE test systems without and with DG

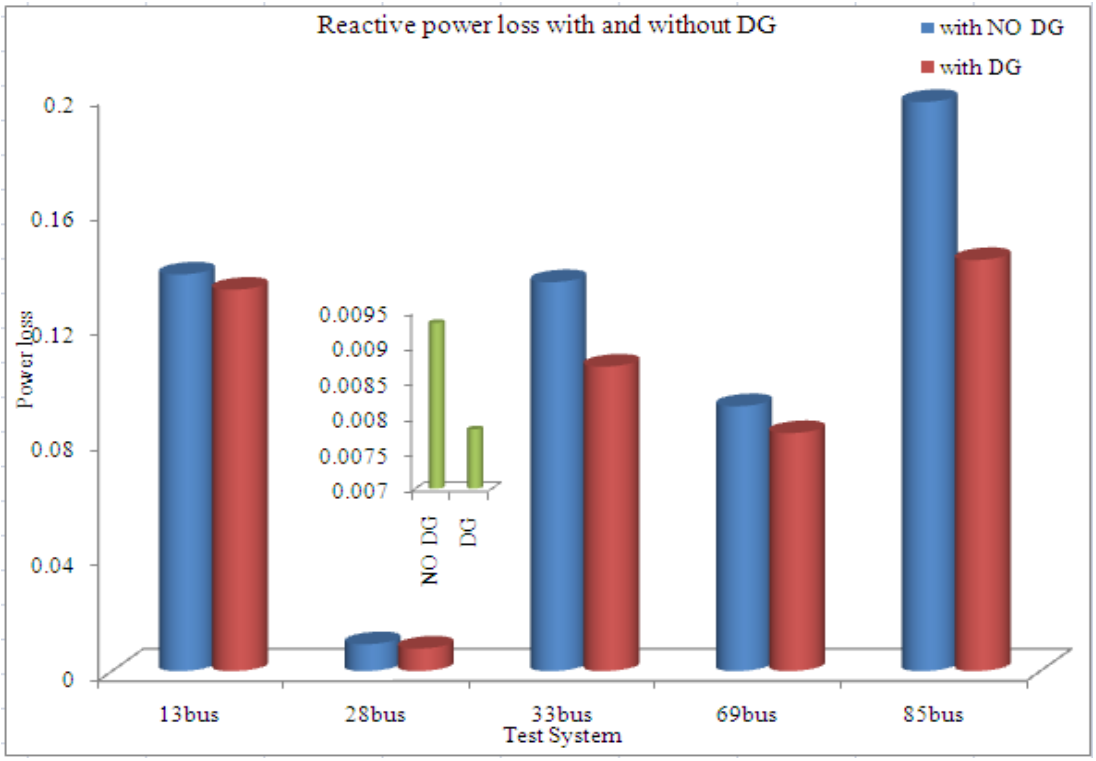

Fig. 5.26: Reactive power loss of different IEEE test system without and with DG

5.11.2 LLRI and VPII

Line loss reduction index and voltage profile improvement index of IEEE test systems used for the case studies are shown in Fig.5.27. Indices of test systems are seemed to be less than one. This means that the penetration of DG provides a positive impact on voltage profile and power loss of radial test system.

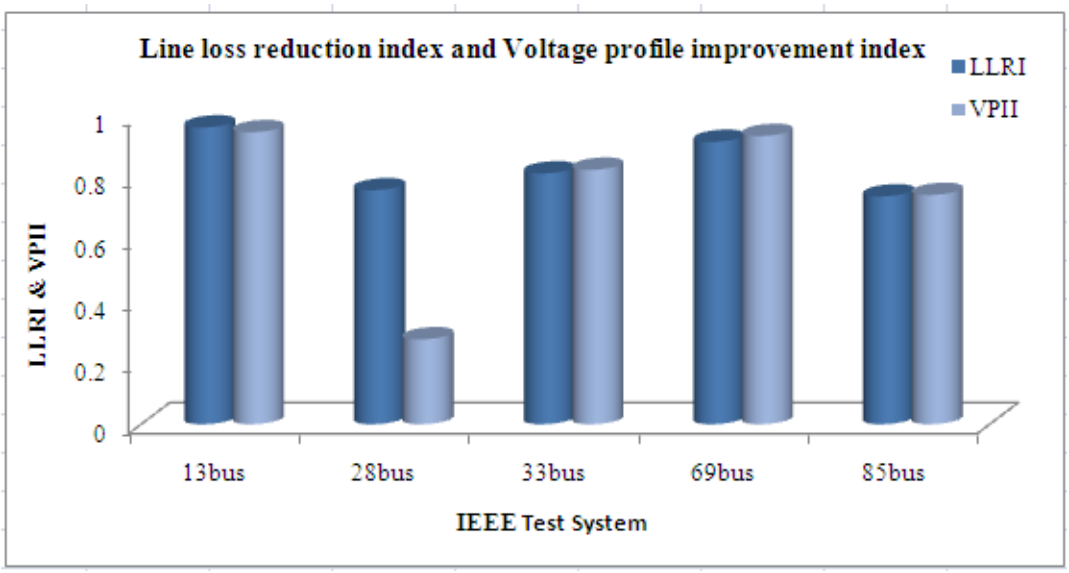

Fig. 5.27: LLRI and VPII of different IEEE test systems

5.11.3 Power Loss Reduction

The active and reactive power loss reduction of IEEE test systems is shown in Table 5.4.

Table 5.4: Percentage reduction of power loss in IEEE test systems

Test System	% reduction(P_{loss}^{dg})	% reduction in (Q_{loss}^{dg})
13 bus	3.7835	3.8322
28 bus	17.991	16.0848
33 bus	18.6865	21.7124
69 bus	13.5973	10.1502
85 bus	26.1292	27.7745

5.11.4 Penetration Level of DG

The penetration level of DG in IEEE test systems is shown in Table 5.5.

Table 5.5: Penetration level of DG in IEEE test systems

Test System	Penetration level (%)
13 bus	37.9651
28 bus	36.8421
33 bus	56.5276
69 bus	26.2889
85 bus	82.8402

5.11.5 Total Operating Cost

Computed values of TOC for IEEE test systems are shown in Table 5.6.

Table 5.6: Operating cost of DG in IEEE test systems

Test System	TOC **(\$)**	ΔOC **(\$)**	$P_{\max}^{dg}$ **(kW)**
13 bus	20675.44	0.6541	6321.6
28 bus	3576.252	0.6274	1140
33 bus	11159.16	1.0013	2229
69 bus	5703.404	0.4998	2282.334
85 bus	11430.24	1.503	1521

5.12 PRACTICAL RADIAL FEEDERS

The proposed approach has been applied on three practical power systems for voltage stability analysis.

i. 18 bus:

Name of the Feeder : Kondaparthy

Name of the Substation to which it is connected : Mamnoor (33/11kV)

Length of the Feeder : 10.55 Km

ii. 22bus:

Name of the feeder : Raghavpur

Name of the Substation to which it is connected : Ghanpur (33/11 kV)

Length of the Feeder : 9.74 Km

iii. 34 bus :

Name of the feeder : Madarmaddi, Dharwad district

No. of tappings : 2

Length of the Feeder : 0.23121 Km and 0.506 Km

The bus data and line data of these feeders are given in the Appendix. BFS algorithm has been applied on these radial feeders to find the voltage profile and power loss. A genetic algorithm is used to find the position and size of DG to be integrated into the grid for maintaining the voltage stability.

5.12.1 Power Loss and Voltage Profile

Voltage profile and power loss of practical systems are shown from Figures 5.28 to 5.31. It is seen that integration of DG improves the voltage profile and reduces the power loss.

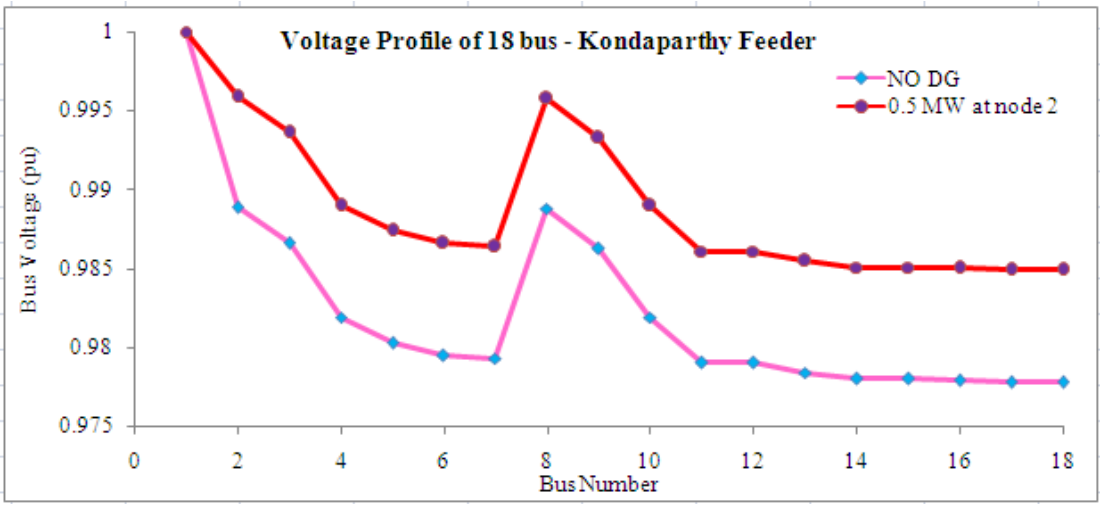

Fig. 5.28: Voltage profile of Kondaparthy feeder without and with DG

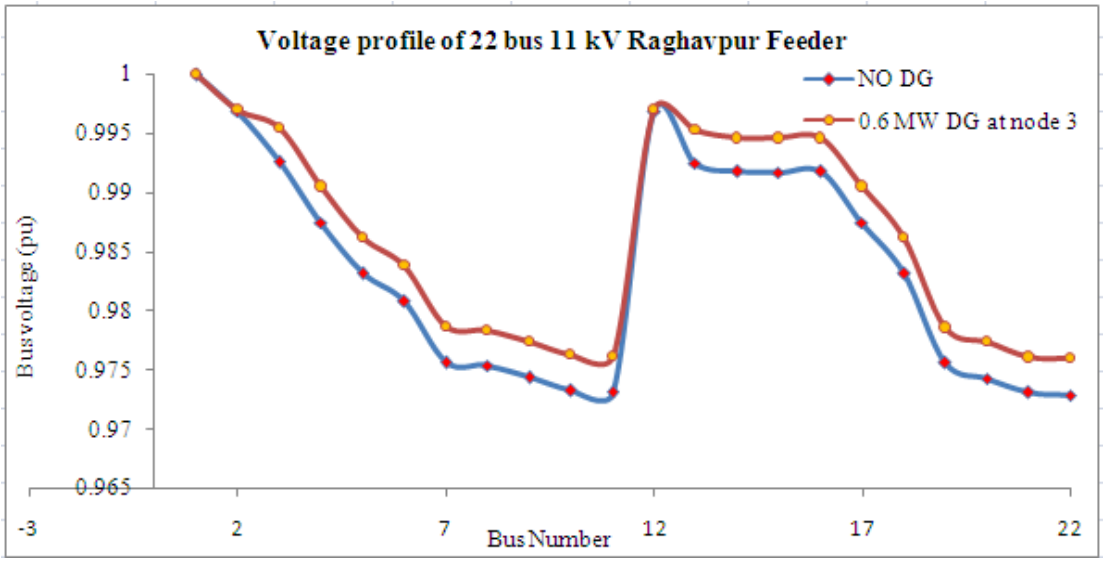

Fig. 5.29: Voltage profile of Raghavpur feeder without and with DG

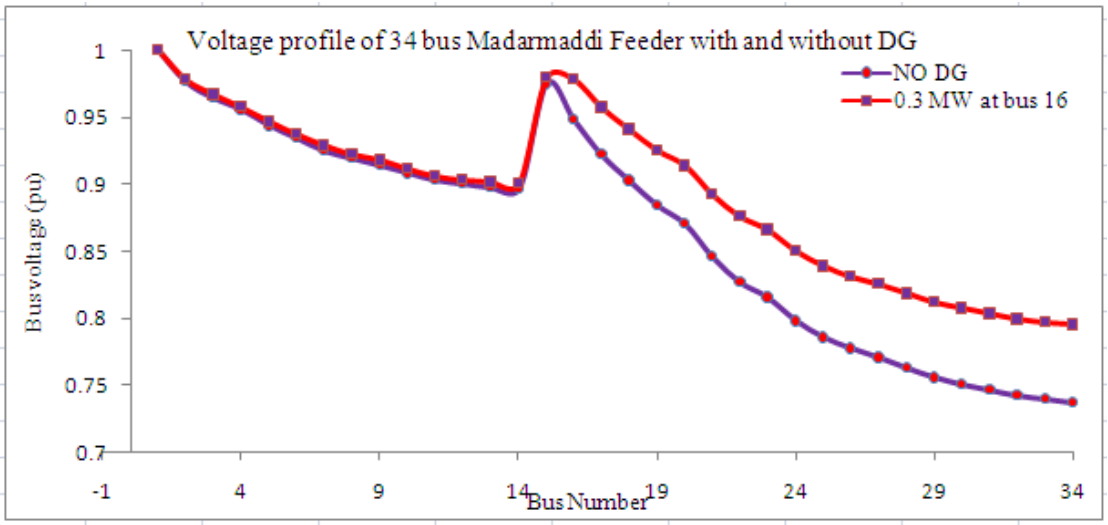

Fig. 5.30: Voltage profile of Madarmaddi feeder without and with DG

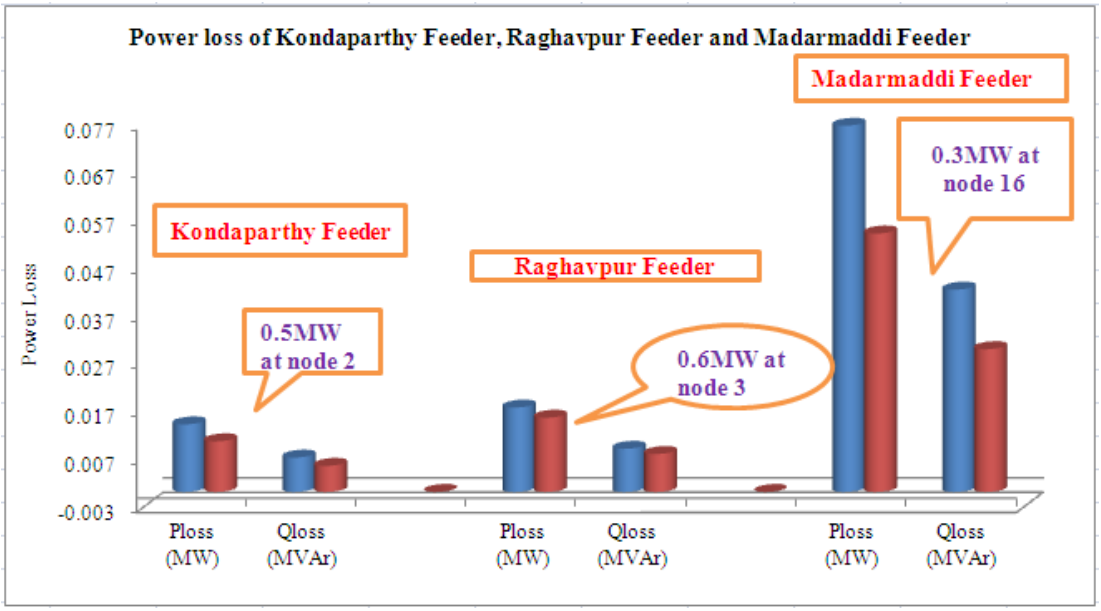

Fig. 5.31: Power loss of practical feeders without and with DG

5.12.2 LLRI and VPII

LLRI and VPII of the practical systems are shown in Fig. 5.32

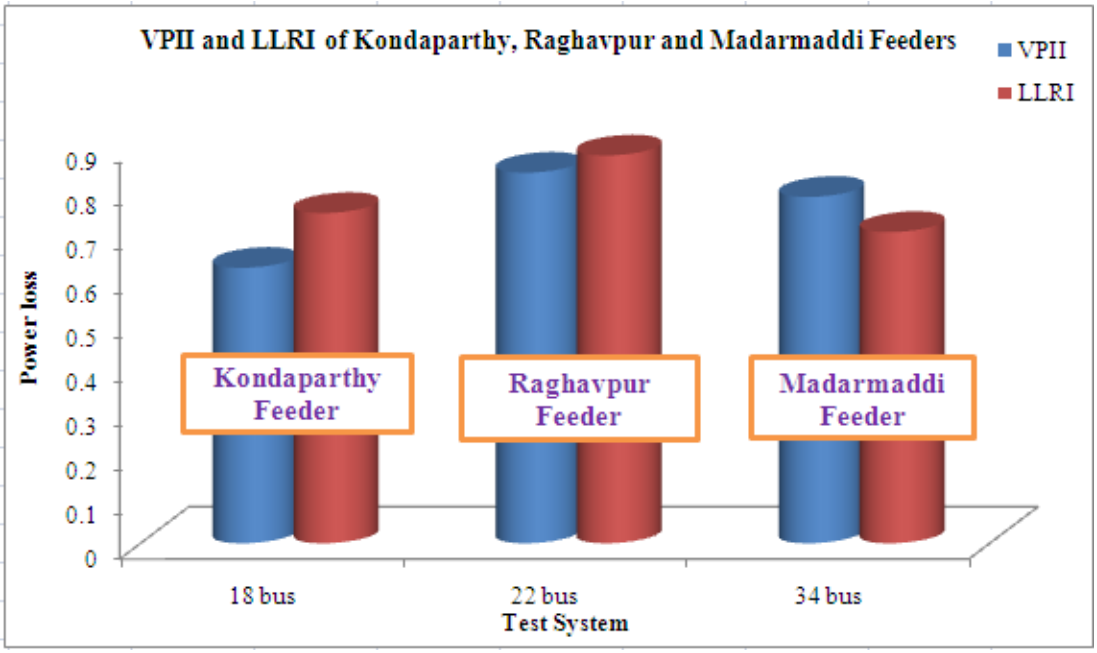

Fig. 5.32: LLRI and VPII of practical systems

5.12.3 Power Loss Reduction

The active and reactive power loss reduction of IEEE test systems is shown in table 5.7.

Table 5.7: Percentage reduction of power loss in practical feeders

Test System	% reduction P_{loss}	% reduction in Q_{loss}
18 bus	25.1	24.06
22 bus	12.05	12.05
34 bus	29.42	29.41

5.12.4 Penetration Level of DG

The penetration level of DG in practical systems is shown in Table 5.8.

Table 5.8: Penetration level of DG in practical feeders

Test System	Penetration level (%)
18 bus	80.183
22 bus	90.592
34 bus	71.839

5.12.5 Total Operating Cost

Operating cost of practical systems is shown in Table 5.9.

Table 5.9: Operating cost of DG in practical feeders

Test System	TOC **(\$)**	ΔOC **(\$)**	$P_{\max}^{dg}$ **(kW)**
18 bus	2542.384	1.359	374.1444
22 bus	3062.152	1.5411	397.3866
34 bus	1716.4	1.3701	250.5588

5.13 MULTIPLE DGs IN RADIAL DISTRIBUTION SYSTEM

Integration of single DG is insufficient to make a positive impact on the radial network and its installation cost is very high compared with multiple DGs. In this regard, the best way to do something in improving voltage stability of RDS is to allocate the optimized size of multiple DGs at proper places [174], [176], [202]-[204]. Integration of multiple DGs at different locations reduces the current flow in branches near to its location so that the net power loss is reduced. In this way, the voltage profile of the whole system can be improved. In IEEE 15 bus test system, it is proved that the active power loss reduction is 7.13% with the integration of 0.4MW size of DG at the 6^{th} bus. When the same DG is placed at the 4^{th} bus, it is found to be 4.52%. From these results, it can be inferred that there exists scope for integration of multiple DGs at various locations for further reduction in power loss and improvement in

voltage profile. Improvement in voltage profile and reduction in power loss are quantified in terms of indices, VPII and LLRI.

From the literature survey, analytical methods for DG allocation which follow two-step procedures may not lead to optimal solution which is a major disadvantage. Further, each DG is added one by one, in case of multiple DG allocation, which may result in missing the optimal solution. Most of the existing meta-heuristic methods considered optimization of DG locations and corresponding sizes sequentially which may not lead to the optimal solution. Even in some methods where sizes and locations were optimized simultaneously, all the buses of the network were considered which increases the search space for locations leading to sub-optimal solutions. Hence, a novel method is required to optimize both DG sizes and locations simultaneously with a reduced searching space.

The algorithmic steps used for multiple DGs in this system are:

1. Run the base load flow (with NO DG)
2. Find the size and location of single DG using BFSA based GA
3. Place DG at the above location and run the load flow
4. Repeat the procedure.

Four cases are considered to show the effectiveness of multiple DGs in improving the voltage stability of IEEE 15 bus radial system.

Case 1: NO DG

Case 2: One DG

Case 3: Two DGs

Case 4: Three DGs

5.13.1 Power Loss and Voltage Profile

Power loss and voltage profile of single DG in comparison with NO DG are discussed in section 5.10.4. From the simulation results shown in Figures 5.33 to 5.35, 7.33% and 25.63% reduction in active power loss, and 6.1% and 25.47% reduction in reactive power loss were obtained with the integration of single DG and two DGs respectively. In this network, integration of three DGs reduced the power loss and improved the voltage profile as shown in Figures 5.33 and 5.34 and Table 5.11. Even though it attains 50% reduction in active power loss, it is seen that the total size of DG exceeds the total connected load. It violates the constraints so that only two DGs can be allocated in this system. Table 5.11 shows the % loss reduction in active and reactive power loss with the integration of multiple DGs.

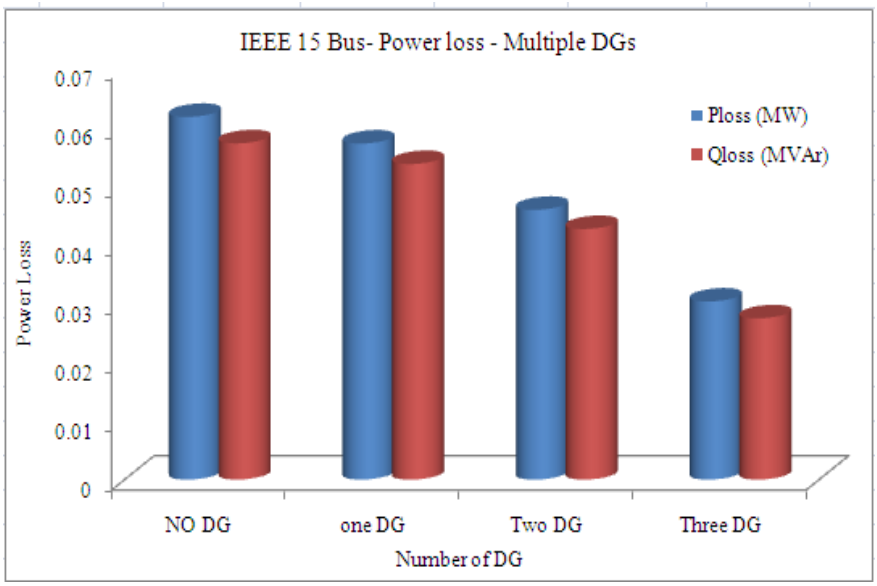

Fig. 5.33: Power loss in IEEE 15 bus RDS with multiple DGs

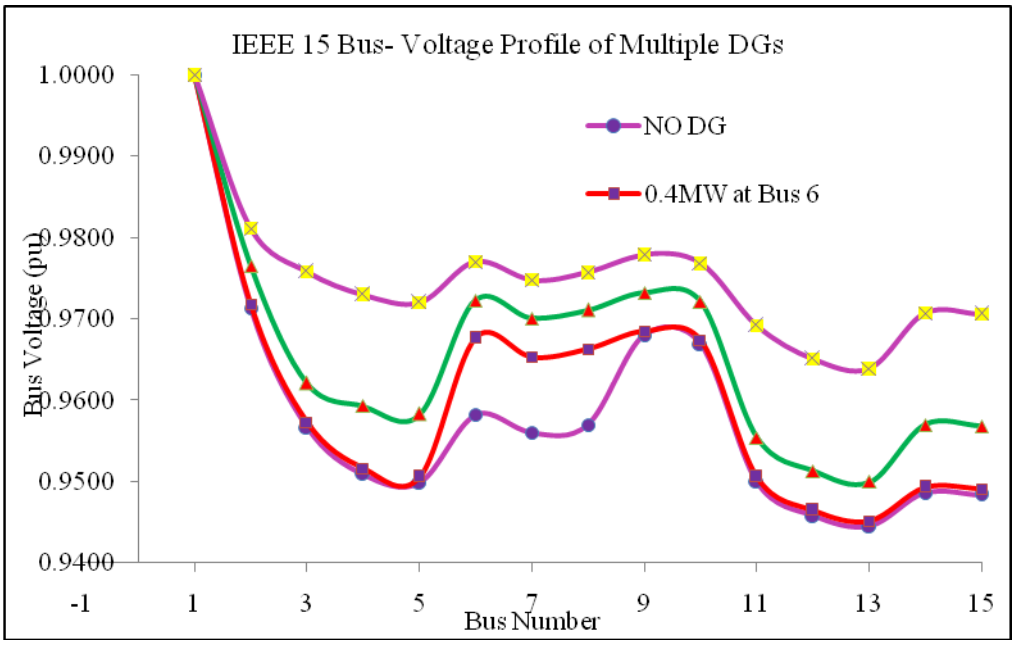

Fig. 5.34: Voltage profile of IEEE 15 bus RDS with multiple DGs

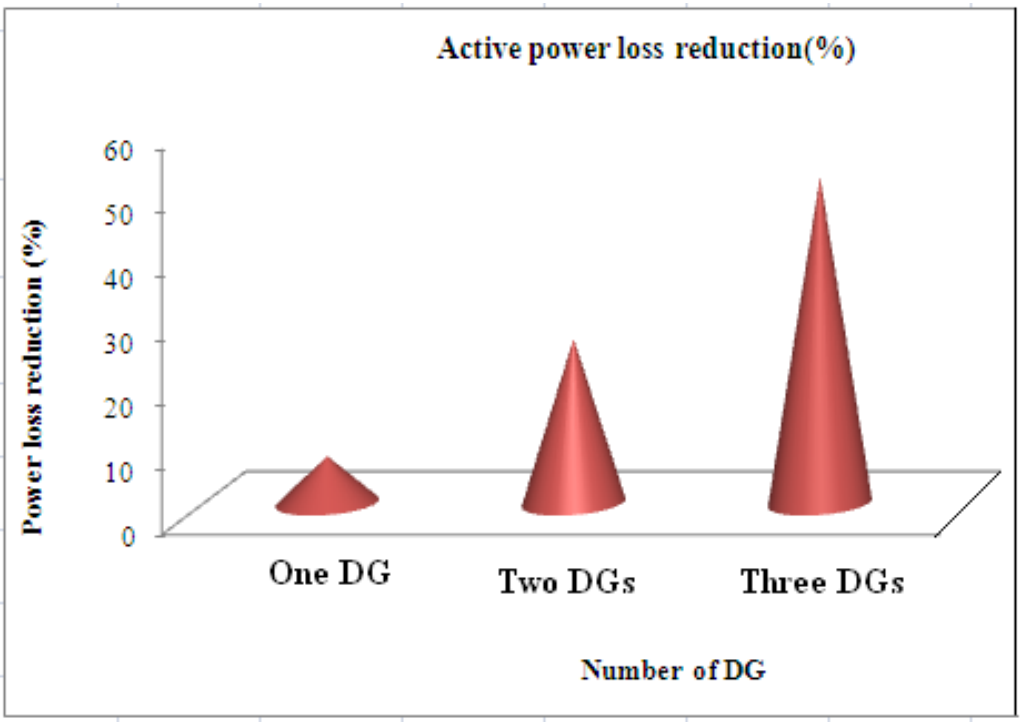

Fig. 5.35: Active power loss reduction with multiple DGs

5.13.2 LLRI and VPII

Technical benefits of DG in practical feeders are shown in Table 5.10.

Table 5.10: VPII and LLRI of IEEE 15 bus RDS integrated with multiple DGs

Number of DG	VPII	LLRI
One DG	0.9444	0.9266
Two DG	0.8195	0.7437

5.13.3 Power Loss Reduction

Percentage reduction in a power loss of IEEE 15 bus is shown in Table 5.11.

Table 5.11: Percentage loss reduction in IEEE 15 bus RDS with multiple DGs

Number of DG	DG size (MW)	Location	Total size of DG (MW)	P_{loss} (MW)	Q_{loss} (MV Ar)	P_{loss} reduction (%)	Q_{loss} reduction (%)
NO DG	NO DG			0.061794	0.057297	0	0
One DG	0.4	6	0.4	0.057259	0.53768	7.33	6.1
Two DGs	0.4	6	0.8	0.045959	0.42701	25.63	25.47
	0.4	4					
Three DGs	0.4	6	1.3	0.030347	0.027471	50.89	52.06
	0.5	3					

5.13.4 Penetration Level of DGs

The penetration level of DG is computed and recorded in Table 5.12. The penetration level exceeds 100% since the integration of three DGs violates the constraint of the maximum size of DG.

Table 5.12: Penetration level of multiple DGs in IEEE 15 bus RDS

Number of DG	Total Size of DG (MW)	Connected Load (MW)	Penetration level (%)
No DG		1.2264	0
One DG	0.4		32.62
TWO DGs	0.8		65.23

5.13.5 Total Operating Cost

Total operating cost and net operating cost are tabulated in Table 5.13.

Table 5.13: Operating cost of multiple DGs in IEEE 15 bus RDS

Number of DG	Total Size of DG (MW)	Ploss (with DG) MW	TOC	Connected load (MW)	P_{DC}max	ΔOC
One DG	0.4	0.057259	2.229	1.2264	0.73584	0.6058
Two DGs	0.8	0.045959	4.184		0.72584	1.1372

5.14 OVERALL FINDINGS

From the analysis, the impact of DG on various systems is concluded as follows:

1. Bus voltage and power loss of radial network are computed with the help of backward forward sweep algorithm.

2. Optimum size and proper location of DG is found out using a genetic algorithm.

3. Computed the power loss and voltage profile by placing the different size of DG at different locations. The results obtained were compared with a genetic algorithm.

4. Considerable reduction in active and reactive power loss was obtained with the integration of single DG.

5. Technical benefits of DG accounted in terms of LLRI and VPII are less than one. Hence, it proved that the location and size of DG in the radial network are optimized.

6. Less searching space and reduced computation time.

7. Computation of penetration level gave an idea about how much active power that can be injected into the network.

8. The maximum size of DG that can be integrated on the network is computed.

9. Total operating cost and net operating cost are calculated.

10. Integration of multiple DG on 15 bus network increases the capacity of overall system so that chance for voltage collapse reduced

5.15 SUMMARY

A novel fast and efficient approach is proposed and presented to identify the suitable location of optimum sized DG/DGs based wind system in an electrical power distribution system for voltage stability enhancement. The proposed approach has been tested on IEEE test systems and practical power systems for illustration purpose. Results obtained for IEEE 15 bus with the proposed approach are compared with those reported in the literature which verifies the applicability and robustness of the proposed method. It offers the benefits of less computation time and storage space. The versatility of the algorithm lends it effectively to computer automation applications in distribution systems. Technical benefits, penetration level and total operating cost are computed. Improvement in voltage stability using multiple DG is also investigated for the IEEE 15 bus test system.

Chapter 6

WEAKEST BUS IDENTIFICATION USING STABILITY INDICES

6.1 INTRODUCTION

The evaluation of voltage stability assessment experiences an increasing attention in the safe operation of the power system. With the restricted amount of power sources and snowballing of power demand of consumers make the existing system to operate at its optimum efficiency [205]. Due to economic and environmental restrictions, distribution networks are not adequately enlarged with increasing loads. Owing to the voltage stability problem, sporadic black outs are occured in several countries. Voltage collapse is the outcome of voltage instability which is the direct cause of black outs. Voltage instability stems from the attempt of load dynamics to restore power consumption beyond the capability of combined transmission and generation systems [206]. Therefore, a detailed study has to be carried out to determine maximum capacity limit just before the system experiences voltage collapse, so that necessary precaution can be taken to avoid system capacity violation.

6.2 VOLTAGE STABILITY

Voltage instability is the major issue faced by a distribution power system due to unpredictable changes in load demand. As the distance between the substation and buses increases, bus voltage reduces which increases power loss. Hence, the system requires active/reactive power compensation to improve voltage profile. Voltage

stability is defined as, "the ability of the power system to provide reactive power or uniform consumption of reactive power by the system itself" [206]. Voltage collapse starts at the most sensitive bus first and then spread out to other sensitive buses. The sensitive bus exhibits some characteristics such as:

- highest critical point
- lowest reactive power margin
- greatest reactive power deficiency
- highest percentage change in voltage

6.3 VOLTAGE STABILITY INDICES

Voltage regulation is the important factor in maintaining the voltage between two buses. Ideally, the drop in the line between two nodes should be zero. In overhead RDS, there is a voltage drop due to the peculiarity of high R/X ratio and hence voltage instability and increased power loss are the major drawbacks. In this system, there is no anti-resistance element to reduce this drop to zero or to improve the voltage regulation. To enhance voltage profile and increasing system efficiency, supporting devices have to be added to the system so that the line current and losses could be significantly reduced and improves the system efficiency [207].

Voltage stability assessment is a major issue in monitoring the power system stability. Voltage stability indices (VSI) are powerful tools to evaluate the stability limit by gauging the proximity of a given operating point to voltage instability. These indices are used to precisely predict the proximity of voltage instability of the electric power

system. Different VSI has been proposed in the literature for voltage stability assessment which can identify the weakest bus or most sensitive bus. It is an indicator which helps the operator to understand the severity of voltage collapse and to initiate remedial measures to prevent it.

Power quality is a major issue in the wind integrated distribution system, so that additional alternative is needed to provide reactive support. Improper integration of DG adversely affects the voltage stability and hence the performance of customer equipment. VSI can be used for the placement of DG/CPD, detecting the weakest lines and buses and triggering the countermeasures against voltage instability. The main objective is to quantify the closeness of a particular point to the steady state voltage stability margin. These indices are very useful in designing and planning operations or to help the operators in real time operation of power system. In the case of integration of DGs or CPDs to the utility grid, these indices help in reducing of search space for the optimization process [206].

Important features of stability indices are:

- Easily identify the position at which real or reactive power support needs
- Less computation time
- Less computer memory required

Researchers have developed various indices for identifying the weakest node at which the voltage collapse starts first [208]-[211].

Important voltage stability indices discussed in the literature are:

1. Voltage stability Indicator (VSI)
2. Bus Voltage Stability Index (BVSI)
3. Fast Voltage Stability Index (FVSI)
4. Sensitivity Analysis Factor (SAF)
5. Loss Sensitivity Factor (LSF)

In this work, backward-forward sweep algorithm (BFSA) based stability index methods are used for determining the suitable location of active/reactive support. These indices were tested on IEEE-15 bus test system to verify the performance of the proposed indices. Results showed that stability indices are very good indicators in predicting the occurrence of system collapse and hence necessary action can be taken to avoid such incident. Effectiveness has been demonstrated using different case studies on IEEE 15 bus radial distribution test system.

6.4 V OLTAGE STABILITY INDEX (VSI)

Consider a two bus network having sending and receiving end voltages are $V_i\angle\delta_i$ and $V_j\angle\delta_j$ respectively, shown in chapter 5 (Fig. 5.1). Load at bus j is $P_j + jQ_j$ and $I(i)$ is the current flowing from bus i to bus j.

If line shunt admittances are neglected, the current flowing from i^{th} bus to j^{th} bus is

$$I(i) = \frac{|V_i|\angle\delta_i - |V_j|\angle\delta_j}{R(k) + jX(k)} \tag{6.1}$$

Also,

$$I(i) = \frac{P_j - j\,Q_j}{V_j^*} \tag{6.2}$$

Equating (6.1) and (6.2),

$$\frac{|V_i|\angle\delta_i - |V_j|\angle\delta_j}{R(k) + jX(k)} = \frac{P_j - j\,Q_j}{V_j^*}$$

$$[|V_i|\angle\delta_i - |V_j|\angle\delta_j] * [|V_j|\angle -\delta_j] = [P_j - j\,Q_j][R(k) - jX(k)] \tag{6.3}$$

Equating real and imaginary parts of (6.3),

$$V_i * V_j \cos(\delta_i - \delta_j) - V_j^2 = P_j * R(k) + Q_j * X(k) \tag{6.4}$$

$$V_i * V_j \sin(\delta_i - \delta_j) = P_j * X(k) - Q_j * R(k) \tag{6.5}$$

In the radial distribution system, the angle of sending end voltage and receiving end voltage is almost equal. Hence,

$\delta_i - \delta_j = 0$.

Then equation (6.4) becomes

$$V_i * V_j - V_j^2 = P_j * R(k) + Q_j * X(k) \tag{6.6}$$

$$I(i) = \frac{P_j - j\,Q_j}{V_j^*} \tag{6.7}$$

From (6.6) and (6.7)

$$V_j^2 - V_i * V_j + P_j * R(k) + \frac{R(k) * Q_j^2}{P_j} = 0 \tag{6.8}$$

$$V_j^2 - V_i * V_j + \frac{R(k) * \left[P_j^2 + Q_j^2\right]}{P_j} = 0 \tag{6.9}$$

The real roots of the equation (6.9)

$$V_i^2 - \frac{4*R(k)*\left[P_j^2+Q_j^2\right]}{P_j} \geq 0 \tag{6.10}$$

$$\frac{4*R(k)*\left[P_j^2+Q_j^2\right]}{Vi^2*P_j} \leq 1 \tag{6.11}$$

Voltage Stability Index is defined as:

$$\text{VSI} = \frac{4*R(k)*\left[P_j^2+Q_j^2\right]}{Vi^2*P_j} \tag{6.12}$$

The node is highly unstable if its VSI is near or greater than unity [212]. So the value of VSI should be less than unity for good stability which means that the particular node is a healthy one.

6.4.1 ALGORITHM FOR VSI

The algorithm for finding the position of DG/CPD in the radial system is explained below.

Step 1: Read the system Data.

Step 2: Identify the nodes and branches beyond each node.

Step 3: Calculate the exact load feeding through each node.

Step 4: Assign bus with larger capacity as Slack.

Step 5: Assign flat start profile 1 pu (per unit).

Step 6: Perform BFSA to find node voltage.

Step 7: Check for convergence of node voltage.

Step 8: If not converged, replace node voltage with updated value, otherwise go to step 6.

Step 9: Set node voltage.

Step 10: Compute VSI of each branch

Step 11: Identify the branch having maximum VSI

Step 12: Print the result.

6.4.2 Voltage Stability Index Profile

The best optimal location is found out using voltage stability index (VSI) which ranks the priority list of buses having high voltage instability. As the load at the bus increases above a certain limit, there occurs a greater chance of becoming a weak bus. The concept of VSI has been applied, to verify the correctness of the location of DG/CPD determined from GA based BFS algorithm. VSI reduces the search space and makes the node identification easy. Figure 6.1 gives VSI analysis of 15 bus radial system. By arranging the rank of sensitivities of each node in descending order, the bus having highest VSI gives the highest priority which needs active/reactive power support. From this analysis, it is found that bus 2 has the first priority and second priority for bus 6. Since the bus 2 is near the substation, it does not require any active power supplementation. Bus 6 having second priority and hence, it is considered as the best location requiring active power support.

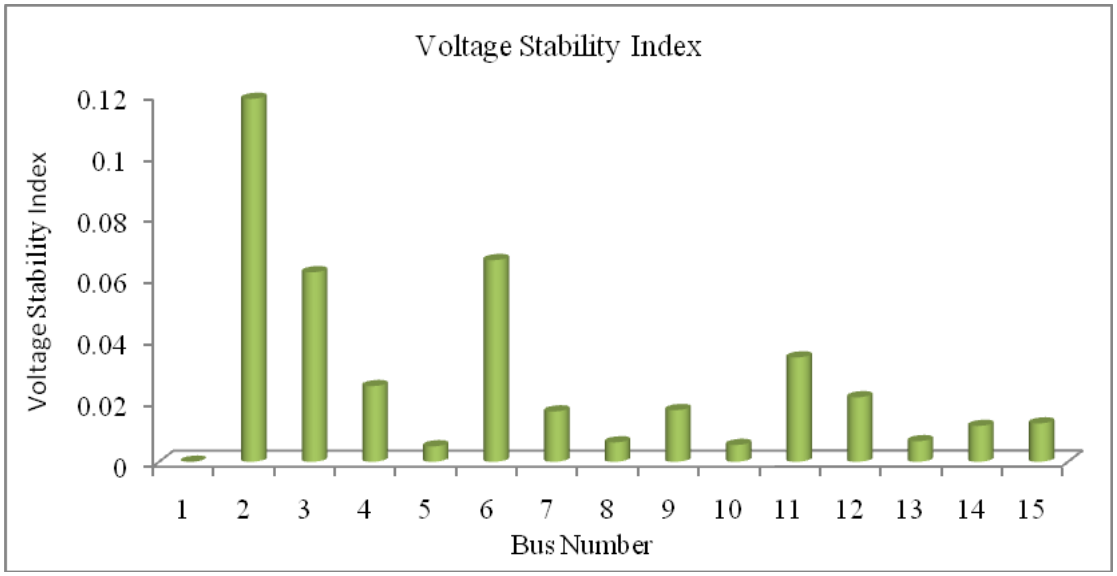

Fig. 6.1: Voltage stability index of IEEE 15 bus RDS

6.4.3 Case Study Analysis Based on VSI

The authenticity of the location of the weakest node is assured with the help of VSI. Four cases are considered to select the optimal size and location of DG.

Case 1: Radial Distribution System without DG

Load flow analysis is conducted in an IEEE-15 bus test system, to obtain voltage profile and power loss. The active and reactive power losses are computed as 0.06179 MW and 0.05729 MVAr respectively. From the voltage profile shown in Fig. 6.2, it is found that the far end buses suffer from voltage instability.

Case 2: Connecting optimum size of DG at location for minimum power loss

The optimized size of DG and its location in the radial network is presented in Chapter V. It is seen that 0.4 MW size of DG placed at node 6 reduces the power loss and improves the voltage profile. Obtained active and reactive power losses are 0.057259 MW and 0.53768 MVAr respectively.

Case 3: Connecting optimum size of DG at the weakest branch of the RDS

From the analysis of VSI, the branch connecting bus 6 and bus 8 is found to be the weakest. If bus 8 is treated as weakest bus and when 0.4 MW size of DG placed at this bus, the active and reactive power losses are increased to 0.06137 MW and 0.05691 MVAr respectively.

Case 4: Connecting a size of DG with minimum power loss at weakest branch

Load flow analysis is carried out by placing the different size of DG at the weakest node 8; then, it is found that power loss is minimum with placing a size of 0.1 MW of DG. It is observed that active and reactive power loss are not much reduced and found to be 0.06016 MW and 0.05576 MVAr respectively.

Case 5: Connecting the DG at the optimal location of the RDS

In this case, DG of 0.1 MW placed at optimal location node 6 and power loss are computed. It is found that active and reactive power losses are 0.058807 MW and 0.054812 MVAr respectively.

6.4.4 Voltage Profile

Voltage profile and power loss obtained from the case studies are presented in Fig. 6.2 and Fig. 6.3 respectively. From the voltage profile, it is seen that voltage is reduced in the main feeder and lateral feeder buses concerning substation voltage (1 pu) when DG is not placed. The analysis shows that the two locations for placing DG are either bus 6 or bus 8 of the weakest branch 6-8. Further, it is observed that when a

single DG of size 0.4 MW is placed at node 6 gave a positive impact on voltage profile of lateral feeder buses 6, 7, 8, 9 and 10 which are nearer to the substation. If the same size of DG placed at the other end of branch 6-8, the voltage is not much improved. Hence, it is clear that a considerable improvement in voltage profile can be attained only when 0.4 MW size of DG placed at bus 6 in the lateral feeder.

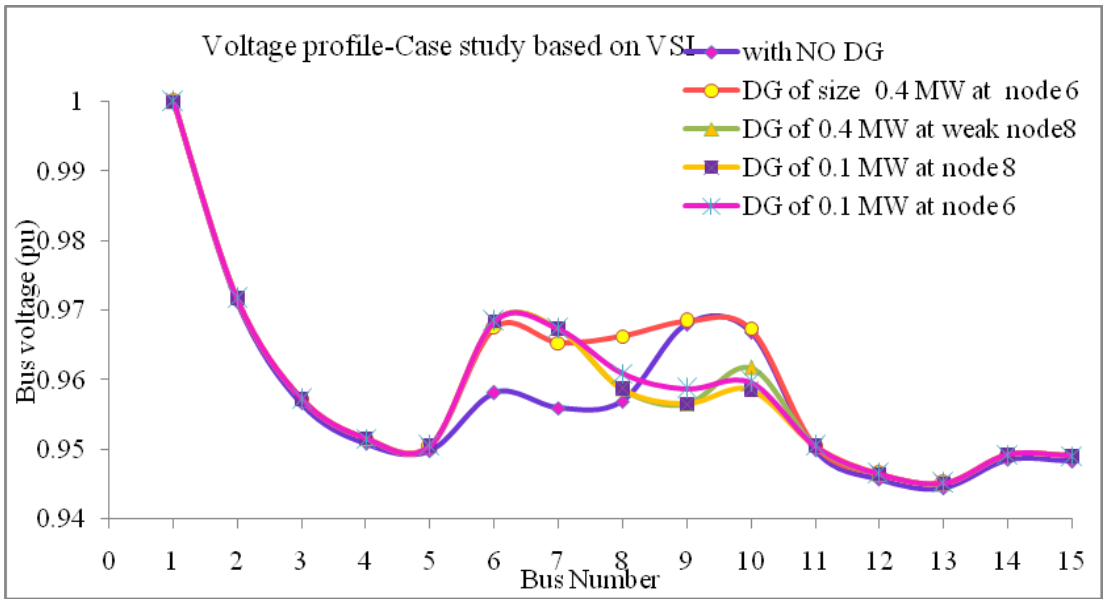

Fig. 6.2: Voltage profile of IEEE 15 bus RDS based on case study analysis using VSI

6.4.5 Power loss

From Fig. 6.3, the power loss is high when DG is not placed. When 0.4 MW DG is placed at either bus 6 or bus 8, the power loss gets reduced. Further, it is observed that considerable reduction in power loss could be obtained by placing 0.4 MW size of DG placed at bus 6 than at bus 8. Hence, it is inferred that power loss cannot be reduced if the location is not optimal.

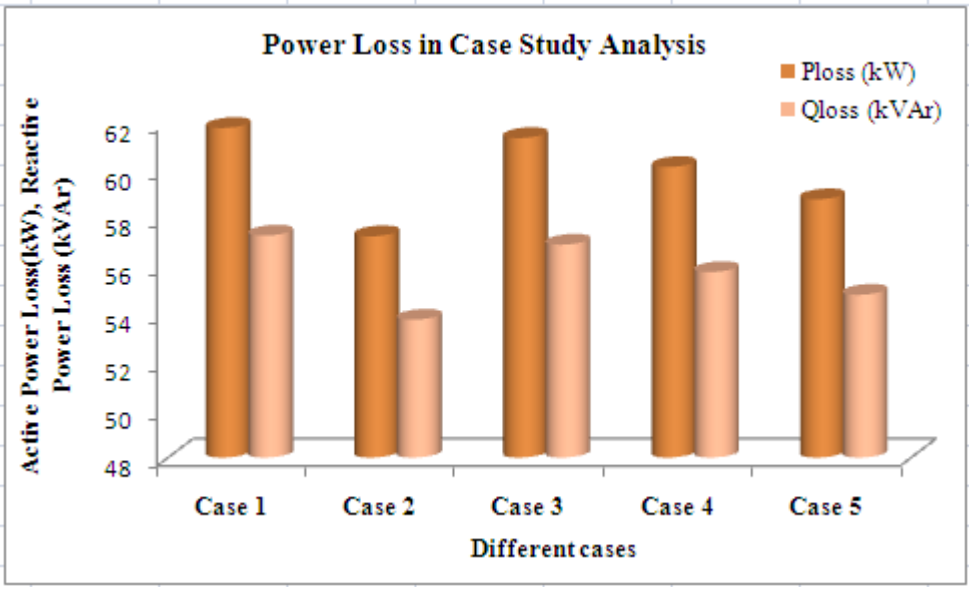

Fig. 6.3: Power Loss of IEEE 15 bus RDS based on case study analysis using VSI

6.5 BUS VOLTAGE STABILITY INDEX (BVSI)

One of the searching methods to find the weak node is bus voltage stability index (BVSI). The node at which the DG is to be located can be easily identified by reducing the searching space. This index gives a priority list of buses suffering from voltage stability. Hence, BVSI is a good indicator of the weak bus. It is calculated by integrating each bus at a time by a DG of 20% size of maximum feeder loading capacity. After putting DG at individual nodes one at a time, voltage profile is obtained and BVSI of each node is calculated using equation

Bus Voltage Stability Index is defined as:

$$\text{BVSI} = \sqrt{\frac{\sum_{j=1}^{N} (1-V_j)^2}{N}} \qquad (6.13)$$

where V_j is the voltage at j^{th} the node and N is the number of nodes. The sensitivity indices are ranked in ascending order to form priority list. Select the node with the

least BVSI is the best location for DG placement. Load flow analysis has to be carried out by placing the different size of DG's with small increments at the above-said node. From the load flow analysis, the DG corresponds to minimum losses and maximum voltage profile has to be taken as the optimized size of DG.

6.5.1 Algorithm for BVSI

Step 1: Run load flow for base case

Step 2: Calculate BVSI of each node by penetrating DG of size 20% of maximum feeder loading capacity.

Step 3: Rank the sensitivities of all nodes in descending order

Step 4: Select the bus with the highest priority and place the DG at that bus

Step 5: Change the size of DG in small steps and calculate power loss for each by running load flow

Step 6: Store the size of DG that gives minimum loss

Step 7: Compare the loss with the previous solution. If the loss is less than the previous solution, store this solution.

Step 8: Repeat the steps 5 to 8 for all buses in the priority list

Step 9: Print the result

6.5.2 Bus Voltage Stability Index Profile

As the load at the bus increases above a certain limit, there occurs a great chance of becoming a weak bus. The concept of BVSI has been applied to establish the authenticity of the optimal location of DG in radial system. The total connected load in the IEEE-15 bus radial distribution system is 1.2264 MW. The index, BVSI is computed by placing 0.245 MW size of DG (20% of connected load) at all nodes.

Figure 6.5 gives BVSI analysis of 15 bus radial distribution system. By arranging the rank of sensitivities of each node in descending order, the bus having high BVSI gives the highest priority which needs active power. From this analysis, it is found that bus 2 which is very near to the substation has the first priority and it does not require any active power supplementation. The next priorities for bus 3, 6, 11, 12 and goes on as per priority list in the descending order.

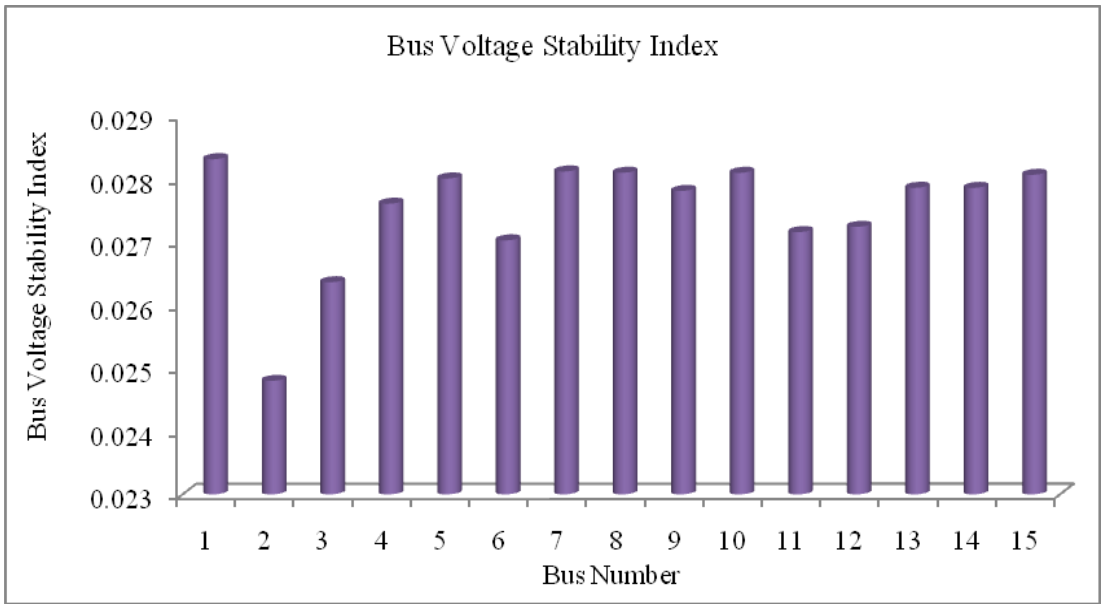

Fig. 6.4: Bus voltage stability index of IEEE 15 bus RDS

6.5.3 Case Study Analysis based on BVSI

Load flow analysis has been carried out in the radial network by placing 0.245 MW DG at different nodes. It can be seen from Fig. 6.5 that the minimum power loss occurs at bus 3 and bus 6 if the bus near to substation (bus 2) is ignored.

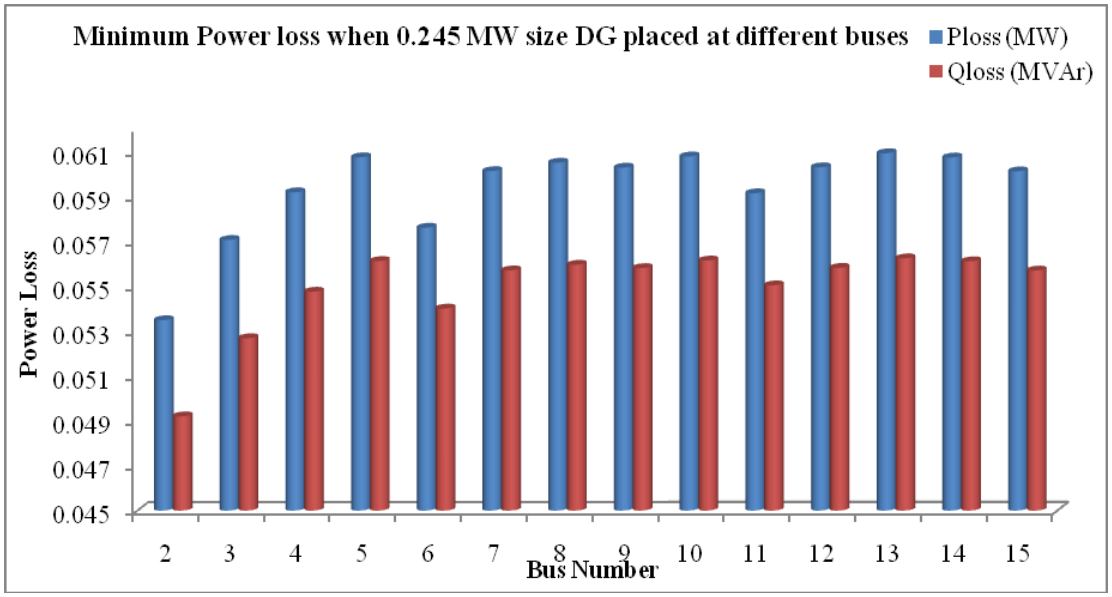

Fig. 6.5: Power loss when 0.245 MW size of DG placed at different buses

Power losses are computed by placing the different size of DG's with small increments at nodes 3 and 6, as shown in Fig.6.6 and Fig.6.7 respectively. It is observed that power loss is minimum when 0.7 MW size DG placed at node 3 and 0.4 MW DG placed at node 6. On comparison with DG at node 6, the power loss is found to be slightly less at node 3, but the large size of DG is required. Then, bus number 6 has the third priority which needs active power support. It is clearly shown in Fig. 6.7 that the power loss first decreases and then increases as the size of DG increases. It results that the DG of size 0.4 MW placed at node 6 gives minimum power loss and maximum voltage profile.

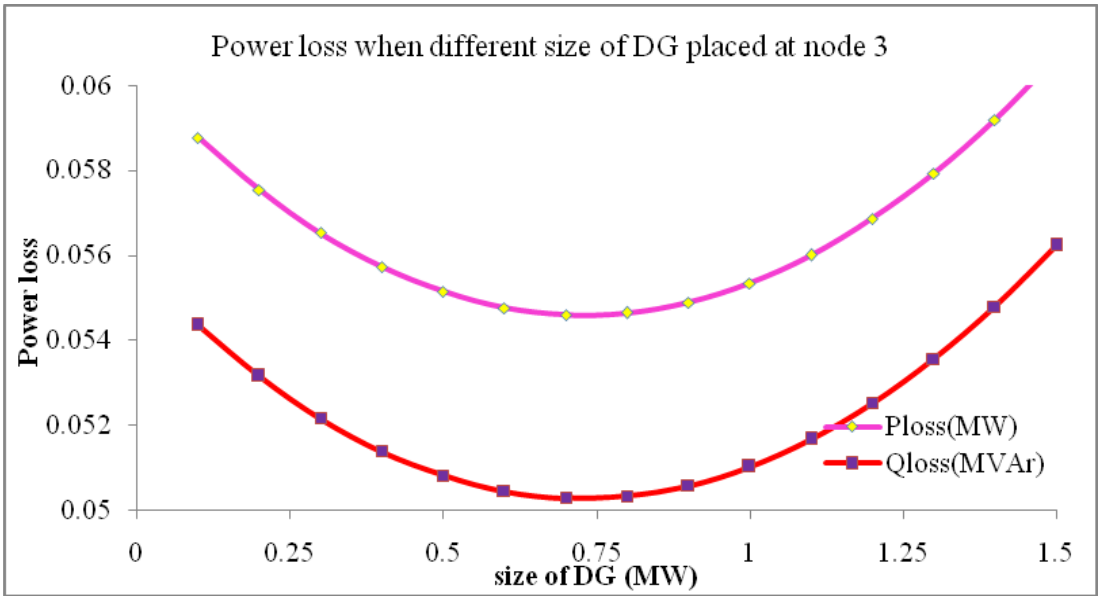

Fig. 6.6: Power loss at bus 3 for different size of DG

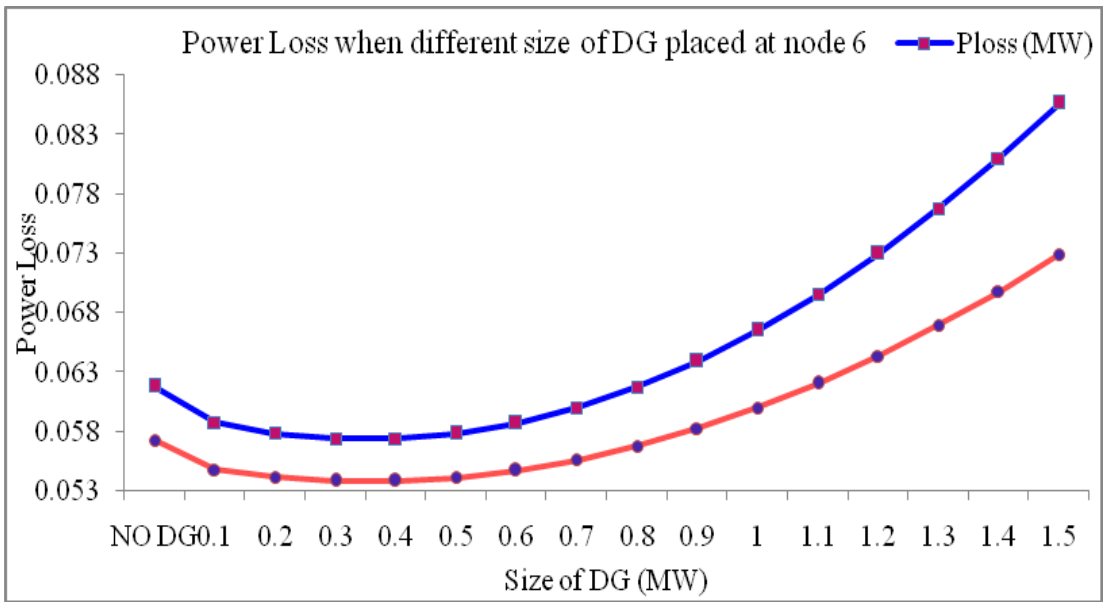

Fig. 6.7: Power loss at bus 6 for different size of DG

Voltage profile of these two cases is shown in Fig. 6.8. It clearly depicts that integration of DG improves the voltage of its nearby nodes.

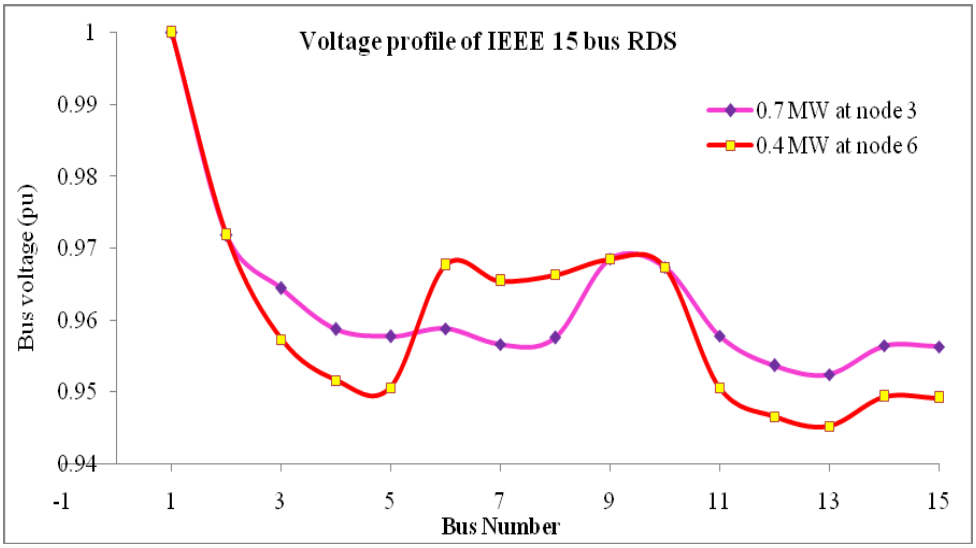

Fig. 6.8: Voltage profile when 0.7 MW placed at node 3 and 0.4 MW placed at node 6

6.6 FAST VOLTAGE STABILITY INDEX (FVSI)

FVSI is used to indicate the stressfulness of a line in the distribution system. The advantage of this method lies in the simplicity of numerical calculations and expressiveness of the results. FVSI is derived from the voltage quadratic equation at the receiving bus on a two-bus system [213].

$$V_j^2 - \left(\frac{R(k)}{X(k)}\sin\delta_{ij} + \cos\delta_{ij}\right)V_i V_j + \left(X(k) + \frac{R(k)^2}{X(k)}\right)Q_j = 0 \tag{6.14}$$

To obtain the roots of V_j, the discriminate is set greater than or equal to zero.

Therefore,

$$\left[\left(\frac{R(k)}{X(k)}\sin\delta_{ij} + \cos\delta_{ij}\right)V_i\right]^2 - \left(X(k) + \frac{R(k)^2}{X(k)}\right)Q_j \geq 0 \tag{6.15}$$

$$\frac{4Z(k)^2 * Q_j * X(k)}{V_j^2\left(R(k)\sin\delta_{ij} + X(k)\cos\delta_{ij}\right)^2} \leq 1 \tag{6.16}$$

Since $\delta_{ij} = \delta_i - \delta_j$ is normally very small, then

$$\delta_{ij} \approx 0, \quad R(k)\sin\delta_{ij} \approx 0 \text{ and } X(k)\cos\delta_{ij} \approx X(k)$$

Hence, Fast Voltage Stability Index is defined as:

$$\text{FVSI} = \frac{4Z(k)^2 Q_j}{V_i^2 X(k)} \tag{6.17}$$

As the value of FVSI of a particular line reaches to unity, it indicates that the line is insecure and close to instability point which may lead to voltage collapse in the entire system. Therefore, the value of this index should be less than unity for a stable condition.

6.6.1 Algorithm for FVSI

Step 1: Read input data

Step 2: Perform load flow

Step 3: Compute the node voltages and Power losses

Step 4: Compute FVSI of each branch

Step 5: Identify the branch having maximum FVSI

Step 6: Sort in descending order

Step 7: Find bus number having high FVSI

6.6.2 Fast Voltage Stability Index Profile

The location in the radial system at which voltage collapse starts first is found out with an index named fast voltage stability index (FVSI), which ranks the priority list of buses having high voltage instability in descending order. FVSI of each line is computed and shown in Fig. 6.9.

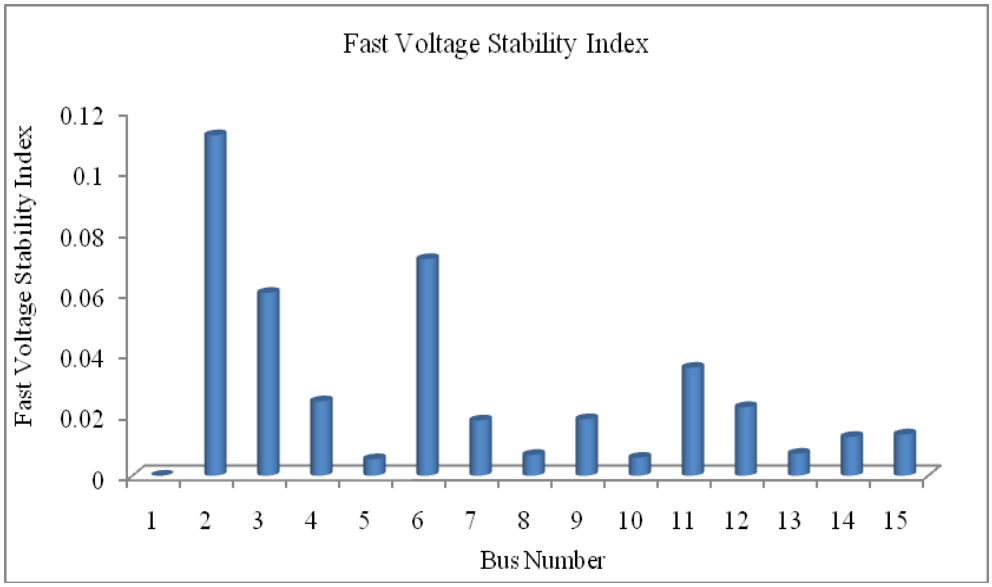

Fig. 6.9: Fast voltage stability index of IEEE 15 bus RDS

From the Fig. 6.9, it found that bus 6 has the first priority when bus 2 is ignored so that the best location of DG can be selected as bus 6.

6.6.3 Case Study Analysis Based on Connected Load

The size of DG can be computed by connecting DG of size varies from 10 – 100% of the total connected load at the node from BVSI analysis. It is seen that when 30% of the connected load placed at node 6, then active and reactive power losses are found to be 0.057342 MW and 0.053824 MVAr respectively, and when 60% of the connected load placed at node 3, then active and reactive power losses are found as 0.054588 MW and 0.050277 MVAr respectively. It is shown in Fig. 6.10. Total connected load in this network is 1.2264 MW. Even though the power loss at node 3 is less than that of node 6, the size of the DG is double to that at node 6. Hence, it is compromised that the suitable size of DG is 30% of connected load, i.e., 0.36792 MW and location is node 6.

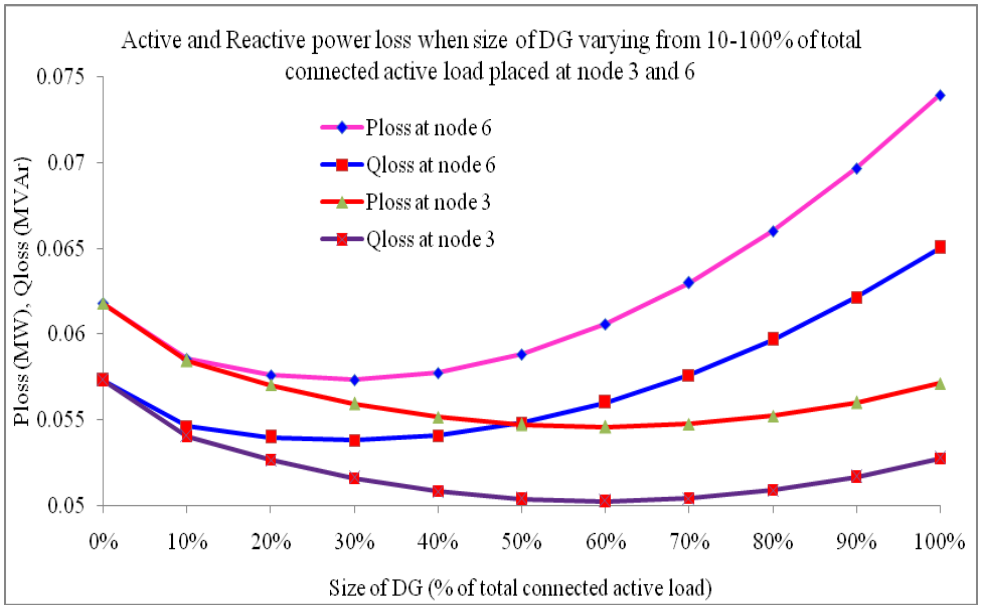

Fig. 6.10: Power loss when 10-100% connected active load placed at node 6 and node 3

Voltage profile of the case study is shown in Fig. 6.11

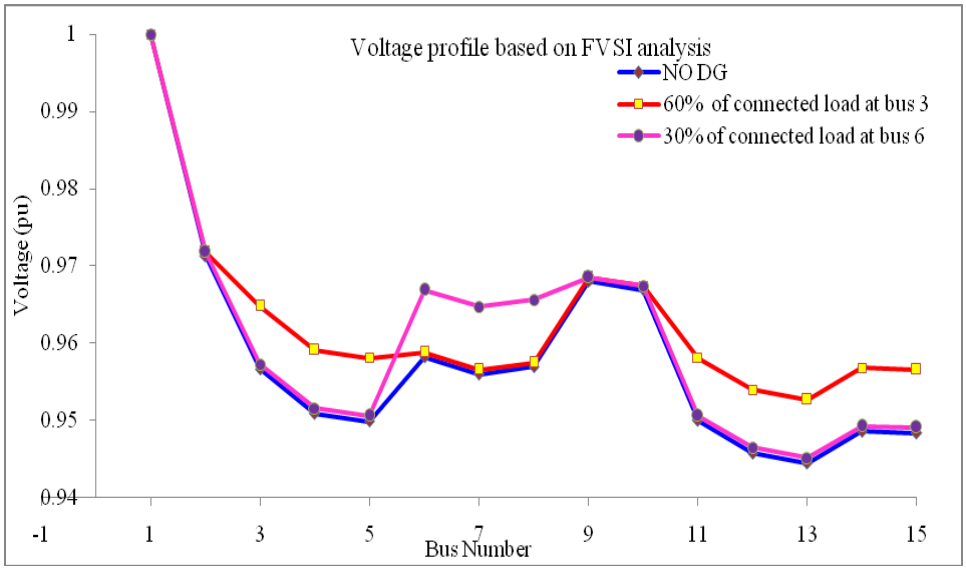

Fig. 6.11: Voltage profile when 30% and 60% of connected active load placed at node 6 and node 3

6.7 SENSITIVITY ANALYSIS FACTOR (SAF)

An index named sensitivity analysis factor (SAF) is derived for finding the optimal location of DG in a radial distribution system. This index is calculated for each branch and sorted from highest to the smallest value. It gives the priority list for the location of DG. The DG should be placed at the end of the branch having highest SAF. Under stable operation, its value should be less than unity. This indicates that the maximum voltage instability occurs at the bus having highest index [182].

For the bus having sending end node i and receiving end node j,

$$P_{loss}^{ndg} = I(i)^2 R(k)$$

$$I(i) = \left(\frac{P_j^{eff} + Q_j^{eff}}{V_j} \right)^* = \frac{P_j^{eff} - Q_j^{eff}}{V_j^*}$$

$$P_{j_{loss}} = \frac{\left(\left(P_j^{eff} \right)^2 + \left(Q_j^{eff} \right)^2 \right) R(k)}{|V_j|^2} \tag{6.18}$$

where P_j^{eff} = total effective active power supplied beyond j^{th} the node

Q_j^{eff} = total effective reactive power supplied beyond j^{th} node

$R(k)$ = resistance of k^{th} branch

For the system loss reduction to be maximized, the rate of change of P_{loss} with respect to the injected power becomes zero. From this, the Sensitivity Analysis Factor (SAF) is derived as

$$\frac{\partial P_{loss}}{\partial P_j^{eff}} = \frac{2 \times P_j^{eff} \times R(k)}{|V_j|^2} \tag{6.19}$$

The SAF is computed for all the nodes and ranked in the descending order so that the candidate buses for the DG placement can be detected in the order of highest SAF. Fig. 6.12 shows the SAF of IEEE 15 bus radial system from which it is understood that the bus 6 is having the highest SAF. It is meant that bus 6 is the weakest bus at which the maximum active/reactive power support can be given to avoid the tendency for the start of voltage collapse.

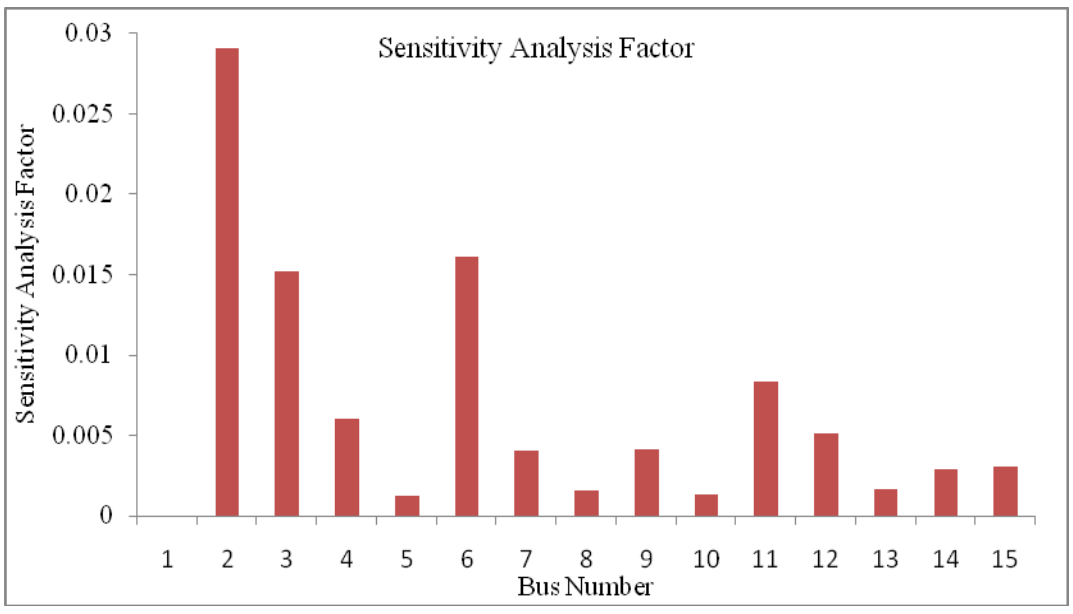

Fig. 6.12: Sensitivity analysis factor of IEEE 15 bus RDS

The maximum load that is possible to be connected to this weakest bus to maintain stability before the system reaches its bifurcation point is computed. For computing the maximum reactive power that can be injected into this bus, the reactive power is increased by a step size of 0.1 MVAr in addition to the connected reactive load. Variations in voltage at this node are observed. The bus voltage at any node should be within 1 ± 0.5 pu. System violation will be experienced if the load at this bus exceeds the maximum load. The increase in voltage at bus 6 versus an increase in reactive power at this bus is shown in Fig. 6.13. It is observed that the maximum load that can be applied to bus 6 to maintain the voltage stability is 3.8 MVAr. Voltage violation results if the injection of reactive power is beyond 3.8 MVAr.

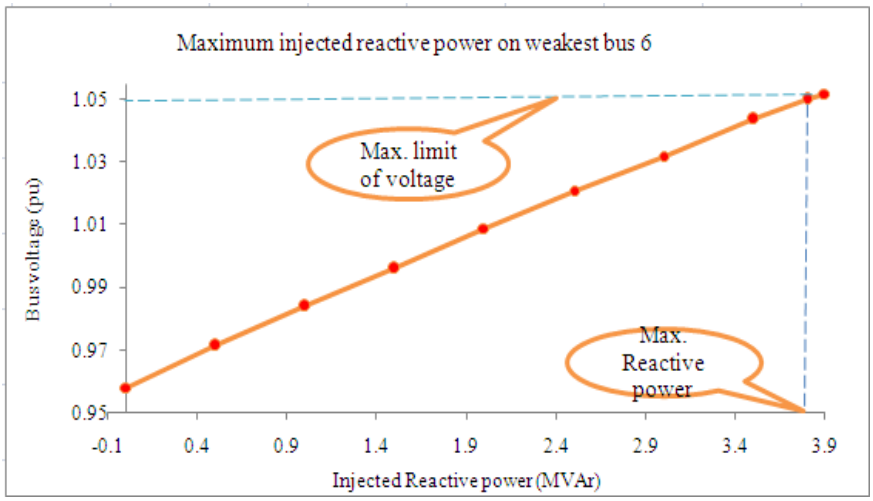

Fig. 6.13: Injected reactive power versus bus voltage at bus 6

6.8 LOSS SENSITIVITY FACTOR (LSF)

Loss Sensitivity Factor (LSF) helps in finding the weakest bus for which the priority has been aimed at giving the real power support. The first priority is identified as the prime location of single DG. The priority list of LSF reduces the searching space for the optimization procedure [214].

Consider, $P_j^{eff} + Q_j^{eff}$ is the effective load connected at the receiving end j of distribution line. The active power loss and reactive power loss in the line between i and j can be expressed as

$$P_{loss} = \frac{\left(\left(P_j^{eff}\right)^2 + \left(Q_j^{eff}\right)^2\right) \times R(k)}{{V_j}^2} \tag{6.20}$$

$$Q_{j_{loss}} = \frac{\left(\left(P_j^{eff}\right)^2 + \left(Q_j^{eff}\right)^2\right) \times X(k)}{{V_j}^2} \tag{6.21}$$

Then LSF can be obtained from the above equations,

$$\frac{\partial P_{loss}}{\partial Q_j^{eff}} = \frac{2 \times Q_j^{eff} \times R(k)}{|V_j|^2} \tag{6.22}$$

$$\frac{\partial Q_{loss}}{\partial Q_j^{eff}} = \frac{2 \times Q_j^{eff} \times X(k)}{|V_j|^2} \tag{6.23}$$

Loss Sensitivity Factor for each node are calculated with the help of load flow analysis and arranged in descending order to get the priority list for placing the DG or CPDs in the radial system. From the priority list, the end bus of the lines which have less than normalized voltage is considered as the weakest nodes which need real or reactive power support to improve the voltage at that locations. LSF of each node is shown in Fig. 6.14. From Fig. 6.14, it can be observed that bus 6 has the highest priority while omitting the buses 2 and 3.

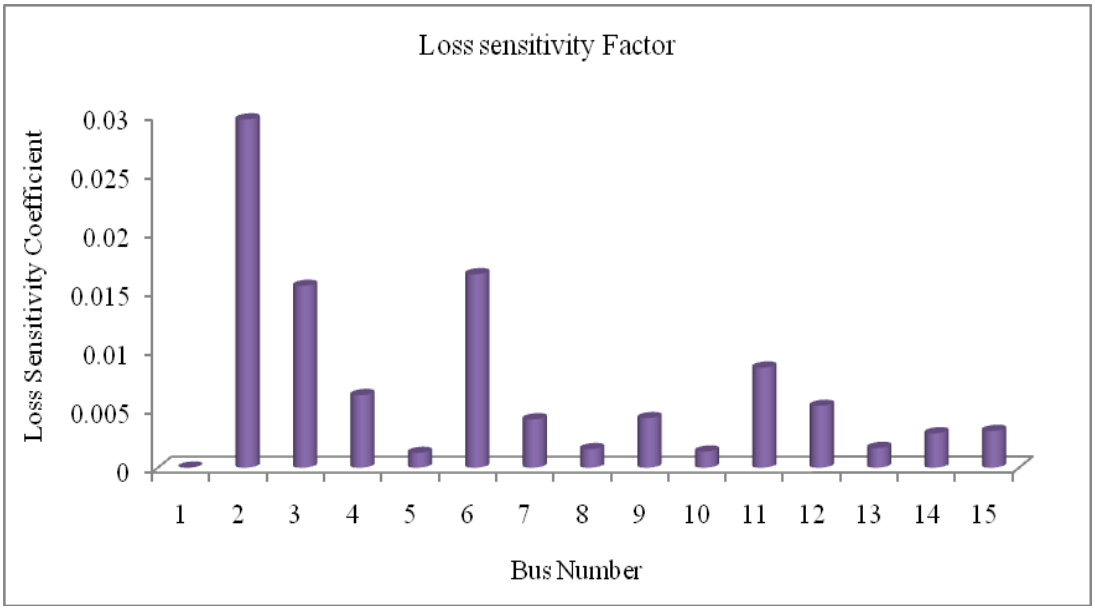

Fig. 6.14: Loss sensitivity factor of IEEE 15 bus RDS

6.9 SUMMARY

The work presents a successful analysis of the weakest bus identification in IEEE 15 bus radial distribution system. Different voltage stability indices are used to determine the origin of voltage collapse. Identification of weakest node is assured with the help of case studies using stability indices. SAF helps in finding the weakest bus at which maximum load is possible to be connected to maintain stability. The violation of the system is in terms of exceeding the voltage limit at this particular bus is also observed.

CHAPTER 7

PLACEMENT OF D-STATCOM IN RDS

7.1 INTRODUCTION

In an electrical power system, the reactive power is vital for reliability, power quality, power loss and voltage stability. The rapid technology advancements in industrial or domestic areas make more stresses on power system so that it adversely affects the voltage profile and power loss. Under this circumstance, the generator could not generate sufficient reactive power to meet the consumer requirements and losses in the system [215], [216]. Power system operators are constantly striving to give guaranteed sufficient security margin to the power system network. But it is a difficult task for the operators considering uncertainties in demand-supply level.

The term PQ has become one of the widely discussed topics in the electrical power industry. The large use of nonlinear loads gives rise to PQ problems. PQ issues such as voltage sag, voltage swell etc. may have an impact on customer devices causing malfunction of devices and cost on the loss of production [217]. Voltage sag is one of the severe power quality issues that affect industrial equipment [218], [219].

Voltage stability covers a wide range of long term and short term, small signal and large signal effects. Under long-term small disturbance, voltage stability is a major issue in wind power applications [220]. In such cases, the dynamic compensation device is a solution for exchanging the reactive power between wind farms and distribution networks.

The literature review [221], [222], [143]-[148] show that power system stress is relieved by injecting adequate reactive power. PE-based CPDs such as DVR, D-STATCOM, UPQC are prevalently used to address PQ problems in power distribution networks. In this work, GA based BFSA is used to optimally place the reactive power compensation device in a distribution network. The result is validated using BIBC-BCBV based stability index method.

7.2 OPTIMAL ALLOCATION OF D-STATCOM

The total electrical power generation is equal to the customer power demand plus the distribution losses. The customer requires active and reactive power based on the load characteristics. The reactive power also accounts for a portion of the total losses. The wind farm contributes a major part of the power in RES integrated distribution systems. DFIG type and squirrel cage induction generators are widely used for wind power generation. It consumes reactive power from the grid. It tends to slow down the voltage restoration after a voltage collapse, leading to voltage and rotor instability [221]. Hence, CPDs have been applied in distribution networks to regulate the bus voltage by providing an adequate amount of reactive power. D-STATCOM or DVR is predicted to play a significant role in the radial system only through proper allocation and sizing. Optimal placement of such devices helps to maximize the loadability, power loss minimization, stability enhancement, reactive power compensation and PQ enhancement such as voltage regulation, voltage balancing, and flicker suppression. In this chapter, GA based BFS algorithm has been applied on IEEE 15 bus radial distribution network for finding the size and location of reactive power support.

7.3 METHODOLOGY

Since it is assumed that D-STATCOM gives only the reactive power support, the optimization algorithm is based on minimization of total reactive power loss in the system.

7.3.1 Objective Function

Power loss is computed for different ratings of D-STATCOM placed at each feeder point. Since it is assumed that the D-STATCOM gives reactive power supply only, the optimization algorithm is based on minimization of total reactive power. To find the optimal size of D-STATCOM, the reactive power loss minimization is taken as the objective of the problem. GA is used to optimize the size of D-STATCOM.

The objective function:

$$g_{(x)} = \frac{Q^{dst}_{loss(x)}}{Q^{ndst}_{loss}} \tag{7.1}$$

where, x represents the chromosome value (size of D-STATCOM in kVAr).

$Q^{dst}_{loss(x)}$ - Total system reactive power loss with D-STATCOM of x kVAr rating

Q^{ndst}_{loss} - Total system reactive power loss without D-STATCOM

7.3.2 Constraints

The reactive power injected by each D-STATCOM is restricted by lower and upper limits $Q_{\min}^{dst}$ and $Q_{\max}^{dst}$. It is based on the total connected reactive load of the network system.

So, the constraints used for the optimization of D-STATCOM capacity are:

$$Q_{\min}^{dst} \le Q^{dst} \le Q_{\max}^{dst} \tag{7.2}$$

$$V_{\min} \le V \le V_{\max} \tag{7.3}$$

7.3.3 Algorithm for finding size and location of D-STATCOM

Step 1: Read input data

Step 2: Perform load flow analysis without D-STATCOM and compute node voltages, net real and reactive power losses

Step 3: Set the bus number (*j*) of D-STATCOM as one

Step 4: If bus number is greater than total no. of bus (*N*), then find the minimum reactive power loss, otherwise, set the size of D-STATCOM Q^{dst} as zero

Step 5: If Q^{dst} is greater than the net reactive load, bus number is incremented by one. Otherwise, run power flow and calculate active and reactive power loss

Step 6: D-STATCOM size is incremented with a step size of 100 kVAr

Step 7: Check the node voltage within 1± 0.05 pu
Otherwise, reject unsuitable values and go to step 3

Step 8: For minimum reactive power loss, find optimum location (*j*) and size Q^{dst} of D-STATCOM

Step 9: Conduct load flow by placing Q^{dst} at the optimal location

Step 10: Print the results

7.4 D-STATCOM IN IEEE 15 BUS RADIAL SYSTEM

Load flow is carried out to find voltage profile and power loss with and without D-STATCOM. Initially, power loss and voltage profile are found with no integration of D-STATCOM. Then, size of D-STATCOM is varied from 0.1 MVAr to 1.2 MVAr and placed at each individual bus. The power loss and voltage profile are computed.

Power Loss and Voltage Profile

Table 7.1 showed the variation in power loss when 0.4 MVAr size of D-STATCOM integrated at bus 4 and bus 6. It can be seen that the power loss is considerably reduced with the integration of D-STATCOM at bus 4 than at bus 6.

Table 7.1: Power loss on IEEE15 bus RDS with and without D-STATCOM

System	P_{loss} (MW)	Q_{loss} (MVAr)
NO D-STATCOM	0.06179	0.05729
0.4 MVAr at bus 4	**0.044956**	**0.04087**
0.4 MVAr at bus 6	0.048081	0.0448

It is computed that the active power loss reduction is 27.243% and reactive power loss reduction is 28.661% respectively when 0.4 MVAr placed at bus 4 and 22.18% and 21.8% respectively at bus 6. The proper amount of reactive power at the far end of the main feeder reduces the power loss in the main feeders as well as in the lateral feeders. Power loss reduction in 15 bus network with and without D-STATCOM is shown in Fig. 7.1.

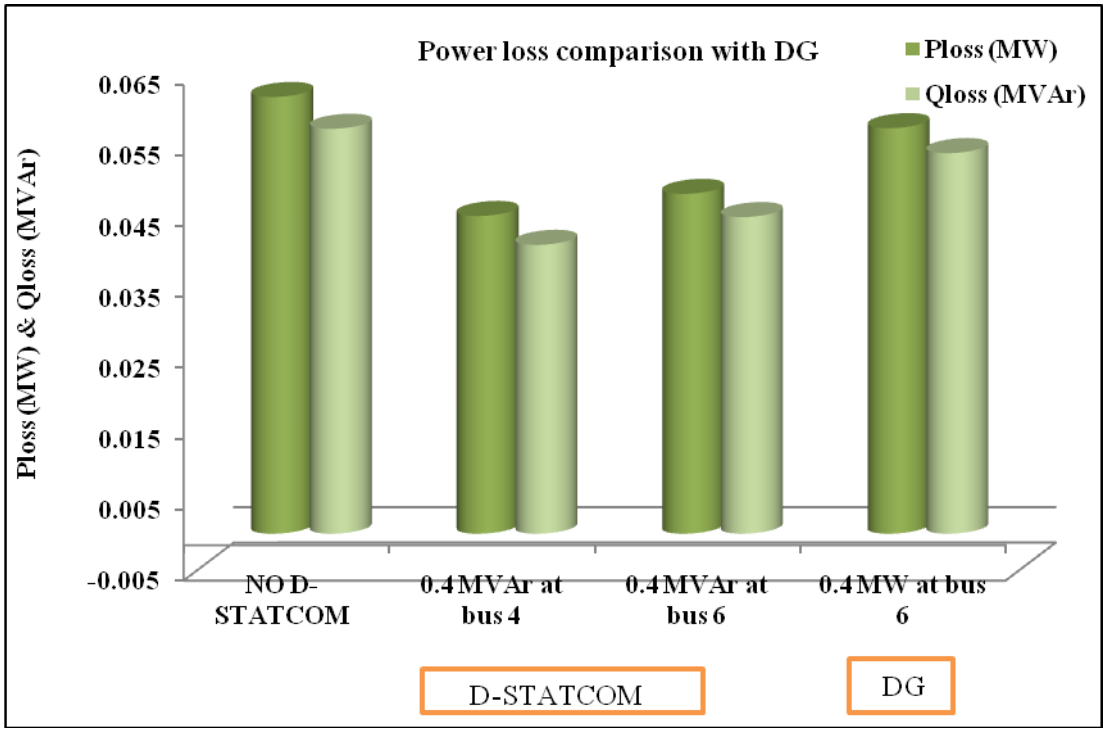

Fig. 7.1: Power loss without and with D-STATCOM

In comparison with DG, it can be seen that the integration of 0.4 MVAr at bus 4 reduces the power loss to a large extent than 0.4 MVAr at bus 6 and 0.4 MW DG at bus 6. It explicitly shows that the D-STATCOM is preferable in this test system for reducing the power loss and improving the voltage profile. The effect of D-STATCOM installation on voltage profile of main feeders and lateral feeders are investigated. Voltage is minimum at bus 13 which is improved from 0.9445 pu to 0.9535 pu with the use of 0.4 MVAr at bus 4 and found that the buses with under or over voltage problem are completely recovered. But, the integration of 0.4 MVAr at bus 6 improved this voltage to 0.9493 only and can be seen that buses with under or over voltage problem are completely recovered except at this bus. Voltage profile of 15 bus system with and without D-STATCOM is shown in Fig. 7.2. It is seen that when 0.4MVAr D-STATCOM is integrated at bus 4, the voltage gets improved at some buses. When integrated at bus 6, the voltage improvement takes place at some other buses.

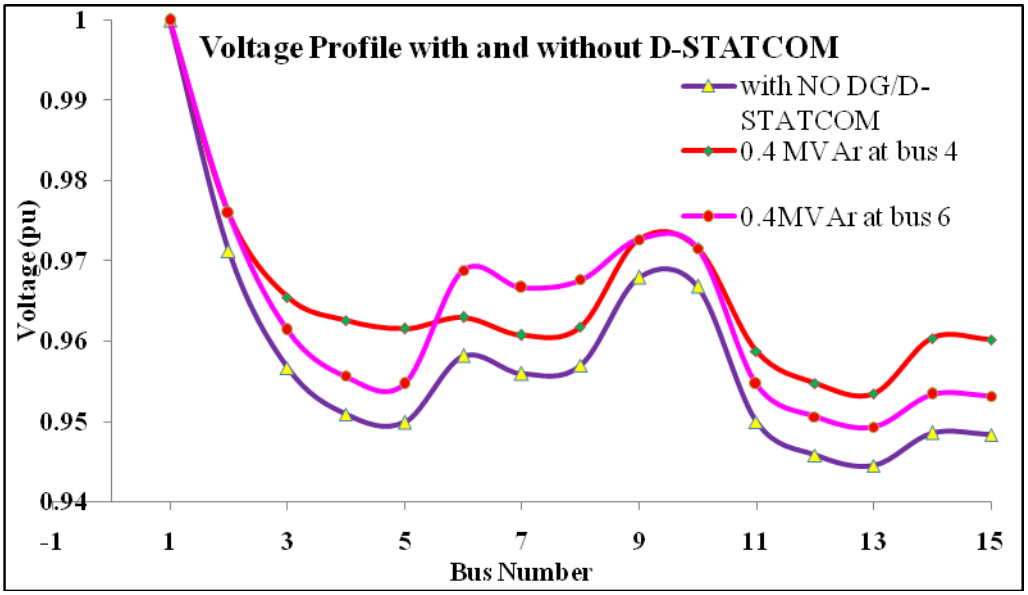

Fig. 7.2: Voltage profile without and with D-STATCOM

7.5 D-STATCOM IN DG INTEGRATED RDS

IEEE 15 bus radial system integrated with DG is taken as the test system. The algorithm used in Section 7.3.3 has been applied in this test system. Size and location of D-STATCOM are computed to reduce the power loss and enhance the voltage stability.

Power Loss and Voltage Profile

Table 7.2 shows the impact of D-STATCOM on power loss in DG integrated test system. Different DG-D-STATCOM combinations are taken for the analysis of power loss.

Table 7.2: Power loss on 15 bus RDS with combination of DG and D-STATCOM

	System	P_{loss} (MW)	Q_{loss} (MVAr)
Case 1	NO D-STATCOM	0.06179	0.05729
Case 2	0.4 MVAr D-STATCOM (4) & 0.4 MW DG (6)	**0.041664**	**0.03795**
Case 3	0.4 MVAr D-STATCOM (6) &0.4 MW DG (6)	0.051063	0.04645
Case 4	0.4 MVAr D-STATCOM (4) &0.4 MW DG (4)	0.045153	0.041073
Case 5	0.4 MVAr D-STATCOM (6) & 0.4 MW DG (4)	0.045629	0.04241

When 0.4 MW size DG integrated at bus 6 is taken as the test system, then 0.4 MVAr D-STATCOM integrated at bus 4 and bus 6 reduces the active power loss by 32.57% and 17.36% respectively and reactive power loss by 33.76% and 18.92% respectively. When the same DG is integrated at bus 4, 0.4 MVAr D-STATCOM at bus 4 and bus 6 reduces the active power loss by 26.93% and 26.15% and reactive power loss by 28.31% and 25.97% respectively. The percentage reduction in the power loss for the above four cases is clearly shown in Fig. 7.3. It can be inferred that the integration of 0.4MVAr D-STATCOM at bus 4 in the DG integrated test system gives considerable reduction in the power loss.

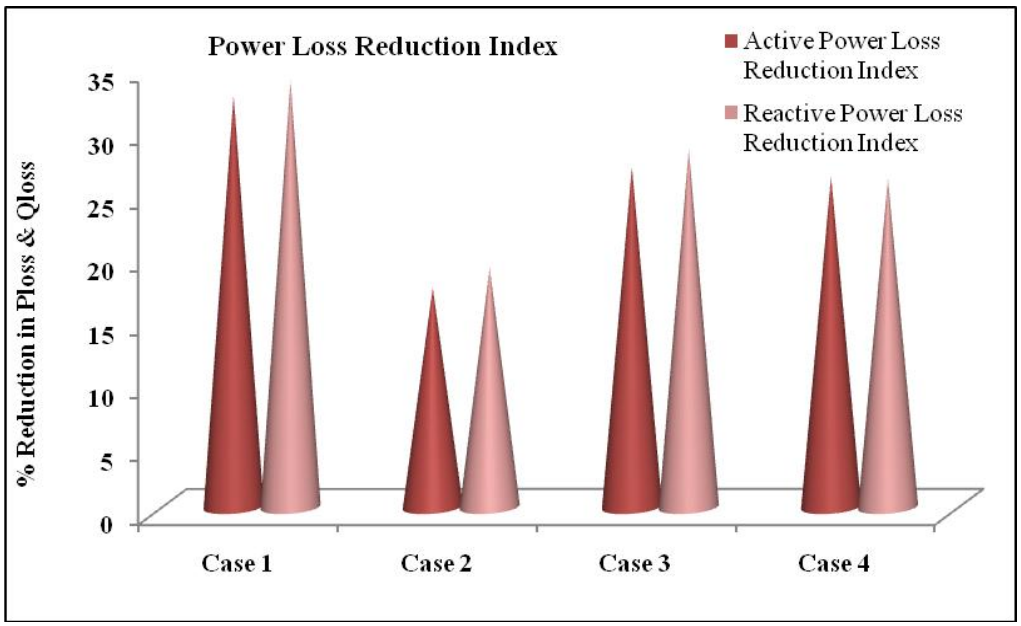

Fig. 7.3: Percentage power loss reduction Index for different combinations of DG and D-STATCOM

Impact of DG-D-STATCOM combination on the voltage profile is shown in Fig. 7.4. It can be seen that the integration of 0.4 MVAr size D-STATCOM at bus 4 and 0.4 MW size DG at bus 6 results in a comparatively high impact on the voltage profile than other D-STATCOM-DG combinations.

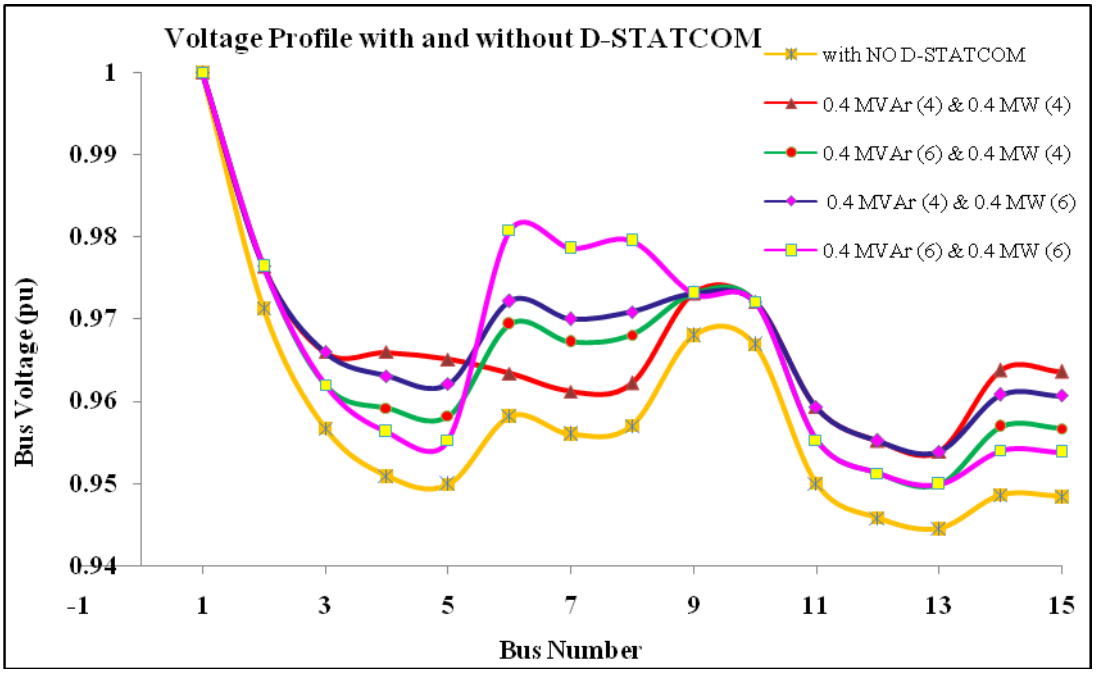

Fig. 7.4: Voltage profile with different combinations of DG and D-STATCOM

7.6 D-STATCOM IN MULTIPLE DG INTEGRATED RDS

In Chapter 5, the location and size of multiple DGs are already discussed. Then, the load flow is carried out to obtain the size of D-STATCOM in multiple DG integrated radial system. The impact of DG and D-STATCOM on the voltage profile and power loss is computed.

The four cases taken to enhancing better voltage stability and power loss reduction in the radial system are:

Case 1: NO DG and D-STATCOM

Case 2: One DG and D-STATCOM

Case 3: Two DGs and D-STATCOM

Case 4: Three DGs and D-STATCOM

Power loss, power loss reduction index and voltage profile are shown in Figures 7.5 to 7.7.

Power Loss analysis

From Fig 7.5, it is observed that the total loss is minimum when three DGs and D-STATCOM are integrated with the radial distribution system. The total active power loss of the system without DG/D-STATCOM is 0.061794 MW and it is reduced to 0.010735 MW with three DGs and D-STATCOM. The results are tabulated in Table 7. 3.

Table 7.3: Reduction in power loss with combination of DGs and D-STATCOM

Number of DG	**Size and location of DG (MW)**		**Total size of DG (MW)**	**Size and location of D-STATCOM (MVAr)**		P_{loss} **(MW)**	Q_{loss} **(MVAr)**	P_{loss} **Reduction (%)**	Q_{loss} **Reduction (%)**
NO DG	-	-	-	NO D-STATCOM	-	0.061794	0.057297	0	0
One DG	0.4	6	0.4	0.4	4	0.041664	0.03795	32.57	33.76
Two DGs	0.4	6	0.8	1	3	0.012885	0.010447	79.15	81.76
	0.4	4							
Three DGs	0.4	6	1.3	0.9	4	0.010735	0.008379	82.63	85.37
	0.4	4							
	0.5	3							

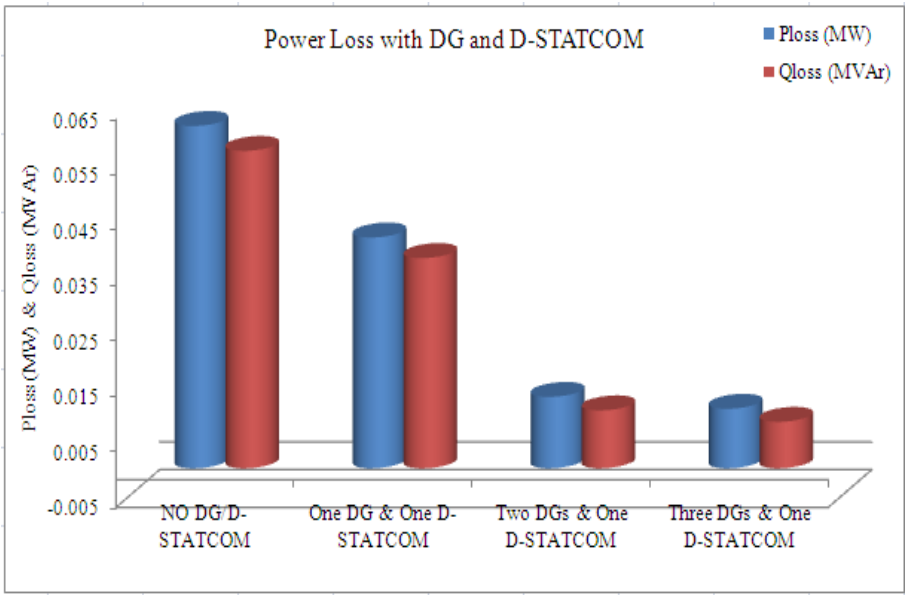

Fig. 7.5: Power Loss with multiple DGs and D-STATCOM

Power Loss Reduction Index

Active and reactive power loss reduction index with multiple DGs and single D-STATCOM are shown in Fig. 7.6. From this, it can be seen that the power loss reduction index is high with the integration of multiple DGs and D-STATCOM at proper places.

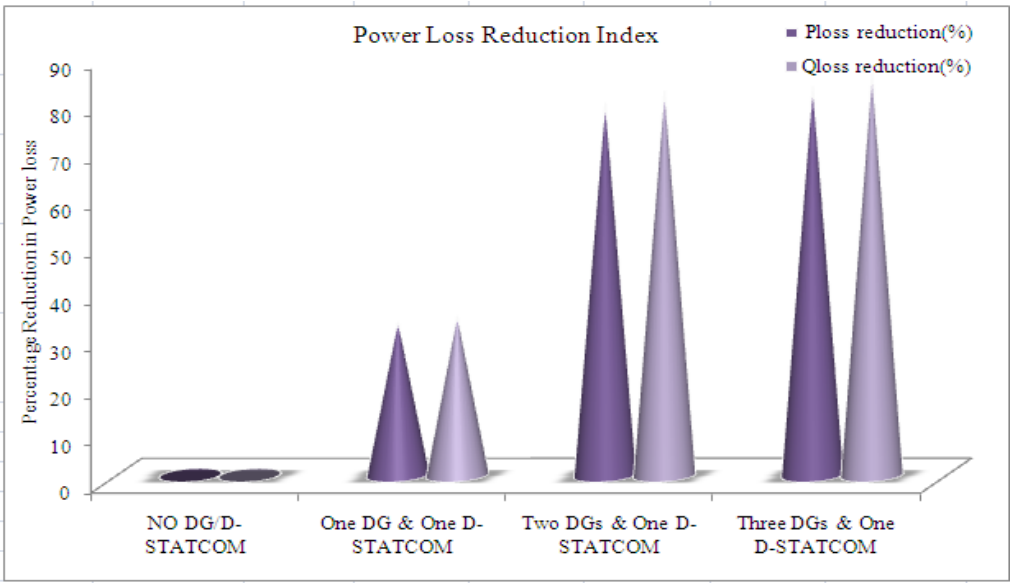

Fig. 7.6: Power Loss reduction Index with multiple DGs and D-STATCOM

Voltage analysis

Voltage profile improvement of all the nodes in the radial network with the integration of multiple DGs and D-STATCOM is shown in Fig. 7.7. It is found that the voltage at bus 13 is improved from 0.9445 pu to 0.9887 pu with the integration of three DGs and D-STATCOM with the objective of minimization of total loss. And also, it is seen that the voltage at all nodes is found to be within the constraints (1.05 pu). This means that under/over voltage problem can be completely recovered with the integration of multiple DGs and D-STATCOM.

It is inferred that better voltage stability enhancement can be achieved with the help of properly allocated optimized multiple DGs combined with D-STATCOM.

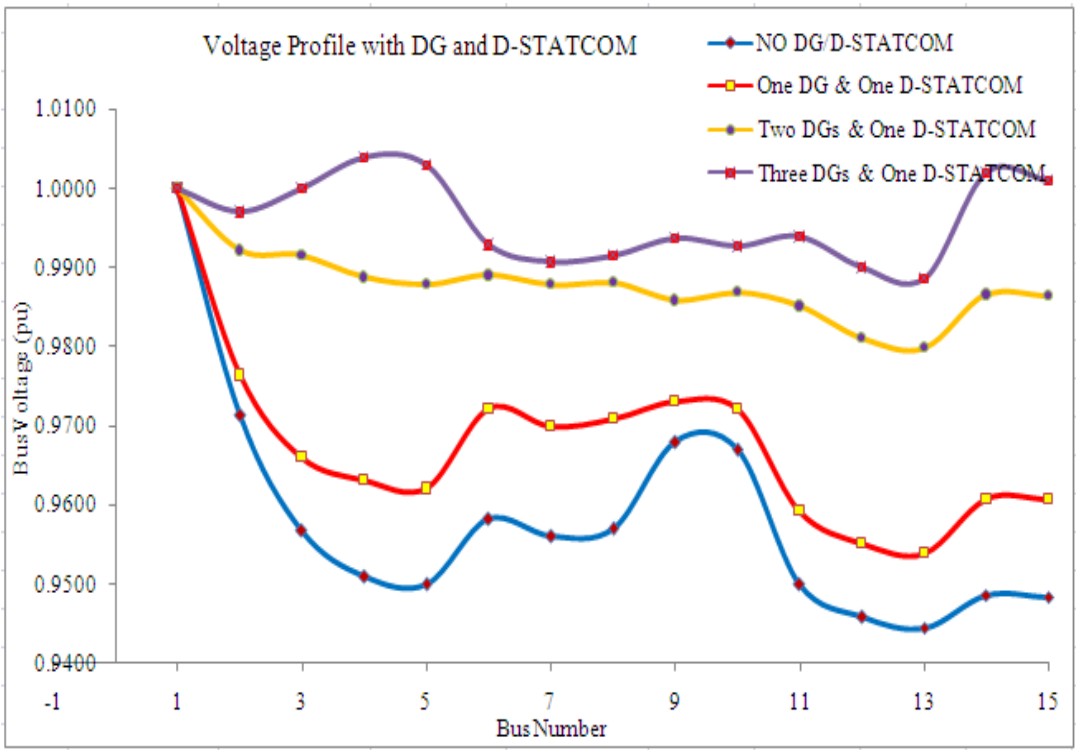

Fig. 7.7: Voltage profile with multiple DGs and D-STATCOM

7.7 STEADY STATE MODELING OF D-STATCOM

To find the size of D-STATCOM and its impact on the voltage profile of radial network, steady-state modeling is used [223][224]. Consider two bus systems in which one bus is taken as reference bus and the other bus having bus voltage less than the reference voltage. D-STATCOM is connected to this bus for improving its bus voltage. Single line diagram of two bus network and its phasor diagram are shown in Figures 7.8 and 7.9.

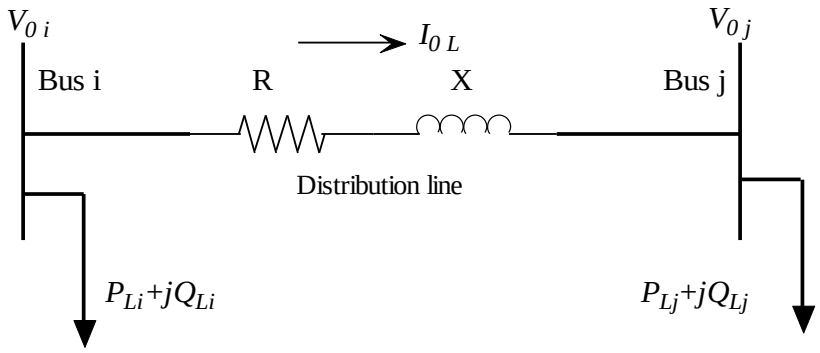

Fig. 7.8: Single line diagram of two bus network

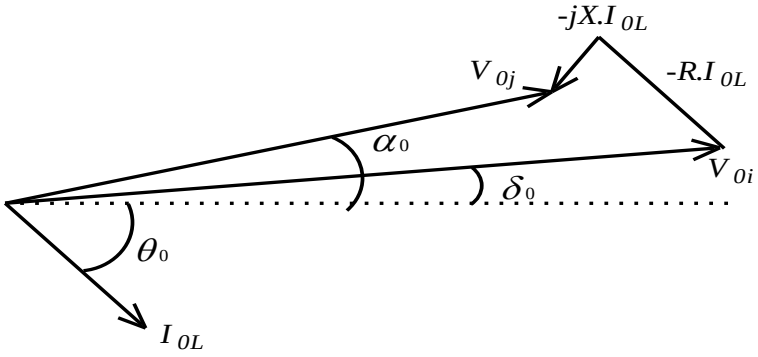

Fig. 7.9: Phasor diagram of voltage and current of two bus network

Generally, bus voltages are less than 1 pu and it can be increased with the help of D-STATCOM. From Fig. 7.9, the relationship between voltage and current can be written as

$$V_{0j}\angle\alpha_0 = V_{0i}\angle\delta_0 - (R + jX)I_{0L}\angle\theta_0 \qquad (7.2)$$

where

$V_{0j}\angle\alpha_0$: voltage of bus j before compensation

$V_{0i}\angle\delta_0$: voltage of bus j before compensation

$R + jX$: line impedance between buses i and j

$I_{0L}\angle\theta_0$: line current before compensation

The voltage at bus i and j and current are computed from load flow calculations. D-STATCOM is used for voltage regulation in the steady-state condition by injecting reactive power to the system. The current through D-STATCOM I_{dst} must be kept in quadrature with the voltage of the system. In the steady-state condition, the integration of D-STATCOM makes changes in the bus voltages, especially neighboring buses of its location and branch currents of the network. The schematic diagram of two bus network connected with D-STATCOM and its phasor diagram is shown in Figures 7.10 and 7.11. Integration of D-STATCOM changes the voltage of bus j from V_j to V_j^{new}.

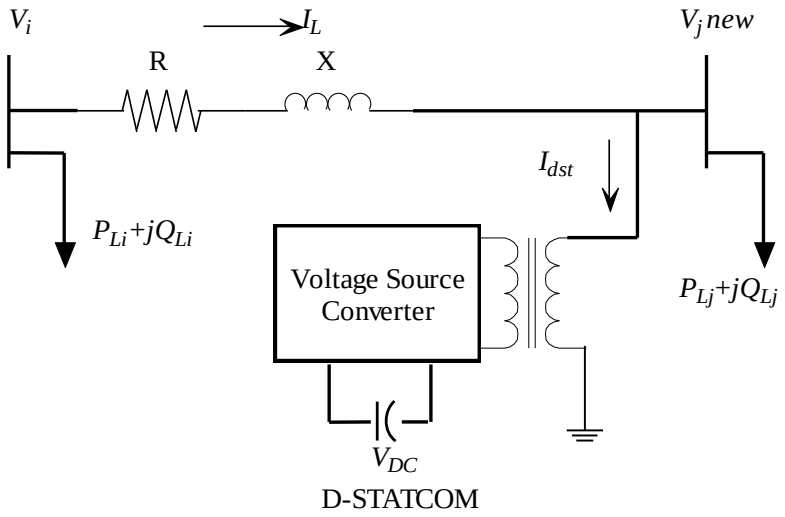

Fig. 7.10: Single line diagram of two bus network with D-STATCOM

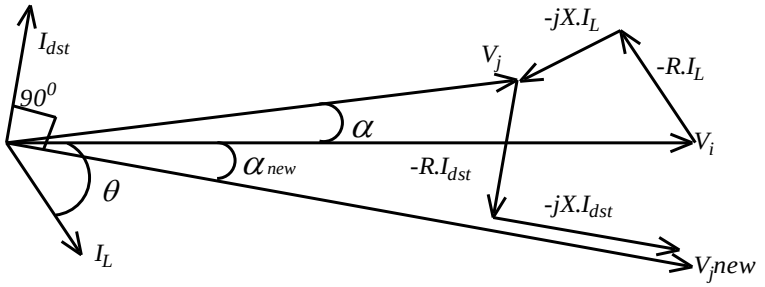

Fig. 7.11: Phasor diagram of voltage and current of two bus network with D-STATCOM

For the sake of simplicity, the angle δ of sending end bus is assumed to be zero.

From Figures 7.10 and 7.11, it can be seen that

$$\angle I_{dst} = \frac{\pi}{2} + \alpha_{new}, \qquad \alpha_{new} \leq 0 \tag{7.3}$$

$$V_j^{new} \angle \alpha_{new} = V_i \angle \delta - (R + jX) I_L \angle \theta - (R + jX) I_{dst} \angle (\alpha_{new} + \frac{\pi}{2}) \tag{7.4}$$

where, $I_{dst} \angle (\alpha_{new} + \frac{\pi}{2})$ is the injected current by D-STATCOM.

$V_j^{new} \angle \alpha_{new}$: voltage of bus j after compensation by D-STATCOM

$V_i \angle \delta$: voltage of bus i after compensation by D-STATCOM

$I_L\angle\theta$: line current after D-STATCOM installation

Voltage $V_i\angle\delta$ and current $I_L\angle\theta$ are computed from load flow calculations.

Separating real and imaginary parts of eqn. 7.4,

$$V_j^{new}\cos\alpha_{new} = \mathrm{Re}al(V_i\angle\delta) - \mathrm{Re}al(ZI_L\angle\theta) - RI_{dst}\cos(\alpha_{new}+\frac{\pi}{2}) + XI_{dst}\sin(\alpha_{new}+\frac{\pi}{2}) \quad (7.5)$$

and

$$V_j^{new}\sin\alpha_{new} = \mathrm{Im}(V_i\angle\delta) - \mathrm{Im}(ZI_L\angle\theta) - XI_{dst}\cos(\alpha_{new}+\frac{\pi}{2}) - RI_{dst}\sin(\alpha_{new}+\frac{\pi}{2}) \quad (7.6)$$

Let

$$a_1 = \mathrm{Re}al(V_i\angle\delta) - \mathrm{Re}al(ZI_L\angle\theta)$$

$$a_2 = \mathrm{Im}(V_i\angle\delta) - \mathrm{Im}(ZI_L\angle\theta)$$

$$b = V_j^{new}$$

$$c_1 = -R$$
$$c_2 = -X$$
$$x_1 = I_{dst}$$
$$x_2 = \alpha_{new}$$

$$b\cos x_2 = a_1 - c_1x_1\sin x_2 - c_2x_1\cos x_2 \quad (7.7)$$

$$b\sin x_2 = a_2 - c_2x_1\sin x_2 + c_1x_1\cos x_2 \quad (7.8)$$

where a_1, a_2, c_1 and c_2 are constants, x_1 and x_2 are variables and b is the magnitude of the compensated voltage at the j^{th} bus (1 pu) are to be determined. Rearranging the equations 7.7 and 7.8, then

$$x_1 = \frac{b\cos x_2 - a_2}{-c_1 \sin x_2 - c_2 \cos x_2} \tag{7.9}$$

and

$$x_1 = \frac{b\sin x_2 - a_2}{-c_2 \sin x_2 + c_1 \cos x_2} \tag{7.10}$$

By equating equations 7.9 and 7.10, then

$$(a_1c_2 - a_2c_1)\sin x_2 + (-a_1c_1 - a_2c_2)\cos x_2 + bc_1 = 0 \tag{7.11}$$

Take $x = \sin x_2$ and squaring both sides of eqn. 7.11, then the following equation is derived.

$$(k_1^2 + k_2^2)x^2 + (2k_1bc_1)x + (b^2c_1^2 - k_2^2) = 0 \tag{7.12}$$

Where

$$k_1 = a_1c_2 - a_2c_1$$
$$k_2 = a_1c_1 + a_2c_2$$

Therefore, $x = \frac{-B \pm \sqrt{\Delta}}{2A}$ (7.13)

where

$$\Delta = B^2 - 4AC$$
$$B = k_1bc_1$$
$$A = k_1^2 + k_2^2$$
$$C = b^2c_1^2 - k_2^2$$

After computing x, then, $x_2 = \alpha_{new}$.

It can be written as $x_2 = \sin^{-1} x$ (7.14)

Thus, $x_1 = I_{dst}$

Injected reactive power by D-STATCOM can be written as:

$$jQ^{dst} = \vec{V}_j^{new} * \vec{I}_{dst}^{\,*} \tag{7.15}$$

Where

$$\vec{V}_j^{new} = V_j^{new} \angle \alpha_{new} \tag{7.16}$$

$$\vec{I}_{dst} = I_{dst} \angle (\alpha_{new} + \frac{\pi}{2}) \tag{7.17}$$

7.8 BIBC-BCBV METHOD

A direct approach named bus injection to branch-current (BIBC) matrix and branch current to bus-voltage (BCBV) matrix [225], [226] has been used for the load flow analysis of radial distribution network. In this method, the formulation of time-consuming Jacobian matrix or admittance matrix, required in conventional methods is avoided.

Equivalent current injection

Complex load S_j at j^{th} node can be expressed as

$$S_j = P_j + jQ_j \qquad j = 1, 2....., n \tag{7.18}$$

Equivalent current injection at k^{th} iteration is computed as

$$I_j^k = I_j^r(V_j^k) + jI_j^i(V_j^k) = \left(\frac{P_j + jQ_j}{V_j^k} \right)^* \tag{7.19}$$

Where,

S_j : complex power at j^{th} the node.

P_j : real power at the j^{th} node.

Q_j : reactive power at j^{th} node

V_j^k : bus voltage at k^{th} iteration for j^{th} the node.

I_j^k : equivalent current injection at k^{th} iteration for the j^{th} node.

I_j^r : real parts of equivalent current injection at k^{th} iteration for $j^{th\ the}$ node.

I_j^i : imaginary parts of equivalent current injection at k^{th} iteration for $j^{th\ the}$ node.

Formulation of BIBC matrix

Formulation of Bus-injection to Branch-current (BIBC) matrix is explained with the help of simple distribution system shown in Fig. 7.12.

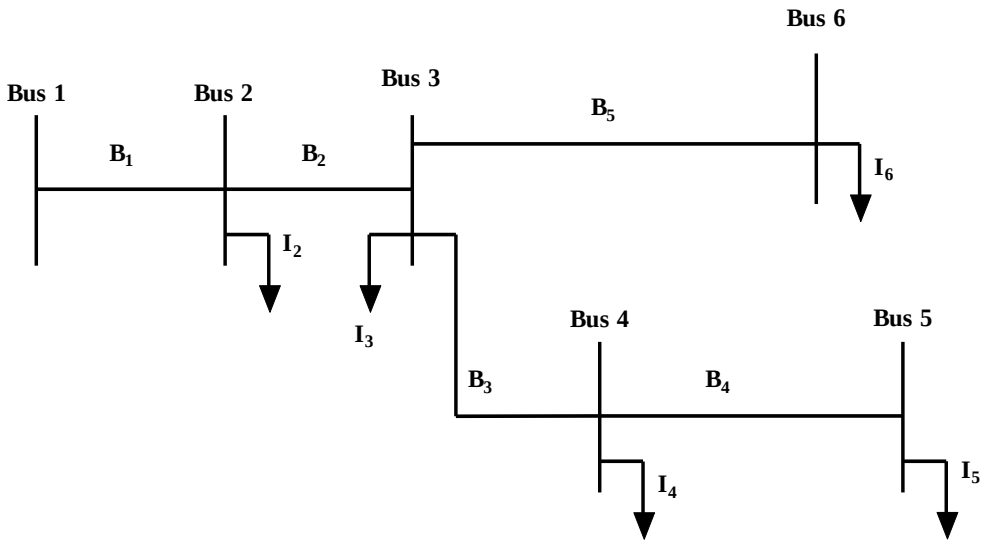

Fig. 7.12: Single line diagram of radial distribution system

Power injections at each bus can be converted to the equivalent current injections using Eqn. 7.19 and a set of equations can be written by applying KCL at each node. From Fig. 7.12, the branch currents can be expressed as:

$$
\begin{aligned}
B_1 &= I_2 + I_3 + I_4 + I_5 + I_6 \\
B_2 &= I_3 + I_4 + I_5 + I_6 \\
B_3 &= I_4 + I_5 \\
B_4 &= I_5 \\
B_5 &= I_6
\end{aligned}
\qquad
\begin{bmatrix} B_1 \\ B_2 \\ B_3 \\ B_4 \\ B_5 \end{bmatrix} =
\begin{bmatrix} 1 & 1 & 1 & 1 & 1 \\ 0 & 1 & 1 & 1 & 1 \\ 0 & 0 & 1 & 1 & 0 \\ 0 & 0 & 0 & 1 & 0 \\ 0 & 0 & 0 & 0 & 1 \end{bmatrix}
\begin{bmatrix} I_1 \\ I_2 \\ I_3 \\ I_4 \\ I_5 \end{bmatrix}
\tag{7.20}
$$

The general form as of Eqn. (7.20) can be expressed as:

$$
[B] = [BIBC][I] \tag{7.21}
$$

Formulation of BCBV matrix

The Branch-Current to Bus voltage (BCBV) matrix summarizes the relation between branch current and bus voltages. The relationship between the branch currents and bus voltages is given as,

$$
\begin{aligned}
V_2 &= V_1 - B_1 Z_{12} \\
V_3 &= V_2 - B_2 Z_{23} \\
V_4 &= V_3 - B_3 Z_{34} \\
V_5 &= V_4 - B_4 Z_{45} \\
V_6 &= V_3 - B_5 Z_{36}
\end{aligned}
$$

According to KVL, the voltage of bus 4 is given by,

$$
V_4 = V_1 - B_1 Z_{12} - B_2 Z_{23} - B_3 Z_{34} \tag{7.22}
$$

Similar procedures can be utilized for other buses, and the BCBV matrix can be derived as:

$$
\begin{bmatrix} V_1 \\ V_1 \\ V_1 \\ V_1 \\ V_1 \end{bmatrix} -
\begin{bmatrix} V_2 \\ V_3 \\ V_4 \\ V_5 \\ V_6 \end{bmatrix} =
\begin{bmatrix} Z_{12} & 0 & 0 & 0 & 0 \\ Z_{12} & Z_{23} & 0 & 0 & 0 \\ Z_{12} & Z_{23} & Z_{34} & 0 & 0 \\ Z_{12} & Z_{23} & Z_{34} & Z_{45} & 0 \\ Z_{12} & Z_{23} & 0 & 0 & Z_{36} \end{bmatrix}
\begin{bmatrix} B_1 \\ B_2 \\ B_3 \\ B_4 \\ B_5 \end{bmatrix}
\tag{7.23}
$$

The general form of Eqn. (7.23) can be expressed as:

$$[\Delta V]=[BCBV][B] \tag{7.24}$$

By replacing off-diagonal elements of BCBV matrix with zeros, we get the diagonal impedance matrix ZD.

Taking the transpose of BIBC matrix,

$$[ZD]=\begin{bmatrix} Z_{12} & 0 & 0 & 0 & 0 \\ 0 & Z_{23} & 0 & 0 & 0 \\ 0 & 0 & Z_{34} & 0 & 0 \\ 0 & 0 & 0 & Z_{45} & 0 \\ 0 & 0 & 0 & 0 & Z_{36} \end{bmatrix} \tag{7.25}$$

$$[BIBC]^T=\begin{bmatrix} 1 & 0 & 0 & 0 & 0 \\ 1 & 1 & 0 & 0 & 0 \\ 1 & 1 & 1 & 0 & 0 \\ 1 & 1 & 1 & 1 & 0 \\ 1 & 1 & 0 & 0 & 1 \end{bmatrix} \tag{7.26}$$

Multiplying Eqn. (7.25) and Eqn. (7.26) gives,

$$[BIBC]^T.[ZD]=\begin{bmatrix} 1 & 0 & 0 & 0 & 0 \\ 1 & 1 & 0 & 0 & 0 \\ 1 & 1 & 1 & 0 & 0 \\ 1 & 1 & 1 & 1 & 0 \\ 1 & 1 & 0 & 0 & 1 \end{bmatrix}\begin{bmatrix} Z_{12} & 0 & 0 & 0 & 0 \\ 0 & Z_{23} & 0 & 0 & 0 \\ 0 & 0 & Z_{34} & 0 & 0 \\ 0 & 0 & 0 & Z_{45} & 0 \\ 0 & 0 & 0 & 0 & Z_{36} \end{bmatrix}$$

$$=\begin{bmatrix} Z_{12} & 0 & 0 & 0 & 0 \\ Z_{12} & Z_{23} & 0 & 0 & 0 \\ Z_{12} & Z_{23} & Z_{34} & 0 & 0 \\ Z_{12} & Z_{23} & Z_{34} & Z_{45} & 0 \\ Z_{12} & Z_{23} & 0 & 0 & Z_{36} \end{bmatrix}=[BCBV] \tag{7.27}$$

So,[$BCBV$] matrix is the product of transpose of [$BIBC$] and diagonal impedance matrix [ZD].

$$[BCBV]=[BIBC]^T.[ZD] \tag{7.28}$$

Substituting Eqn. (3.20) in Eqn. (3.17) gives,

$$[\Delta V]=[BIBC]^T.[ZD].[B] \tag{7.29}$$

Combining Eqn. (7.28) and Eqn. (7.29) gives,

$$[\Delta V]=[BIBC]^T.[ZD].[BIBC].[I] \tag{7.30}$$

Distribution Load Flow (DLF) matrix is obtained as the product of BCBV and BIBC matrices.

$$[DLF]=[BCBV].[BIBC]=[BIBC]^T.[ZD].[BIBC] \tag{7.31}$$

So, Eqn. (7.30) can be expressed as,

$$[\Delta V]=[DLF].[I] \tag{7.32}$$

For the $(k+1)^{th}$ iteration,

$$\left[\Delta V^{k+1}\right]=[DLF].\left[I^k\right] \tag{7.33}$$

Where,

$$I_j^k=\left(\frac{P_j+jQ_j}{V_j^k}\right)^*$$

From Eqn.(7.33) ,

$$\left[\Delta V^{k+1}\right]=\left[V^0\right]-\left[V^{k+1}\right] \tag{7.34}$$

So,

$$\left[V^{k+1}\right]=\left[V^{0}\right]-\left[\Delta V^{k+1}\right] \tag{7.35}$$

The solution for the load flow can be obtained by solving eqns. (7.33) and (7.35) iteratively.

The total power loss can be expressed as a function of the bus current injections

$$P_{loss}=\sum_{k=1}^{nb}\left|B_k\right|^2.R_k=\left[R\right]^T.\left|\left[BIBC\right]\left[I\right]\right|^2 \tag{7.36}$$

where, R_k is the resistance of k^{th} branch and nb is the number of branches.

7.9 SIZE OF D-STATCOM USING ANALYTICAL METHOD

In IEEE 15 bus test system, an attempt is carried out to find the size of D-STATCOM using the analytical method. D-STATCOM is placed at bus 4 and load flow analysis has been carried out based on BIBC-BCBV method. Algorithm for finding the size of D-STATCOM is given in Section 7.9.1.

7.9.1 Algorithm for finding size of D-STATCOM

Step 1: Read line data and bus data.

Step 2: Perform load flow algorithm

Step 3: Find voltage profile and power loss

Step 4: Assume voltage profile of candidate bus as 1 pu

Step 5: Calculate injected reactive power and phase angle of D-STATCOM

Step 6: Update reactive power of candidate bus

Step 7: Perform load flow with the updated reactive power of candidate bus.

Step 8: Print voltage profile and power loss

7.9.2 Power Loss and Voltage Profile

Based on BIBC-BCBV method, the power loss and voltage profile are computed without the integration of D-STATCOM. Then, the size of D-STATCOM is computed using the analytical method. The power loss and voltage profile are observed by placing this D-STATCOM at bus 4. It is seen that 0.3650207 MVAr size of D-STATCOM reduces the active power loss from 0.0550069 MW to 0.0416316 MW and reactive power loss from 0.0509702 MVAr to 0.0378962 MVAr respectively which is depicted in Table 7.4. The reduction in the active and reactive power loss is found to be 24.32% and 25.65% respectively. Further, the same size of D-STATCOM placed at each node for computing the power loss is shown in Fig. 7.13. It is seen that the power loss is minimum at bus 4.

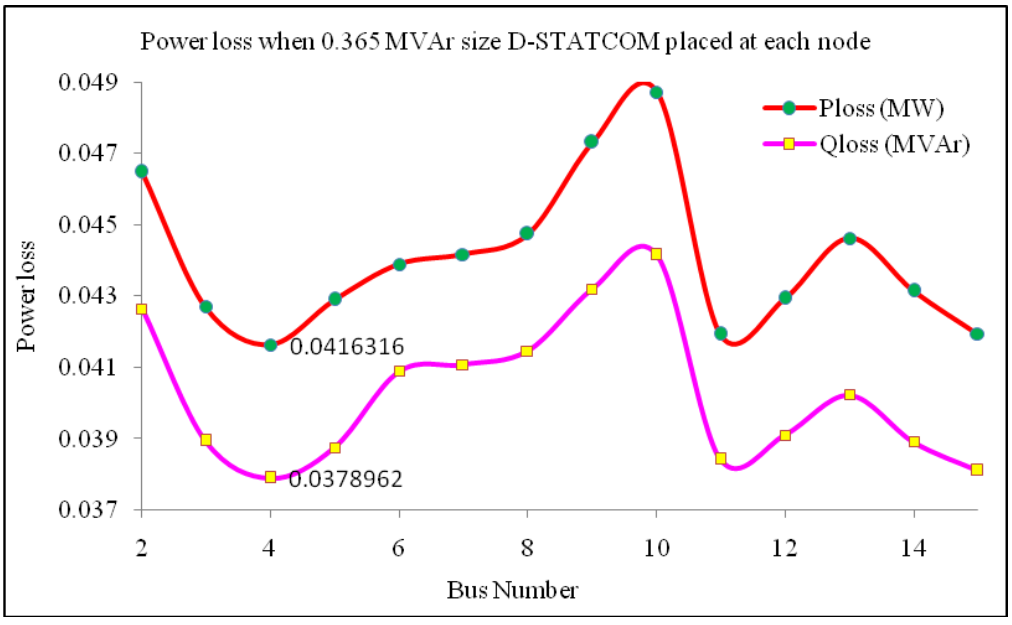

Fig. 7.13: Voltage profile of IEEE15 bus RDS when 0.365 MVAr D-STATCOM placed at each node

Table 7.4: Power loss in IEEE 15 bus RDS with and without D-STATCOM

Power loss	System without D-STATCOM	System with D-STATCOM
P_{loss} (MW)	0.0550069	0.0416316
Q_{loss} (MVAr)	0.0509702	0.0378962

From Fig. 7.14, it is found that the integration of 0.3650207 MVAr size of D-STATCOM improves the voltage profile when it is placed at bus 4. And also, it is seen that the size of D-STATCOM computed using BIBC-BCBV based analytical method is comparable to that of GA based on BFS algorithm. While comparing these two methods, it is observed that both voltage profiles are following the same pattern (Fig. 7.2 and Fig.7.14)

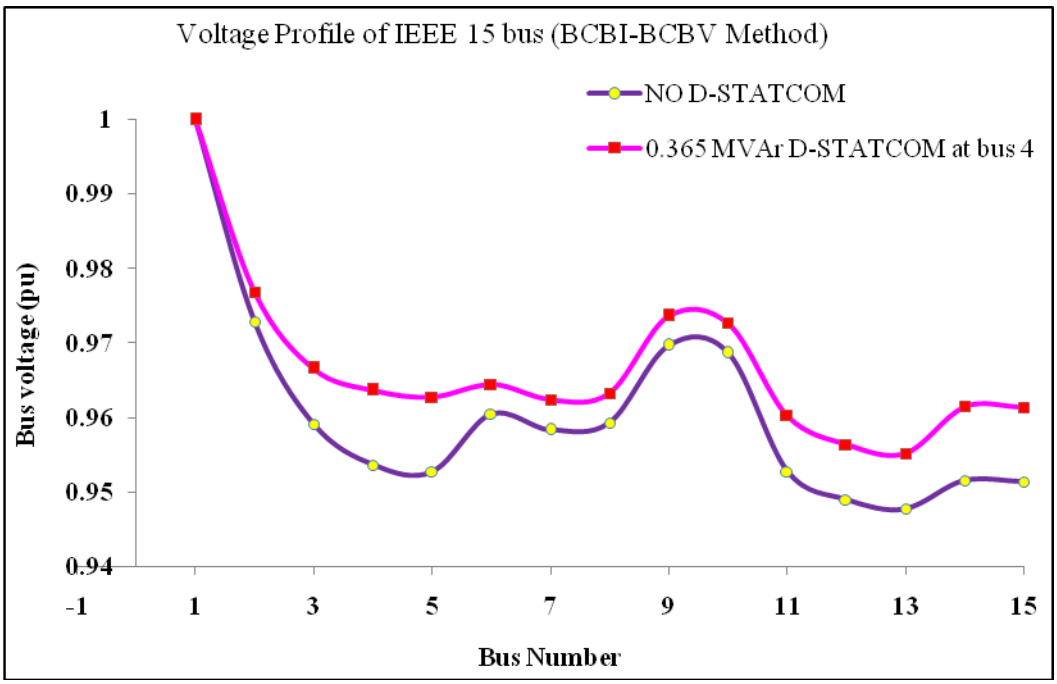

Fig. 7.14: Voltage profile of IEEE15 bus RDS without and with 0.365 MVAr D-STATCOM at bus 4

7.10 SUMMARY

Optimal allocation of DG and D-STATCOM has been significant in the present scenario where integration of DG has increased due to the growing demand. The increase in demand resulted in more DG sources being included in the system like a wind farm, solar panels that have, in turn, affected the reactive power requirement of the system. Hence, it has necessitated the need for D-STATCOM in DG integrated systems. In this work, BFS algorithm has been applied to find the location and size of D-STATCOM in IEEE 15 bus test system. It is inferred that the total loss is minimum when 0.4 MVAr size of D-STATCOM is placed at bus 4. The voltage of all the nodes are improved, particularly the nearby nodes 5, 14 and 15 and thereby the system became more reliable. Further, the position and size of D-STATCOM in multiple DG integrated radial network have been computed for observing the enhancement in voltage profile. BIBC-BCBV based analytical method is used to affirm the size and location of D-STATCOM in this radial network. From the results obtained, it is seen that better enhancement of voltage stability is achieved with the proper placement of optimized DG and D-STATCOM. Hence, it is inferred that the location and size of DG/D-STATCOM is a prime factor for achieving better voltage stability enhancement.

CHAPTER 8

MODELING OF DG AND CPD INTEGRATED RADIAL DISTRIBUTION SYSTEM

8.1 INTRODUCTION

Power supply system, transmission, and distribution networks have to be expanded to meet the increase in demand. Integration of DG based systems is a viable option to meet the growing demand and helps to operate the system within security limits, ensuring the stability. CPDs can be used for solving PQ issues caused by an increase in the use of nonlinear loads. In this work, IEEE 15 bus radial distribution network has been taken for voltage stability as well as PQ analysis.

8.2 THEVENIN'S EQUIVALENT CIRCUIT MODEL OF RDS

The practical distribution network of IEEE 15 bus can be reduced to an equivalent single line network for the investigation related to PQ issues. Thevenin's equivalent circuit model of IEEE 15 bus radial network is taken as the test system which is shown in Fig. 8.1. The total connected active and reactive load in the test system are 1.2264 MW and 1.251 MVAr respectively. From BFSA based load flow analysis, the active and reactive power losses are found to be 0.061791 MW and 0.057295 MVAr respectively. Using these values, the equivalent resistance and inductance of 15 bus test system are computed.

$$r_{eq} = \frac{P_{loss}}{P_{tl}^2 + Q_{tl}^2} = \frac{0.061791}{1.2264^2 + 1.251^2} = 0.0201345\Omega \quad (8.1)$$

$$x_{eq} = \frac{Q_{loss}}{P_{tl}^2 + Q_{tl}^2} = \frac{0.057295}{1.2264^2 + 1.251^2} = 0.01867\Omega \quad (8.2)$$

From Equations 8.1 to 8.2, the equivalent resistance and inductance for 23.2 km length of distribution feeder are computed as 0.0201345 Ω and 0.01867 Ω respectively. A test load of $1.2264 + j1.251$is connected at PCC of the test system.

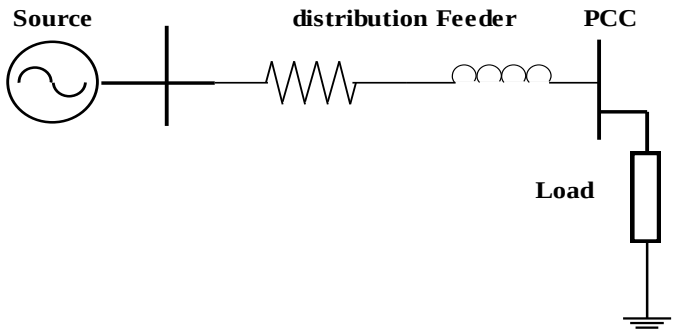

Fig. 8.1: Thevenin's equivalent circuit model of IEEE 15 bus radial network

In the Thevenin's equivalent test system, distribution feeder is connected between the voltage source and test load such as linear, nonlinear and unbalanced load. The parameters are given in Table 8.1. The test system is modeled in SIMULINK.

Table 8.1: System parameters of Thevenin's equivalent circuit of IEEE 15 bus RDS

System Parameters	
Source	11kV, 50 Hz
Test load	$1.2264 + j1.251$
Feeder impedance	$0.0201345 + j0.01867\Omega$

To understand the performance of the test system, simulations are carried out on the system with different loads, wind farm and CPDs. Effects of the wind farm as well as the effectiveness of D-STATCOM and DVR on the test system are discussed in this chapter.

8.2.1 Linear Load Condition

Test system with distribution feeder of resistance 0.0201345 Ω and inductive reactance of 0.01867 Ω is connected to a voltage source of 11kV and a test load of 1.2264+ *j*1.251 is shown in Fig. 8.2. Simulation is carried out on the system to observe the parameters, voltage, and current at the source and load side.

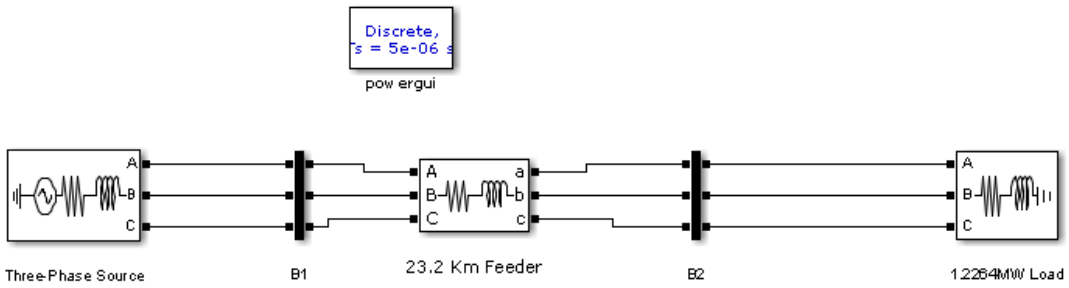

Fig. 8.2: Simulink model of test system connected to test load

Voltage and current waveform at the source and load side are shown in Figures 8.3 and 8.4. While comparing the voltage and current spectra of source and load, it is seen that the voltage and current at both sides are equal in magnitude and sinusoidal. Since the test load connected at PCC is acting as a linear load, the harmonics were not present in source and load side.

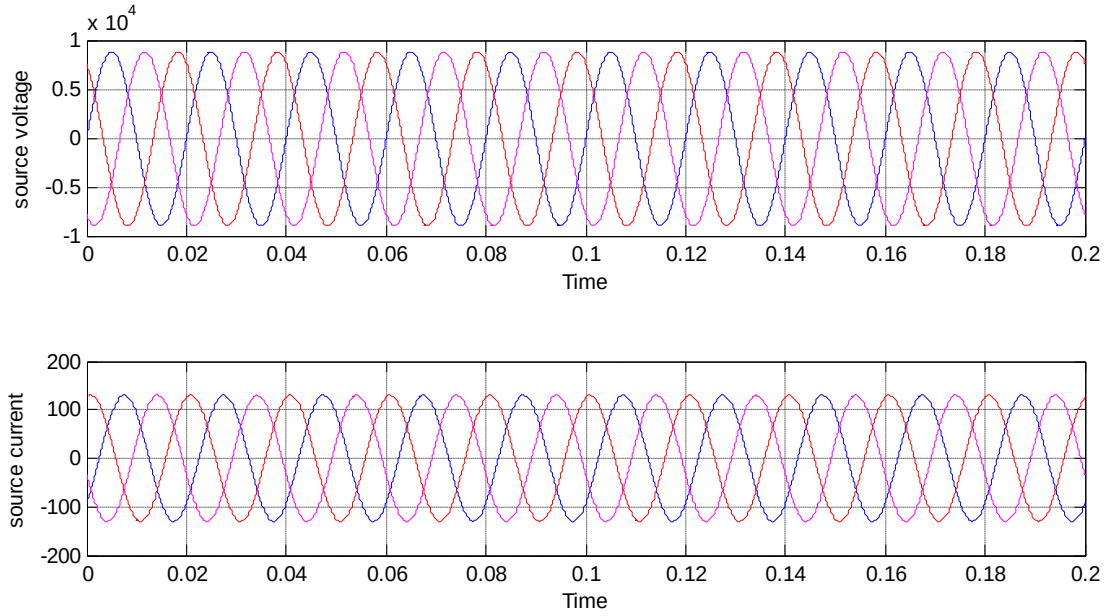

Fig. 8.3: Voltage and current at source side under linear load condition

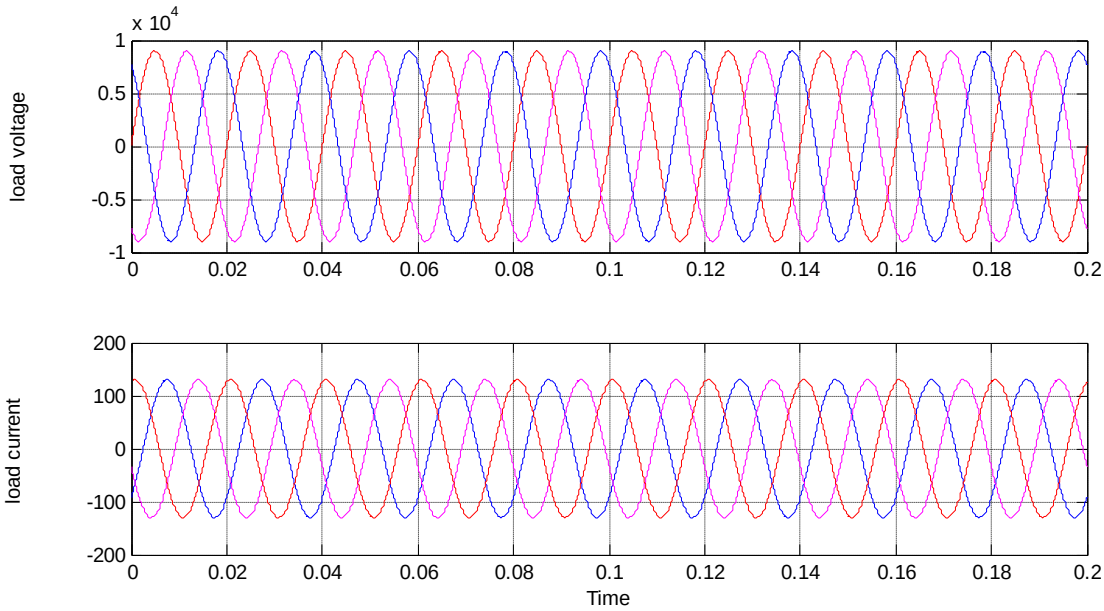

Fig. 8.4: Voltage and current at load side under linear load condition

Figure 8.5 and Figure 8.6 shows the active and reactive power waveforms at the source and load side. It is understood that the active and reactive power demand of linear load is fully supplied by the source.

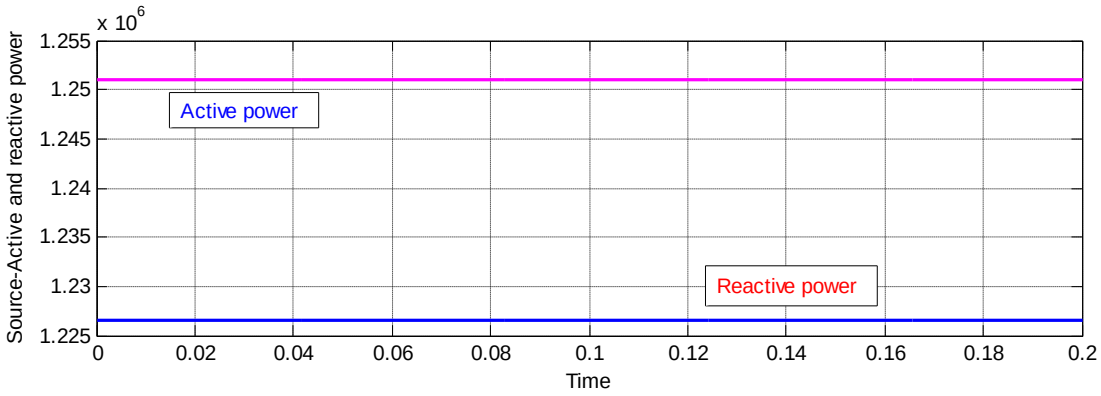

Fig. 8.5: Active and reactive power at source side under linear load condition

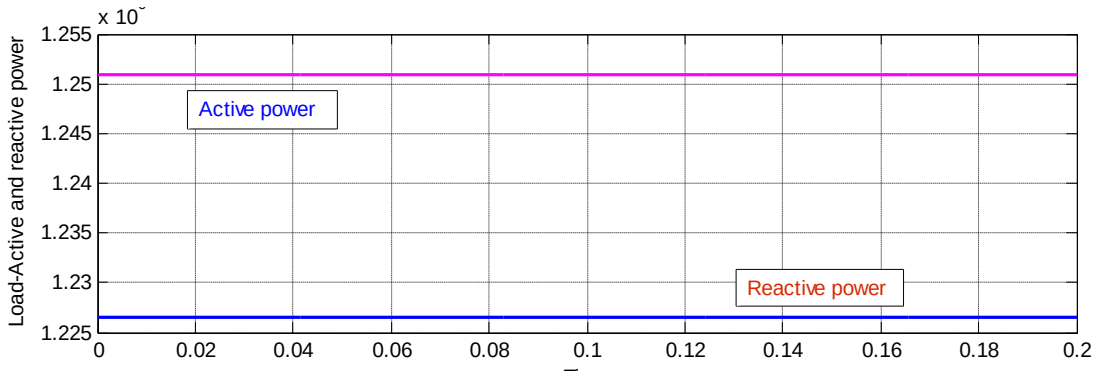

Fig. 8.6: Active and reactive power at load side under linear load condition

8.2.2 Nonlinear Load Condition

A nonlinear load is connected to the test load at PCC through a breaker. Simulation results are shown in Figures 8.7 and 8.8. Comparing the voltage spectra at the source and load side, it is found that they are equal in magnitude and are sinusoidal.

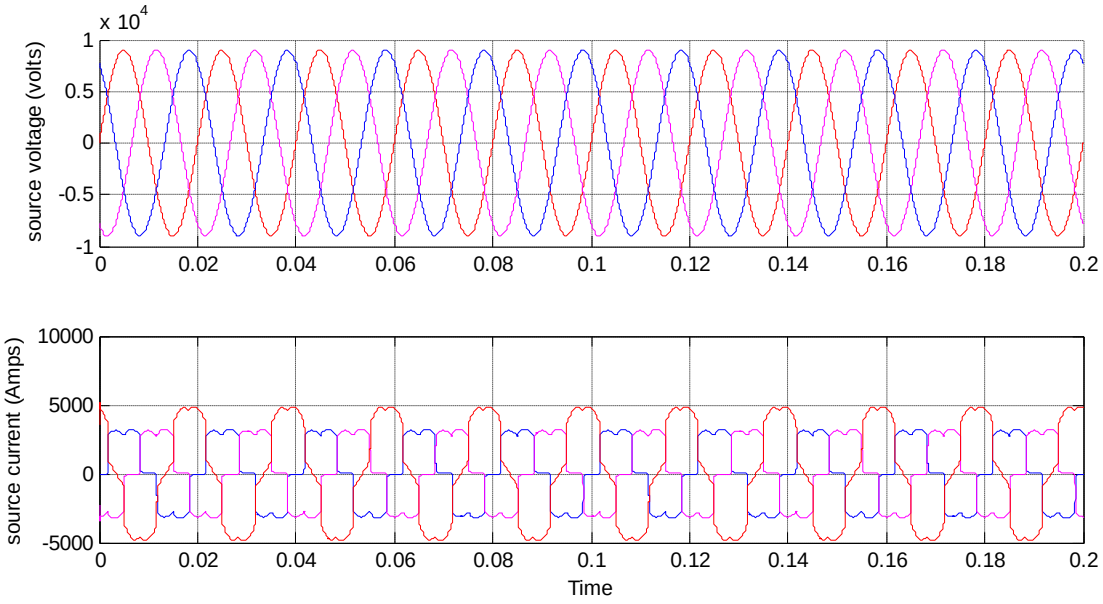

Fig. 8.7: Voltage and current at source side under nonlinear load condition

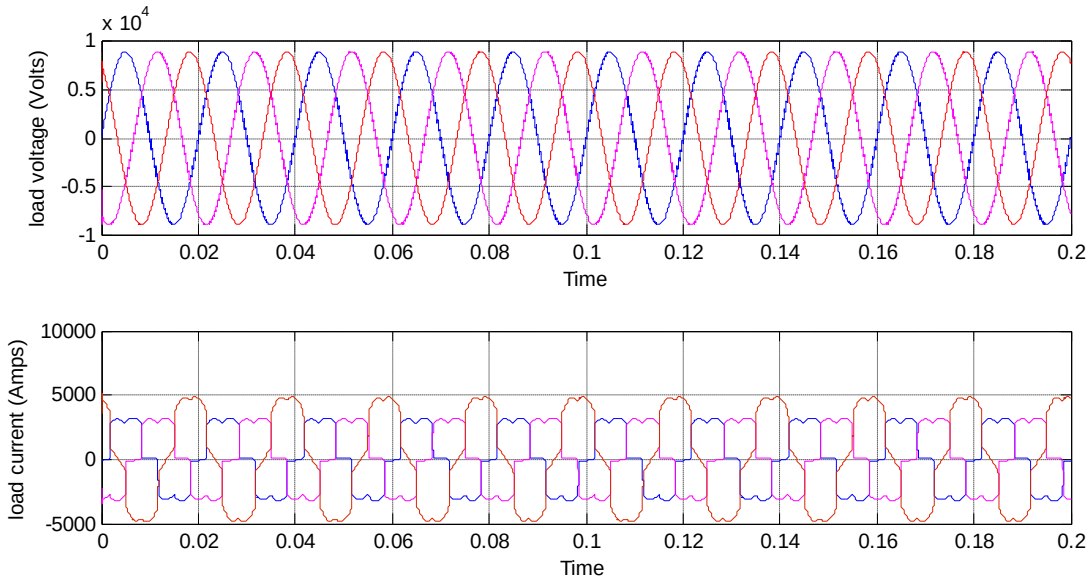

Fig. 8.8: Voltage and current at load side under nonlinear load condition

But, the current spectra are distorted due to the presence of harmonics under nonlinear load condition. It is clear that the harmonics in the load currents affect the source and therefore the system requires a harmonic current compensator.

8.2.3 Unbalanced Load Condition

Simulation is carried out on the test system connected to an unbalanced load on which R, Y and B phases are open for 0.1-0.5 sec. The voltage and current waveforms were observed at the source and load side. It is found that the current is distorted for this duration which is shown in Figures 8.9 and 8.10. It is due to the unbalanced system which draws an unbalanced current from the source.

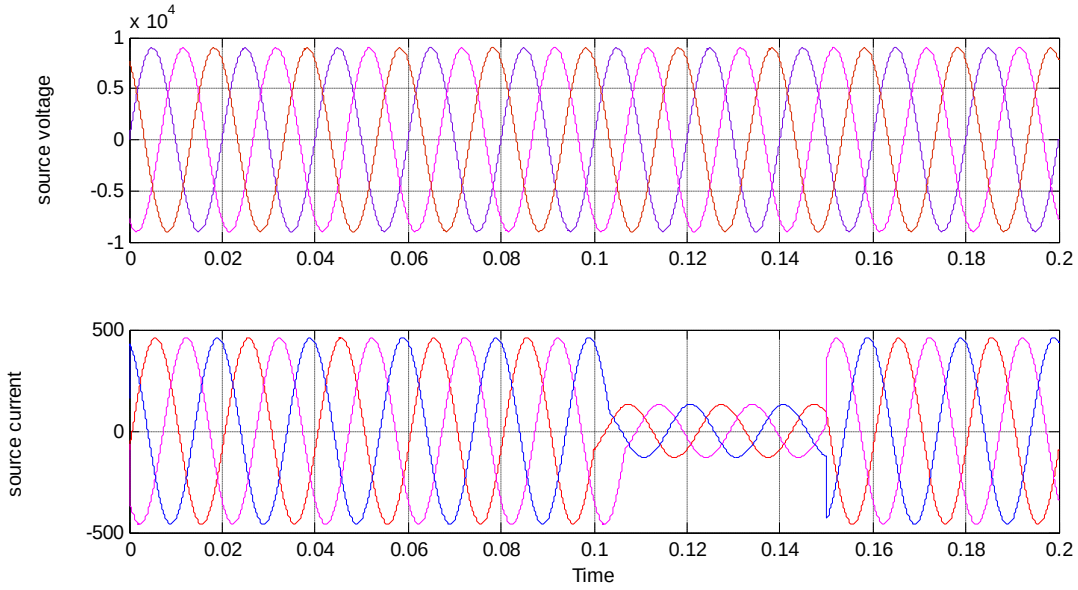

Fig. 8.9: Voltage and current at source side under unbalanced load condition

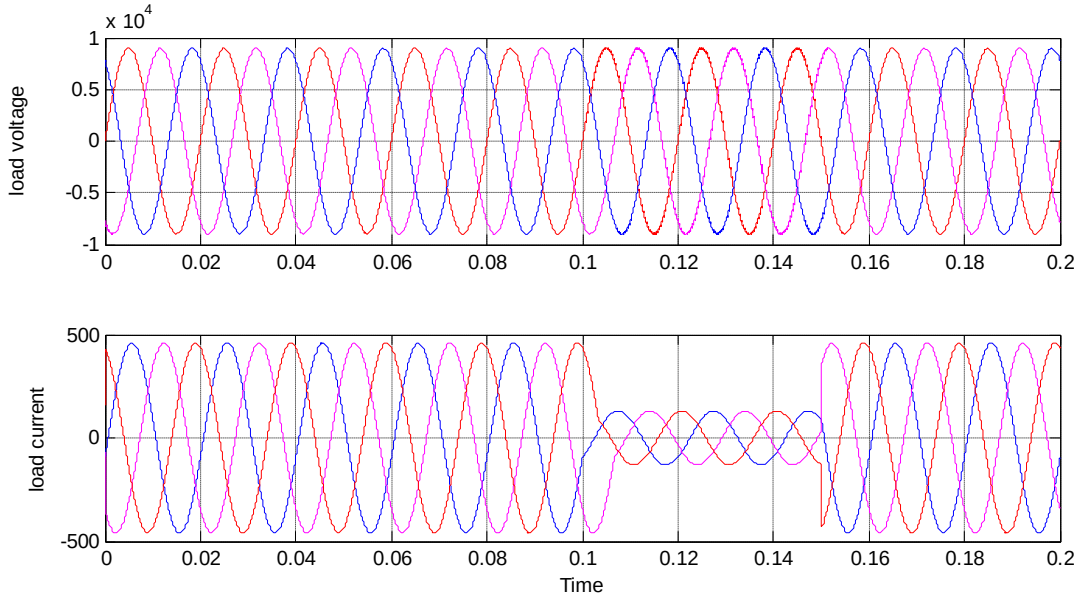

Fig. 8.10: Voltage and current at load side under unbalanced load condition

8.2.4 Combined Load Condition

Simulations are carried out in the system in which all types of loads are connected at PCC, and then, the voltage and current waveforms are monitored. Simulation results are shown in Figures 8.11 and 8.12. It is found that the voltage waveform is sinusoidal but, the current waveform is distorted at both sides.

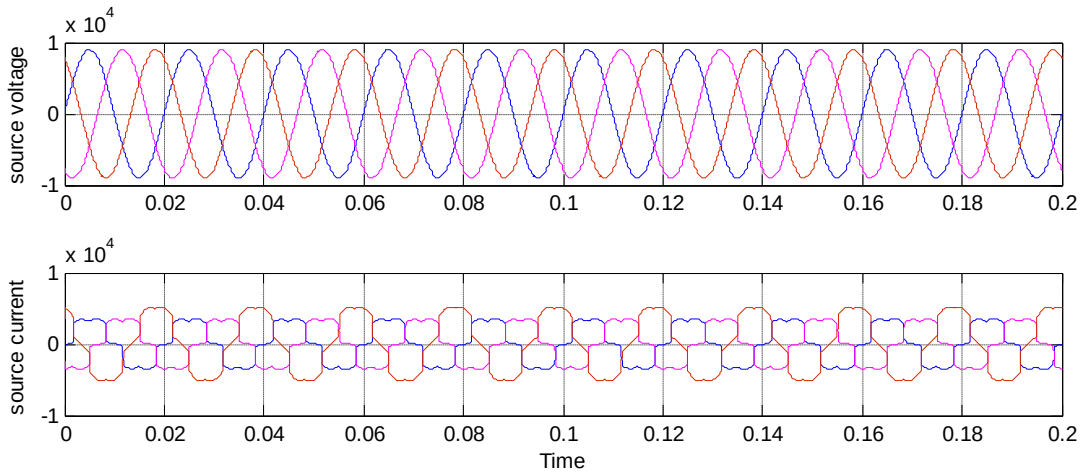

Fig. 8.11: Voltage and current at source side under combined load condition

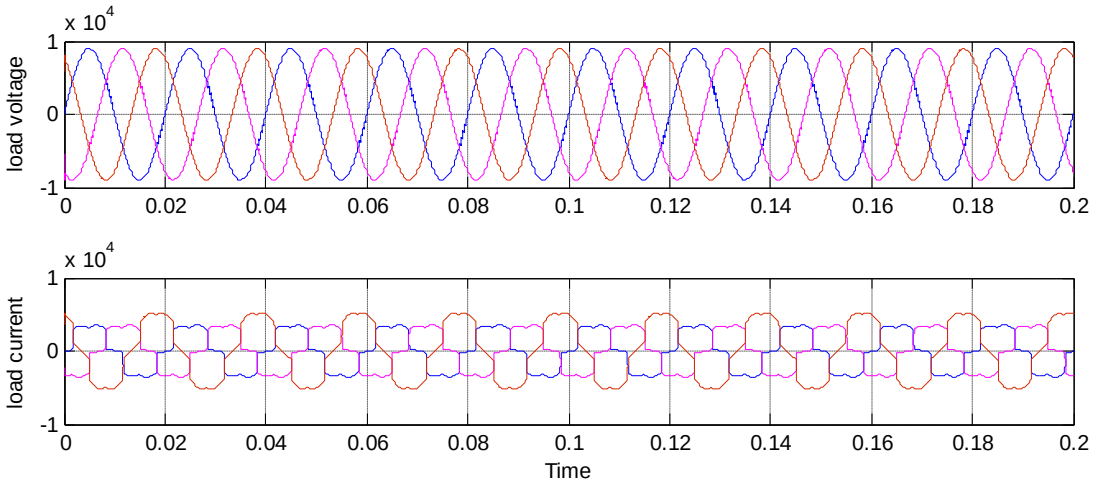

Fig. 8.12: Voltage and current at load side under combined load condition

Simulation results showed that the harmonic currents present in the test system due to nonlinear and unbalanced loads at PCC appears as an unbalanced linear load to the

grid. Effect of different types of fault on the radial network is already discussed in Chapter 4. In both the cases, it is observed that PQ issues can crop up either due to system faults or due to the presence of nonlinear loads. Shunt connected grid interfacing inverter can be used as the shunt active filter for compensating current harmonics and reactive power injection/absorption device for improving the voltage sag and voltage swell. DVR and D-STATCOM are used as a mitigating device in this work.

8.3 IMPACT OF DVR ON TEST SYSTEM

The model of DVR connected with test system is shown in Fig. 8.13. It is connected in series with the distribution line at PCC to which the test load is connected. Voltage sag occurs mainly due to LG fault and overload problem and, voltage swell occurs mostly when a heavy load turns off. In this section, the compensation of voltage sag and voltage swell with the use of DVR is demonstrated.

8.3.1 Voltage Sag Compensation

Model of the system consists of a programmable source, distribution line, test load and DVR. Voltage sag and voltage swell are created using the programmable device. DVR consists of voltage source converter (VSC), dc link, passive filter and boosting transformer. The output of VSC is connected to the grid through a transformer. The primary side of the transformer is connected in series with the distribution line and the output of VSC is connected to the secondary of the transformer.

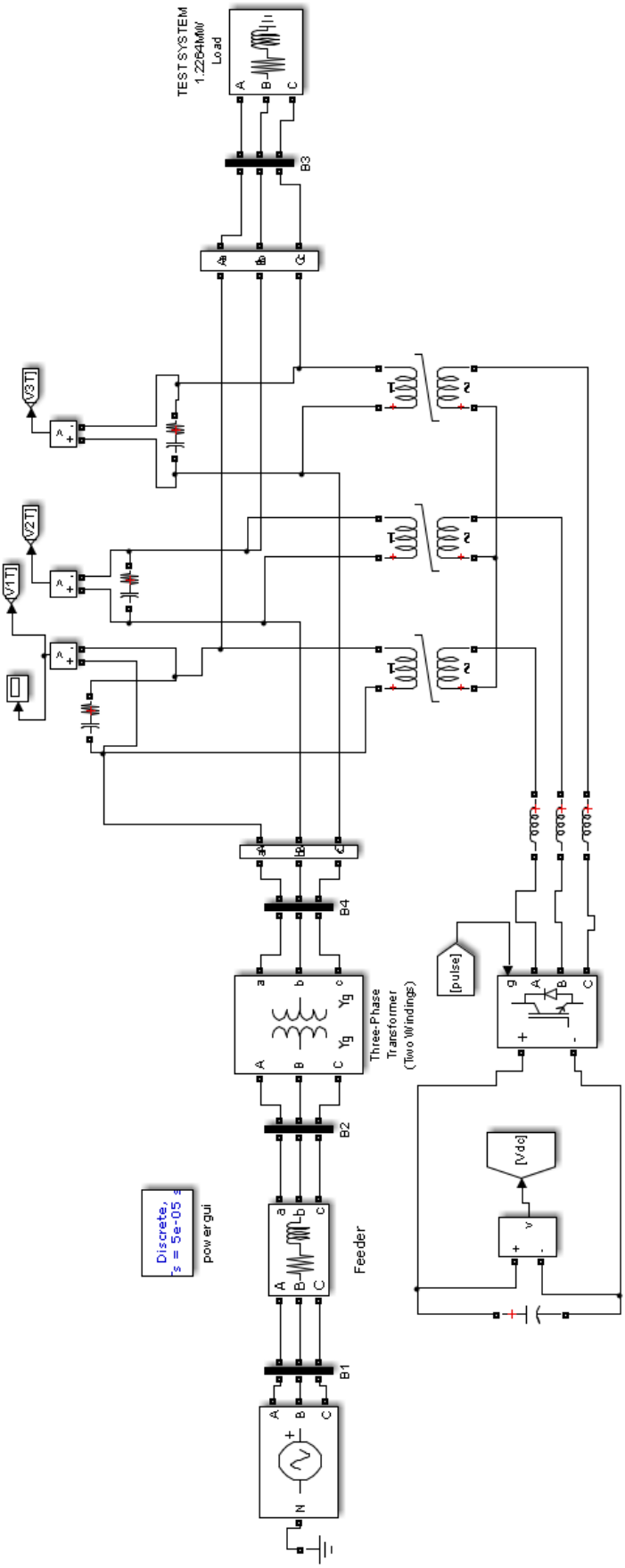

Fig. 8.13: Simulink model of DVR integrated test system

In normal condition, DVR did not inject or absorb any reactive power to the system. It is meant that there is no voltage distortion at the load side and source side and hence both voltages are found to be 1 pu, shown in Fig. 8.14. Then, system voltage is reduced to 0.8 pu from 1pu for 1-3 sec. Reflection of sag in source side on the load side is shown in Fig. 8.15. From Fig. 8.15, it is seen that the voltage at the source and load side are 0.8 pu.

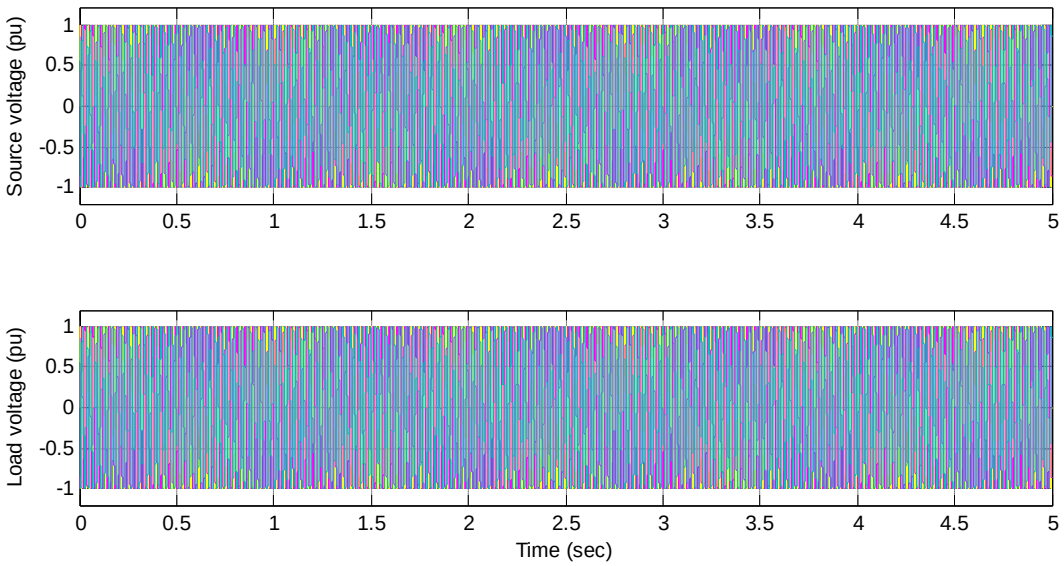

Fig. 8.14: Voltage at source and load side without sag

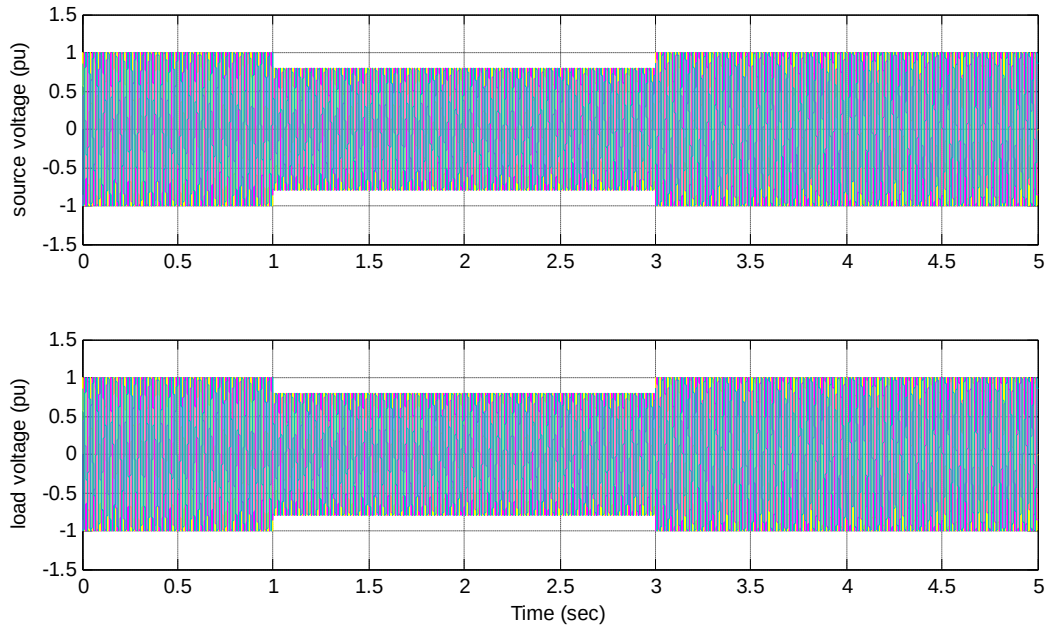

Fig. 8.15: Voltage at source and load side with a voltage sag of 20%

To mitigate the voltage sag, a discrete PWM based control scheme is used. The load voltage at PCC (V_{pcc}) is first sensed, and its magnitude is compared with the reference voltage (V_{ref}). If V_{pcc} is less than V_{ref}, then DVR injects sufficient voltage to compensate the missing voltage. In self-supported DVR, the injected voltage is in quadrature with the line current. The power absorbed or supplied is zero under steady state condition and the voltage injected by DVR is in quadrature with feeder current. The voltage injected by DVR (V_c) is used to maintain V_{pcc} at 1pu. It has direct axis component (V_{cd}) in phase with the current used to meet the power losses in VSC of DVR and thereby regulate the DC bus voltage and quadrature axis component (V_{cq}) is used to regulate the PCC voltage at a constant magnitude.

The control is based on synchronous rotating frame theory [227]. Fig. 8.16 shows the control scheme of DVR. The synchronous reference frame method is used for estimation of V_{ref}, which is based on the transformation of voltage in the synchronously rotating d-q frame. The source voltage or V_{pcc} is converted to rotating reference frame using abc-dq0 conversion called Parks Transformation.

The components of voltages in d-axis and q-axis are

$$V_d = V_d^{dc} + V_d^{ac} \tag{8.3}$$

$$V_q = V_q^{dc} + V_q^{ac} \tag{8.4}$$

The low pass filter is used to eliminate the harmonics and oscillatory components. PI controller is used to maintaining dc bus voltage across the capacitor of DVR.

$$V_{cap} = V_{cap}{}^{n-1} + K_{p1}(V_{de}{}^{n} - V_{de}{}^{n-1}) + K_{i1}V_{de}{}^{n} \quad (8.5)$$

where $V_{de}{}^{n} = V_{dc}{}^{*} - V_{dc}{}^{n}$ which is the error between the reference and sensed dc voltage at n^{th} the sampling instant. K_p And K_i is the proportional and integral gain of PI controller. The reference d-axis voltage,

$$V_d{}^{*} = V_d{}^{dc} - V_{cap} \quad (8.6)$$

To maintain the amplitude of load voltage to 1pu, another PI controller is used. The output of this PI controller is considered as the reactive component of voltage $V_{q(r)}$ which is used to regulate the load voltage. The amplitude of load voltage (PCC voltage),

$$V_l = \sqrt{\frac{2}{3}} \times \sqrt{\left(V_l{}^{a}\right)^2 + \left(V_l{}^{b}\right)^2 + \left(V_l{}^{c}\right)^2} \quad (8.7)$$

where $V_l{}^{a}$, $V_l{}^{b}$ and $V_l{}^{c}$ are ac voltages.

$$V_{q(r)} = V_{q(r)}{}^{n-1} + K_{p2}(V_{pe}{}^{n} - V_{pe}{}^{n-1}) + K_{i2}V_{pe}{}^{n} \quad (8.8)$$

where $V_{pe}{}^{n} = V_l{}^{*} - V_l{}^{n}$ is the error between the reference and actual PCC voltage at the n^{th} sampling instant.

The reference load quadrature axis voltage

$$V_q{}^{*} = V_q{}^{dc} + V_{q(r)} \quad (8.9)$$

The reference voltage $V_l{}^{a*}$, $V_l{}^{b*}$ and $V_l{}^{c*}$ in the a-b-c frame is obtained by inverse parks transformation, dq0 to a-b-c.

$$\begin{bmatrix} V_a \\ V_b \\ V_c \end{bmatrix} = \sqrt{\frac{2}{3}} \times \begin{bmatrix} \cos\theta & -\sin\theta & \frac{\sqrt{2}}{2} \\ \cos\left(\theta - \frac{2\pi}{3}\right) & -\sin\left(\theta - \frac{2\pi}{3}\right) & \frac{\sqrt{2}}{2} \\ \cos\left(\theta + \frac{2\pi}{3}\right) & -\sin\left(\theta + \frac{2\pi}{3}\right) & \frac{\sqrt{2}}{2} \end{bmatrix} \begin{bmatrix} V_d \\ V_q \\ 0 \end{bmatrix}$$

The error between sensed load voltage, V_{pcc} and V_{ref} is used to generate a pulse for VSC of DVR. PWM generator generates pulses for carrier-based PWM converters using two-level topology. The pulses are generated by comparing a triangular carrier waveform to a reference modulating the signal.

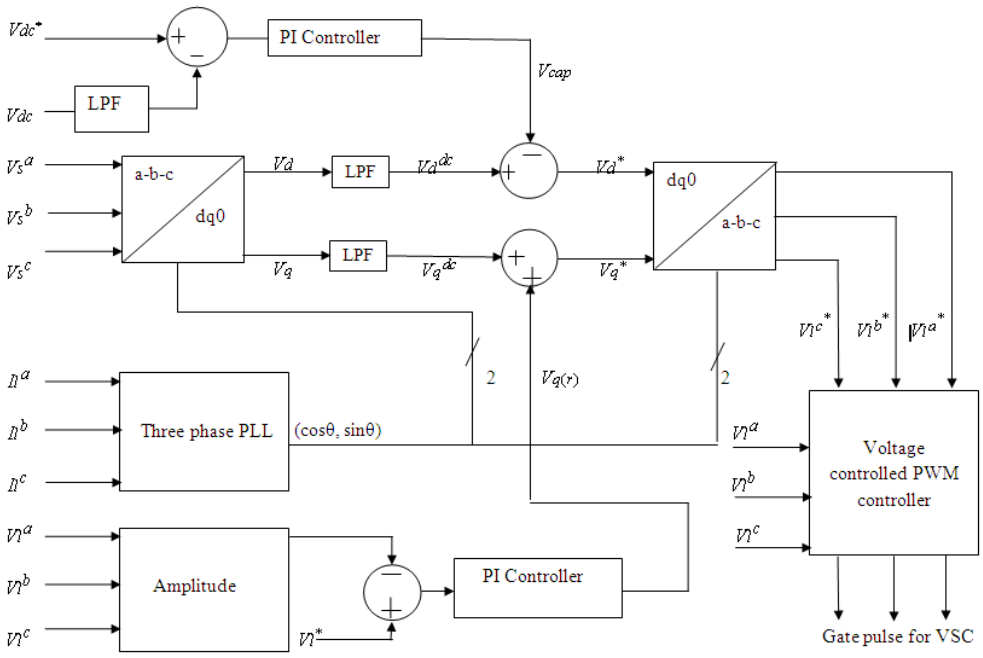

Fig. 8.16: Control scheme of self-supported DVR

Voltage sag improvement achieved with the help of DVR is as shown in Fig. 8.17. It is seen that the voltage at load side or PCC is raised from 0.8 pu to 1 pu with the effective control of DVR on the test system. This means that VSC injects sufficient amount of reactive power at PCC. The voltage across the capacitor is found to be 150V.

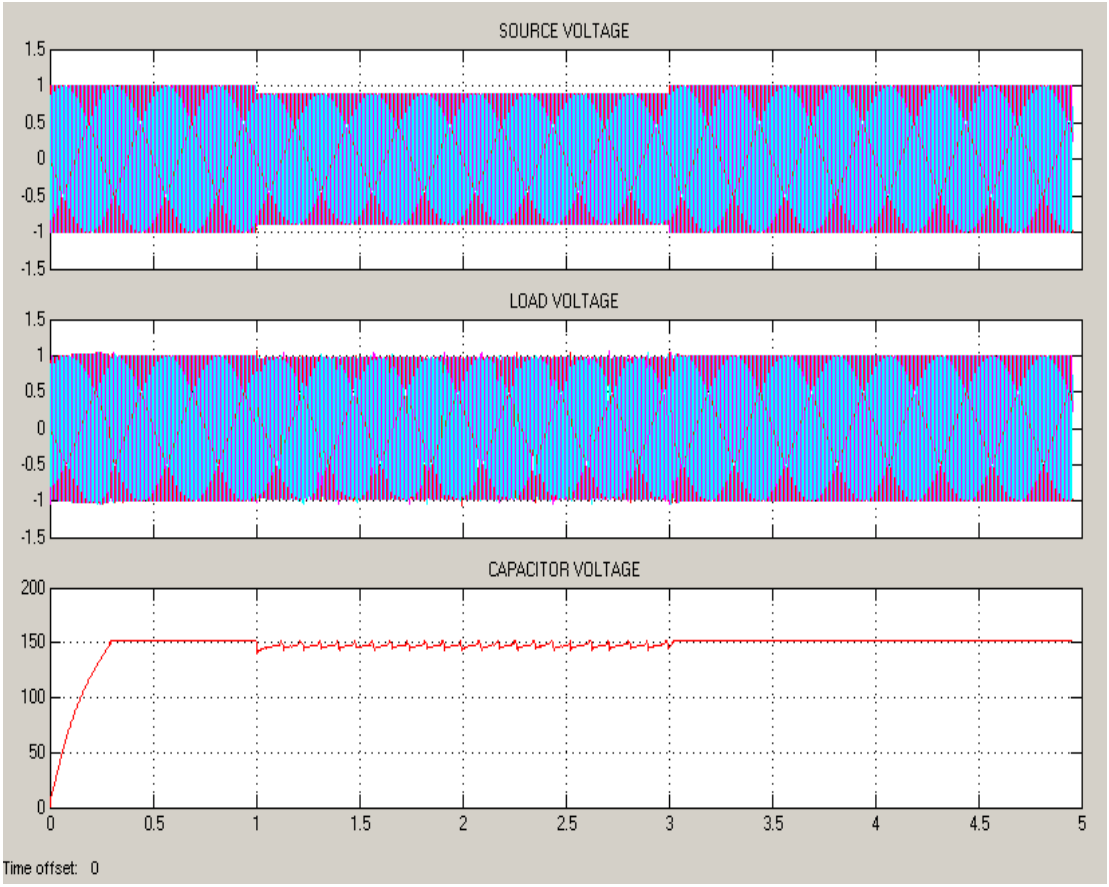

Fig. 8.17: Voltage sag mitigation using DVR and capacitor voltage.

8.3.2 Voltage Swell Compensation

In this work, the system voltage is increased to 1.2 pu for 1-3 sec. Swell in source side reflection on the load side is shown in Fig. 8.18. It is seen that the voltage at source and load side is 1.2 pu.

If the V_{pcc} is greater than V_{ref}, then DVR absorbs the reactive power to minimize the effects of the voltage at PCC. The voltage swell compensation is shown in Fig. 8.19. The voltage at load side is reduced from 1.2 pu to 1 pu with the effective control of DVR. The capacitor voltage is found to be 150V.

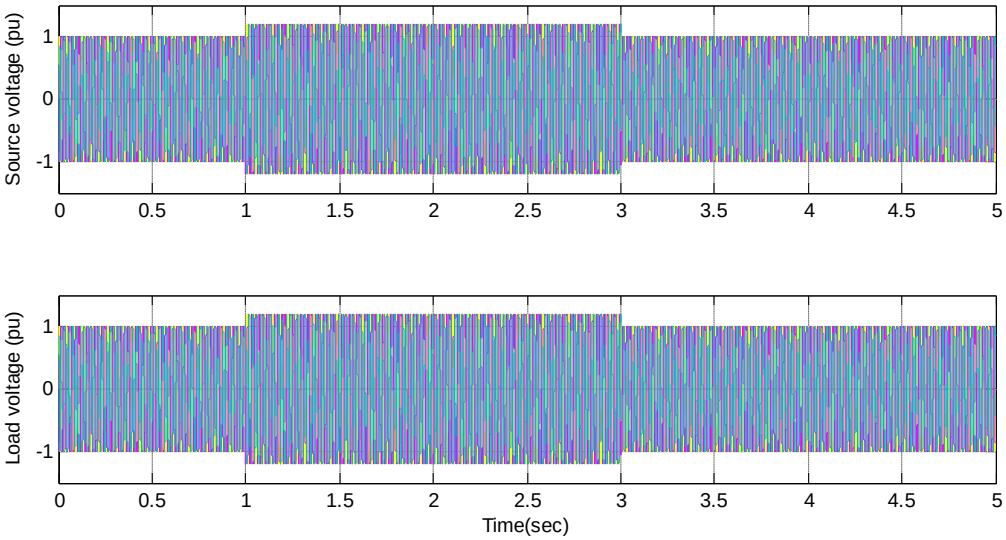

Fig. 8.18: Voltage at source and load side with a voltage swell of 20%

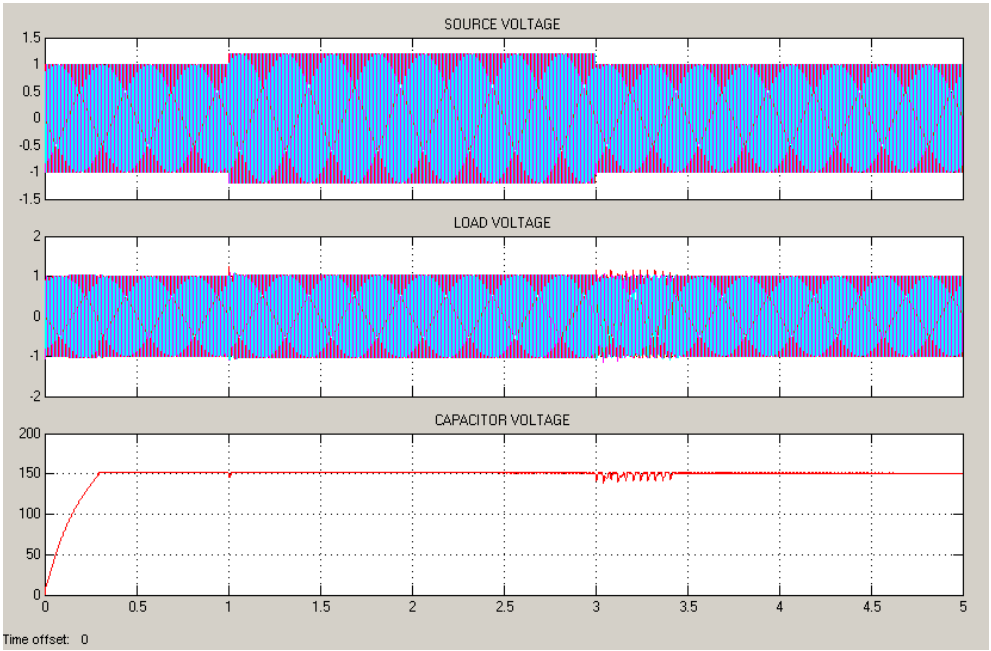

Fig. 8.19: Voltage swell mitigation using DVR and capacitor voltage.

8.4 IMPACT OF D-STATCOM ON TEST SYSTEM

Model of D-STATCOM integrated with the test system is shown in Fig. 8.20. The mitigating device D-STATCOM is connected in parallel with the test load at PCC. Another load is connected to the PCC through the circuit breaker to create voltage sag at the load side. The control scheme of D-STATCOM is shown in Fig. 8.21.

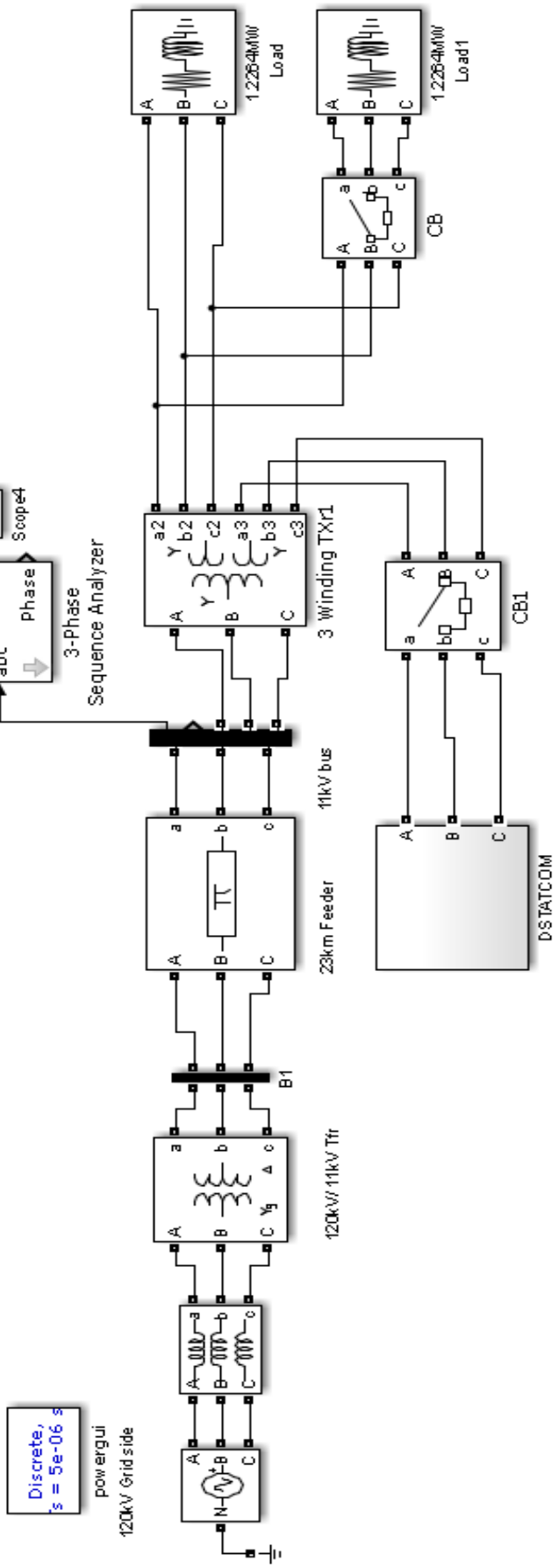

Fig. 8.20: Simulink model of D-STATCOM integrated test system

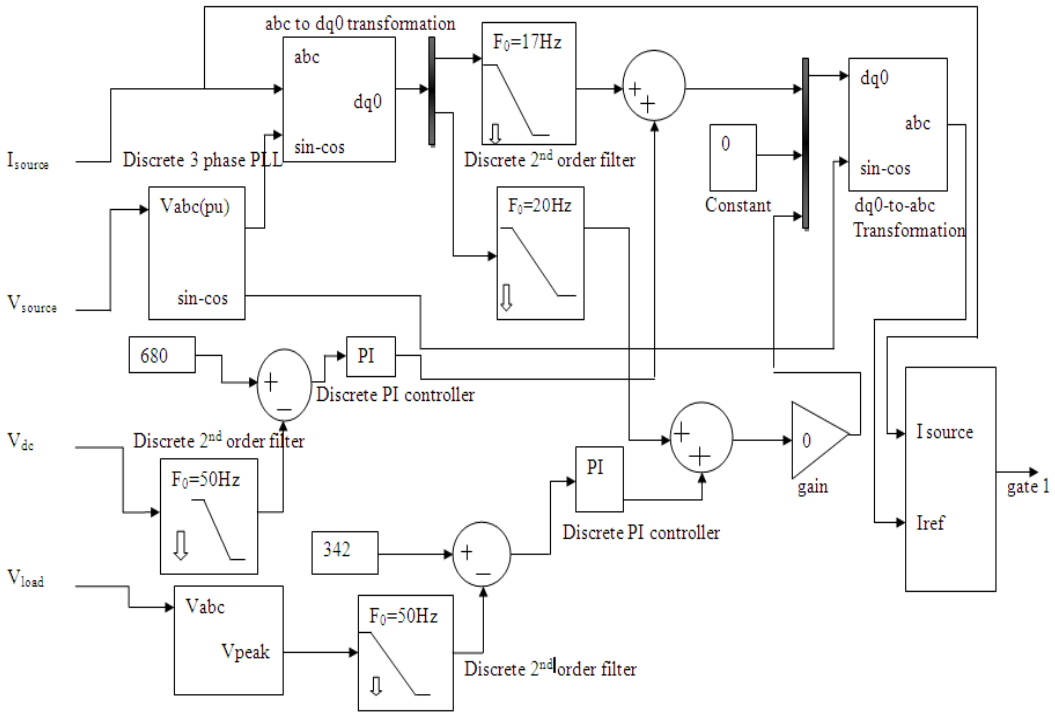

Fig. 8.21: Control scheme of D-STATCOM

When D-STATCOM is not connected to the test system, then the voltage at PCC is found to be 1 pu as is shown in Fig. 8.22. The circuit breaker is used to make a fault on the load side for 0.06-0.14 seconds. It is seen from Fig. 8.23 that the voltage is reduced from 1 pu to 0.95 pu. During this period, D-STATCOM provides sufficient amount of reactive power to meet the missing voltage and thereby the voltage at PCC is improved as it is evident from Fig. 8.24.

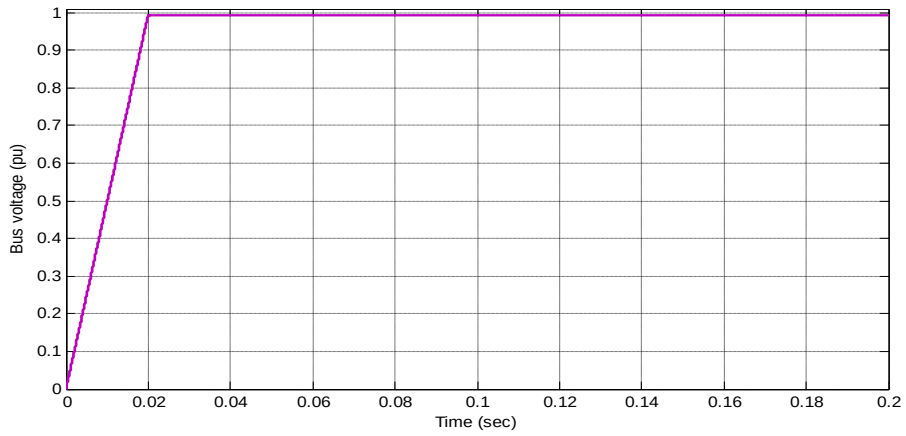

Fig. 8.22: Voltage at PCC without D-STATCOM

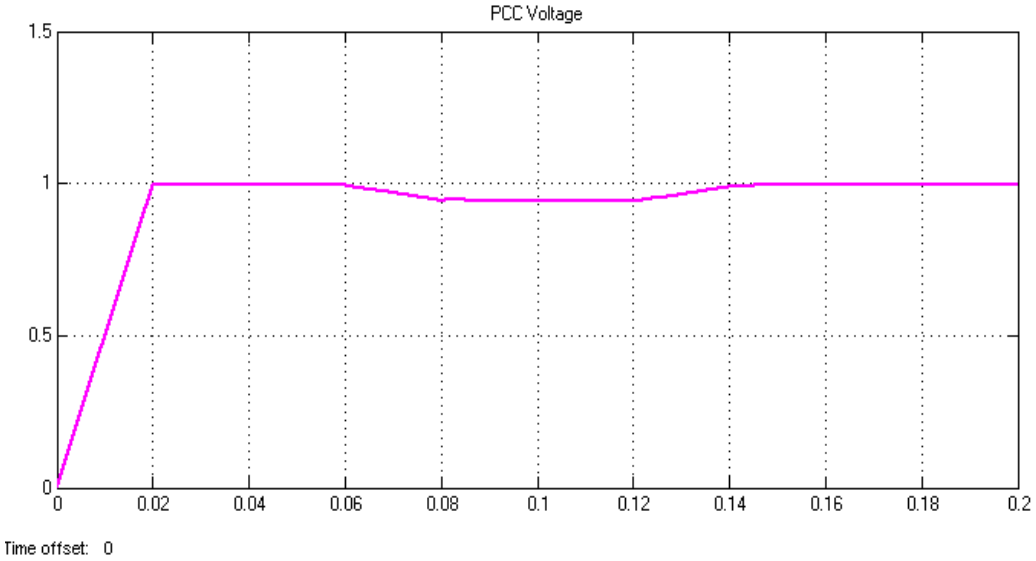

Fig. 8.23: Voltage sag under fault condition

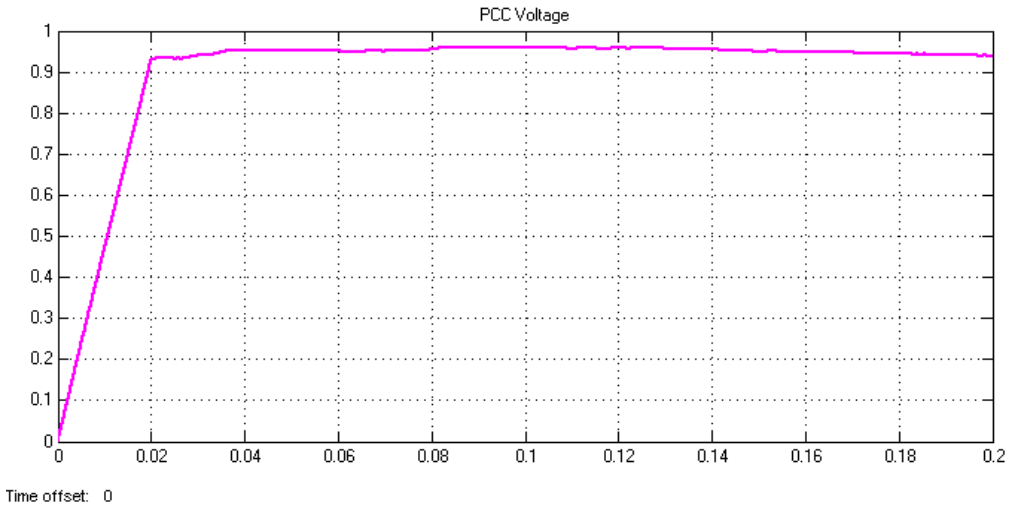

Fig. 8.24: Mitigated voltage at load side with D-STATCOM

8.5 DG ON TEST SYSTEM

Model of 400 kW size of DG on the test system is shown in Fig. 8.25. The wind-based system acts as the active power source so that the reactive power injection to the grid is zero. DG and test load are connected at PCC.

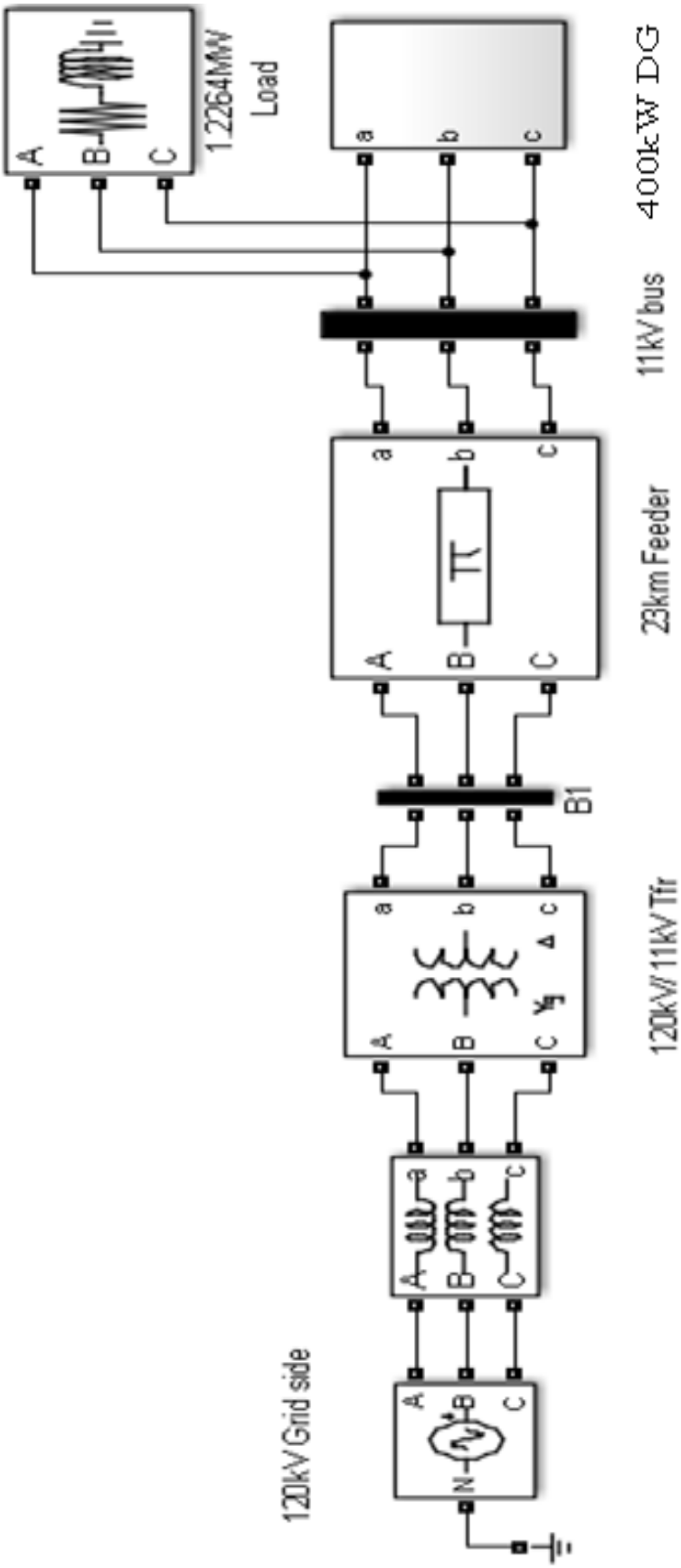

Fig. 8.25: DG integrated IEEE 15 bus RDS

Figure 8.26 shows the output of 400 kW wind system. The terminal voltage of the wind system is found to be 1 pu. DG provides active power only so that the active power output obtained from the wind-based system is 400 kW and reactive power output is zero.

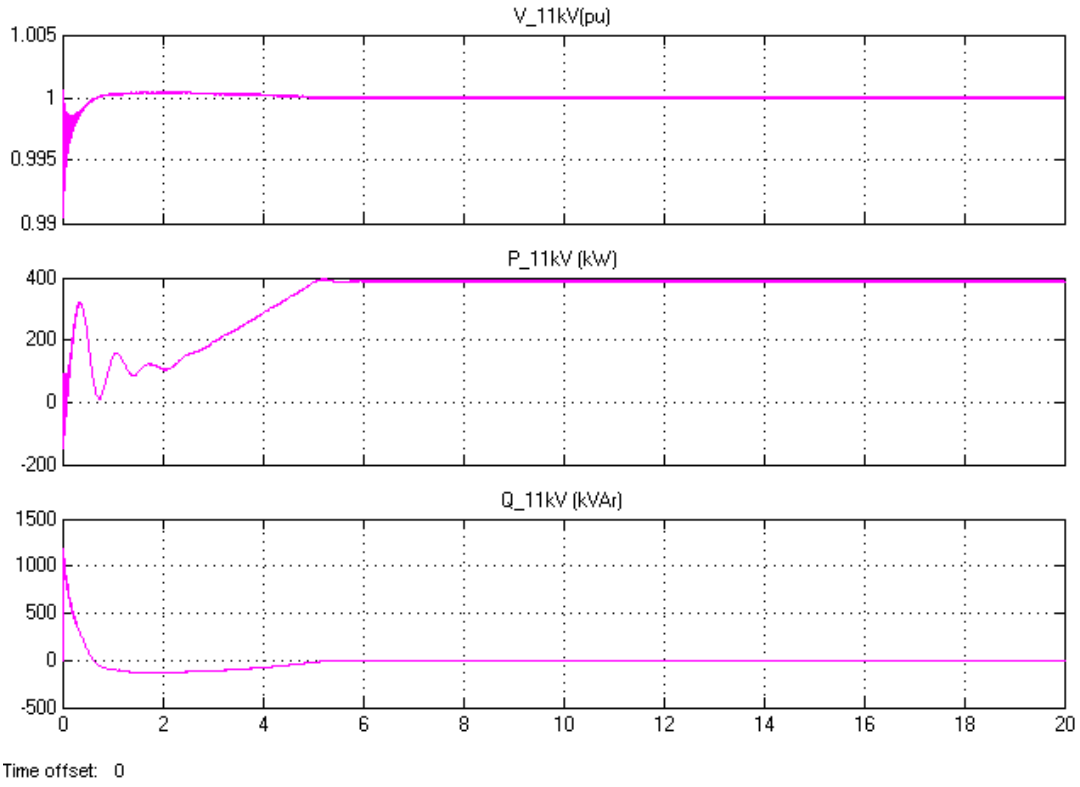

Fig. 8.26: Voltage, active and reactive power output of 400 kW wind system

Results obtained from integration of DG on the test system are shown in Fig. 8.27. The terminal voltage at PCC of this system is found to be nearly equal to 1pu. The active power of load connected at PCC is 1226.4kW. Active and reactive power output at PCC is then found to be nearly equal to 826kW and 0kVAr respectively.

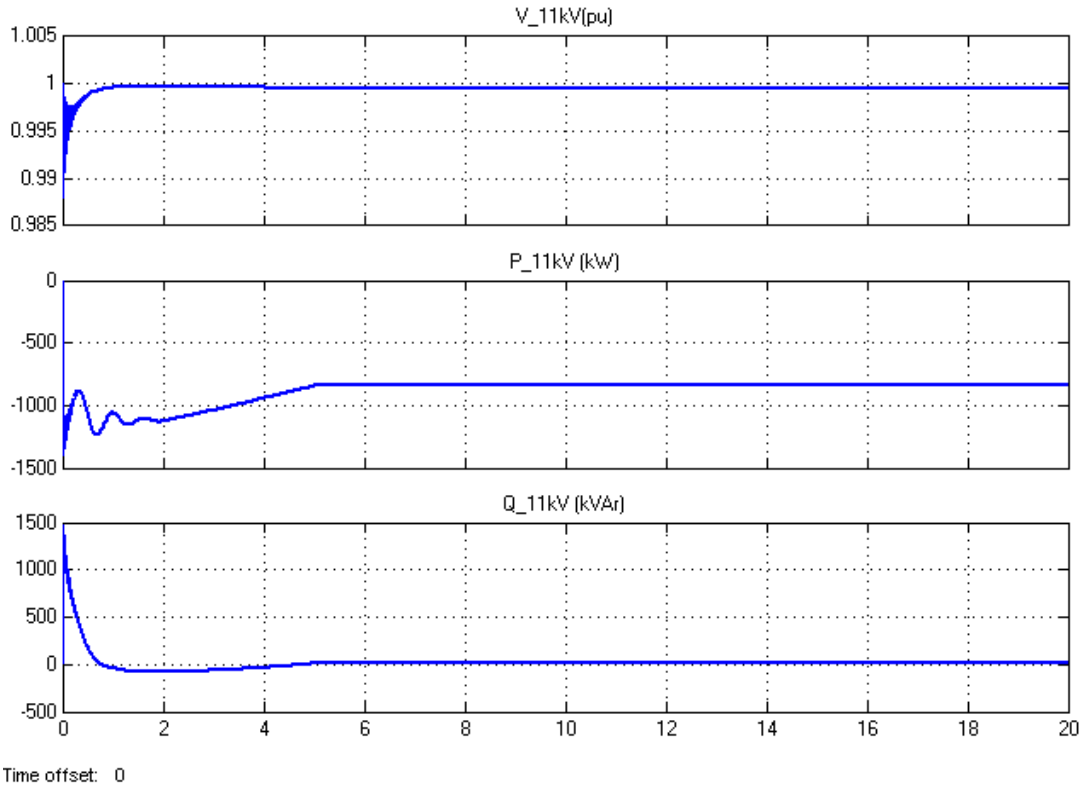

Fig. 8.27: Voltage, active and reactive power at PCC in DG integrated test system

8.6 DG AND D-STATCOM ON TEST SYSTEM

Figure 8.28 shows that the load, DG, and D-STATCOM are connected at PCC. If there is no disturbance in the system, then there is no voltage drop at the source side and load side. Therefore, the load voltage is found to be 1pu as shown in Fig. 8.29. Active and reactive power at wind side was found to be 0.4 pu (400kW) and 0 pu (0kVAr) respectively as shown in Fig. 8.30. Active and reactive power at source side is shown in Fig. 8.31.

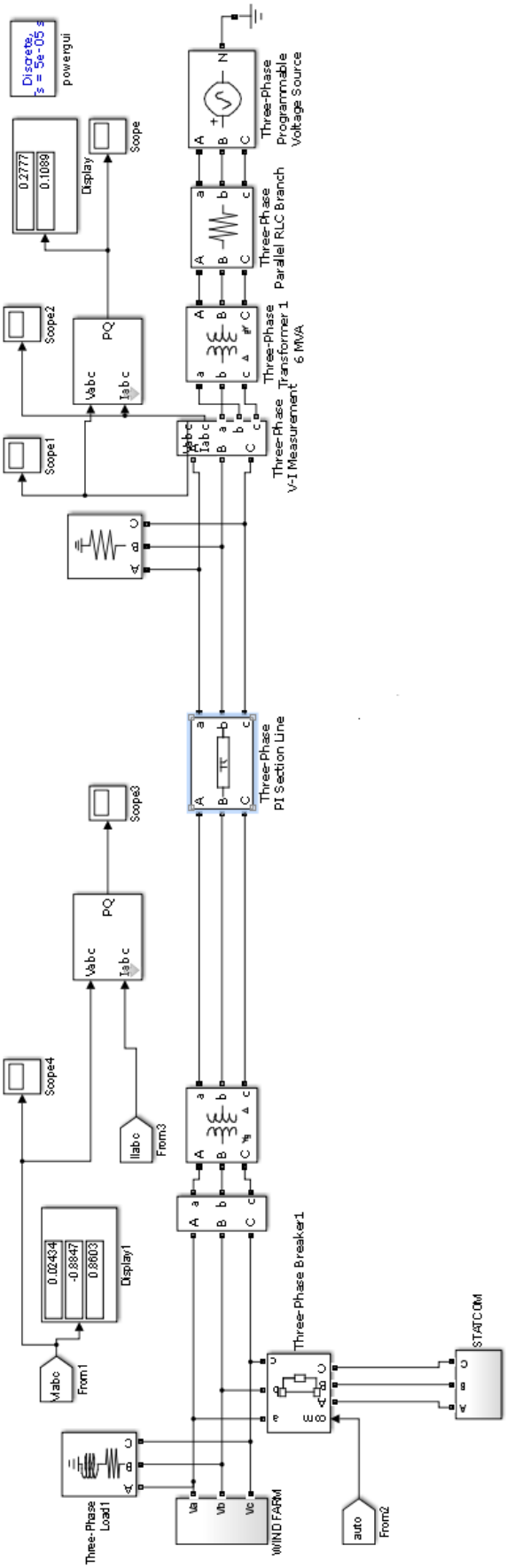

Fig. 8.28: Simulink model of DG integrated test system

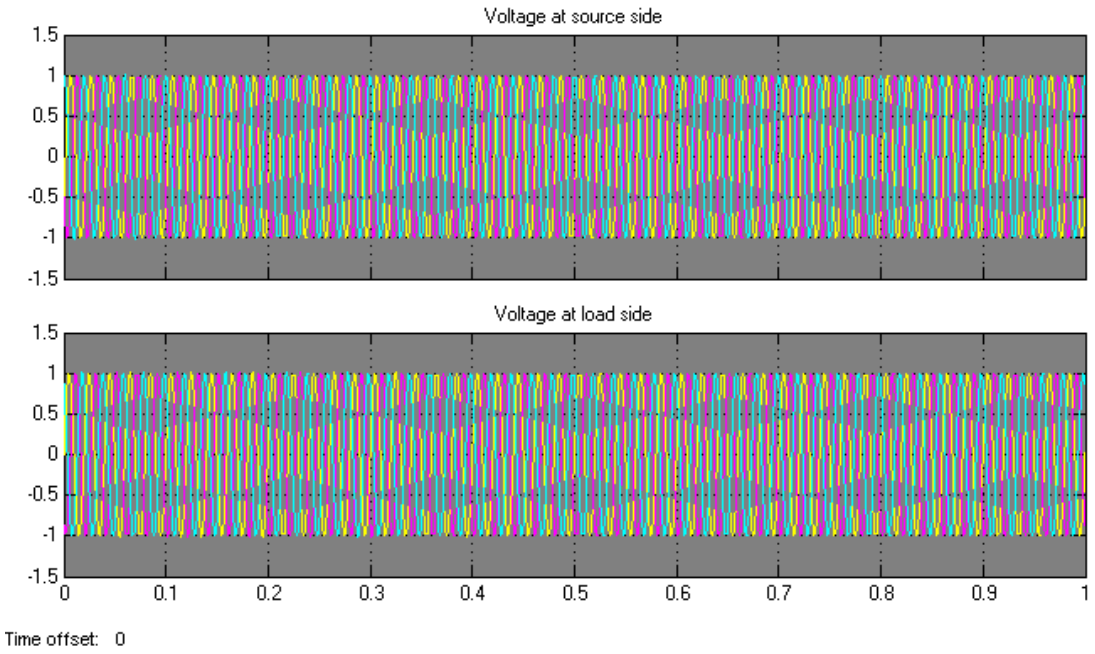

Fig. 8.29: Source voltage and load voltage of DG integrated test system

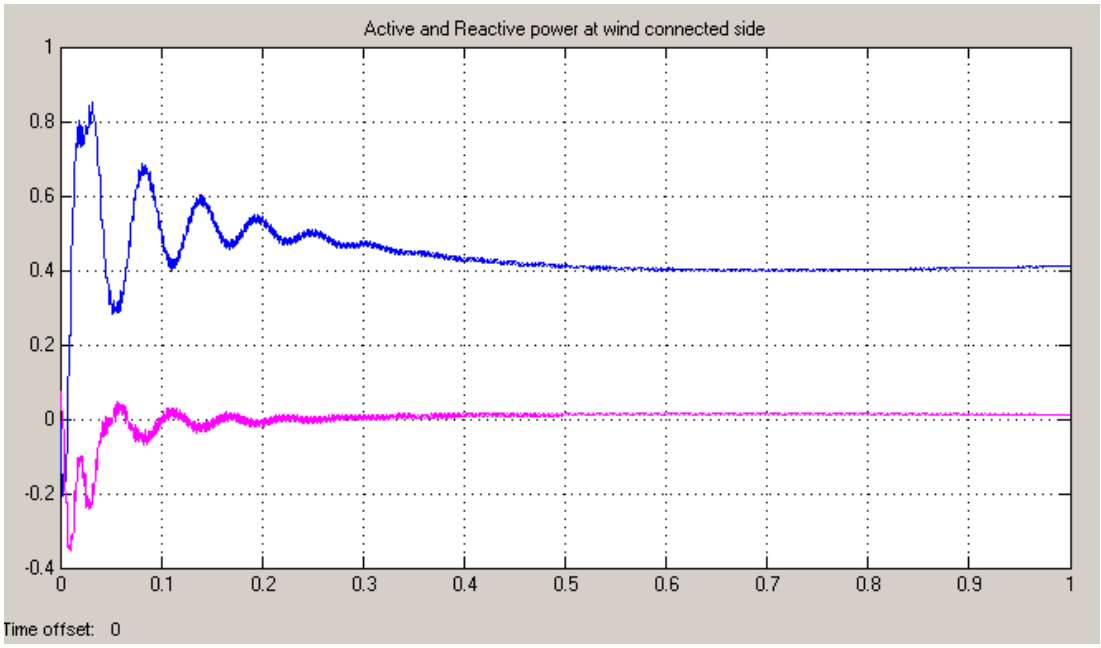

Fig. 8.30: Active and reactive power at PCC when DG of 400 kW connected at load side

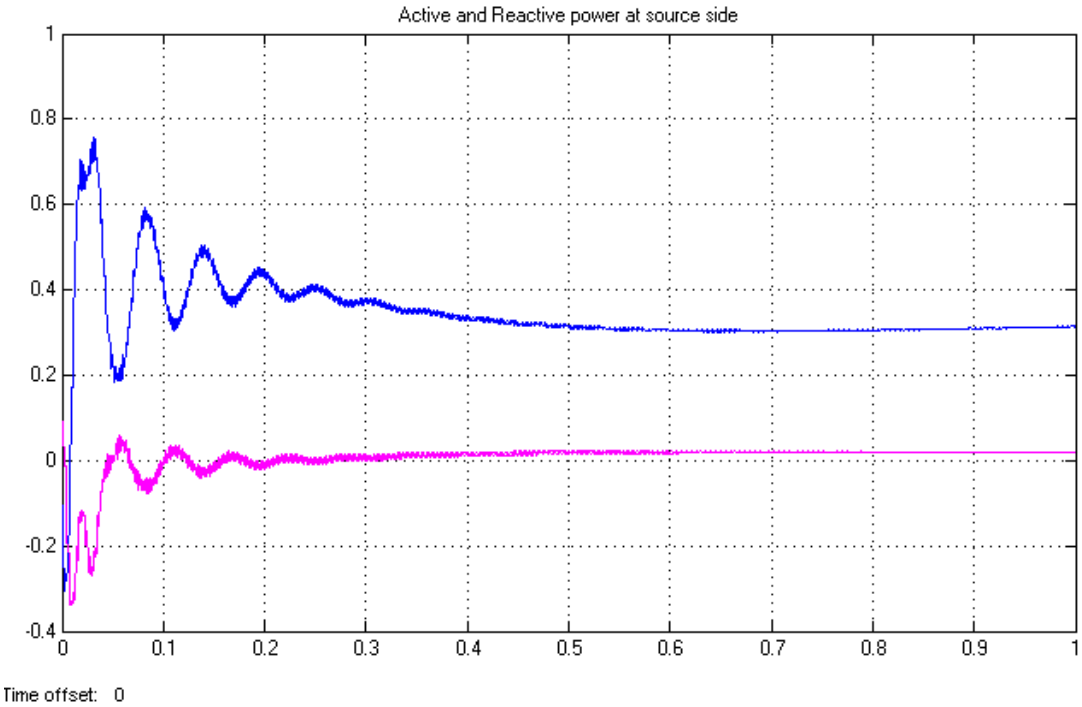

Fig. 8.31: Active and reactive power at source side when DG of 400 kW connected at load side

When a disturbance occurs for 0.3-0.5 seconds, then the effect of disturbance will reflect on both source and load side. The disturbance at source and load side for this period is shown in Figures 8.32 and 8.33. D-STATCOM will act as a mitigating device during the period of disturbance so that the voltage is recovered at load side. Figure 8.34 showed the source and load voltage under fault condition with D-STATCOM. The capacitor voltage is found to be 350V as shown in Fig. 8.35.

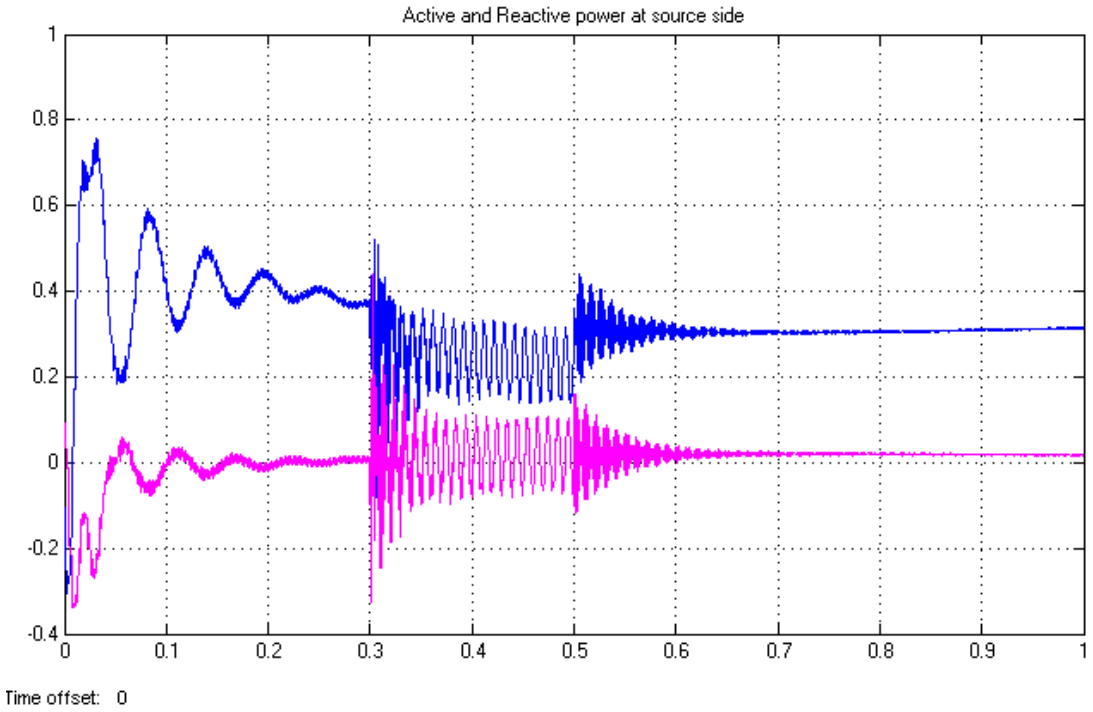

Fig. 8.32: Source power in DG integrated system under fault condition

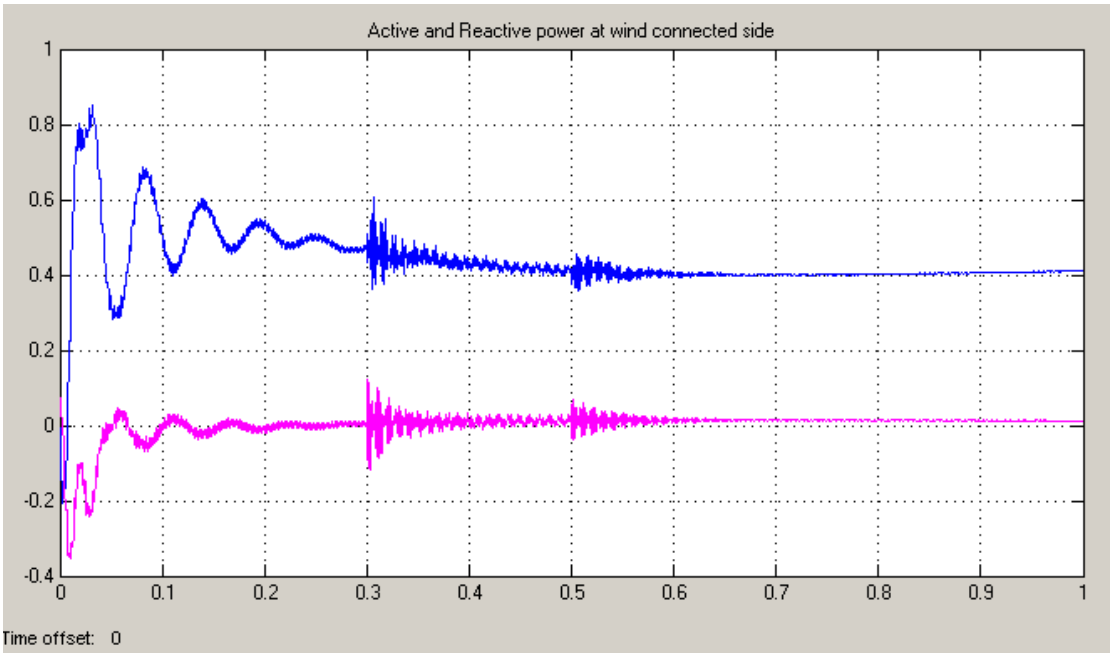

Fig. 8.33: Load power in DG integrated system under fault condition

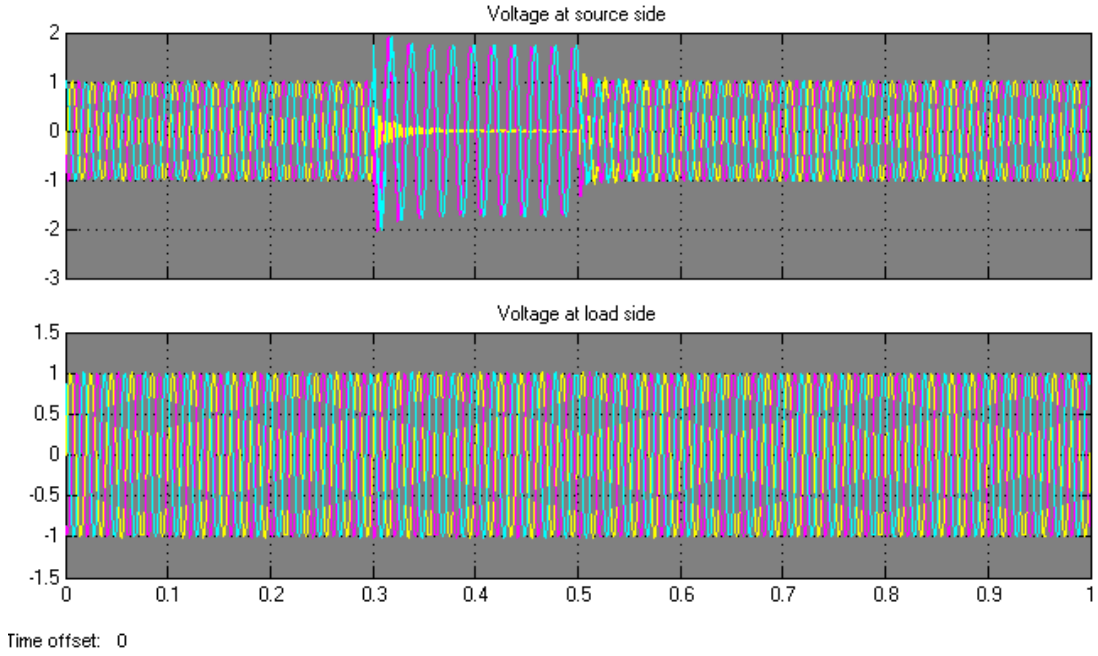

Fig. 8.34: Source and load voltage with D-STATCOM

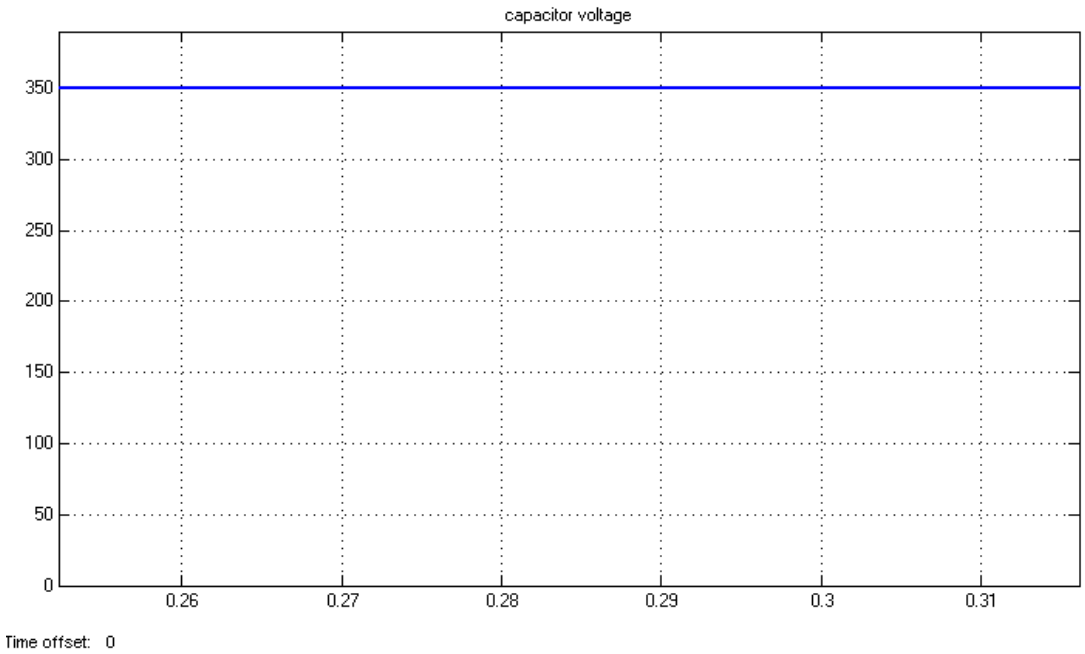

Fig. 8.35: Capacitor voltage of D-STATCOM

In DG integrated radial network, the effectiveness of DVR and D-STATCOM in mitigating voltage sag at load and source side are demonstrated. It is seen that the integration of DVR or D-STATCOM is a better choice to provide reactive power compensation in the normal test system as well as DG connected test system.

8.7 PRACTICAL RADIAL DISTRIBUTION SYSTEM

An attempt has been made to investigate the effectiveness of DG, D-STATCOM combination for voltage compensation in a practical IEEE 15 bus test system. In Chapter 5, the optimal location and size of DG in various practical test systems such as 15 bus, 28 bus, 33 bus etc., have been investigated.

8.7.1 IEEE 15 BUS RDS

Simulink model of IEEE 15 bus RDS test system is shown in Fig. 8.36. Simulation is carried out on the system to obtain the voltage profile. It is observed that the voltage profile is followed almost the same pattern as that is obtained from MATLAB programming using BFS algorithm. Comparison of voltage profiles is given in Fig. 8.37.

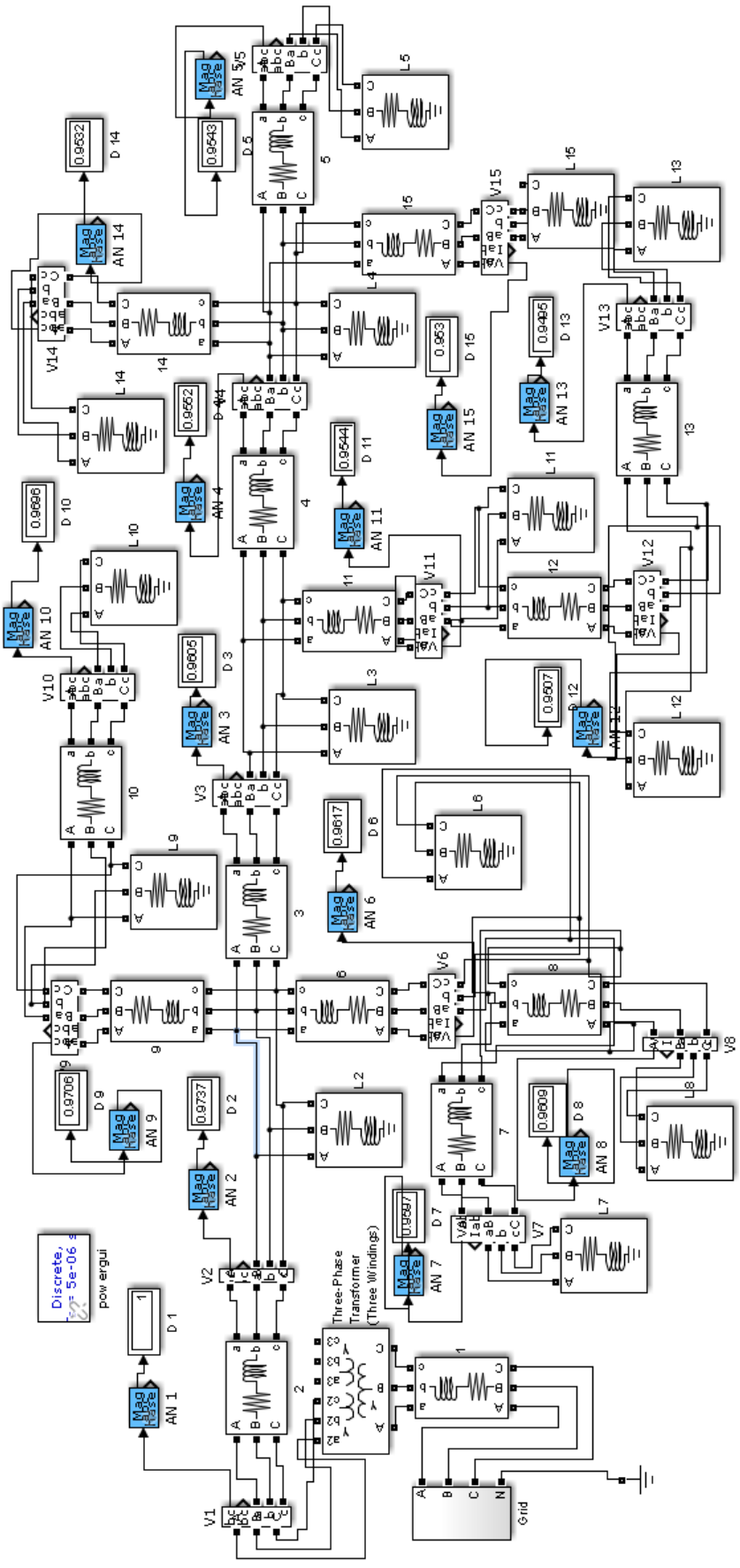

Fig. 8.36: Simulink model of IEEE 15 bus RDS

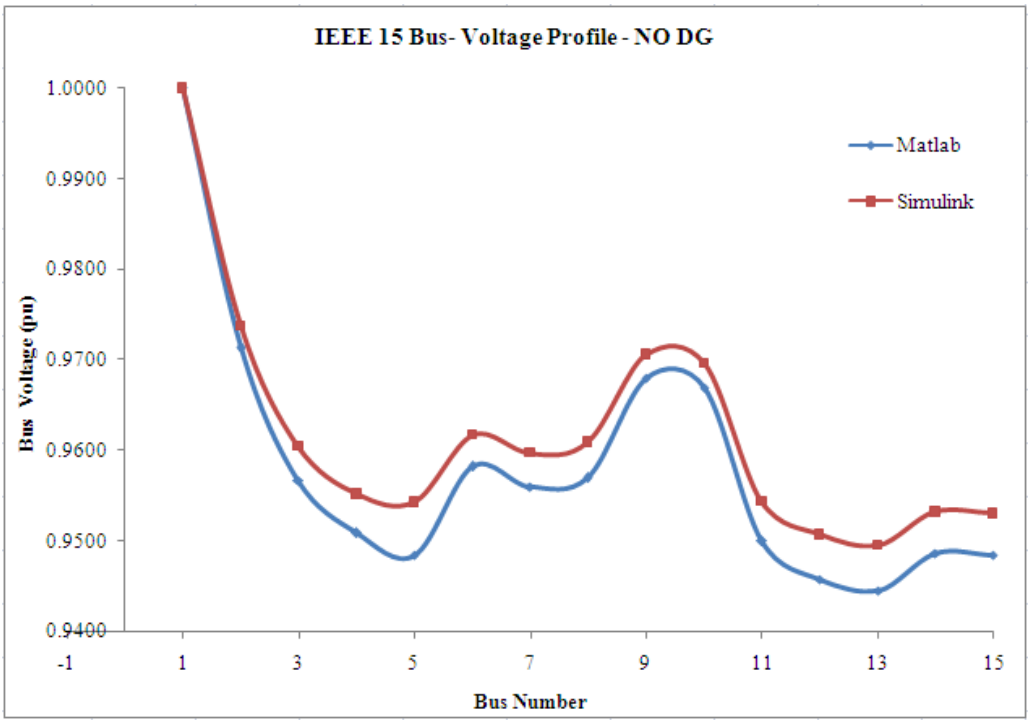

Fig. 8.37: Voltage profile of IEEE 15 bus RDS – A comparison between Matlab programming and Simulink modeling

8.7.2 DG integrated IEEE 15 Bus RDS

Load flow analysis using BFS algorithm provided an improved voltage profile with the integration of 400 kW size of DG placed at bus 6. It is obtained that when the same size of DG is placed at bus 4, then the voltage at far end buses, particularly 4, 5, 14 and 15 are improved more than DG at bus 6. IEEE 15 bus system is modified in two ways in such a way that 400 kW wind-based system is connected with load at bus 6 which is shown in Fig. 8.38 and at bus 4 that is shown in Fig. 8.39. Simulation is carried out on these two modified systems for finding the impact of DG on the voltage profile. Voltage profile of these two systems is shown in Fig. 8.40. Voltage profile obtained from modeling follows almost the same pattern to the result obtained from simulation, shown in Fig. 5.19. On comparing these two voltage profiles, it is observed that when 400 kW size of DG placed at bus 6 and bus 4 together gave an improved voltage at far end buses.

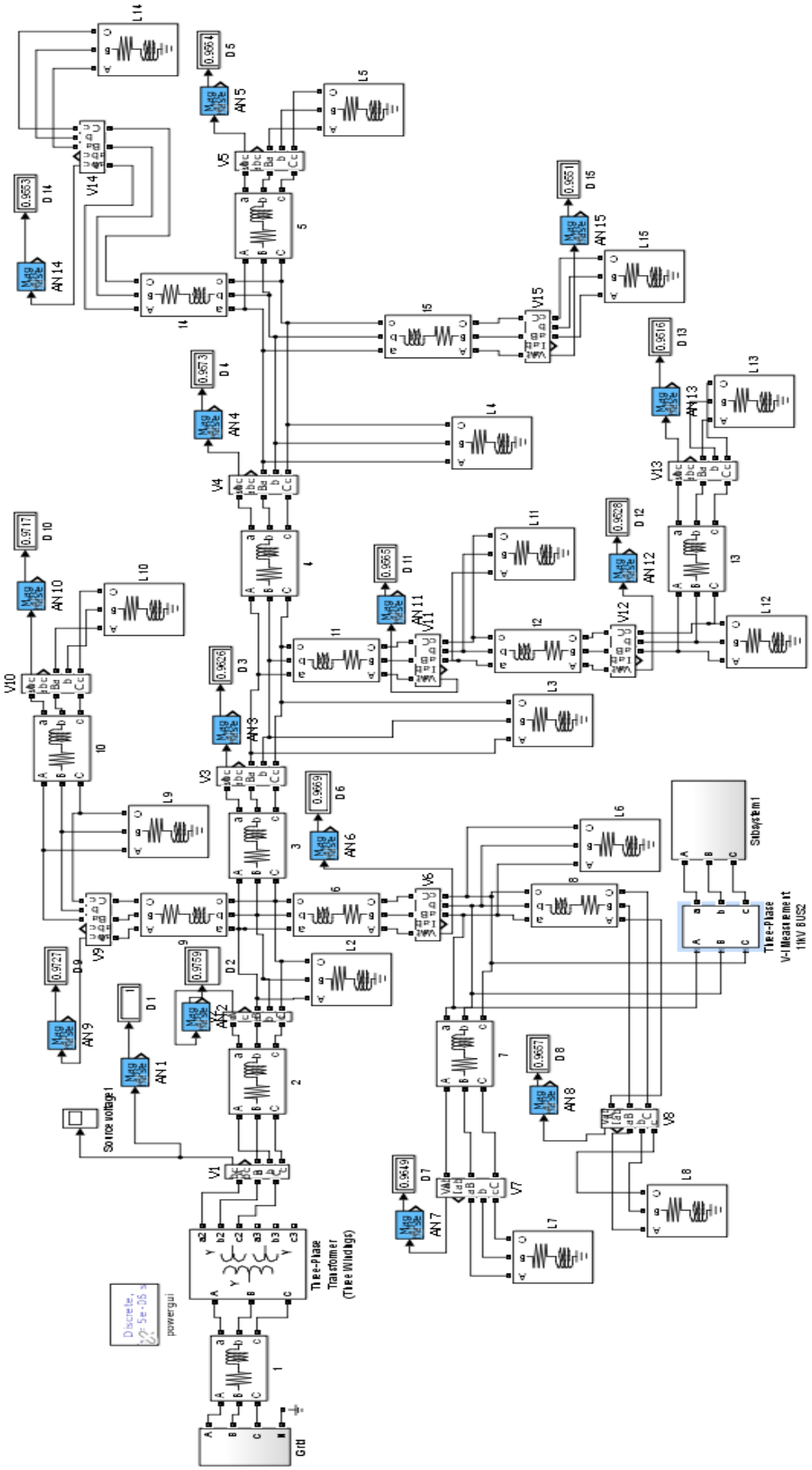

Fig. 8.38: Simulink model of IEEE 15 bus RDS with integration of 0.4 MW DG at bus 6

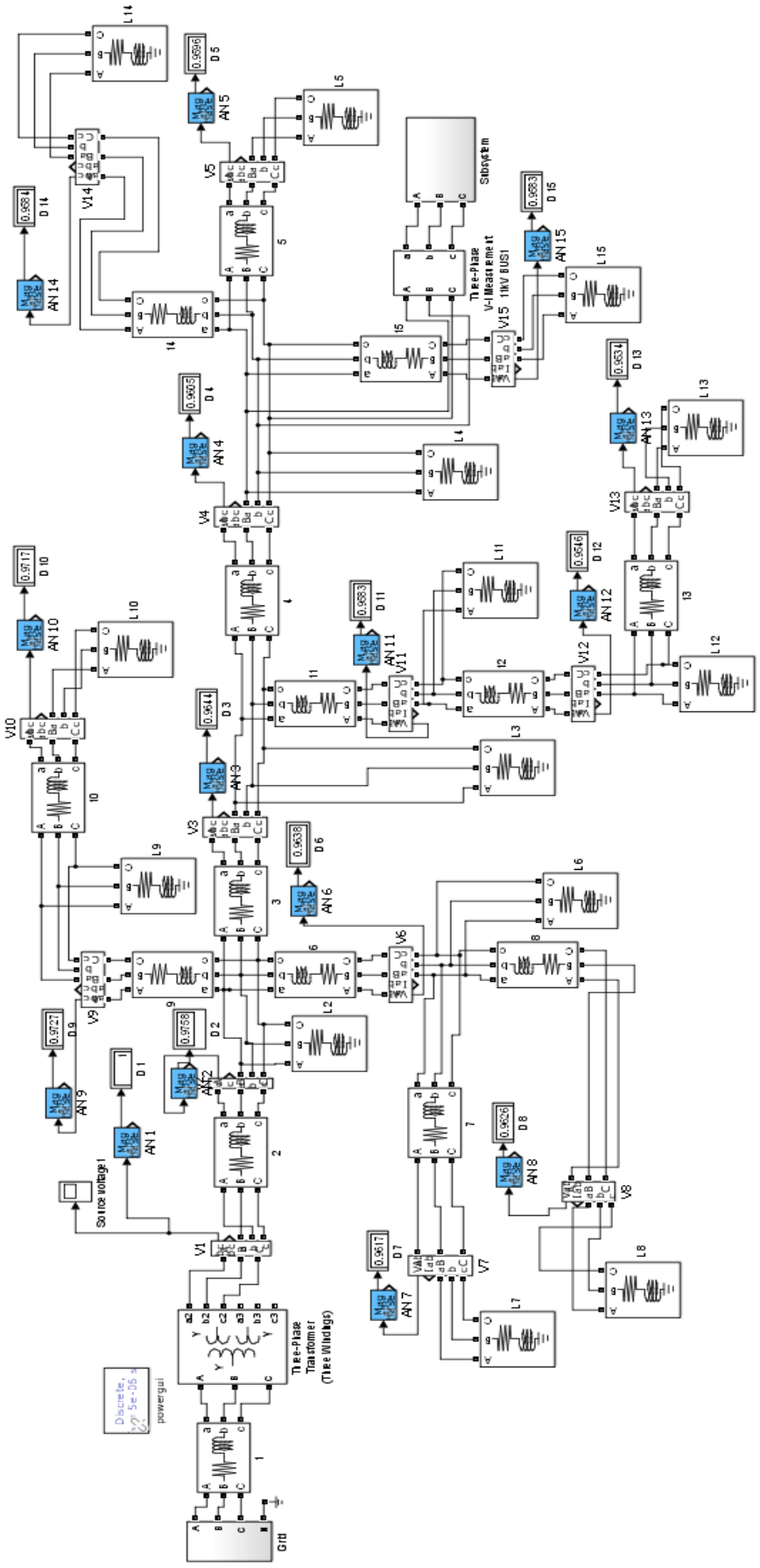

Fig. 8.39: Simulink model of IEEE 15 bus RDS with integration of 0.4 MW at bus 4

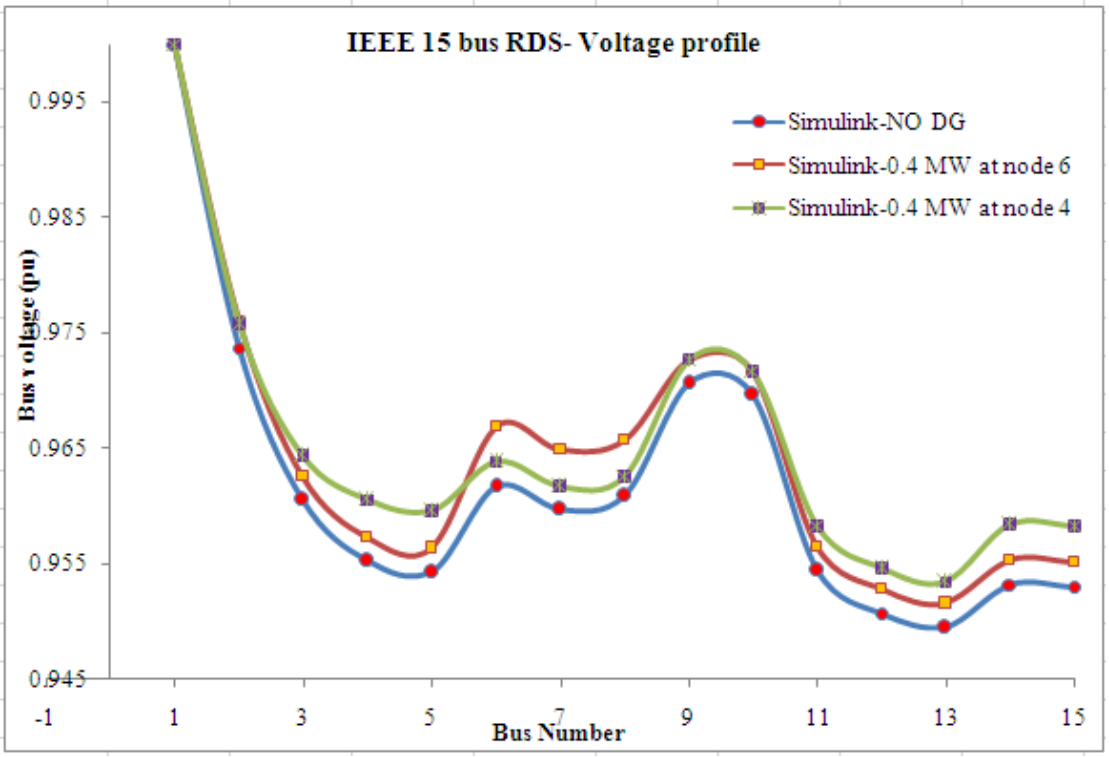

Fig. 8.40: Comparison of voltage profile of IEEE 15 bus RDS with integration of 0.4MW DG at bus 4 and bus 6

8.7.3 D-STATCOM integrated IEEE 15 Bus RDS

Simulation results showed that the bus voltage at far end bus 14 is 0.9543 pu, as seen from Fig. 8.41. In this radial network, a fault is created at far end bus 14 for 0.3-0.5sec so that the voltage at bus 14 comes down to 0.82 pu. Integration of D-STATCOM provides sufficient reactive power to meet the missing voltage thereby increasing the voltage to 1 pu. The voltage sag and its mitigation are shown in Figures 8.42 and 8.43.

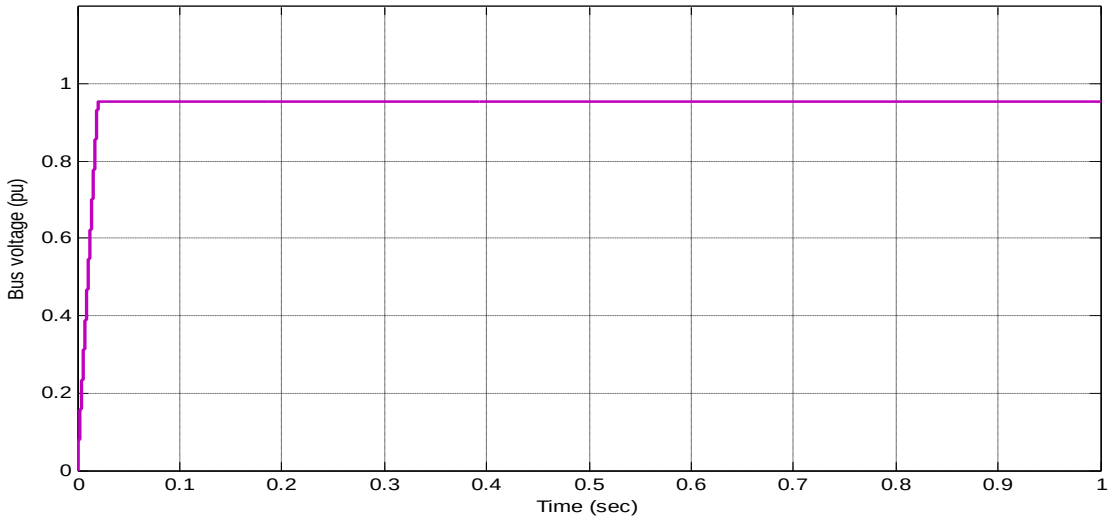

Fig. 8.41: Load voltage at bus 14 without fault

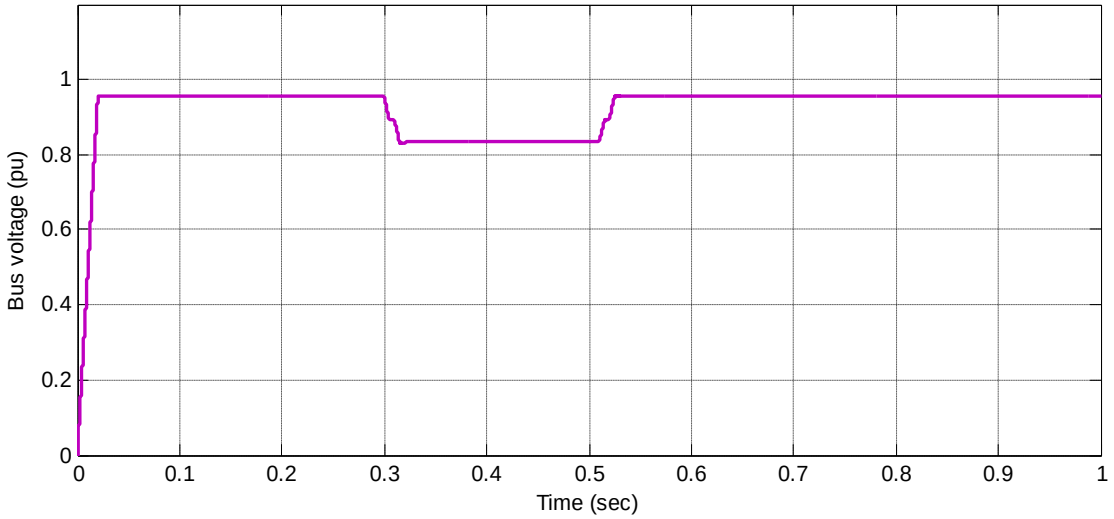

Fig. 8.42: Load voltage at Bus 14 with fault

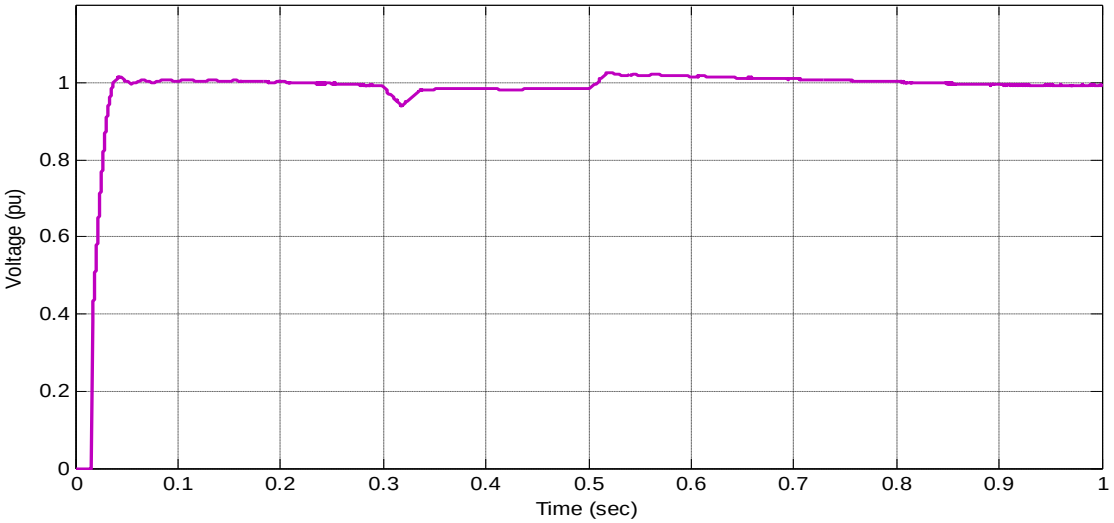

Fig. 8.43: Load voltage at bus 14 with D-STATCOM

From the various analysis conducted on the radial network, it is observed that the integration of the suitable size of DG at the proper place gave an improved voltage profile. Moreover, multiple DGs at suitable locations can enhance better voltage stability in the system. Results showed that the disturbance on the system could be reduced with the use of D-STATCOM.

8.8 SUMMARY

In this chapter, the Thevenin's equivalent model of IEEE 15 bus test system has been presented and performance of the model for various types of loads like linear, nonlinear and unbalanced is demonstrated. On measuring the voltage and current at PCC, it is observed that the nonlinear loads can introduce PQ issues in the test system. The effectiveness of DVR and D-STATCOM in the improvement of voltage sag and voltage swell is established through investigations to observe the enhancing capability of CPDs at the terminal of the linear load. The test system is modified with integration of 400 kW wind-based system, in which D-STATCOM is used as the mitigating device to enhance PQ issue at PCC. Further, the performance of D-STATCOM is tested through SIMULINK model of IEEE 15 bus radial distribution network integrated with 400 kW wind-based system. It can be inferred that DVR and D-STATCOM perform accurately for PQ issues, particularly voltage sag and voltage swell in linear load condition.

CONCLUSIONS

9.1 Conclusions

Growth rate of power sources is not comparable with the power demand in the existing system, leading to energy deficit particularly in peak time, makes it necessary to use all the available energy sources to its maximum capacity. Increased demands on electric power and absence of long-term planning cause security concerns and impair the quality of supply. Due to the economic and environmental restrictions, radial distribution networks are not adequately enlarged with increasing loads. Gas, fossil fuels and other energy alternatives collectively pose a threat to power plant operators and end users. In recent times, renewable energy sources have been getting prominence in power generation as their costs decline while the price of oil and gas continue to fluctuate.

In power systems where, RE based system delivers a significant proportion of power, voltage stability and power quality are important issues which require serious attention. Increase in usage of nonlinear loads, particularly in the industrial sector is a major cause for power quality issues which may even lead to voltage collapse and subsequently partial or full system blackout. To ensure a reliable supply of quality power, effective operational strategies have to be adapted by the utilities.

In the case of normal distribution test system as well as wind integrated test system, simulation results demonstrated the feasibility and effectiveness of the custom power devices in mitigating voltage sag under different fault conditions. Due to the reactive

support is given by the wind generator at the customer or load side, the terminal voltage is not much reduced in wind integrated system. On comparison, D-STATCOM provides excellent performance than DVR in voltage sag mitigation during a fault condition. SSTS helps to transfer the power from unhealthy feeder to the healthy feeder at a very high speed particularly in the wind integrated system.

Integration of renewable energy based distributed generation (DG) systems, particularly of wind and solar photo-voltaic (SPV) based systems have attained wide acceptance in many countries, as the cost of power generation has come down and it is comparable with that of electricity generated from fossil fuels. In this context, the determination of optimal size and location of renewable energy based DGs have become a very crucial issue. To enhance the voltage stability, an algorithm is formulated for optimizing the size of DGs within the constraints with an objective of minimizing the active power loss.

The applicability and robustness of BFS algorithm have been tested in different IEEE test systems as well as practical power systems. In IEEE 15 bus radial system, the voltage stability enhancement is attained with the integration of 0.4 MW size of DG placed at bus 6. Power loss reduction index and voltage profile improvement index quantifies the effectiveness of optimized DG in the radial network. Moreover, the maximum capacity of DG/DGs that can be added to the existing system to improve the voltage stability is also computed. Simulation results showed that the proper location of optimized DG/DGs in different radial network reduces the power loss and thereby improves the voltage stability.

Severe voltage instability in the network results in sudden voltage crisis which can seriously affect the end users. To facilitate timely intervention by the operator to alleviate the crisis, adequate knowledge of the root cause is an essential pre-requisite. Stability indices help the operators to take the initiative to address the impeding problems and in turn facilitate improvement in voltage stability. Effectiveness of various stability indices have been tested on IEEE 15 bus radial distribution system and demonstrated further with the help of case studies. Theses indices show the close agreement and are comparable as an early warning tool to voltage collapse. From the various stability indices analysis, bus 6 is identified as the weakest bus so that it requires active/reactive support. While comparing the GA based BFS algorithm and voltage stability indices analysis, the position of active/reactive power injected is found to be same. Maximum amount of reactive power that can be injected into this bus to maintain the voltage stability within the limit is also calculated.

To find the location and size of reactive power support, an algorithm is developed with an objective of minimizing reactive power loss. Further, this algorithm has been tested in multiple DG integrated radial network for observing the enhancement in voltage profile. Results are verified using BIBC-BCBV based analytical method to affirm the size and location of D-STATCOM. From the GA based BFS algorithm, the size of reactive power support is found to be 0.4 MVAr at bus 4. The power loss and voltage profile are computed with the integration of multiple DGs by placing 0.4 MVAr at bus 4. From the results obtained, it is inferred that no buses having under/over voltage problem. From the obtained results of the BIBC-BCBV method, the size of D-STATCOM is found to be 0.365 MVAr which gives minimum power loss. The size and location are reaffirmed by this method.

An integrated model of DG and custom power devices have been developed and applied in Thevenin's equivalent model of the radial network and IEEE 15 bus test system to assess the effectiveness of mitigating voltage sag. Simulation results depicted that the DVR and D-STATCOM perform accurately in the normal radial system as well as wind integrated radial system for PQ issues, particularly voltage sag and voltage swell in linear load condition.

9.2 Suggestions for Future Research

- Optimum size and location of different DG systems like wind, solar photo-voltaic (SPV), small hydel, etc. in a radial network using multi-objective programming can be attempted.
- Development of optimization model of DG systems incorporating DG systems integrating with energy storage can be explored.
- Rescheduling of power at peak time with the help of proper coordination technologies can be attempted.
- Based on this model, the impact of custom power devices on power quality can be assessed, and possible remedies can be suggested.
- Hardware implementation of this model can be attempted for real-time validation.
- Demand side management can be offered to the prompt application of renewable energy sources.

REFERENCES

[1] M.H.J. Bollen, *Understanding Power Quality Problems: Voltage Sags and Interruptions*, New York, IEEE Press, 1999.

[2] N.G. Hingorani and L. Gyugyi, *Understanding FACTS: Concepts and Technology of Flexible AC Transmission Systems*, 1st edition, The Institute of Electrical and Electronics Engineers, 2000.

[3] Prabha Kundur, Neal J.Balu and Mark G. Lauby, *Power system Stability and Control*, New York. Mc-Graw Hill, Professional, 1994.

[4] W.Tinney and C. Hart, "Power Flow Solution by Newton's Method," *IEEE Trans. on Power Apparatus and Systems*, vol.PAS-86, no.11, pp.1449-1460, November 1967.

[5] B. Stott and O. Alsac, "Fast Decoupled Load-flow," *IEEE Trans. on Power Apparatus and Systems*, vol.PAS-93, no.3, pp.859-869, May 1974.

[6] F. Zhang and C. S. Cheng, "A Modified Newton Method for Radial Distribution System Power Flow Analysis," *IEEE Trans. on Power Systems*, vol.12, no.1, pp.389-397, February 1997.

[7] H. L. Nguyen, "Newton-Raphson Method in Complex Form," *IEEE Trans. on Power Systems*, vol.12, no.3, pp.1355-1359, August 1997.

[8] Whei-Min Lin and Jen-HaoTeng, "Three-Phase Distribution Network Fast-Decoupled Power Flow Solutions," *Int. J. of Electrical Power and Energy Systems*, vol. 22, pp.375-380, 2000.

[9] T. H. Chen et al., "Distribution System Power Flow Analysis- A Rigid Approach", *IEEE Trans. on Power Delivery*, vol.6, no.3,pp.1146-1153, July1991.

[10] J. H. Teng, "A Modified Gauss-Seidel Algorithm of Three-phase Power Flow Analysis In Distribution Networks", *Int. J. of Electrical Power and Energy Systems*, vol.24, pp.97-102, 2002.

[11] S. Iwamoto and Y.A. Tamura, "Load-flow Calculation Method for Ill−Conditioned Power Systems", *IEEE Trans. on Power Apparatus And Systems*, vol. PAS−100, no.4,pp.1706−1713, April 1981.

[12] S. Tripathy *et al*, "Load-Flow Solutions for Ill- Conditioned Power Systems by a Newton-Like Method," *IEEE Trans. on Power Apparatus and Systems*, vol.PAS-101, no.10, pp.3648-3657, 1982.

[13] W.H. Kersting and Mendive, "A Method to Teach the Design and Operation of a Distribution System," *IEEE Trans. on Power Apparatus and Systems*, vol.PAS-103, no.7, pp.1945-1952, 1984.

[14] R.A. Stevens *et al.*, "Performance of Conventional Power Flow Routines for Real Time Distribution Automation Application," *Proc.18th Southeastern Symposium on Systems Theory: IEEE Computer Society*, 1986, pp.196-200.

[15] D. Shirmohammadi, "A Compensation Based Power Flow Method for Weakly Meshed Distribution and Transmission Network," *IEEE Trans. on Power Systems*, vol. 3, no. 2, pp.753-762, 1988.

[16] G. X. Luo and A. Semlyen, "Efficient Load Flow for Large Weakly Meshed Networks," *IEEE Trans. on Power Systems*, vol.5, no.4, pp.1309-1316, 1990.

[17] C.G. Renato, "New Method for the Analysis of Distribution Networks," *IEEE Trans. on Power Delivery*, vol.5, no.1, pp.391-396, January 1989.

[18] D. Das *et al.*, "Simple and Efficient Method for Load Flow Solution of Radial Distribution Networks," *Int. J. of Electrical Power & Energy Systems*, vol.17, no.5, pp.335-346, 1995.

[19] S. Goswami and S. Basu, "Direct Solution of Distribution Systems," *IEEE Proc. on Generation, Transmission and Distribution*, vol.138, no.1, pp.78-88, January 1991.

[20] M.H. Haque, "Efficient Load-flow Method for Distribution Systems with Radial or Mesh Configuration," *IEEE Proc. on Generation, Transmission, Distribution*, vol.143, no.1, pp.33-39, January 1996.

[21] S. Ghosh and D. Das, "Method for Load−Flow Solution of Radial Distribution Networks," *IEEE Proc. on Generation, Transmission and Distribution*, vol.146, no.6, pp.641–648, November 1999.

[22] P.R. Bijwe and G.K. Vishwanadha Raju, "Fuzzy distribution power flow for weakly meshed systems," *IEEE Trans. Power Syst.*, vol. 21,no.4, pp.1645-52, 2006.

[23] S. Sivanagaraju *et.al*, "A loop based loop flow method for weakly meshed distribution network," *ARPN J. of Engineering and Applied Sciences*, vol. 3, no. 4, August 2008.

[24] S. Ghosh and K. Sherpa, "An Efficient Method for Load−Flow Solution of Radial Distribution Networks," *Proc. of Int. J. of Electrical Power and Energy Systems*, Spring 2008.

[25] A. Kumar and Aravindhababu, "An Improved Power Flow Technique for Distribution Systems," *J. of Computer Science, Informatics and Electrical Engineering*, vol.3, Issue 1, 2009.

[26] A. Augugliaro *et.al*,"A Backward sweep method for power flow solution in distribution networks," *Int. J. of Electrical Power and Energy Systems*, vol.32, pp. 271–280, 2010.

[27] D. Das *et.al* , "Novel Method for Solving Radial Distribution Networks," *IEE Proc. on Generation, Transmission and Distribution*, vol.141, no.4, pp.291-298, July 1994.

[28] U. Eminoglu and M.H. Hocaoglu, "A New Power Flow Method For Radial Distribution Systems Including Voltage Dependent Load Models," *Int. J. of Electric Power Systems Research*, vol.76, pp.106–114, 2005.

[29] D.P.Sharma *et.al*," An Improved Mechanism of a Leaf Node Identification for Radial Distribution Network," *IEEE Power and Energy Conference organized by university of Illinois*, U.S.A, 25-26 February, 2011.

[30] Srihari Mandava *et.al*, "A new load flow method for radial distribution system," *Int. Conf. on Advances in Electrical Engg*., 2014.

[31] Tanveer Hsain *et.al*, "load flow analysis in radial and mesh distribution system using ZIP model," *Int. Conf. on Global Trends in Signal Processing, Information Computing and Communication, 2016*

[32] T. Griffin *et. al*, "Placement of Dispersed Generations Systems for Reduced Losses," *Proc. of the 33rd Hawaii Int. Conf. on System Sciences*, 2000.

[33] H. L. Willis, "Analytical Methods and Rules of Thumb for Modeling DG-Distribution Interaction," *IEEE Power Engineering Society Summer Meeting*, vol. 3, Issue, pp. 1643 – 1644, 2000.

[34] Parizad A *et.al*, "Optimal placement of distributed generation with sensitivity factors considering voltage stability and losses indices," *18th Iranian Conf. on Electrical Engineering (ICEE)*, 2010

[35] J. O. Kim *et.al*, "Dispersed generation planning using improved Hereford Ranch algorithm," *Int. J. Electric Power System Research*, vol.47, no.1, pp. 47–55, 1998 .

[36] M. Gandomkar and M. Vakilian, "Optimal distributed generation allocation in distribution network using Hereford Ranch algorithm," *Proc. of the 8th Int. Conf. on Electrical Machines and Systems*, volume 2, Issue , pp. 916 – 918, 2005.

[37] Walid El-Khattam *et. al*, "Stochastic Power Flow Analysis of Electrical Distributed Generation Systems," *IEEE Meeting Power Engineering Society*, vol. 1, pp. 141-143, 2003.

[38] C. L. T. Borges and D. M. Falcao, "Optimal distributed generation allocation for reliability, losses, and voltage improvement," *Int. J. Power Energy Syst*., vol.28, no.6, pp. 413–420, 2006.

[39] Y. Alinejad-Beromi *et. al*, "Using Genetic Algorithm for Distributed Generation Allocation to Reduce Losses and Improve Voltage Profile," *IEEE UPEC*, pp. 954-959, *2007*.

[40] A. A. Abou El-Ela *et.al*, "Maximal optimal benefits of distributed generation using genetic algorithms," *Int. J. of Electric Power Systems Research*, vol. 80, pp. 869–877, 2010.

[41] M. Gandomkar *et. al*, "A Combination of Genetic Algorithm and Simulated Annealing for Optimal DG Allocation in Distribution Networks," *IEEE CCECE/CCGEI*, Saskatoon, May 2005.

[42] Z.M.Yasin *et.al*, "Optimal Sizing of Distributed Generation by using Quantum-Inspired Evolutionary Programming," *4th Int. Power Engineering and Optimization Conf. (PEOCO2010)*, 23-24, June 2010

[43] K.-H. Kim *et.al*, "Dispersed generator placement using fuzzy-GA in distribution systems," *in Proc. 2002 IEEE Power Engineering Soc. Summer Meeting*, vol. 3, Chicago, IL, July 2002, pp. 1148–1153.

[44] K Nara et.al, "Application of tabu search to optimal placement of distributed generators," *IEEE Power Engineering Society Winter Meeting*, 2001, volume: 2, pp.918 –923.

[45] M. R. Aghaebrahimi and M. Amiri,"An Immune-Based Optimization Method for Distributed Generation Placement in order to Minimize Power Losses," *1st Int. Conf. on Sustainable Power Generation and Supply (SUPERGEN)*, Nanjing, China, April 6- 7, 2009.

[46] Mohammad Falahi Sohi et.al, "Applying BCO Algorithm to Solve the Optimal DG Placement and Sizing Problem," *5th Int. Power Engineering and Optimization Conf. (PEOCO2011)*, Malaysia ,2011

[47] A Marimuthu *et.al*, "Optimal allocation and sizing of DG in a radial distribution system using whale optimization algorithm," *Int. Conf. on Innovations in green energy and healthcare technologies*, 2017.

[48] Ontoseno Penangsang *et.al*, " Optimal placement and sizing of distributed generation in radial distribution system using K-means clustering method," *Int. seminar on Intelligent technologies and its applications*, 2017.

[49] Maryam majidi *et.al*, "Optimal DG allocation and sizing in radial distribution networks by Cuckoo search algorithm," *Int. Conf. on Intelligent system application to power systems*, 2017.

[50] G. Mohan and P. Aravindbabu, "A novel placement algorithm for voltage stability enhancement in distribution system," *Int. J. of Electronics Engineering*, vol. 1, no. 1, pp. 83-87, 2009.

[51] G Rajendar and B. Banakara, "A novel algorithm for capacitor placement to improve voltage stability of radial and meshed power systems," *J. of Information Engineering and Applications*, vol. 2, no.11, pp. 47-58, 2012.

[52] C. W. Taylor, *Power System Voltage Stability*, McGraw-Hill, Inc., 1994.

[53] Tareq Aziz *et. al*, "Distributed Generators Placement for Loadability Enhancement Based on Reactive Power Margin," *Proc. of the 9th Int. Power and Energy Conf. IPEC2010*, 27 - 29 October 2010.

[54] K.R. Vadivelu and G. V. Marutheswar, "Maximum loadability estimation for weak bus identification using fast voltage stability index in a power transmission system by real-time approach," (2014).

[55] A.E. Abedelatti *et. al*. "Weakest Bus Based on Voltage Indices and Loadability" IEEE 2004.

[56] A. Devi Lakshmi and A. Chaithanya, "A New Analytical Method for the Sizing and Siting of DG in Radial System to Minimize Real Power Losses," *Int. J. of Computational Engineering Research*, vol 2, no.7, pp. 31-37, 2012.

[57] A. Parizad *et. al*, "Optimal placement of distributed generation with sensitivity factors considering voltage stability and losses indices," *Electrical Engineering (ICEE), 2010, 18th Iranian Conf. on*. IEEE, 2010.

[58] Naderi *et.al*, "Determination of the performance of the distribution static compensator (D-STATCOM) in distribution network," *Electricity Distribution (CIRED 2013), 22nd In. Conf. and Exhibition on*. IET, 2013.

[59] Chanda *et.al*, "Identification of weak buses in a power network using novel voltage stability indicator in radial distribution system," *Power Electronics (IICPE), 2010, India Int. Conf. on*. IEEE, 2011.

[60] Hussain and S. M. Suhail, "Identification of weak buses using Voltage Stability Indicator and its voltage profile improvement by using D-STATCOM in radial distribution systems," *IOSR J. of Electrical And Electronics Engineering (IOSRJEEE)* vol.2, no. 4, pp.17-23, 2012.

[61] Taher et.al, "Optimal location and sizing of D-STATCOM in distribution systems by immune algorithm," *Int. J. of Electrical Power & Energy Systems*, 60, pp. 34-44, 2014.

[62] Aslanzadeh *et al.*,"Comparision of voltage stability indicators in distribution systems," *Indian J. Sci. Res* vol. 2, no. 1, pp. 5-10, 2014.

[63] Adedayo Ademola Yusuff, "Voltage stability index based on standard deviation to mean ratio for identification of weak nodes," *AFRICON*, 2017IEEE

[64] A. Ghosh *et al*., *Power quality enhancement using custom power devices*, Kluwer Academic Publishers, 2002.

[65] A. Cetin *et al*., "Reactive power compensation of coal convertor drives by using D-STATCOMs," in Conf. Record of the 2007 IEEE Industry Applications Conf. Forty-Second IAS Annual Meeting, vols. 1-5, 2007, pp.1731-1740.

[66] S. Xu *et al*., "Development of a D-STATCOM prototype based on cascade inverter with isolation transformer for unbalanced load compensation," October1994.

[67] M. Brent Hughes and John S. Chan, "Canadian National Power Quality Survey", Power tech Labs Inc , Canada and B.C Hydro, Canada, 1992.

[68] J. Bumett, "Survey of Power Quality in High-Rise Air Conditioned Buildings", *Power Electronics and Variable-Speed Drives Conf*., 26-28

[69] H. F. Bilgin and M. Ermis, "Design and Implementation of a Current-Source Converter for Use in Industry Applications of D-STATCOM," *IEEE Trans. on Power Electronics*, vol.25, no.8, pp.1943-1957, 2010.

[70] Mahmoud zadehbagheri *et.al*., "Performance Evaluation of Custom Power Devices in Power Distribution Networks to Power Quality Improvement: A Review," *Int. J. of Scientific & Engineering Research*, vol. 4, Issue 5, 2013.

[71] R. Sirjani *et.al*.,"Optimal placement and sizing of Static Var Compensators in power systems using Improved Harmony Search Algorithm," *Przeglad Elektrotechniczny*, vol. 87, no.7, pp.214-218, 2011.

[72] R. Sirjani *et.al*., "A hybrid BCO/HS algorithm for optimal placement and sizing of static Var compensators in power systems," in *Proc. of the 10th WSEAS Int. conf. on System science and simulation in engineering*, World Scientific and Engineering Academy and Society (WSEAS): Penang, Malaysia. pp. 54-59, 2011.

[73] R. Jahani *et al*., "Optimal Placement of Unified Power Flow Controller in Power System by a New Advanced Heuristic Method," *Technical and Physical Problems of Engineering*, vol. 2, no.5, pp.13-18, 2010.

[74] S. Sherin Jasper, "Artificial Neural Network Controlled DSTATCOM for Power Quality improvement," *Int. J. of innovative research in electrical, electronics, instrumentation and control engg*., vol.3, no. 5,2015

[75] A. R. Jordehi and J. Jasni, "Heuristic methods for solution of FACTS optimization problem in power systems," in *IEEE Student Conf. on Research and Development (SCOReD)*, 2011, pp.30-35.

[76] T.Orfanogianni and R. Bacher, "Steady-state optimization in power systems with series FACTS devices," *IEEE Trans. on Power Systems*, vol.18, no.1, pp.19-26, 2003.

[77] A. A. Eajal and M. El-Hawary, "Optimal capacitor placement and sizing in unbalanced distribution systems with harmonics consideration using particle swarm optimization," *IEEE Trans. on Power Delivery*, vol.25, No.3, pp.1734-1741, 2010.

[78] A. Parastar *et al*., "Optimal location of FACTS devices in a power system using modified particle swarm optimization," *in 42nd Int. Universities Power Engineering Conf. (UPEC)*, 2007, pp.1122-1128.

[79] G.K. Venayagamoorthy, "Dynamic optimization of a multi-machine power system with a FACTS device using identification and control Object Nets," in *39th IAS Annual Meeting on Industry Applications Conf.*, 2004, pp.2643-2650.

[80] P.A.D.V. Raj *et al*., "Particle Swarm Optimization Based Energy Optimized Dynamic Voltage Restorer," in *Joint Int. Conf. on Power System Technology and IEEE Power India Conference*, 2008, 1-6.

[81] F. Pilo *et al*., "Optimal placement of custom power devices to mitigate voltage dips in distribution networks. in *13th Int. Conf. on Harmonics and Quality of Power*, 2008, pp.1-7.

[82] O. Amanifar and M.E.H. Golshan,"Mitigation of Voltage Sag by Optimal Distributed Generation Placement and Sizing in Distribution Systems with Economic Consideration Using Particle Swarm Optimization," in *Int. Power System Conf.*, 2011, Tehran, Iran.

[83] R. Ghazi and H. Kamal, "Optimal size and placement of DVR's in distribution system using simulated annealing (SA), in *18th Int. Conf. and Exhibition on Electricity Distribution (CIRED 2005)*, 2005, pp. 75-82.

[84] Z. Yan and J. V. Milanovic,"Voltage sag cost reduction with optimally placed FACTS devices," in *9th Int. Conf. on Electrical Power Quality and Utilisation*, 2007, pp.1-6.

[85] C.S. Chang and Y. Zhemin,"Distributed mitigation of voltage sag by optimal placement of series compensation devices based on stochastic

assessment," *IEEE Trans.on Power Systems*, vol. 19, no.2, pp.788-795, 2004.

[86] Y. Zhang and J.V. Milanovic, "Global Voltage Sag Mitigation With FACTS-Based Devices," *IEEE Trans. on Power Delivery*, vol. 25,no.4, pp. 2842-2850, 2010.

[87] C. Vira and Y.Y. Haimes, *Multiobjective decision making:theory and methodology*, 1983, North-Holland.

[88] E. Rashedi *et al*., "GSA: a gravitational search algorithm," *Information Sciences*, vol. 179, no.13, pp.2232-2248, 2009.

[89] N. Salman *et al*.,"Reliability Improvement in Distribution Systems by Optimal Placement of DSTATCOM Using Binary Gravitational Search Algorithm,"*Przeglad Elektrotechniczny (Electrical Review)*, vol.88, no.2, pp. 295-299, 2012.

[90] D. Tanti *et al*., "An Ann Based Approach for Optimal Placement of Dstatcom for Voltage Sag Mitigation," *Int. J. of Engineering Science*, vol.3 no.2, pp.827-835, 2010.

[91] Rosli Omar and Nasrudin Abd Rahim,"Modeling and Simulation for Voltage Sags/Swells Mitigation Using Dynamic Voltage Restorer (DVR)," in *Pro. of Australasian Universities Power Engineering Conference*, Sydney, NSW, 2008, pp. 1-5.

[92] S. Sadaiappan *et al*.,"Modeling and Simulation of Series Compensator to Mitigate Power Quality Problems," *Int. J. of Engineering Science and Technology*, vol. 2, no. 12, pp. 7385-7394, 2010.

[93] Chong Han *et al*., "Evaluation of Cascade –Multilevel Converter Based STATCOM for Arc Furnace Flicker Mitigation," *IEEE Trans. on Industry Applications*, vol. 43, no. 2, 2007

[94] K. A. Schwabe *et al*., "A Dynamic Exercise in Reducing Deer Vehicle Collisions: Management through Vehicle Mitigation Techniques and Hunting," *J. of Agricultural and Resource Economics*, vol. 27, no. 1, pp. 261-268.

[95] S. Rahmani *et. al*., "A New Combination of Shunt Hybrid Power Filter and Thyristor Controlled Reactor for Harmonics and Reactive Power Compensation," *IEEE Electrical Power & Energy Conf*., pp.1-6, 2009.

[96] Tejas Zaveri *et al*., "Load compensation using DSTATCOM in three - phase, three-wire distribution system under various source voltage and delta connected load conditions," *Int. J. of Electrical Power and Energy Systems*, vol. 41, pp. 34-43, 2012.

[97] Mohammad H. Moradi and Younes Mohammadi, "Voltage sag source location: A review with introduction of a new method,"*Int. J. of Electrical Power and Energy Systems,* vol. 43, pp. 29–39, 2012.

[98] E. Najafi and A.H.M. Yatim, "A novel current mode controller for a static compensator utilizing Goertzel algorithm to mitigate voltage sags," *Energy Conversion and Management*, vol. 52, no. 4, pp. 1999-2008, April 2011.

[99] Tejas Zaveri *et. al.*, "Control Techniques for Power Quality Improvement in Delta Connected Load using DSTATCOM," *IEEE Int. Conf. on Electric Machines & Drives (IEMDC),* 2011, pp.1397-1402.

[100] N. Sudhakar *et. al*., "Mitigation of EMI in DC-DC converter using analogue chaotic PWM technique", *Int. Conf. on Sustainable Energy and Intelligent Systems (SEISCON 2011),* 2011, pp.272-277.

[101] T. K. Abdel-Galil *et. al*., "Effect of New Deregulation Policy on Power Quality Monitoring and Mitigation Techniques", *Transmission and Distribution Conference and Exposition,* vol. 1, pp.554-560, 2001.

[102] A.A.C. Reyna,"Applications of the differential evolution optimization algorithm in power systems planning, operation and control," 2006, Citeseer.

[103] K. Hwang, *Advanced computer architecture: parallelism, scalability, programmability*. vol. 199. 1993: McGraw-Hill Singapore.

[104] M. Gen and R. Cheng, Genetic *algorithms and engineering optimization*, Vol. 7. 2000: Wiley-interscience.

[105] S. Favuzza et al., "Adaptive and dynamic ant colony search algorithm for optimal distribution systems reinforcement strategy," *Applied Intelligence*, vol.24, no.1, pp.31-42, 2006.

[106] S. Toune et. al., "Comparative study of modern heuristic algorithms to service restoration in distribution systems," *IEEE Trans. on Power Delivery*, vol. 17, no.1, pp. 173-181, 2002.

[107] S. Gerbex et. al., "Optimal location of multi-type FACTS devices in a power system by means of genetic algorithms," *IEEE Trans. on Power Systems*, vol.16, no.3, pp.537-544, 2001.

[108] Singh S P, Rao A R. "Optimal allocation of capacitors in distribution systems using particle swarm optimization". *Electrical Power Energy System*,43. pp. 1267–1275,2012.

[109] M.M. El Metwally *et al*., "Optimal allocation of FACTS devices in power system using genetic algorithms," in *12th Int. Middle-East Power System Conf.*, 2008. pp.1-4.

[110] M. Mosaad *et al*.,"On-Line Optimal Power Flow Using Evolutionary Programming Techniques," *Thammasat Int. J. of Science and Technology*, vol.15, no.1, 2010

[111] Masoud Farhoodnea *et. al*., "A Comprehensive Review of Optimization Techniques Applied for Placement and Sizing of Custom Power Devices in Distribution Networks," *Przegląd Elektrotechniczny*, pp. 261-265, 2012.

[112] Joseph Sanam *et. al*, "Allocation of D-STATCOM and DG in distribution systems to reduce power loss using ESM algorithm," *IEEE Int. Conf. on Power electronics, Intelligent control and Energy systems*, 2016

[113] Joseph Sanam *et. al*, "Forecasting of AELC and TESC of distribution systems with the optimal allocation of D-STATCOM," *IEEE Innovative Smart Grid Technologies-ASIA*, 2016

[114] Ashutosh Kumar Tagore *et. al*, "Impact of DG and D-STATCOM allocation in radial distribution system for reducing harmonics," *Int. Conf. on Computing, Commn. and networking technologies*, 2017

[115] Alireza Lorestani *et.al*,"A novel analytical-heuristic approach for placement of multiple distributed generator in distribution network," *Smart Grid conference*, 2016.

[116] T Yuvaraj *et.al*, "Optimal Allocation of DG and DSTATCOM in Radial Distribution System Using Cuckoo Search Optimization Algorithm," *Modelling and Simulation in Engineering*, 2017

[117] Anju Bala *et.al*, "Design and Implementation of three phase three level inverter based D-STATCOM," *Int. Conf. on Power, Control and Embedded Systems*, 2017.

[118] C. Venkatesh and D. Srikanth Kumar, "Modelling of nonlinear loads and estimation of harmonics in industrial distribution system," *15^{th} National Power System conf.*, IIT Bombay, 2008, pp. 592-597.

[119] Ravneet Kaur, and Jayati Vaish," "A new era in electricity production using renewable sources," *Int. J. of Emerging Technology and Advanced Engineering*, vol. 3, pp. 410-413, Feb 2013.

[120] 10.391J Sustainable Energy Spring 2000 – Term Paper by Murray J. Height.

[121] S. Heier, *Grid integration of wind energy conversion systems*, Translated by Rachel Waddington, John Wiley, 1998. ISBN-10.

[122] Mohd Ikhwan Bin Muhammad Ridzuan, "Modeling and Simulation of Power Conditioning for Grid-Connected PV/Wind Hybrid Generation System," Faculty of Electrical Engineering, University Teknologi Malaysia, Johor Bahru, 2009

[123] Philippe Maibach *et. al*, "STATCOM Technology for wind parks to meet grid code requirements,'2000.

[124] "Solar Electric Power System," in http://cogeneration.net/solar- electric-power systems/, R. E. I. R. Cogeneration: News and Technologies, Ed.

[125] Prasanna Kumar Biswal et al., "Distributed Generation: Benefits, Issues and Challenges," *Grenze Int. J. of Engineering and Technology*, vol. 1, no. 1, January 2015

[126] K. Purchala and R. Belmans,"Distributed generation and the grid integration issues", 2005.

[127] "The potential benefits of DG and rate related issues that may impede their expansion"- A study pursuant to section 1817 of the Energy Policy Act of 2005.

[128] A. Lovins and C. Lotspeich,"Energy Surprises for the 21st Century, *J. of Int. Affairs*, vol. 53, no. 1, 1999.

[129] DPCA (2000) *Distributed Power Coalition of America*, www site, http://www. dpc.org/

[130] D. Maskovitz, (2000) *Profits and Progress through Distributed Resources*, The Regulatory Assistance Project (RAPMAINE), http://www. rapmaine.org/ P&pdr.htm

[131] J. Douglas, "The Electricity Technology Roadmap: Power Delivery in the 21st Century," J. of Electric Power Research Institute (EPRI), Summer, 1999.

[132] F. M. Shelor,"Mini-Merchants for Distributed Generation," *Power Engineering*, vol.102, no. 8, pp. 34-38, 1998.

[133] E. Jeffs, "Rush to CHP," *Independent Energy*, v24, n4, p3, 1994.

[134] Munson, D. and T. Kaarsberg, "Unleashing Innovation in Electricity Generation," *Issues in Science and Technology*, National Academy of Sciences, Spring, 1998.

[135] T. Hennagir,"Indochinese Power Progress," *Independent Energy*, v25, n6, pp3, 1995.

[136] MNRE-Annual Report 2015-16

[137] MNRE- Strategic plan for New and Renewable energy sector for the period 2011-17, February 2011.

[138] Ackermann Thomas *et al*., "Distributed generation: a definition," Int. J. of Electrical Power System Research, vol. 57, pp.195–204,2001.

[139] C. Zhan *et al*., "Battery Energy Storage for Voltage Dip Mitigation," *Power Electronics and Variable Speed Drives*, Conf. Publication No. 475, IEE September 2000.

[140] Central Electricity Regulatory Commission- Indian Electricity Grid Code:Web- www.cercind.gov.in

[141] V. Sureshkumar, and Ahmed F. Zobba,"Power quality and stability improvement in wind park system using STATCOM," *Jordan J. of Mechanical and Industrial Engg*, vol. 4, pp. 169-176, Jan 2010.

[142] R. Sreeram Kumar, *Lecture notes on Flexible AC Transmission Systems*, 1st edition, The Institution of Engineers, *2003.*

[143] Roger C. Dugan, *Electrical Power Systems Quality*, New York, Tata McGraw Hill, 2003.

[144] Prafull A. Desale et. al, "Brief Review Paper on the Custom Power Devices for Power Quality Improvement", IEEE 2002.

[145] Narain G. Hingorani, "Introducing Custom Power", *IEEE Spectrum*, June 1995, pp. 41-48.

[146] Ravilla Madhusudan and G. Ramamohan Rao, " Modeling and Simulation of D-STATCOM for Power Quality Problems-Voltage Sags and Swells based on sinusoidal pulse width modulation," *IEEE Int. Conf. on Advances in Engg., Science and Management*, pp. 436-441, March 2012.

[147] N. Hamzah and M R Muhamad, " Investigation on the effectiveness of DVR for voltage sag mitigation," *IEEE conf. on Research and Development*, 2007.

[148] Yash pal *et al*., " A Review of Compensating Type Custom Power Devices for Power Quality Improvement", IEEE, 2008.

[149] Mokhtari et al.,"Performance Evaluation of Thyristor Based Static Transfer Switch", *IEEE Trans. on Power Delivery*, vol. 15, No. 3, pp. 960- 966, July, 2000.

[150] H. Mokhtari , and M. R. Iravani, "Effect of source Phase Difference on Static Transfer Switch Performance", *IEEE Trans. on Power Delivery*, vol. 22,no. 2, pp. 1125-1131, April, 2007.

[151] P. T. Cheng, and Y. H. Chen , "Design of an Impulse Commutation Bridge for the Solid-State Transfer Switch", *IEEE Trans. on Industry Applications*, vol. 44, no. 4, pp. 1249-1258, July/August, 2008.

[152] Ankush Sharma,"Review Paper on Applications of D-STATCOM in Distribution System', *Int. J. of Science and Modern Engineering*, vol. 2, Issue 11, 2014.

[153] Nwohu Mark Ndubuka, " Power quality enhancement of Nigerian power distribution systems by use of D-STATCOM," *Int. J. of Electrical and Power Engg.*, vol. 5 , pp. 8-12, 2011.

[154] E. Babaei and M. Farhadi Kangarlu, "Voltage Quality improvement by a DVR based on a direct three phase converter with fictitious DC link," *IET Gener., Transm., Distrib*, vol. 5, pp. 814-823, 2011.

[155] D. Murali and M. Rajaram, " Simulation and implementation of DVR for voltage sag compensation," *Int. J. of Computer Applications*, vol. 23, pp. 26-30, June 2011.

[156] Ashwin Kumar Sahoo and T. Thyagarajan, " Transient studies of FACTS and Custom Power Equipment," *Int. J. of Recent Trends in Engg*., vol. 1, May 2009.

[157] Olimpo Anaya-Lara and E. Acha, " Modeling and analysis of custom power systems by PSCAD/EMTDC," *IEEE Trans. On power delivery, vol. 17, no.1, pp. 266-271, January* 2002.

[158] S. S. Choi et al., "Dynamic voltage restoration with minimum energy injection," *IEEE Trans. Power Syst*., vol. 15, no. 1, pp. 51–57, Feb. 2000.

[159] Mahesh A Patel and Ankit R Patel, " Use of PWM Techniques for power quality improvement," *Int. J. of Recent Trends in Engg*., vol. 1, May 2009.

[160] Ravilla madhusudan and G. Ramamohan Rao, " Modeling and Simulation of a Dynamic Voltage Restorer(DVR) for Power Quality Problems-Voltage Sags and Swells," *IEEE Int. Conf. on Advances in Engg., Science and Management*, pp. 442-447, March 2012.

[161] Ned Mohan, *Power Electronics-Converters, Applications and design*, New Delhi, John Wiley & Sons, 2003.

[162] A. Sannino and J. Svensson, "Power-electronic solutions to power-quality problems", *Int. J. of Electric Power Systems Research*, vol. 66, Issue 1,pp. 71-76, July 2003.

[163] Tahir Mahmood and Muhammad Ahmad Choudhry, "Medium voltage three phase static transfer switch operation: simulation and modeling," *Mehran University research journal of engineering and technology*, vol.29, no.4, Oct. 2010.

[164] Moschakis, M. N. and N. D. Hatziargyriou, "A Detailed Model for a Thyristor-Based Static Transfer Switch", *IEEE Trans. on Power Delivery*, volume 18, no. 4, pp. 1442-1449, October 2003.

[165] M. A. Hannan, and Aini Hussain,"A simulation model of solid state transfer switch for protection in distribution systems," *J. of Applied Sciences*, vol.6, no.9, pp. 1993-1999, 2006.

[166] L. Gyugyi,"Dynamic compensation of ac transmission lines by solid state synchronous voltage sources," *IEEE Trans. Power Delivery*, vol.9, pp. 904-911, April 1994.

[167] Mokhtari, H. , and Iravani, M. R ., "Effect of source Phase Difference on Static Transfer Switch Performance", IEEE Transactions on Power Delivery, Volume 22,No. 2, pp. 1125-1131, April, 2007.

[168] Sanjay Jain *et. al.*, Ganga Agnihotri and Renuka Kamdar, "Siting and Sizing of DG in medium primary Radial distribution system with enhanced voltage stability," Chinese J. of Engg., pp. 1-9, 2014.

[169] Mokhtari, H., Dewan, S .B ., Lehn, P , Martinez, J.A., and Iravani, M.R., "Benchmark Systems for Digital Computer Simulation of a Static Transfer Switch", IEEE Transactions on Power Delivery, Volume 16, No. 4, pp. 724-731, October, 2001.

[170] K R Padiyar, *FACTS controllers in Transmission and distribution*, New Age International, New Delhi, 2007.

[171] Thakur, T. and Jaswanti Dhiman. "A new approach to load flow solutions for radial distribution system." *Transmission & Distribution Conference and Exposition: Latin America, 2006. TDC'06. IEEE/PES*. IEEE, 2006.

[172] M. H. Moradi and M Abedini."A Combination of GA and PSO for optimal DG location and sizing in distribution systems. *Int. J. of Electrical Power and Energy Systems,*vol.34, pp.66-74, 2012.

[173] Tuba Gozel and M Hakan Hocaoglu,"An analytical method for the sizing and siting of distributed generators in radial systems" *Int. J. of Electric Power Systems research*, pp. 912-918, 2009.

[174] Satish Kumar Injeti and N Prema Kumar,"A novel approach to identify optimal access point and capacity of multiple DG's in a small, medium and large scale radial distribution systems. *Int. J. of Electrical Power and Energy Systems*, pp. 142-151, 2013.

[175] T. N. Shukla and S. P Singh,"Optimal sizing of distributed generation placed on radial distribution systems. *Int. Jou. of Electric power components and systems*," pp. 260-274, 2010.

[176] Partha Kayal and C. K Chanda,"Placement of wind and solar based DGs in distribution system for power loss minimisation and voltage stability improvement," *Int. Jou. of Electrical Power and Energy Systems*, pp. 795-809, 2013.

[177] K. Uma Rao, *Power system operation and Control*, John Wiley & Sons, 2013.

[178] Ke Jia and Tianshu Bi,"Advanced Islanding detection utilized in distribution systems with DFIG" *Int. J. of Electrical Power and Energy Systems*, vol. 63, pp. 113-123, 2014.

[179] M. A. Junjieet al.,"Size and location of DG in distribution system based on Immune algorithm," *System Engg. Procedia*,vol. 4, pp.124-132, 2012.

[180] Ranjan R and D Das, "Simple and Efficient computer Algorithm to solve radial distribution networks," *Int. J. of Electric power components and Systems*, vol.31,pp. 95-107, 2003.

[181] M. Chakravarty and D. Das,"Voltage stability analysis of radial distribution networks," *Int. J. of Electric Power and Energy Systems*, vol.23, pp.129-135, 2001.

[182] Aman, M.M., Jasmon, G.B., Mokhlis, H. and Bakar, A.H.A. (2014) 'Optimal placement and sizing of a DG based on a new power stability index', *Int. Journal of Electrical Power and Energy Systems*, Vol. 43, No. 1, pp.1296–1304.

[183] C. Rueda-Medina Augusto *et. al*., "Mixedinteger linear programming approach for optimal type, size and allocation of distributed generation in radial distribution systems", *Electr Power Syst Res*. 97.pp.133–143.2013.

[184] R. B. Ranjan et. al., "Voltage stability analysis of radial distribution networks," *Int. J. of Electric Power components and Systems*, vol.33. pp.501-511, 2004.

[185] Subin Sunny and P Balaji, "The better optimization technique for the placement of DG in order to reduce overall cost of power system," *Int. J. of Engg. and Advanced Technology*,vol. 2, pp.159-162, 2013.

[186] K. Nagaraju et al., "A novel method for optimal distributed generator placement in radial distribution systems," *Int. J. of Distributed Generation and Alternative Energy*,vol. 26, pp. 7-19, 2011.

[187] Injeti Satishkumar and Premakumar Navuri,"Optimal access point and capacity of distributed generators in radial distribution systems for loss minimisation including load models," *Int. J. of Distributed Generation and Alternative Energy*, vol. 29, 2014.

[188] S. Rajasekharan and G. A. Vijayalakshmi Pai, *Neural Networks, fuzzy logic and genetic algorithm*, Prentice Hall of India Pvt. Ltd.,2003 Edn.

[189] Zahra Boor and Seyyed Mehdi Hosseini, " GA based optimal placement of DGs for loss reduction and reliability improvement in distribution networks with time varying loads", *Int. J. of Intelligent systems and applications*, vol.4, pp.55-63, 2013.

[190] Majid Davoodi et al., "Optimal capacitor placement in distribution networks using genetic algorithm", *Indian J. of Science and Technology*, vol.5, no.7, pp.3054-3058, 2012.

[191] K. varesi,"Optimal allocation of DG units for power loss reduction and voltage profile improvement of distribution networks using PSO algorithm," *World academy of science, Engg. And Technology*, vol.5, pp. 12-26, 2011.

[192] S.Vijayabaskar and T. Manigandan, " Analysis of radial distribution system optimization with FACTS devices using hybrid heuristic technique," *J. of Theoreticsl and applied information technology,* vol. 58, no.2, 2013.

[193] S. Devi and M. Geethanjali, "Optimal location and sizing of distribution static synchronous series compensator using PSO algorithm," *Int. J. of Electrical Power and Energy systems,*vol. 62, pp.646-653, 2014.

[194] Ali Aref and Mohsen Davoudi, "Optimal distributed generation planning in RDS using Body Immune Algorithm," *J. of Basic and applied scientific research*, vol. 2, no. 6, pp. 6277-6284, 2012

[195] M.M. Aman *et al*., "Optimal placement and sizing of a DG based on a new power stability index and line losses," *Int. J. of Electrical Power and Energy Systems,* vol.43, pp.1296-1304, 2012.

[196] M Karimi and A Shahriari,"Impact of load modeling in distribution state estimation," *IEEE Int. Power Engg. And optimization Conf*., pp. 67-71, 2012.

[197] M M Aman, G B Jasmon," Optimum simultaneous DG and capacitor placement on the basis of minimization of power losses," *Int. J. of computer and electrical engg*., vol.5,no.5, pp.516-522, 2013.

[198] D Sai Krishna Kanth, P Suresh Babu and M. Padma Lalitha, " siting and sizing of DG for power loss and THD reduction, voltage improvement using PSO and sensitivity analysis," *Int. J. of engg. Research aand development*, vol.9, 1-7, 2013.

[199] T. N. Shukla and S. P Singh,"Allocation of optimal distributed generation using GA for minimum system losses in radial distribution networks," *Int. J. of Engg., Science and Technology*, vol. 2, no. 3, pp. 94-106, 2010.

[200] Duong Quoc Hung, and Mithulananthan N,"Optimal placement of dispatchable and nondispatchable renewable DG units in distribution networks for minimizing energy loss," *Int J. of Electrical Power and Energy Systems*, vol. 55, pp. 179-186, 2014.

[201] D. Rama Prabha and T. Jayabarathi,"Optimal placement and sizing of multiple distributed generating units in distribution networks by invasive

weed optimization algorithm," *Aim Shams Engineering Journal*, vol. 7, pp.683-694, 2016.

[202] Devi, A. Lakshmi and A. Chaithanya,"A New Analytical Method for the Sizing and Siting of DG in Radial System to Minimize Real Power Losses." *International Journal Of Computational Engineering Research* 2.7 (2012): 31-37.

[203] K R Devabalaji, K Ravi,"Optimal size and siting of multiple DG and D-STATCOM in RDS using Bacterial foraging optimization algorithm," *Ain Shams Engg. Journal*, vol. 7, pp.959-971, 2016.

[204] Khyati Mistry, Ranjit Roy,"CRPSO based optimal placement of multi-distributed generation in radial distribution system," *IEEE Int. Conf. on Power and Energy*, pp.852-857, 2012.

[205] H. H. Goh et al., "Comparative study of line voltage stability indices for voltage collapse forecasting in power transmission system," *Rio de Janeiro Brazil*, vol. 13, no. 2 part II, 2015

[206] Kundur P et. al., "Definition and classification of power system stability," *IEEE Trans. Power Systems*, vol.19, no. 3, pp.1387–1401, 2004

[207] T.V. Cutsem, *Voltage stability of electric power system*, Springer, 1998

[208] V.V.S.N. Murthy and Ashwani Kumar,"Comparison of optimal DG allocation methods in radial distribution systems based on sensitivity approaches," *Int. J. Electrical Power and Energy Systems*, vol.53, pp.450-467, 2013.

[209] Vadivelu, K. R. and G. V. Marutheswar, "Maximum loadability estimation for weak bus identification using fast voltage stability index in a power transmission system by real-time approach." (2014).

[210] Jain, Abhinav, A. R. Gupta and Ashwani Kumar, "An efficient method for D-STATCOM placement in radial distribution system." *Power Electronics (IICPE), 2014 IEEE 6th India International Conference on*. IEEE, 2014.

[211] Zahra Boor and Seyyed Mehdi Hosseini, " GA based optimal placement of DGs for loss reduction and reliability improvement in distribution networks with time varying loads", *Int. J. of Intelligent Systems and Applications*, vol. 4, pp.55-63, 2014.

[212] Atma Ram Gupta and Ashwani Kumar, "Energy savings using D-STATCOM placement in radial distribution system," *Procedia Computer Science* , vol. 70, pp.558 – 564, 2015.

[213] Pinki Yadav et. al., "Enhancement of voltage stability in power system using UPQC," *IOSR J. of Electrical and Electronics Engineering*, vol. 9, Issue 1 pp. 76-82, 2014.

[214] S. Devi and M. Geethanjali,"Optimal location and sizing determination of DG and D-STATCOM using PSO algorithm," *Int. J. of Electrical Power and Energy systems*, vol. 62, pp.562-570, 2014.

[215] Srinivasarao et. al.,"Optimal capacitor placement in a RDS using plant growth simulation algorithm," *Int. J. Electrical power and Energy system*, vol. 33, pp. 1133-1139, 2011.

[216] S. Uma Maheswaran and N. O. Guna Sekhar,"Reactive power contribution of multiple STATCOM using particle swarm optimization," *Int. J. of Engg. And Technology*, vol. 5, no.1, pp.122-126, 2013.

[217] Rosli Omar and Nasrudin Abd Rahim,"New control technique applied in DVR for voltage sag mitigation," *American J. of Engg. And applied sciences,* vol. 3, no. 1, pp. 858-864, 2010.

[218] Hendri *et. al.*, "Construction of a prototype D-Statcom for voltage sag mitigation," *European J. of scientific research*, vol. 30, no.1, pp. 112-127 2009.

[219] S. V. Ravikumar and S. Siva Nagaraju, " Simulation of D-Statcom and DVR in power systems," *APRN J. of Engg. And Applied Sciences,* vol.2, no.3, pp. 7-13, 2007.

[220] Bin Wang *et al.*, " Voltage sag estimation for power distribution systems," *IEEE Trans. on power systems*, vol. 20, no. 2, pp.806-812, 2005.

[221] V. Salehi *et al.*, " Improvement of voltage stability in wind farm connection to distribution network using FACTS devices," *IEEE*, pp. 4242-4247, 2006.

[222] P. Vasudevanaidu and Y. Narendra Kumar,"A new simple modeling and analysis of custom power controllers," *IEEE 3rd Int. Conf. on Power systems*, Kharagpur, Dec. 2009.

[223] S. M. Suhail Hussain and M Subbaramiah, " An Analytical Approach for Optimal location of DSTATCOM in Radial Distribution System," *IEEE*, 2013.

[224] Mehdi Hosseini *et al.*, " Modeling of series and shunt distribution FACTS devices in distribution systems load flow," *J. Electrical systems*, pp.1-12, 2008.

[225] Teng Jen-Hao,"A direct approach for distribution system load flow solutions," *IEEE Trans. Evol. Comput.*, vol. 18, pp.882–887, 2003.

[226] S. G. Bharathi Dasan et al., "Optimal siting and sizing of hybrid distributed generation using EP," *3rd IEEE Int. Conf. on power systems*, 2009.

[227] A. Ghosh et al., "Design of a capacitor supported DVR for unbalanced and distorted loads," *IEEE Trans. On power delivery*, vol.19,no.1, pp.405-413, 2004.

A1: Line data and Bus data of IEEE 15 bus Radial distribution system

Sending end node	Receiving end node	R (ohm)	X(ohm)	P(kW)	Q(kVAr)
1	2	1.35309	1.32349	44.1	44.991
2	3	1.17024	1.14464	70	71.4143
3	4	0.84111	0.82271	140	142.8286
4	5	1.52348	1.0276	44.1	44.991
2	9	2.01317	1.3579	70	71.4143
9	10	1.68671	1.1377	44.1	44.991
2	6	2.55727	1.7249	140	142.8286
6	7	1.0882	0.734	140	142.8286
6	8	1.25143	0.8441	70	71.4143
3	11	1.79553	1.2111	140	142.8286
11	12	2.44845	1.6515	70	71.4143
12	13	2.01317	1.3579	44.1	44.991
4	14	2.23081	1.5047	70	71.4143
4	15	1.19702	0.8074	140	142.8286

A2: Total Active power loss when different size of DG placed at different buses

Size of DG (kW)	Active Power Loss (kW)													
	2	3	4	5	6	7	8	9	10	11	12	13	14	15
0	61.7													
100	57.28	58.76	59.67	60.22	58.8	60.03	60.16	59.98	60.22	59.53	59.91	60.23	60.12	60.01
200	54.6	57.5	59.2	60.5	57.8	60	60.34	60.1	60.53	59	60.07	60.62	60.45	60.03
300	52.17	56.52	59.04	61.08	57.4	60.2	60.74	60.58	61.14	59.1	60.68	61.37	61.17	60.2
400	49.9	55.72	59.01	61.92	57.3	60.6	61.37	61.4	62.04	59.4	61.72	62.49	62.29	60.7
500	48.05	55.13	59.09	63.03	57.8	61.2	62.21	62.56	63.23	60	63.19	63.97	63.81	61.3
600	46.3	54.7	59.32	64.4	58.6	62	63.2	64	64.7	61	65	65.8	65.7	62.2
700	44.9	54.5	59.7	66.06	60	63	64.5	65.9	66.4	62	67.4	67.9	68	63.3
800	43.6	54.6	60.2	67.97	61.7	64.2	66.05	68.08	68.4	63.8	70.1	70.5	70.6	64.6
900	42.7	54.8	60	70.1	63	65.5	67.7	70.5	70.8	65.7	73.3	73.3	73.7	66.2
1000	41.9	55.3	61.7	72.5	66.5	67.1	69.6	73.4	73.3	67.9	76.8	76.5	77.1	67.9
1100	41.4	56	62.7	75.2	69.5	68.8	71.8	76.5	76.2	70.4	80.8	80.1	80.8	69.8
1200	41.19	56.8	63	78.2	72.8	70	74.1	80	79.4	73	85.1	84	0.85	72
1300	41.1	57.9	65.1	81.3	76.7	72	76.7	83.8	82.8	76.3	89.9	88.2	89.5	74
1400	41.3	59.1	66	84.8	81	75	79.5	87.9	86.4	79	0.95	92.7	94.3	76
1500	41.7	60.6	68.1	88.5	85.6	77.6	82.4	92.3	90.4	83.3	100	97.5	99.5	60

A3: Total Reactive power loss when different size of DG placed at different buses

Size of DG (kW)	Reactive Power Loss (kVAr)													
	2	3	4	5	6	7	8	9	10	11	12	13	14	15
0	**57.29**													
100	52.9	54.34	55.23	55.76	54.81	55.63	55.72	55.6	55.76	55.3	55.56	55.77	55.7	55.62
200	50.29	543.14	54.86	55.96	54.18	55.65	55.84	55.68	55.98	55.06	55.66	56.03	55.92	55.63
300	47.92	52.16	54.6	56.35	53.8	55.7	56.12	56	56.39	55.05	56.07	56.54	56.41	55.8
400	45.79	51.38	54.5	56.91	53.8	56.07	56.54	56.56	56.99	55.2	56.77	57.3	57.16	56.1
500	48.05	55.13	54.66	57.66	54.1	56.4	57.11	57.34	57.79	55.6	57.77	58.29	58.19	56.5
600	42.25	50.44	54.89	58.59	54.73	57.01	57.82	58.36	58.78	56.31	59.05	59.53	59.47	57.15
700	40.84	50.28	55.2	59.7	55.6	57.6	58.69	59.6	59.97	57.1	60.62	61	61.01	57.8
800	39.66	50.32	55.79	60.99	56.8	58.46	59.7	61.07	61.34	58.22	62.47	62.7	62.81	58.78
900	38.71	50.57	56.4	62.45	58.2	59.3	60.85	62.75	62.9	59.4	64.59	64.63	64.86	59.8
1000	38	51.02	57.2	64.09	60.02	60.4	62.15	64.66	64.65	60.9	66.99	66.8	67.16	60.9
1100	37.51	51.66	58.2	65.9	62.05	61.6	63.59	66.79	66.58	62.6	69.66	69.19	69.7	62.2
1200	37.25	52.51	59.3	67.89	64.3	62.9	65.18	69.13	68.7	64.5	72.6	71.8	72.49	63.7
1300	37.21	53.55	60.6	70.05	66.9	64.3	66.9	71.68	71	66.6	75.8	74.64	75.52	65.3
1400	37.4	54.79	61.9	72.37	69.7	65.8	68.77	74.45	73.47	68.9	79.26	77.7	78.79	67
1500	37.82	56.23	63.5	74.87	72.9	67.5	70.77	77.42	76.13	71.3	82.98	80.97	82.3	68.8

A4: Overall findings in IEEE 15 bus RDS using GA based BFSA

System Parameters	**GA based BFSA**
Active Power loss (P_{loss}) with NO DG (MW)	0.06179
Reactive Power loss (Q_{loss}) with NO DG(MVAr)	0.05729
Optimum size of DG (MW)	0.4
Location of DG	6
Active Power loss with DG (MW)	0.05738
% Reduction in P_{loss}	7.13
Reactive Power loss with DG(MVAr)	0.05385
% Reduction in Q_{loss}	6.0
Maximum voltage (pu)	1.0
Minimum Voltage (pu) with NO DG	0.9445
% Maximum voltage drop	5.55
Minimum Voltage (pu) with DG	0.9452
Location at minimum voltage	13
% Maximum voltage drop	5.48
% Recovery in voltage with DG	0.074
Grid Power (MW) with NO DG	1.28819
Grid Power (MW) with DG	0.88378

A5: Overall findings in IEEE 15 bus RDS with DG and D-STATCOM

System parameter	NO D-STATCOM or DG	Single D-STATCOM only	Single DG only	Two DGs	Three DGs	one DG and D-STATCOM	Two DGs and D-STATCOM	Three DGs and D-STATCOM
Active Power Loss (MW)	0.06179	0.044956	0.05738	0.045959	0.030347	0.041664	0.012885	0.010735
% reduction in P_{loss}		27.243	7.13	25.62	50.88	32.57	79.15	82.63
Reactive Power Loss (MVAr)	0.05729	0.04087	0.05385	0.042701	0.027471	0.03795	0.010447	0.008379
% reduction in Q_{loss}		28.661	6	25.47	52.05	33.75	81.76	85.37
Minimum voltage (pu)	0.9445	0.9662	0.9452	0.95	0.9639	0.95	0.9799	0.9887
Location at minimum voltage	13	13	13	13	13	13	0.13	13
% Voltage drop w.r.t reference voltage	5.55	3.38	5.48	5	3.61	5	2.01	1.13
No. of buses with under or over voltage	5	0	4	0	0	0	0	0
Optimum location		4	6	6	6	6	6	6
				4	4	4	4	4
					3		3	3
								4
Optimum Capacity		0.4MVAr	0.4MW	0.4MW(6) & 0.4MVAr(4)	0.4MW(6) 0.4MW(4) & 0.5MW(3)	0.4 MW(6) & 0.4 MVAr(4)	0.4 MW(6), 0.4 MW(4) & 1 MVAr (3)	0.4MW(6) 0.4MW(4) 0.5MW(3) & 0.9MVAr(4)

LIST OF PUBLICATIONS

International Journals:

1. Bindumol E. K. and C. A. Babu, "Analytical and sensitivity approach for the sizing and placement of DG in radial system", *Advances in Energy Research, An International Journal*, pp. 163-176, Vol. 4, No. 2, 2016.

2. Bindumol E. K. and C. A. Babu, "A novel analytical approach for sizing and placement of DG in radial distribution system", *International Journal of Energy Technology & Policy*, pp. 90-106, Vol. 13, Nos. 1/2, 2017.

International Conferences:

1. Bindumol E. K and C. A. Babu, "Voltage quality improvement by DVR in normal distribution and wind connected systems under different faults," International Conference on Advances in Recent Technologies in Electrical & Electronics (ARTEE), pp. 363-371, September 2013.

2. Bindumol E. K. and C. A. Babu, "Voltage Stability analysis in a radial distribution system using PSCAD and MATLAB," International Conference on Intelligent and Efficient Electrical Systems (ICIEES), pp. 8-13, December 2013

3. Bindumol E. K and C. A. Babu, "Impact of D-STATCOM on voltage sag in normal distribution and wind connected systems under different faults," IEEE International Conference on Advances in Energy Conversion Technologies (ICAECT), pp. 231-236, January 2014.

4. Bindumol E. K and C. A. Babu, "Performance improvement of multiple feeders in wind integrated distribution systems using SSTS," International Conference on Electrical, Electronics, Computer science and Mathematics Physical Education and Management (SARC), pp. 27-32, May 2014.

5. Bindumol E. K and C. A. Babu, "A simple and fast load flow algorithm for sizing and placement of DG in radial distribution system," IEEE International Conference on Electrical, Electronics, Signals, Communication and Optimization (EESCO), pp.1-6, January 2015.

6. Bindumol E K and Babu C A," Impact of D-STATCOM on voltage stability in Radial Distribution System," IEEE International Conference on Energy, Communication, Data Analytics & Soft Computing (ICECDS), August 2017.

7. Bindumol E K and Babu C A," Voltage Stability enhancement of radial distribution system using Optimum Size of D-STATCOM," IEEE Int. Conf. on International Conference On Electrical, Electronics, Computers, Commn, Mechanical And Computing (EECCMC), Jan 2018.

CURRICULUM VITAE

Bindumol E. K. was born in Ernakulam District of Kerala, India in 1973. She obtained her B.Tech Degree in Electrical and Electronics Engineering from M. A. College of Engineering, Kothamangalam, Kerala under Mahatma Gandhi University, Kerala in 1994. She acquired M.Tech degree in Microwave and Radar Electronics from Cochin University of Science and Technology, Kochi in the year 1996. She got selected in NIT, Calicut as Lecturer in the year 1998. Then, she got selected through PSC, Govt. of Kerala for appointment as Lecturer in Electrical Engineering in 1999. Since then, she has been teaching in Government Engineering Colleges in Kerala. Presently she is working as Assistant Professor in Electrical Engineering Department, Govt. Engineering College, Wayanad, Kerala. She has so far published two research papers in international journals and more than ten papers in international/national conferences. Her areas of interest include power system, renewable energy, distributed generation and custom power devices.